

IDENTIFICATION OF MAMMALIAN PROTEINS
INHIBITING APOPTOSIS DOWNSTREAM OF
CYTOCHROME C RELEASE
IN A YEAST SURVIVAL SCREEN

Dissertation
zur Erlangung des Doktorgrades
der Naturwissenschaften

Vorgelegt beim Fachbereich 15-Biologie und Informatik-
der Johann Wolfgang Goethe-Universität
in Frankfurt am Main

by
Marie-Luise Ligia Brezniceanu-Mehedinti
from Paris (France)

Frankfurt am Main 2003
(DF1)

Vom Fachbereich Biologie und Informatik der Johann Wolfgang Goethe-Universität
als Dissertation angenommen.

Dekan:

.....

Gutachter:

.....

Datum der Disputation:

.....

Eidstattliche Erklärung

Ich erkläre hiermit an Eides statt, dass ich die vorliegende Dissertation selbständig und nur mit den angegebenen Hilfsmitteln angefertigt habe.

Frankfurt am Main, den 19. Mai 2003

(Marie-Luise Ligia Brezniceanu-Mehedinti)

Abstract

One of the known apoptotic pathways in mammalian cells involves release of mitochondrial Cytochrome *c* into the cytosol. Cyt *c* then together with ATP or dATP induces a conformational change in the adaptator protein Apaf-1 (a homologue of the *C. elegans* CED4 protein) (Zou, Henzel et al. 1997), leading to its oligomerization and the recruitment of several pro-Casp-9 molecules. This protein complex assembly called "apoptosome" leads to the activation of Casp-9 which then initiates or amplifies the caspase cascade.

The cell death program can be stalled at several points and we were interested in identifying new proteins inhibiting cell death downstream of Cyt *c* release. This thesis describes how I have screened a cDNA library derived from a pool of human breast carcinomas in a yeast-based survival screen, using the *S. pombe* yeast strain HC4 containing an inducible *CED4* construct (James, Gschmeissner et al. 1997). The screen resulted in the identification of six proteins displaying cell death-inhibiting activity in *S. pombe* as well as anti-apoptotic potential in mammalian cells. Those six molecules were RoRet (Ruddy, Kronmal et al. 1997), Aven (Chau, Cheng et al. 2000), Fte-1/S3a (Kho, Wang et al. 1996), PGC2 (Padilla, Kaur et al. 2000; Goetze, Eilers et al. 2002), SAA1-2 β (Moriguchi, Terai et al. 2001) and FBP (Brockstedt, Rickers et al. 1998) of which I selected RoRet, Aven and Fte-1/S3a for further analysis.

RoRet is a new anti-apoptotic molecule that can inhibit the mitochondrial pathway via its PRY-SPRY domain. RoRet does not seem to bind to Apaf-1, and does not co-localize with the activated Apaf-1/Caspase-9 complex.

Aven was published to act as an anti-apoptotic protein and suggested to function via the recruitment of Bcl-X_L to Apaf-1. This work shows that its C-terminal domain can bind to Apaf-1 and has a strong anti-apoptotic activity by itself. Moreover, Aven co-localizes with the activated Apaf-1/Caspase-9 complex suggesting that it is a component of the apoptosome. Furthermore, the expression of Aven is regulated in mammary glands during the pregnancy cycle.

Fte-1/S3a has been already implicated in increased transformation capacity of v-Fos in fibroblasts (Kho and Zarbl 1992; Kho, Wang et al. 1996). This work shows that it has anti-apoptotic activity and can protect against Bak- and Apaf-1-induced apoptosis. It can bind directly to activated Apaf-1 at the linker domain between the WD40 repeats and the CED4-like domain, suggesting that it may protect by sequestering the activated Apaf-1 to some organelles whose nature remains to be determined. Moreover, expression studies on mRNA and protein level showed upregulation of Fte-1/S3a in colon, lung and kidney carcinoma.

Hmgb1 (Flohr, Rogalla et al. 2001; Pasheva, Ugrinova et al. 2002; Stros, Ozaki et al. 2002) was identified during a survival screen performed with a NIH 3T3 mouse fibroblast cDNA library in a Bak-expressing yeast *S. pombe* strain. HMGB1 can protect against Bak-, UV-, FasL- and TRAIL-induced apoptosis. Significant overexpression of HMGB1 was found in breast and colon carcinoma, and elevated mRNA amounts were detected in uterus, colon and stomach carcinoma, suggesting that it may be a tumour marker (Brezniceanu et al., 2003).

Acknowledgements

My very great thanks go to all who helped in the production of this thesis: to all members of the AG-Zörnig, in particular to Dr. Martin Zörnig, who directed and formed me during the past three years; to Prof. Dr. Anna Starzinski-Powitz whose advises were so precious for the outcome of my work and to Prof. Dr. Bernd Groner who allowed me to pursue this work at the Georg-Speyer-Haus; to Dr. Kirsten Völp whose knowledge and experience was always to be consulted and helped me to better target my efforts; to Susanne Bösser who did part of my cloning work and helped me with her technical assistance when I did not have enough hands; to Wiebke Baum for her counsels in IP and Pulldowns, and Ina Oehme for her instruction in the FACS “mysteries”; and to Pr. Dr. Winfried Wels and Dr. Claudia Litterst for their helpful protocols and kind advises.

I also have to thank my mother for her confidence in me and my fiancé for his patience when I was loosing patience. All my thanks as well to my dear friends: Estelle Dubois-Vignal, Sangrichan Giraud-Phomma, Sandra Primault, Mai-Trang Ngotrieu, Dr. Sylvie Pinson, Dr. Cyrile Curat, Schwester Dina Berzan and Elena Lebi-Carp, who against all odds, after so many crisis, depressions and hysterical-repetitive complains, are still my friends.

To all those people it has been a privilege to work and share ideas with, I offer these thanks, and I hope they will remember me kindly.

List of Abbreviations

Ab	antibody
bp	base pair(s)
cDNA	complementary deoxyribonucleic acid
<i>C. elegans</i>	<i>Caenorhabditis elegans</i>
Casp-	Caspase
Cyt <i>c</i>	Cytochrome <i>c</i>
(d)NTP	(2'-deoxy)ribonucleoside triphosphate
(d)ATP	(2'-deoxy)adenosine triphosphate
(d)CTP	(2'-deoxy)cytidine triphosphate
(d)GTP	(2'-deoxy)guanosine triphosphate
(d)TTP	(2'-deoxy)thymidine triphosphate
DMSO	dimethyl sulphoxide
DNA	deoxyribonucleic acid
DNase	deoxyribonuclease
<i>E. coli</i>	<i>Escherichia coli</i>
EDTA	ethylenediaminetetraacetic acid
EMM	Edinburgh minimal medium
EtOH	ethanol
EtBr	ethidium bromide
FBP	fuse binding protein
g	gram
HA	haemagglutinin
HRP	horse radish peroxidase
Ig	immunoglobulin
IP	immuno-precipitation
kb	kilobase
kD	kiloDalton
l	litre
LB	Luria-Bertani medium
M	molar
m	milli
mA	milliAmper
MOPS	3-(N-morpholino)propane sulphonic acid
mRNA	messenger ribonucleic acid
NB	northern blot
NaOAc	sodium acetate
OD	optical density
PAGE	polyacrylamide gel electrophoresis
PBS	phosphate-buffered saline
PCD	program cell death
PCR	polymerase chain reaction
RNA	ribonucleic acid
RNas	ribonuclease

rpm	revolutions per minute
RT-PCR	reverse transcription PCR
SB	southern blot
SDS	sodium dodecyl sulphate
<i>S. cerevisiae</i>	<i>Saccharomyces cerevisiae</i>
<i>S. pombe</i>	<i>Schizosaccharomyces pombe</i>
TBE	Tris-borate-EDTA buffer
TE	Tris-EDTA buffer
TEMED	N, N, N',N',-tetramethylethylenediamine
Tris (Trizma base)	Tris(hydroxymethyl)aminomethane
Tween 20	polyoxyethylenesorbitan monolaurate
u	unit (of enzyme activity)
V	volts
WB	western blot
μ	micro
n	nano
°C	degrees centigrade
x(...)g	gravity

Table

<i>Abstract</i>	4
<i>Acknowledgements</i>	5
<i>List of Abbreviations</i>	6
<i>Table</i>	8
<i>I-Introduction</i>	13
A-Apoptosis-a special form of PCD	13
1-Apoptosis-general considerations.....	13
2-Apoptosis in development and morphogenesis.....	14
3-Apoptosis and genetic integrity.....	14
4-Apoptosis and diseases.....	14
5-Apoptosis and evolution.....	15
6- Key players of the apoptotic process.....	16
B-General pathways	18
1-Programmed Cell Death in unicellular organisms.....	18
2- <i>Caenorhabditis elegans</i>	20
3- <i>Drosophila melanogaster</i>	22
4-Mammals.....	25
4.1-Extrinsic and intrinsic apoptosis pathways.....	25
4.3- p53.....	26
4.2- Caspases.....	28
4.3- The central role of mitochondria.....	31
C-Mitochondria and the apoptosome	32
1- The apoptosome pathway studied through knockout mice.....	32
2-Proapoptotic proteins released from the mitochondria.....	34
2.1-Cytochrome <i>c</i>	34
2.2-Smac/Diablo and Omi/HtrA2.....	34
2.3-Apoptosis-inducing factor (AIF).....	36
2.4-Endonuclease G.....	36
3-Induction of the mitochondria.....	37
3.1-Cleavage of Bid.....	38
3.2-Phosphorylation of Bad.....	38
3.3-Dissociation of Bim and Bmf from the cytoskeleton.....	39
3.4-The role of Bax and Bak.....	40
4-Apoptosis-inhibiting mechanisms.....	41
4.1-The Bcl-2 anti-apoptotic members.....	41
4.2-The IAPs.....	41
4.3-Receptor-mediated survival pathway.....	42

D-Clinical implications of apoptotic pathways disruption.....	43
1-Cancer	43
2-AIDS	45
3-Neurodegenerative disorders	46
4-Autoimmune disease.....	47
E-The goal of the project.....	48
II-Material and methods.....	49
A-The yeast survival screen	49
1-cDNA libraries used for the yeast survival screen	49
1.1- 1 Human mammary carcinoma cDNA-library cloned into the yeast expression vector pART1b, without start codon provided by a linker.	49
1.2- Human mammary carcinoma cDNA-library 2 cloned into the yeast expression vector pART1b, with a start codon provided by a linker.....	50
2-Yeast transformation.....	50
3-Buffers and solutions	51
B-Basic molecular biology	51
1-Mini-Prep.....	51
1.1-QIAGEN column (according to manufacturer's protocol).....	51
1.2-Alkaline Lysis Method.....	51
1.3-Buffers and solutions	51
2-Maxi-Prep.....	52
2.1-QIAGEN column (according to manufacturer's protocol).....	52
2.2-Lithium Chloride Method.....	52
3-Mega-Prep for cDNA Library amplification (QIAGEN column).....	52
4-DNA digestions, and DNA ligations	52
4.1- DNA digestion.....	52
4.2- DNA Phenol-extraction and DNA precipitation	53
4.3- 3'-OH DNA dephosphorylation	53
4.4- Gel extraction	53
4.5- DNA ligation	53
5-Bacterial transformation	54
5.1-Calcium chloride transformation	54
5.2-Bacteria transformation by electroporation.....	54
6-Southern Blot analysis.....	56
6.1- Yeast genomic DNA extraction.....	56
6.2- Protocol for the DNA transfer on the membrane, the insert radioactive labelling and the insert hybridization.....	56
6.3- Buffers and solutions	57
7-Northern Blot analysis	57
7.1- RNA extraction.....	57
7.2-Protocol for the RNA transfer on the membrane, the insert radioactive labelling and the insert hybridization.....	58
7.3- Buffers and solutions	58
8-Western Blot analysis	58
8-1-Protein extract	58
8.2-Protocol.....	59
8.4-Stripping membrane for subsequent hybridizations.....	59

8.4-Buffers and solutions	59
9-GST-pulldowns.....	60
10-Immunoprecipitation	60
10.1-Protocol.....	60
10.2-Buffers and solutions	61
11-PCR and RT-PCR.....	61
11.1- PCR.....	61
11.2- RT-PCR	62
13-Plasmids maps and cloning strategies	62
13.1- pcDNA3.1+/- (<i>Invitrogen</i>).....	62
13.2- In pEGFP-N1 (<i>Clontech</i>).....	63
13.3- In pCR3.3-Gaytway-compatible modified. (parental vector is pCR3.1 from <i>Invitrogen</i>).....	65
13.4- In pGADT7 (<i>Clontech</i>).....	66
13.5- In pArt1 (expression vector for <i>S. pombe</i> kindly provided by Dr. Paul Nurse, NCBR, London).	67
13.6- In pRIP 45 (expression vector for <i>S. pombe</i> kindly provided by Dr. Paul Nurse, NCBR, London).	68
13.7- In pGEX-AHK (expression vector for GST-fusion proteins in BL21 <i>E. coli</i> , fusing gene to GST.	69
13.8- Constructs provided by other research groups	70
14-Yeast Two-Hybrid (Y2H)assay.	74
14.1- β -galactosidase assay.....	74
14.2-Buffers and solutions.....	74
C-Cell culture	74
1-Basic handling	74
2-Transfection	75
3- Apoptosis quantification by LIVE/DEAD assay.....	75
4- Caspase activity assay.	76
5- KIM-2 cells.....	76
5.1-Cell culture	76
5.2-Buffers and solutions	76
D-FACS analysis	77
1-Propidium Iodide staining of fixed cells.....	77
1.1-Fixation.....	77
1.2-PI staining	77
3-Buffers and solutions	77
E-Confocal laser scanning microscopy	77
1-Fixation and antibody staining of cells.....	77
F- Cancer profiling array with tumours cDNA	78
G-Preparation of protein lysates from tumour samples for Western Blot analysis.....	78
1-Protein lysate preparation.	78
2-Buffers and solutions	79
H-Mouse mammary glands mRNA, northern blot analysis.	79
I- Common Drugs and companies	79
J- Tools and equipments.....	80

III-Results.....	82
A-The screens	82
1- The Yeast survival screen.....	82
B-Selection of candidate genes for future investigations.....	83
1-CED-4 expression.....	83
2-Literature analysis of the clones encoding for a protein.....	84
3-Anti-apoptotic potential of the candidate clones in mammalian cells.....	86
3-Computational analysis of Aven, Fte-1 and RoRet.....	91
3.1-Aven:	92
3.2-Fte-1/S3a:.....	93
3.3-RoRet:.....	94
C-Results in <i>S. pombe</i>.....	95
1-The protection potential against Bak- and CED4- induced yeast cell death. ...	95
2-CED4 induces cell death rather than growth arrest in <i>S. pombe</i> and Aven, RoRet and Fte-1 confer protection against CED4 yeast killing.....	97
3-Yeast protection assay in liquid medium.....	98
D-Functional assays	99
1- Apoptosis assays quantified by FACS analysis.....	99
2- Apoptosis quantified by the LIVE/DEAD assays	102
E- Analysis of the molecular pathways by which RoRet, Aven and Fte-1 may inhibit apoptosis	104
1- Analysis of Caspase-9 and -3 cleavage by Western Blot	104
2- Inhibition of Caspase-9 and -3 activity by Aven, RoRet and Fte-1	106
F- Cellular localization of RoRet, Aven and Fte-1, and analysis of their possible interaction with Apaf-1.....	108
1- Apaf-1 interaction studies of RoRet, Aven and Fte-1 in a Two-hybrid system.	108
2- Analysis of the potential interaction of RoRet, Aven and Fte-1 with Apaf-1 using the GST-pull down method.....	110
3- Co-immunoprecipitation of RoRet, Aven and Fte-1 with Apaf-1.....	112
4- Cellular localization of RoRet, Aven, Fte-1 and their deletion mutants, and co-localization studies with Apaf-1 and Caspase-9 by confocal microscopy.....	113
4.1-Co-localization of RoRet, Aven, Fte-1 with Apaf-1 or Caspase-9.....	113
4.2- Are Aven, RoRet and Fte-1 localized in the apoptosome ?.....	115
G-Possible involvement of Aven, Fte-1 and RoRet in mammary gland development and/or tumourigenesis	121
1-Mammary gland development.....	121
2- Kim-2 cells as an <i>in vitro</i> model for differentiation and apoptosis induction in the mammary gland.....	122
2-Aven, Fte-1 and RoRet expression in tumours.....	123
2.1- The cancer profiling arrays.....	123
2.2- Western Blots analysis of tumour lysates.....	126

<i>IV-Identification of HMGB1 in a yeast survival screen as an apoptosis-inhibiting protein.....</i>	<i>126</i>
1-A yeast survival screen with Bak as the “killer” protein led to isolation of HMGB1	126
2-HMGB1 protects mammalian cells against Bak-induced apoptosis.....	128
3-Correlation between HMGB1 expression and tumourigenesis	130
<i>V-Discussion.....</i>	<i>133</i>
A-The survival screen and the selection of the isolated cDNA clones.....	133
B-Analysis of RoRet, Aven and Fte-1 protection in yeast <i>S. pombe</i> and mammalian cells against apoptosis induction by different stimuli	135
1-RoRet, Aven and Fte-1 protect mammalian cells against cells death induced by Bak and Apaf-1 M368L/Caspase-9 overexpression, but protect <i>S.pombe</i> only against CED4 induced cell death.	135
2-RoRet, Aven and Fte-1 protect differently against apoptosis in mammalian cells.	138
C-Analysis of the In vivo relevance of these inhibitors of apoptosis: their possible implication in tissue homeostasis, regulation or tumourigenesis.....	142
D-HMGB1inhibits cell death in yeast and mammalian cells and is overexpressed in certain human tumours.....	143
<i>VII-Summary and outlooks</i>	<i>145</i>
References:.....	146
<i>INDEX.....</i>	<i>162</i>
<i>HMGB-1 inhibits cell death in yeast and mammalian cells and is abundantly expressed in human breast carcinoma.....</i>	<i>162</i>

I-Introduction

A-Apoptosis-a special form of PCD

Apoptosis is a genetically regulated process of cell suicide that is capital to the development, homeostasis and integrity of multicellular organisms. Its importance is such that the dysregulation of mechanisms controlling cell suicide plays a role in the pathogenesis of a wide range of diseases. Different from autophagy and necrosis which have lately also been defined as orchestrated by a genetically programmed mechanism, apoptosis can be defined by specific morphological changes: membrane blebbing, chromatin condensation and fragmentation, and exposure of markers on the outer cytoplasmic cellular membrane like phosphatidyl-serine that will mark the cell for phagocytosis by macrophages. By contrast, autophagy targets a population of cells or entire tissues that will die by the presence of “autophagic vacuoles” in their cytoplasm containing the machinery needed to degrade the dying cell. An early loss of membrane integrity leading to the leakage of cellular components is the hallmark of necrosis. While great progress has been achieved in unveiling of the molecular mechanisms of programmed cell deaths, a new level of complexity, with important therapeutic implications, has begun to emerge, suggesting (i) that several different self-destruction pathways may exist and operate in parallel in cells, and (ii) that molecular effectors of cell suicide may also perform other functions unrelated to cell death induction and crucial to cell survival.

1-Apoptosis-general considerations

Initial questions about the possible existence, mechanisms, and role of physiological cell death emerged during the second half of the 19th century, from the study of animal development, (Clarke and Clarke 1996), (Lockshin and Zakeri 2001), but it is only during the second half of the 20th century that a series of conceptual and experimental advances progressively led to the idea that cells from multicellular animals may have the capacity to activate a program of self-destruction, and that this self-destruction program may be regulated by signals provided by other cells. (Clarke and Clarke 1996), (Lockshin and Zakeri 2001), (Saunders 1966), (Kerr, Wyllie et al. 1972), (Umansky 1982), (Cowan, Fawcett et al. 1984), (Ellis and Horvitz 1986), (Clarke 1990), (Ellis, Yuan et al. 1991). The identification of a genetic regulation of physiological cell death, of the features of its most frequent phenotype, apoptosis, and of its central role, not only in development, but also in adult tissue homeostasis, has led to the idea that all cells all multicellular animals may be intrinsically programmed to self-destruct, and that cell survival continuously depends on the repression of this self-destruction program by other cells, in other words that cells may survive only as long as they are signalled to suppress the induction of a 'default' pathway leading to cell suicide (Kerr, Wyllie et al. 1972), (Vaux 1993), (Hengartner 2000), (Raff 1992).

2-Apoptosis in development and morphogenesis.

The coupling of the fate of each cell to the nature of the interactions with other cells has led to the concept of 'social control' of cell survival and cell death, allowing a stringent regulation of cell numbers, of their tissue localization, and a constant adjustment of the different cell types that constitute our organs and tissues (Raff 1992). This interdependence generated between cells, is one of the bases of life perennity and species plasticity, allowing bodies to build themselves, to constantly reconstruct, and to adapt to ever changing environments. Programmed cell death participates in particular in morphogenesis (the sculpting of the form of embryos like the fingers and toes of hands and feet), in sexual differentiation (in male embryo the Müller channel is deleted by apoptosis), and in the epigenetic self-organization processes (where the cells are selected more by environmental criteria than genetic predestination) that allow the emergence of the two most complex regulatory organs of our body, the immune system and the nervous system (Oppenheim 1991), (Flanagan 1999), (Goldrath and Bevan 1999), (Yuan and Yankner 2000). Indeed during development, an excess of cells is generated in these tissues which are subsequently deleted by apoptosis. For example, in the Thymus where a repertoire of T cells is selected whose receptors have the potential to recognize foreign antigenic peptides, but not auto-antigenic peptides (those cells are cleared by apoptosis) bound to the individual's own MHC molecules (Ashton-Rickardt, Van Kaer et al. 1993; Kishimoto and Sprent 1997; Suzuki, Guinter et al. 1998).

3-Apoptosis and genetic integrity

Specific organ or tissue cell-cell interaction, represents only one dimension of the 'social control' of cell survival and cell death. At another level, each individual cell may be considered as a complex entity, a 'society' by itself, a mingling of heterogeneous organelles and components that behaves as a whole. Thus, self-destruction can occur not only as a response to signals originating from the outside environment of the cell, but also from its inside environment. Accordingly, genetic damage causes the activation of the p53 protein family, that induces either DNA repair and cell cycle arrest, or programmed cell death, a radical and extreme means preventing the emergence of genetic heterogeneity, and the progression towards cancer.(Rich, Allen et al. 2000) Similarly, alterations in endoplasmic reticulum integrity, induced, for example, by abnormal protein folding, (Mehmet 2000) or alterations in mitochondrial activity, such as respiratory chain dysfunction (Wang, Silva et al. 2001) can induce signalling leading to programmed cell death. Thus, cell suicide plays an essential role in the maintenance of the genetic identity and the integrity of the body, by inducing the rapid elimination of altered cells.

4-Apoptosis and diseases

Programmed cell death is also crucial in the adult, by controlling tissue homeostasis, elimination of damaged or abnormal cells, and defense against infections (Cohen 1993),(Ameisen 1994),(Vaux, Haecker et al. 1994),(Williams 1994). Conversely, programmed cell death dysregulation has been proposed to participate in the pathogenesis of many diseases, ranging from cancer and autoimmunity to infectious diseases and neurodegenerative disorders, (Umansky 1982), (Ameisen, Estaquier et al. 1994), (Nagata and Golstein 1995), (Teodoro and Branton 1997),(Evan and Littlewood 1998), (Krammer 2000) leading to the emergence of new concepts of therapeutic intervention, aimed at the selective modulation of the mechanisms involved in the regulation of cell death and cell survival (Yuan and Yankner 2000), (Williams 1991), (Kerbel 1997), (Nicholson 2000). Finally, programmed cell death may also participate in the physiologically regulated process of aging (Umansky 1982), (Migliaccio, Giorgio et al. 1999).(See *Clinical implications*)

5-Apoptosis and evolution

Programmed cell death has been found to operate in all multicellular animals studied so far, including nematodes, insects, amphibians, birds and mammals (Ellis, Yuan et al. 1991), (Meier, Finch et al. 2000), (Vaux and Korsmeyer 1999), (Steller 1995), (Cikala, Wilm et al. 1999). Lately PCD has also been identified in unicellular organisms like bacteria, yeast, *Thetrahymena thermophila* or *Dictyostelium discoideum* (Lewis 2000; Arnoult, Tatischeff et al. 2001; Madeo, Engelhardt et al. 2002), (Christensen, Chemnitz et al. 1998). The evolutionary conservation of this programmed cell death in the animal kingdom points toward some central aspects of its genetic control, and to important aspects of its most frequent phenotype, apoptosis (Saunders 1966), (Ellis, Yuan et al. 1991), (Vaux and Korsmeyer 1999), (Steller 1995), (Cikala, Wilm et al. 1999). In most cases that have been studied to date, programmed cell death is regulated by signals provided by other cells, either in the form of cell-lineage information, of soluble mediators, or of cell-to-cell contacts. Programmed cell death induction may depend on cell-lineage information, such as in the nematode *Caenorhabditis elegans*, on the activation of gene transcription, or, in a more stochastic way, on a combination of cell-lineage information, intercellular signaling, transcription factor activation and cytoplasmic second messengers, such as in mammals (see rev. (Meier, Finch et al. 2000). During the last nine years, homologues of genes involved in the regulation of programmed cell death in *Caenorhabditis elegans* have been identified in sponge (Wiens, Diehl-Seifert et al. 2001), in *Hydra vulgaris* (Cikala, Wilm et al. 1999), in the fruitfly *Drosophila melanogaster* (White, Grether et al. 1994), in *zebrafish* (Inohara and Nunez 2000) and in mammals (Yuan, Shaham et al. 1993), (Hengartner and Horvitz 1994) (Fig.3). As frequently occurs during evolution, however, this striking conservation in both sequences (Vaux and Korsmeyer 1999), (Horvitz 1999) and functional properties (Vaux, Weissman et al. 1992) has been associated with a great level of diversification (Hengartner 2000), (Vaux and Korsmeyer 1999) mostly due to gene duplication. In humans and mice, around twenty gene products that are homologues of the cell death

repressor Ced-9 and its antagonist Egl-1 (the Bcl-2 family) have been identified, as well as more than ten homologues of the executioner protease Ced-3 (the caspase family) and at least three variant of Apaf-1 (apoptotic protease-activating factor 1) the homologue of Ced-4 (Fu, Kelsey et al. 2001).

6- Key players of the apoptotic process

Two apoptotic pathways have been described recently: the extrinsic and the intrinsic pathway. Both of them act through the activation of the cascade of cysteine proteases (caspases). The extrinsic pathway which acts through the activation of initiator caspases can be directly coupled to cell surface receptor signalling, such as Caspase-8 activation induced by the recruitment of the FADD adaptor protein, consecutive to the engagement of 'death' receptors of the CD95/tumor necrosis factor receptor (TNFR) family by their ligands. The intrinsic pathway involves another initiator caspase, Caspase-9, that is activated downstream of the mitochondria outer membrane permeabilization induced by members of the Bax family in response to various pro-apoptotic stimuli, through the release of Cytochrome *c* that activates the Apaf-1 adaptor protein (Fig.1). There are two types of cells described for the death-receptor apoptosis induction: type I cells can activate enough Caspase-8 to activate Caspase-3 and proceed to apoptosis of the cell, the type II cells need to induce the release of pro-apoptotic molecules from the mitochondria (Cytochrome *c*, Smac,...) to activate Caspase-3 through the formation of the apoptosome (Scaffidi, Fulda et al. 1998). In type II cells the intrinsic and extrinsic pathways can cross-talk through the induction of the mitochondria. The initiator caspases are autocatalytically cleaved and activated through recruitment by adaptor proteins that share death-effector domains (DED) or caspase activation and recruitment domains (CARD) with these initiator caspases (Hengartner 2000), (Krammer 2000), (Green 2000), (Thornberry and Lazebnik 1998).

Downstream in the cascade, caspases are termed effector or executionary caspases, such as Caspase-3, -6 and -7, which cleave numerous nuclear and cytoplasmic proteins, thereby inducing several of the typical features of apoptosis (Hengartner 2000), (Nagata 2000) (Fig.6). The activation of these effector caspases requires their initial cleavage by other upstream caspases (initiator caspases) such as Caspase-8 and -9 (Fig.6).

The death repressors (Bcl-2/Bcl-X_L) and their antagonists (Bax/Bak) share the capacity to homodimerize or oligomerize, and to neutralize each other through heterodimerization, and, for some of them, to insert through a carboxyterminal hydrophobic transmembrane domain into the outer membrane of intracellular organelles such as the nucleus, endoplasmic reticulum and mitochondria. While there are alternative views (Finkel 2001), it is generally believed that it is through their control of mitochondrial outer membrane permeability that the Bcl-2/Bax family members exert an important part of their antagonistic effect on cell death and survival, by repressing (Bcl-2) or inducing (Bax) the release of mitochondrial intermembrane space proteins into the cytosol that will favor the induction of cell death (Gross,

McDonnell et al. 1999), (Vander Heiden and Thompson 1999), (Green 2000), (Kroemer and Reed 2000), (Martinou and Green 2001) (Fig.1). Some of these intermembrane space proteins, such as Cytochrome c, Smac/Diablo, and Omi/HtrA2 will induce caspase activation (Green 2000), (Martinou and Green 2001), (Suzuki, Imai et al. 2001), while others, such as AIF (apoptosis inducing factor), (Susin, Lorenzo et al. 1999), or endonuclease G may favor the induction of caspase-independent executionary pathways.

Importantly these multiple pathways of activation, that can amplify each other, can also be repressed at the level of the effector caspases, for example by IAPs (inhibitors of apoptosis proteins) that block the activity of already processed caspases (Goyal 2001). The IAPs themselves can be inhibited by the Smac/Diablo protein, which is released by mitochondria and binds to IAPs, thereby releasing the caspases molecules (Goyal 2001) (Fig.7 and 10).

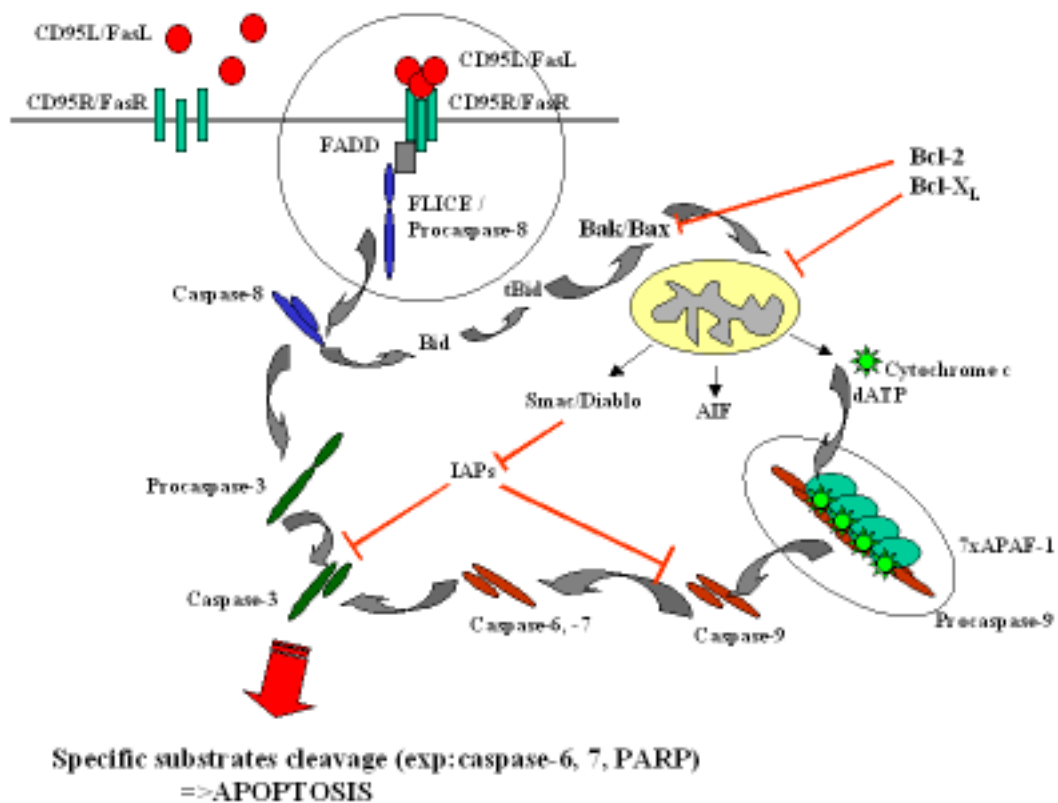


Fig.1: The cell death machinery.

Illustration of the death receptor induced apoptosis, the DISC formation (the circle containing FasL/Fas/FADD/FLICE complex) induced by ligand binding. Then takes place the proteolytic activation of Caspase-8, -9, -6, -7 and -3. The mitochondria is induced by Bak/Bax translocation after Bid cleavage, and release Cytochrome c. The apoptosome formation follows (the circle containing APAF-1/Cytochrome c/Procaspase-9/ATP or dATP) that can activate Caspase-9 and lead to activation of Caspase-3. IAPs, Bcl-2 and Bcl-X_L can inhibit at different levels.

A series of knock-out experiments in mice, including the deletion of genes encoding either members of the Bcl-2/Bax family, the Apaf-1 and FADD adaptor proteins, members of the caspase family, or, more recently, cytochrome *c* or AIF have indicated that each of these proteins controls some, but not all, suicide pathways, in some, but not all, cell types.

Thus, in contrast to the simple paradigm of *Caenorhabditis elegans*, in mammalian cells, programmed cell death can proceed along multiple intracellular molecular pathways, and the pathways followed will not be the same in different cell types, in response to a given death signal, nor in the same cell type, in response to different death signals. In some instances, the molecular pathway leading to self-destruction will even be different in a given cell type, in response to the same death signal, depending on the particular differentiation stage of the cell. Moreover, the complexity of the molecular control of cell survival and cell death also involves various epigenetic mechanisms such as alternative splicing and post-translational modifications (phosphorylation, dephosphorylation, or proteolytic cleavage) that can transform the product of a given gene into either a pro-apoptotic or an anti-apoptotic protein (Yuan and Yankner 2000), (Gross, McDonnell et al. 1999), (Xiang, Chao et al. 1996). These modifications include or example the activation of Bad through dephosphorylation or the cleavage of procaspases in active caspases during the so called “caspase cascade” (Cohen 1997; Thornberry and Lazebnik 1998; Wolf, Witte et al. 2001).

B-General pathways

1-Programmed Cell Death in unicellular organisms

Until very recently, studies on programmed death of free-living unicellular eukaryotes were at a preliminary stage. But as several reports describing apparent programmed cell death in unicellular eukaryotes like *Tetrahymena thermophila* (Christensen, Chemnitz et al. 1998), *Dictyostelium discoïdum* (Arnoult, Tatischeff et al. 2001) or even prokaryotes like bacteria, the idea that unicellulars may commit suicide for the advantage of the colony becomes accepted easier. A theory has emerged that a unicellular organism undergoing PCD in a colony preserving genetic integrity would act the same way a single cell in a multicellular organism would commit suicide to preserve the genetic integrity of a whole body or tissue, or even to allow an evolutive advantage to spread in the species. Staurosporine (a non-specific protein kinase inhibitor inducing apoptosis in cells of higher organisms) was shown to stimulate reactive oxygen species (ROS) production and to kill *Tetrahymena* (Christensen, Chemnitz et al. 1998). Petit and his colleagues (Arnoult, Tatischeff et al. 2001) identified in the slime mold *Dictyostelium discoïdeum* an apoptosis-inducing factor (DdAIF) structurally and functionally similar to the mammalian AIF (Susin, Lorenzo et al. 1999). It was found that DdAIF is involved in cell death caused by adding protoporphyrin IX or differentiation-inducing factor-1 (DIF-1). However, one

should keep in mind that *D. discoideum* at some stage of its life cycle is a multicellular organism (for some other indications of the programmed death of constantly unicellular eukaryotes, see reviews (Ameisen 1996), (Lewis 2000)).

During the last decade, programmed cell death was intensively studied in yeast. The majority of these studies dealt with expression of mammalian pro- and anti-apoptotic proteins in these microorganisms. Kane et al. (Kane, Sarafian et al. 1993) reported that the anti-apoptotic mammalian protein Bcl-2 partially rescued a *S. cerevisiae* yeast mutant lacking superoxide dismutase. Manon and co-workers (Manon, Chaudhuri et al. 1997) found that the pro-apoptotic mammalian protein Bax caused growth arrest of yeast *S. cerevisiae* cells, which was accompanied by Cytochrome *c* release from mitochondria into the cytosol. Coexpression of anti-apoptotic Bcl-x_L prevented the effects of Bax. Ink and al. (Ink, Zornig et al. 1997) studied Bak induced Cell Death in *Schizosaccharomyces pombe*, and found that not only Bak was able to induce yeast cell lethality, but that this lethality could be antagonized by the mammalian anti-apoptotic protein Bcl-x_L. Moreover, in this case cell death was accompanied by morphological feature resembling apoptosis like loss of nuclear membrane integrity, vacuolisation and chromatin condensation and fragmentation (Ink, Zornig et al. 1997). The possibility that cell death may be caused by simple overexpression of a foreign protein was excluded by overexpressing Bcl-x_L (which had phenotype) and by overexpression of a deletion mutant of Bak lacking the BH3 domain necessary to induce apoptosis in mammals (Ink, Zornig et al. 1997). Since this mutant did not kill yeast cells either, it was speculated that some conserved pathways in evolution must be involved in programmed Cell Death in Yeast.

The possibility of using *Schizosaccharomyces pombe* as a model system to study the activity of proteins involved in apoptosis of multicellular organisms, allows the precise functional analysis of these proteins, often in the absence of further, potentially redundant family members. For example James and al. discovered a death-inducing function of CED4 in yeast (James, Gschmeissner et al. 1997). Indeed the authors could show that CED4 could induce active cell death in *S. pombe*, and that this cell death was accompanied by the translocation of CED4 from the ER and mitochondria to the nucleus. In dying yeast cells CED4 was co-localizing with the condensed chromatin. Moreover, the authors could show that yeast killing by CED4 could be inhibited by CED9 co-expression, but not by CED9L (an inactive mutant in *C. elegans*) or p35 co-expression (James, Gschmeissner et al. 1997). CED4 directly interacts with CED9 as shown by the authors using *S. cerevisiae* for yeast-two-hybrid studies. The observed effects strongly suggest that some evolutionary programmed cell death pathway has been conserved from unicellular organisms to mammals.

Later Manon and co-workers (Manon, Chaudhuri et al. 1997; Priault, Camougrand et al. 1999) found that neither cytochrome *c* nor ATP/ADP antiporter are required for the Bax-induced death of yeast *S. cerevisiae*, moreover yeast Cytochrome *c* injection was not able to induce yeast cell death. Thus, Cytochrome *c* release might be a side effect of Bax. For example, it is known that Bax, if added together with mitochondrial porin, induces permeabilization of an artificial phospholipid membrane for Cytochrome *c* (Shimizu, Ide et al. 2000). It was found that porin is required for the killing of yeast by Bax (Shimizu, Shinohara et al. 2000). The Bax-induced death of yeast seemed to be a consequence of an oxidative stress since co-expression of some

plant proteins preventing Bax-induced ROS burst rescued the Bax-expressing yeast (Levine, Belenghi et al. 2001), (Moon, Baek et al. 2002).

Some other studies have demonstrated that certain mutations in the yeast genome result in death showing features of apoptosis like chromatin condensation, cytoplasmic vacuolisation, and loss of nuclear and organelles membrane integrity (Madeo, Frohlich et al. 1997). A *Saccharomyces cerevisiae* mutant in cell division cycle gene CDC48 shows typical markers of apoptosis: membrane staining with annexin V, indicating an exposure of phosphatidylserine at the outer layer of the cytoplasmic membrane, DNA fragmentation and chromatin condensation and fragmentation (Madeo, Frohlich et al. 1997).

Other cases were described which point to programmed death for example of yeast treated by a lethal dose of some toxic compounds. Madeo et al. (Madeo, Frohlich et al. 1999) and Corte-Real et al. (Ludovico, Sousa et al. 2001) reported that H₂O₂ or acetate kill yeast *S. cerevisiae*, the death being accompanied by some typical apoptotic features. The discovery of a yeast caspase YCA1 in 2002 by Madeo and Al. (Madeo, Engelhardt et al. 2002) who succeeded in finding in *S. cerevisiae* a meta-caspase, a key enzyme of the animal apoptotic cascade (this discovery was, in fact, predicted by Koonin, Dixit and their bioinformatic colleagues analyzing the yeast genome (Uren, O'Rourke et al. 2000)). Madeo et al. (Madeo, Engelhardt et al. 2002) studied a 52 kDa protein, the amino acids sequence of which resembled that of mammalian caspases. It was found that overexpression of the enzyme resulted in removal of a 12 kDa fragment of this protein and appearance of the caspase-like proteolytic activity. When the potentially catalytic cysteine 297 of the protein was mutated, no formation of the 12 kDa product could be observed. Moreover, overexpression of the 52 kDa protein reduced viability of the prolonged yeast culture. Addition of H₂O₂ to the yeast overexpressing p52 cell extract hydrolyzation of typical caspase substrates. Deletion of the corresponding gene increased the lethal dose of H₂O₂ by a factor of 3 and entailed appearance of 6–8% 'immortal' cells surviving more than 28 days under nutrient-depleted conditions whereas all the wild-type cells died within 10 days. The authors called the 52 kDa protein yeast caspase 1 (YCA1). Madeo et al. (Madeo, Engelhardt et al. 2002) identified one more component of the YCA1-mediated yeast programmed death. It was shown that the absence of a protein encoded by the Ygl129c gene completely prevented the death caused by the YCA1 overexpression. As indicated by Berger et al. (Berger, Brigl et al. 2000), this protein is an ortholog of the animal mitochondrial protein DAP-3, which is involved in apoptosis induced by some cytokines (Kissil, Cohen et al. 1999).

2- *Caenorhabditis elegans*

The first evidence for the existence of genetic information specific for the control of cell death was provided by pioneering experiments in the nematode *Caenorhabditis elegans*, (Ellis and Horvitz 1986), (Ellis, Yuan et al. 1991), (Horvitz, Shaham et al. 1994; Horvitz 1999) a metazoan whose phylogenic divergence predates ours by several hundred million years and whose body is constituted of exactly 959

somatic cells. During the development of *C. elegans*, 131 of the somatic cells die by apoptosis, and are rapidly ingested by neighboring cells. The investigation of genetic mutants revealed that the survival or death of most, if not all, cells during development depends on the presence, and expression, of only four genes, *ced-3*, *ced-4*, *ced-9*, and *egl-1* (Hengartner 2000), (Horvitz 1999) (Fig.2). In addition to these four gene products involved in the control of self-destruction and survival, there are at least seven gene products that allow the rapid ingestion of the dying cells by its neighbours, (Savill and Fadok 2000), (Horvitz 1999). Ced-3, a key protein in the induction of cell death is an aspartate-directed cystein protease (a caspase) that, like most proteases, is synthesized as an inactive pro-enzyme precursor, and requires cleavage to become active. Ced-4 is an adaptor protein that, by oligomerizing and binding the Ced-3 pro-enzyme, induces Ced-3 autocatalytic cleavage and activation. Ced-9 is a repressor of cell death that, by binding Ced-4, prevents it from activating Ced-3. Finally, Egl-1, which is transcriptionally upregulated is an antagonist of Ced-9, that by binding Ced-9 prevents its protective effect, releasing Ced-4 from Ced-9, and allowing Ced-4 to activate Ced-3 and to trigger self-destruction.

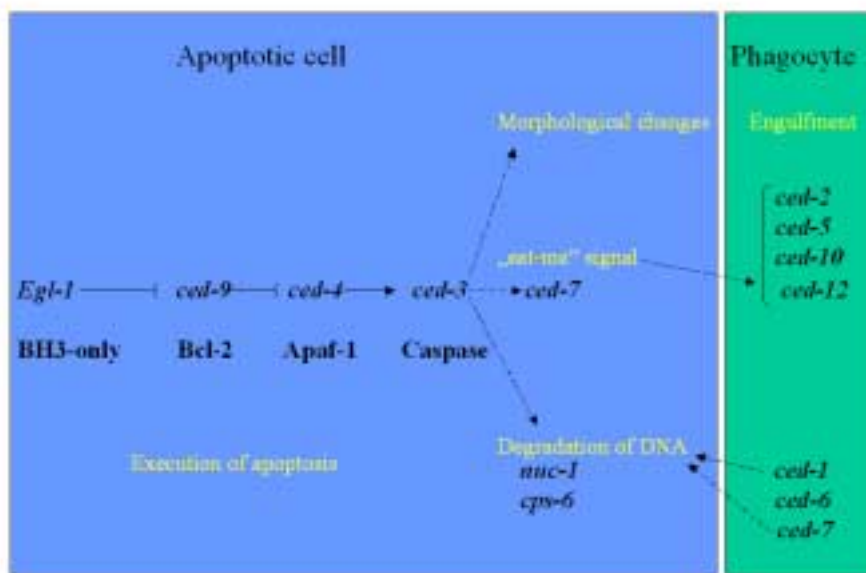


Fig.2: The genetic pathway of apoptosis in *C. elegans* and their mammalian homologues. Egl-1 inhibits CED-9 inhibition of CED-3 activation by CED-9. CED-3 activation results in morphological changes, expression of phagocytosis-signal proteins and DNA degradation.

These findings provided a new paradigm: a simple genetic module suffices to control the fate of all somatic cells in response to the various cell-lineage and cell-type specific signals involved in cell differentiation and embryonic development. At the same time, these findings also illustrate the ambiguity intrinsic to the concept of a 'death program'. Indeed, Ced-3 is an executioner of cell death, but only if Ced-4 is present and available; Ced-4 is an activator of the executioner, but only if Ced-9 is lacking or not available; and Ced-9 is a repressor of cell death, but only if Egl-1 is

lacking, or not available. In other words, the completion of the 'death program' will depend, in each cell, on the interactions between each of these four proteins, that depend, at least in part, on their respective expression level, regulated by cell signalling during development (Fig.2). Very recent findings have also suggested that the activation of the Ced-3 protease may not obligatorily represent a 'point of no return' beyond which cells are condemned to die, and that an unexpected form of social control may be involved in the process of cell death. Indeed, while Ced-3 activation seems required for the initiation of self-destruction, the execution of cell death also requires the expression of the proteins involved in the ingestion of dying cells, in the neighbouring surviving cells (Hoepfner, Hengartner et al. 2001),(Reddien, Cameron et al. 2001).

3-*Drosophila melanogaster*

Regulation of cell death has also been extensively studied in *Drosophila*. Flies with mutations in the caspase *dcp-1* (*drosophila caspase-1*) die as larvae with tumours or are infertile because of defects associated with oogenesis (Song, McCall et al. 1997; McCall and Steller 1998). Furthermore, flies with a strong null mutations in *dark* gene (the *drosophila* homologue of *Apaf-1*) die during metamorphosis, have defects in nervous system cell death and often develop tumours (Rodriguez, Oliver et al. 1999). Furthermore, Kumar and colleagues have recently reported that DARK may form an apoptosome complex which is built by Apaf-1 and Caspase-9 or homologues in mammalian cells and which results in the activation of Caspase-9) by recruitment of the fly Caspase-9 homologue DRONC (Dorstyn, Colussi et al. 1999; Dorstyn, Read et al. 2002). Mutations in the inhibitor of apoptosis (IAP) gene *diap* result in massive ectopic cell death and embryonic lethality owing to the activity of caspases (Wang, Hawkins et al. 1999; Goyal, McCall et al. 2000) (Fig.3). Recent studies have shown that deletion of *dark* suppresses this dramatic *diap*^{-/-} phenotype, indicating that caspase-activated cell death requires input from *dark* (Rodriguez, Chen et al. 2002). Although initial experiments indicated that DARK interacted with Cytochrome *c* (Rodriguez, Oliver et al. 1999), two recent studies suggest that fly apoptosomes do not require this protein as a cofactor for their assembly. In addition, the *Drosophila* Reaper protein has been found to promote mitochondrial Cytochrome *c* release upon addition to a *Xenopus* cell-free system (Evans, Kuwana et al. 1997). Thus, although the recent data suggest that the *Drosophila* apoptosome may be regulated in a Cytochrome *c*-independent manner, it remains possible that Cytochrome *c* may participate in *Drosophila* PCD in some ways.

Table 1 | **Cell-death genes are conserved in different organisms**

Relationships are conserved within the generic signalling hierarchy

CED-9 → CED-4 → CED-3
 Bcl-2 → Apaf-1 → Caspases

Gene sequences and functions are conserved




Gene family	Worm	Fly	Mouse
			
Caspases	<i>ced-3, csp-1, csp-2</i>	<i>Dredd, Dronc, Dream/Strica, Dcp-1, Drice, Decay, Daydream/Damm</i>	Caspases 1–14
Bcl-2	<i>ced-9, egl-1</i>	<i>Debcl-1/Drob-1/Dborg-1/Dbok, Buffy/Dborg-2</i>	<i>Bcl-2, Bcl-x, Bcl-w, Mcl-1, A1, Diva, Bax, Bak, Bok, Bik, Bik, Bid, Bad, Hrk, Bim, Bnip, Nix</i>
APAF-1	<i>ced-4</i>	<i>ark/dark/hac-1/dApaf-1</i>	<i>Apaf-1</i>
IAP	<i>bir-1, bir-2</i>	<i>diap-1, diap-2, dbruce, deterin</i>	<i>Xiap, c-iap1, C-ap2, hILP-2, ml-iap, naip, survivin, bruce</i>
RHG domain	?	<i>rpr, hid, grim, sickle</i>	<i>Smac/DIABLO, Omi/HtrA2</i>

Fig.3: Conserved genes and pathways throughout evolution. (*Molecular Cell biology*, 2002, (Baehrecke 2002)).

A unique feature of *Drosophila* is that the products of three closely linked genes, *reaper* (*rpr*), *head involution defective* (*Hid*), and *grim*, control essentially all developmental-related PCD in this organism (White, Grether et al. 1994). Rpr, Hid and Grim share a short region of homology at their N-termini, known as the RHG (Rpr, Hid, Grim) motif, and this region is both necessary and sufficient for binding to the *Drosophila* IAPs, DIAP1 and DIAP2. While the RHG (for Rpr, Hid and Grim) proteins were initially thought to contain pro-apoptotic activities that could be repressed by the fly IAPs, recent studies suggest that the RHG proteins act by repressing the caspase-inhibitory function of DIAP1 and DIAP2 (Wang, Hawkins et al. 1999; Goyal, McCall et al. 2000). *Drosophila* embryos that lack *rpr*, *hid* and *grim* expression due to deletion of the H99 interval, are essentially devoid of all PCD (White, Grether et al. 1994) (Fig.4). Studies from several laboratories have also shown that apoptosis due to DIAP1 loss is both DARK- and DRONC-dependent. This suggests that the loss of DIAP1 is sufficient to activate the apoptosome (Rodriguez, Chen et al. 2002; Zimmermann, Ricci et al. 2002). Taken together with the observation that Cytochrome c may not be a required cofactor for apoptosome assembly in the fly, these data suggest that caspase activation in *Drosophila* may be regulated primarily through neutralization of DIAP1-mediated repression of DARK-dependent caspase activation. Two possibilities have been proposed: either DARK/DRONC apoptosomes may have a propensity to assemble spontaneously, which is normally prevented through DIAP1-mediated inhibition of DRONC activity. It is also possible that in addition to neutralization of DIAP1 function, a second signal provided by neighbouring cells is required to promote DARK-dependent activation of DRONC (Zimmermann, Ricci et al. 2002).

Using an *in vitro* ubiquitination assay, Ryoo et al. provide convincing evidence that the binding of Rpr to DIAP1 activates the intrinsic E3 ubiquitin-ligase activities of this protein towards itself (Ryoo, Bergmann et al. 2002). Thus, Rpr-induced DIAP1 downregulation *in vivo* is almost certainly due to proteasome-mediated destruction of this protein as a consequence of polyubiquitination. Steller and colleagues identified a *Drosophila* mutant, *ubcD1/effete* (which encodes an E2 ubiquitin-conjugating enzyme) (White, Grether et al. 1994), that dominantly suppressed Rpr-induced cell death. UBCD1 was found to interact physically with DIAP1 and to promote Rpr-induced DIAP1 polyubiquitination *in vitro*. Morgue, another protein belonging to a class of enzymes known as ubiquitin conjugating enzyme variants (UEVs), can also interact with DIAP1 and probably acts in concert with UBCD1 to polyubiquitinate DIAP1 (Hays, Wickline et al. 2002) (Fig.4). Evidence that DIAP1 promotes the ubiquitination of DRONC have been provided by Meier and colleagues, however, it is not clear whether this targets DRONC for proteasome-mediated destruction (Wilson, Goyal et al. 2002).

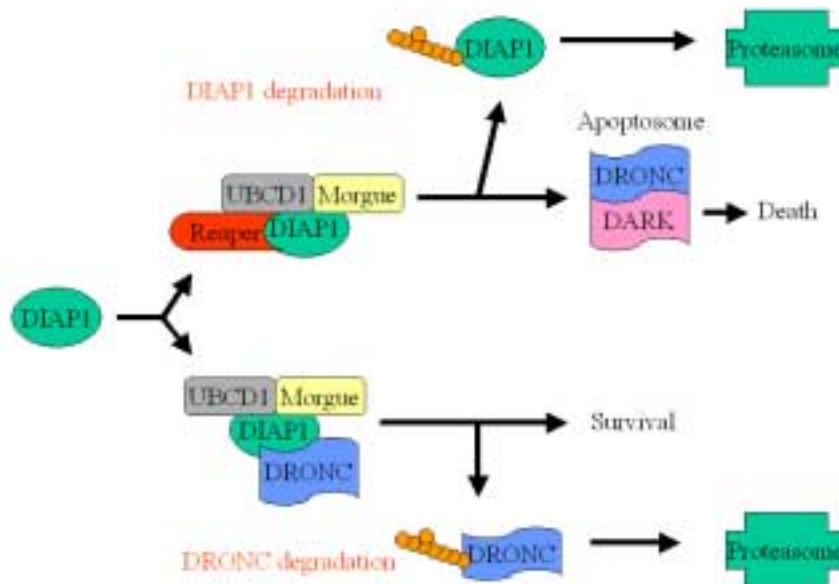


Fig.4: Regulation of DIAP1 stability by Reaper in the fly *D. melanogaster*. Autoubiquitination of DIAP1 is stimulated by the binding of Reaper (and possibly by Hid) in a reaction catalysed by an E2 conjugase (UBCD1), assisted by Morgue (E2-like). DIAP1 degradation results from the assembly of the DARK/DRONC apoptosome. When DARK is absent, the DIAP1/DRONK complex allows ubiquitination and degradation of DRONK.

4-Mammals

4.1-Extrinsic and intrinsic apoptosis pathways

Many more gene members have been described for the mammals Bcl-2 family, Caspase-family and BH3-only family, resulting in an increased complexity in the different interacting and cross-talking apoptotic pathways. Two general apoptosis pathways have been identified in mammalian cells: the extrinsic and the intrinsic apoptosis pathway. The extrinsic pathway is also called death receptor pathway. Upon ligation, death receptors such as CD95 and TNF-R1 bind to and oligomerize adaptor proteins and procaspases (Fig.1). FADD, which contains a DD (death domain, protein interaction domain), is recruited directly to CD95 and indirectly (through TRADD) to TNF-R1, resulting in the recruitment (through the DEDs: death effector domain, interaction) and autoactivation of Caspase-8 (Fig.7). The complex formed by CD95, FADD and Caspase-8 is called DISC (death inducing signal complex) and has been characterized biochemically in P. Kramer's group (Muzio, Chinnaiyan et al. 1996; Scaffidi, Fulda et al. 1998; Scaffidi, Kramer et al. 1999; Scaffidi, Schmitz et al. 1999). In an analogous manner, the adaptor protein RAIDD/CRADD, which contains a CARD (Caspase recruitment domain), can associate with TNF-R1 and promote activation of pro-Caspase-2 ((Ahmad, Srinivasula et al. 1997); (Duan and Dixit 1997), (Li, Bergeron et al. 1997)).

Based on their structure and role in cell death pathways, caspases can be divided into initiator and effector caspases. Effector caspases generally contain only a short prodomain and cleave diverse cellular substrates, whereas initiator caspases have a long prodomain and exert regulatory roles by cleaving and activating downstream effector caspases (Fig.6). Activation of initiator caspases is mediated by recruitment of these proteases to protein complexes, thereby increasing the local concentration of caspases. Two general types of interaction have been identified ((Martin, Siegel et al. 1998); (Muzio, Stockwell et al. 1998); (Srinivasula, Ahmad et al. 1998)). Pro-Caspase-8 and -10 each contain two tandem death effector domains (DEDs), while pro-Caspase-1, -2, -4, and -9 contain a caspase-recruitment domain (CARD). In each case, the procaspases bind to adaptor molecules containing similar domains, and they either directly aggregate or interact with other molecules. Although not related, CARDS and DEDs have a similar structure composed of amphipathic, antiparallel α -helices, which are also present in the death domain DD of death receptors, and in adaptor proteins like FADD (Fig.5).

Besides death receptor-mediated apoptosis, a related but different way of caspase activation exists that is triggered for instance by cytotoxic drugs or p53 and essentially controlled by mitochondria. This is the so-called intrinsic or mitochondrial pathway. In early phases of apoptosis, mitochondria release cytochrome c which, together with dATP or ATP, activates the adaptor protein Apaf1 ((Li, Nijhawan et al. 1997)). Apaf1 binds to the prodomain of pro-Caspase-9 via CARD-CARD interaction, while a different region of Apaf1 self-associates resulting in Caspase-9 activation (for more details see: *Proapoptotic proteins released from the mitochondria*).

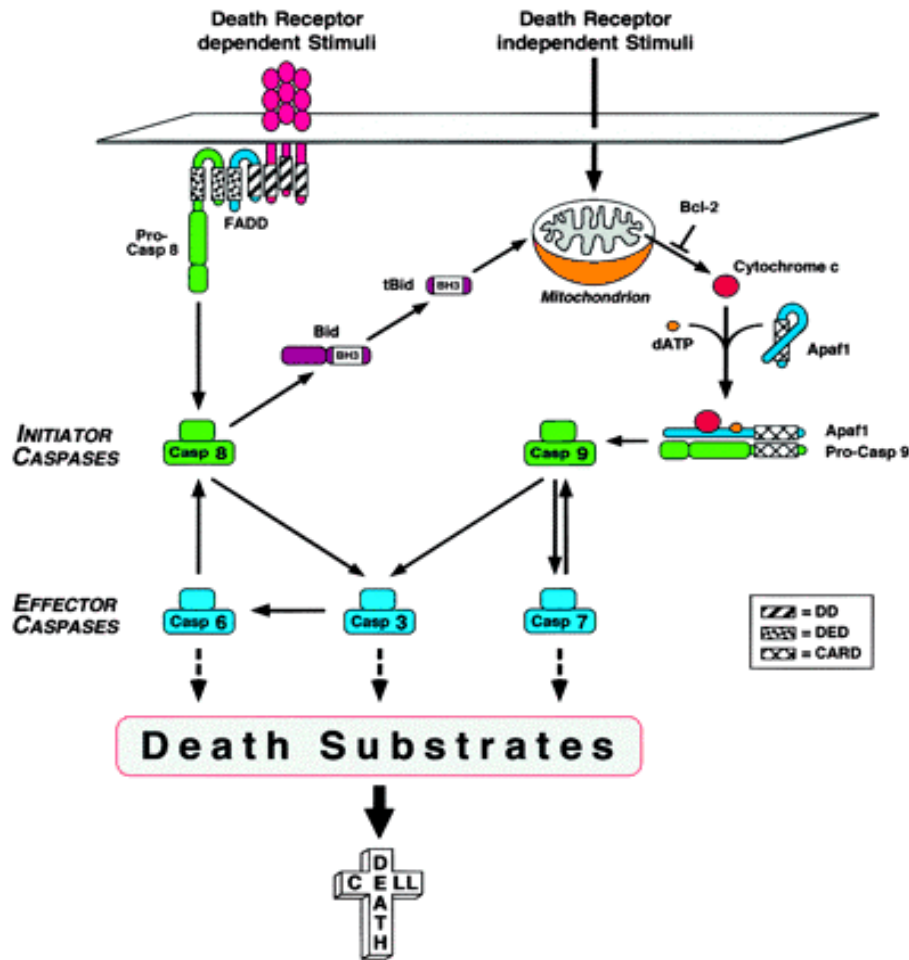


Fig.5: Role of the recruitment domains in the two principal signalling pathways of Apoptosis (*Immunity*, 1999 (Los, Wesselborg et al. 1999)).

One pathway (left) involves ligation of death receptors, resulting in the recruitment of the adaptor protein FADD through interaction between the death domains (DD) of both molecules. The death effector domain (DED) of FADD in turn recruits pro-Caspase-8, which is cleaved and activated at the receptor complex. Another pathway (right), which is triggered by many apoptotic stimuli, is initiated at the mitochondrion.

4.3- p53

One of the central molecule in the apoptotic pathways is p53. Various stress stimuli such as cytotoxic drugs, γ -irradiation, heat shock, hypoxia, osmotic shock, and DNA-damaging agents stabilize the tumor suppressor protein p53, which promotes cell-cycle arrest to enable DNA repair or apoptosis to eliminate defective cells (Levine 1997), (Herr and Debatin 2001). However, it is still largely unknown how p53 selects the pathways of G1 arrest or apoptosis. One hypothesis is that the proline-rich domain (residues 64-92) (Venot, Maratrat et al. 1998), (Walker and Levine 1996) and a recently identified transcriptional activation domain (residues 43-63) (Zhu, Zhou et al. 1998) are necessary for mediation of apoptosis because deletion of either of these

2 domains abolishes this activity. On the other hand, it has been shown that phosphorylation and acetylation play important roles for regulating biological activities of p53 (Giaccia and Kastan 1998), (Prives 1998). Although the functions of these modifications are not fully characterized, they are likely to regulate the binding of p53 with its negative regulator, Mdm2. Other negative regulatory mechanisms involve binding of JNK to p53, which mediates ubiquitination and proteolytic removal of p53 (Fuchs, Adler et al. 1998), and the retinoblastoma gene product (Rb), which prevents the apoptotic function of p53 (Haupt, Rowan et al. 1995), (Morgenbesser, Williams et al. 1994). Both p53 inhibitors, Rb and Mdm2, are cleaved by caspases during apoptosis (An and Dou 1996), (Erhardt, Tomaselli et al. 1997), (Janicke, Walker et al. 1996), suggesting a positive self-regulation of programmed cell death and close connection to key cell-cycle regulators. The transcriptional activating function of p53 is a major component of its biological effects. Many p53 target genes have been identified, and those functions have been characterized. Cell-cycle arrest that is dependent on p53 requires transactivation of p21^{Waf1}, GADD45, and cyclin G. Pro-apoptotic p53 target proteins include Bax, PIG genes, CD95, DR5 (a receptor for the death ligand TRAIL), IGF-BP3, Rpr (in *Drosophila*), Cdc42 (a Ras-like GTPase), Noxa (a Bcl-2 family protein), and p53AIP1 (Oda, Ohki et al. 2000), (Levine 1997), (Brodsky, Nordstrom et al. 2000), (Muller, Wilder et al. 1998), (Oda, Arakawa et al. 2000), (Owen-Schaub, Zhang et al. 1995), (Sheikh, Burns et al. 1998), (Thomas, Giesler et al. 2000), (Wu, Burns et al. 1999).

The mechanism by which p53-induces apoptosis is described involving the translocation of p53 to the mitochondria, thus activating the Apaf-1/caspase-9 pathway (Soengas, Alarcon et al. 1999; Sansome, Zaika et al. 2001; Mihara, Erster et al. 2003), death receptor signalling (Muller, Strand et al. 1997), (Bennett, Macdonald et al. 1998), (Munsch, Watanabe-Fukunaga et al. 2000), and cleavage of downstream caspases (Li, Dietz et al. 1999). For example, cells expressing mutant p53 fail to induce CD95 and are less sensitive to drug-induced apoptosis (Muller, Strand et al. 1997), (Newton and Strasser 2000). Independently of transcription, p53 may facilitate the transport of CD95 from Golgi stores to the membrane, leading to death receptor aggregation (Bennett, Macdonald et al. 1998). However, in some cases CD95 is not essential for p53-mediated apoptosis, and p53-dependent up-regulation of CD95 does not obligatory induce apoptosis (O'Connor, Harris et al. 2000). An additional route by which p53 may signal apoptosis is through the production of ROS, which influence the mitochondrial membrane potential without involving Cytochrome *c* release (Li, Dietz et al. 1999), (Johnson, Yu et al. 1996). In particular, the p53-inducible gene PIG3 shares homology with an NADPH-quinone oxidoreductase, which generates ROS. When overexpressed alone, PIG3 fails to initiate apoptosis, implying that other signals must be activated in parallel (Polyak, Xia et al. 1997). Recently, p53 itself was shown to cause caspase activation in cell-free extracts from E1A/ras-transformed, but not normal, fibroblasts by a mechanism independent of transcription or presence of Bax or Cytochrome *c* (Ding, McGill et al. 1998). Activation of caspases by p53 is mediated by the c-Myc oncogene (Ravi, Bedi et al. 2001). Apparently, p53 can transduce apoptotic signals through protein-protein interactions, thereby modulating p53-dependent caspase activation. Another mechanism by which p53 promotes apoptosis is through activation of the Ras-like GTPase Cdc42, which results in the

JNK1-induced phosphorylation of Bcl-2 (Thomas, Giesler et al. 2000). All these pathways and their components are explained in detail in the following chapters.

4.2- Caspases

Mammalian caspases comprise a group of at least fourteen members that can promote apoptosis ((Cohen 1997), (Nicholson and Thornberry 1997), (Cryns and Yuan 1998), (Schulze-Osthoff, Ferrari et al. 1998)).

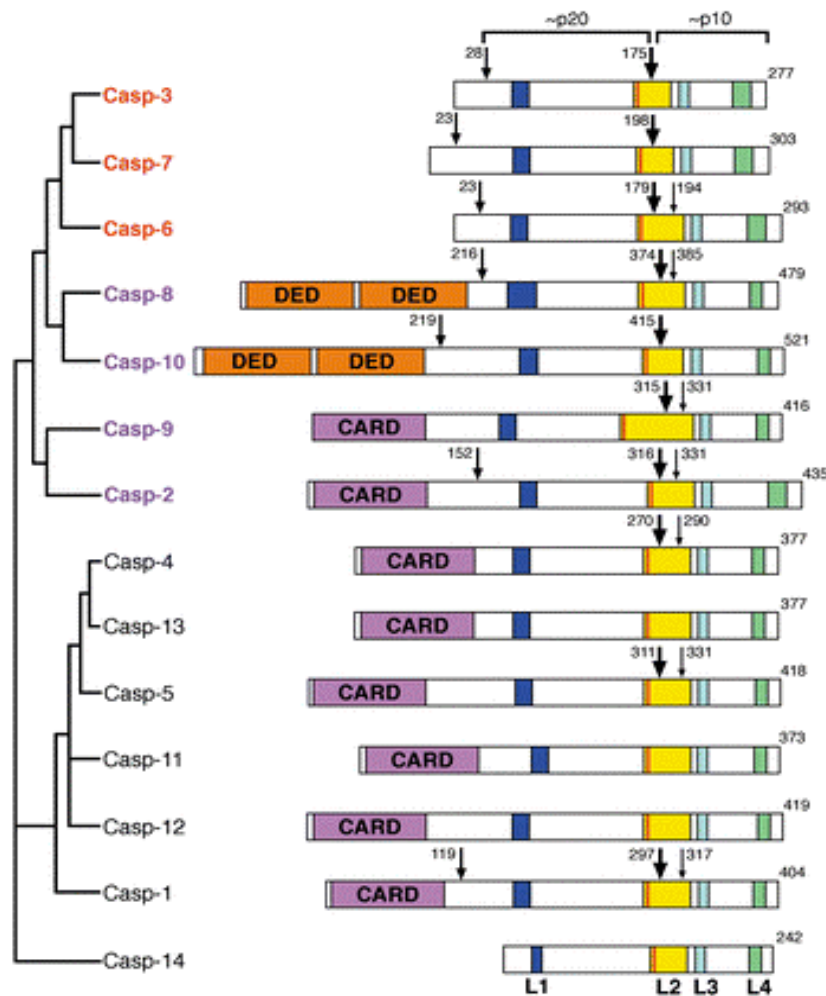


Fig.6: Schematic diagram of the mammalian caspases (*Molecular Cell*, 2002 (Shi 2002)).

Except Caspase-11 (mouse), -12 (mouse) and -13 (bovine), all listed caspases are of human origin. Their phylogenetic relationship (left) appears to correlate with their function in apoptosis or inflammation. Initially expressed as zymogens, pro-caspases are activated either by auto-catalytical cleavage induced by the forced proximity created in complexes like the DISC or the apoptosome (Caspase-8 or -9), either by cleavage by an other upstream active caspase (Caspase-3, -6 and -7). The initiator and effector caspases are labelled in purple and red, respectively. The position of the first activation cleavage (between the large and small subunits) is highlighted with a large arrow while additional sites of cleavage are represented by medium and small arrows.

Some caspases, like Caspase-1, generate mature proinflammatory cytokines and thereby regulate immune responses. Based on phylogenetic analysis and positional scanning studies of their peptide substrates, caspases are divided into three subfamilies: The ICE-like protease family includes Caspase-1, -4, -5, -13, and -14 as well as murine Caspase-11 and -12. The CED-3 subfamily includes Caspase-3, -6, -7, -8, -9, and -10, whereas the third subfamily consists of only one member, Caspase-2 (Fig.6). Within each subfamily, the peptide sequence preferences in the substrates are similar ((Thornberry, Rano et al. 1997); (Garcia-Calvo, Peterson et al. 1998)). Because at least in some cases different caspases can cleave the same substrates, this illustrates some degree of functional redundancy within the caspase family. Caspases exist as latent zymogens that contain an N-terminal prodomain followed by the region that forms two subunits with the catalytic domain. The core of the catalytic center is formed by the conserved pentapeptide sequence QACXG (the central cysteine has given its name to the caspase family). The proforms of caspases are activated by proteolytic cleavage at specific aspartate residues. Generally, an initial cleavage event separates the C-terminal short subunit from the rest of the molecule, allowing assembly of an active protease that autocatalytically cleaves off its prodomain. As deduced from the crystal structure of Caspase-1 and Caspase-3, the mature enzyme of all caspases is a heterotetrameric complex composed of two large subunits and two small subunits ((Walker, Talanian et al. 1994); (Wilson, Black et al. 1994); (Rotonda, Nicholson et al. 1996); (Mittl, Di Marco et al. 1997)). Once activated, some caspases can propagate activation of other family members and thus initiate a proteolytic cascade (Fig.1).

Although caspases are the essential components of many, if not all apoptotic pathways, their precise physiological role remains controversial. Indeed, Caspase-8 has been shown for example to be important for T-cell proliferation (Newton, Harris et al. 1998; Strasser and Newton 1999), (Hueber, Zornig et al. 2000), (Salmena, Lemmers et al. 2003) and caspases activation was shown to be crucial in monocytic differentiation of myeloid leukaemia cells (Pandey, Nakazawa et al. 2000). Very recent studies using gene targeting and transgene technologies have provided some answers to questions like “are caspases simply redundant or do they play specific roles in specific apoptotic pathways?” or “are the molecular components of apoptosis only implicated in apoptosis or are they important also for other pathways like proliferation and differentiation?”. These studies have shed new light on the distinctive role of individual caspases in cell death as well as in other unexpected biological processes. Caspase-1 was originally identified as interleukin 1 β -converting enzyme (ICE), the protease that cleaves the precursor of IL-1 β into the active cytokine ((Cerretti, Kozlosky et al. 1992)). More recently, Caspase-1 has been shown to further process the cytokine precursors of IL-16 and IL-18. Furthermore studies from knockout (KO) mice indicated that Caspase-1 mediates partially apoptosis induced by IFN- γ . In this scenario, a positive amplification loop between IFN- γ and Caspase-1 seems to exist. IFN- γ is able to induce Caspase-1 expression through activation of the STAT (signal transducer and activator of transcription) signaling pathway (Chin, Kitagawa et al. 1997).

Homozygous disruption of the mouse *caspase-8* gene was found to be lethal in utero ((Varfolomeev, Schuchmann et al. 1998)). However, whereas Caspase-3^{-/-} mice

exhibited profound brain defects, Caspase-8^{-/-} embryos presumably died from cardiac failure. Two salient features of Caspase-8 null mice were impaired heart muscle development and abdominal hemorrhage. Extensive erythrocytosis was present also in other organs such as liver and lung. The fact that the heart was hypotrophic rather than enlarged strongly suggests that Caspase-8 may be involved in the transmission of survival rather than death signals. This is supported by the fact that hematopoietic precursor cells from KO mice revealed a strongly impaired colony-forming activity. Disruption of Caspase-8 thus appears to result in a primary or secondary depletion of the hematopoietic precursor pool ((Varfolomeev, Schuchmann et al. 1998)). Embryonic fibroblasts deficient in Caspase-8 were completely resistant to apoptosis mediated by death receptors, such as CD95, TNF-R1 and DR3, whereas they retained sensitivity to a wide range of apoptotic stimuli including UV irradiation, ceramide, chemotherapeutic drugs, and infection with the cytopathic vesicular stomatitis virus. A Jurkat T cell line deficient in Caspase-8 is not only completely resistant to death receptor-induced apoptosis, but also partially resistant to cell death induced by UV irradiation, adriamycin, and etoposide ((Juo, Kuo et al. 1998)). Complementation of these cells with Caspase-8 restores apoptosis sensitivity. In addition, adenoviral E1A induces pro-Caspase-8 processing and apoptosis in cells deleted of FADD, indicating the existence of alternative activation pathways ((Nguyen, Branton et al. 1998)). Thus, these findings indicate that Caspase-8 plays a necessary and non-redundant role in apoptosis induction by death receptors.

FADD KO mice brought further insights to this rather complicated death-induction/proliferation mechanisms. Like Caspase-8 KO mice, gene targeting of the adaptor protein FADD results in a lethal phenotype with profound signs of cardiac failure and haemorrhage ((Yeh, Pompa et al. 1998)). Since FADD^{-/-} mice die in utero, T cell maturation has been analyzed in chimeric mice deficient for the recombination activating gene product RAG1, which activates rearrangement of immunoglobulin and T cell receptor genes ((Zhang, Cado et al. 1998)). T lymphocytes from FADD^{-/-} chimera were completely resistant to CD95-induced apoptosis. Thymocyte populations were apparently normal in newborn chimeras. As these mice age, their thymocytes, however, decreased to undetectable levels, although peripheral T cells were present. Thus, FADD^{-/-} mice seem to be inefficient in maintaining thymic cellularity possibly due to an intrinsic survival defect. Activation-induced proliferation was impaired in FADD^{-/-} T cells, despite normal production of IL-2. Thus, this suggests a rather unexpected connection between cell proliferation and apoptosis ((Zhang, Cado et al. 1998)). A growth-promoting activity of FADD is supported by the phenotype of transgenic mice expressing a dominant-negative FADD mutant (FADD-DN) under control of a T cell-specific promoter ((Newton, Harris et al. 1998), (Zornig, Hueber et al. 1998), (Walsh, Wen et al. 1998)). Expression of FADD-DN enhanced negative selection of self-reactive thymic lymphocytes. FADD-DN mice displayed increased apoptosis and reduced proliferation and clonogenic growth of mitogen-activated T cells. Interestingly, this impaired T cell proliferation was not observed in CD95-deficient mice or animals overexpressing the viral caspase inhibitor CrmA ((Smith, Strasser et al. 1996)). Thus, signaling through FADD does not lead exclusively to cell death, but under certain circumstances can promote cell survival and proliferation.

4.3- The central role of mitochondria

An early step in apoptosis is the mitochondrial release of Cytochrome *c* into the cytosol which, together with dATP or ATP, binds to the CED-4 homolog Apaf1. This event leads to a conformational change which induces oligomerization of the molecule in a heptamer resembling a wheel with seven spokes and a hub. In each of the seven Apaf-1 monomers, the CARD and part of the NBD (nucleotide binding domain) contribute to the hub, whereas the remainder of the Apaf-1 molecule (its carboxy-terminal moiety) forms a Y-shaped spoke (Acehan, Jiang et al. 2002), (Adams and Cory 2002). Subsequently, procaspase-9 binds to the complex through CARD/CARD interactions (Fig.5). This oligomerization of Apaf-1 and pro-caspase-9 forms the mega-complex called apoptosome. The mitochondrial (but not the death receptor) pathway is inhibited by Bcl-2. Antiapoptotic members of the Bcl-2 family may interfere with the relocalization of cytochrome *c* or with the binding of Cytochrome *c* to Apaf-1 (see: *How cells are protected from apoptosis*).

A comparison of the so far established KO mice allows the separation of distinct *in vivo* apoptotic pathways that are strikingly cell type-specific and differentially utilized in response to certain stimuli (Scaffidi, Fulda et al. 1998). First, the classical death receptor pathway that is Caspase-3- dependent but can be independent of Caspase-9 (in the so-called type I cells). The existence of this pathway is exemplified in activated T cells. Caspase-3 deficiency protects activated T cells from apoptosis induced by anti-CD95, TRAIL, and anti-CD3, whereas Caspase-9 deficiency has no obvious effect. Secondly, the classical mitochondrial pathway (intrinsic pathway or death receptor pathway in type II cells) that is dependent on Apaf-1 and Caspase-9. For example, embryonic stem cells from both Apaf1^{-/-} and Caspase-9^{-/-} mice are resistant to several apoptotic signals including UV and γ -irradiation or chemotherapeutic drugs (Fig.1).

Following activation of the initiator caspases Caspase-8 or Caspase-9, the two pathways, extrinsic and intrinsic, converge on the activation of the effector Caspase-3, -6, and -7, which finally cleave various “death” substrates. Because Caspase-8 cleaves Bid and generates a truncated, proapoptotic BH3-containing fragment (tBid) that induces cytochrome *c* release, both pathways (intrinsic and death receptor pathway in type II cells) cross-communicate. Caspase-8, in turn, can be also activated by Caspase-6 following Caspase-9 cleavage, thereby amplifying the apoptotic signal (Ghayur, Banerjee et al. 1997), (Gu, Kuida et al. 1997), (Fantuzzi, Puren et al. 1998). Here again, the generation of KO mice helped to unravel the role of Caspase-3 in apoptosis. Indeed, gene targeting of Caspase-3 generated mice with profound defects in apoptosis ((Kuida, Zheng et al. 1996); (Woo, Hakem et al. 1998)). The most pronounced effect is seen in the central nervous system, while no discernible abnormalities are found in embryonic heart, lung, liver, or kidney. Caspase-3 deficient

animals show massive hyperplasia and ectopic cell masses of the brain with a variety of disorganized cellular structures. Hence, Caspase-3 plays a critical role during morphogenetic cell death in the mouse brain. The central role of Caspase-3 for induction of apoptosis has been shown also in hepatocytes and thymocytes derived from KO mice ((Zheng, Schlosser et al. 1998)).

Although *caspase-3*^{-/-} hepatocytes or thymocytes were killed at a similar rate as control cells when cocultured with CD95 ligand-expressing 3T3 cells, wild-type cells displayed typical apoptotic features such as cytoplasmic blebbing and nuclear fragmentation within 6 hr, while none of these events was observed for Casp3^{-/-} cells. The cleavage of various caspase substrates implicated in apoptotic events, including gelsolin, fodrin, lamin B, and DFF/ICAD, an endonuclease inhibitor, was delayed or absent in the Caspase-3^{-/-} cells. Thus, the altered cleavage of these key substrates is likely to be responsible for the aberrant apoptotic phenotype in Caspase-3-deficient cells. Although Caspase-3 is highly expressed in cells of hematopoietic origin, lack of Caspase-3 did not affect immature T and B cell development ((Kuida, Zheng et al. 1996)). Gene-targeted mice contained fewer thymocytes, related to their overall smaller size. Surprisingly, thymocytes from Caspase-3^{-/-} and wild-type mice were equally sensitive to induction of apoptosis by anti-CD95, dexamethasone, ceramide, staurosporin, and γ -irradiation. Using Caspase-3^{-/-} lymphocytes from RAG1^{-/-} mice, it was shown that peripheral T cells were resistant to activation-induced cell death and apoptosis triggered by anti-CD3 and anti-CD95 ((Woo, Hakem et al. 1998)). The requirement for intact Caspase-3 appeared to dependent on the apoptotic stimulus. In embryonic stem cells, Caspase-3 was necessary for efficient apoptosis following UV irradiation, but not γ -irradiation or cytotoxic killing of target cells. Conversely, the same stimulus can show tissue specific consequences: TNF- α treatment induced normal levels of apoptosis in Caspase-3^{-/-} thymocytes, but defective apoptosis in oncogene-transformed fibroblasts ((Woo, Hakem et al. 1998)). Hence, the consequences of Caspase-3 deficiency appear to be remarkably context-dependent with apoptotic defects being both cell type and stimulus-specific.

C-Mitochondria and the apoptosome

The complex role of mitochondria in mammalian cell apoptosis came into focus when biochemical studies identified several mitochondrial proteins that are able to activate cellular apoptotic programs directly (Liu, Kim et al. 1996; Susin, Lorenzo et al. 1999; Du, Fang et al. 2000; Li, Luo et al. 2001). Normally, these proteins reside in the intermembrane space of mitochondria. In response to a variety of apoptotic stimuli, they are released to the cytosol and/or the nucleus. They promote apoptosis either by activating caspases and nucleases, or by neutralizing cytosolic inhibitors of this process (Fig.7).

1- The apoptosome pathway studied through knockout mice.

The two major components of the apoptosome are Apaf-1 and Caspase-9. Recently both Caspase-9 and Apaf-1 deficient mice have been generated (Cecconi et al., 1998; Hakem et al., 1998; Kuida et al., 1998; Yoshida et al., 1998). The phenotypes of these mice resembled Caspase-3 deficient animals in that they primarily developed brain malformations and overgrowth with excess cells in the central nervous system. The ectopic cell masses consisted of differentiated postmitotic cells that had escaped apoptosis. A nearly 10-fold reduction of TUNEL-positive cells was found in the brain of Caspase-9^{-/-} mice at E12.5. In situ immunostaining showed the absence of Caspase-3 activation in vivo. Both Caspase-9- and Apaf-1 deficient mice died at about day 16.5 of development. Unlike the brain, other non-neural organs such as heart, lung, and liver or spinal cord were unaffected and appeared remarkably normal. The similar phenotypes of Caspase-3, Caspase-9, and Apaf-1 deficient mice therefore indicate that the molecules act in line in a common apoptotic pathway. It is interesting to note that the phenotypes of the three KO mice are similar, but do not accurately mimic each other. Although disruption of either Caspase-9 or Caspase-3 caused brain malformations, the abnormalities were more severe in mice lacking Caspase-9. Caspase-3-deficient cells rarely exhibited an overt exencephaly abnormality. One possibility to account for this difference in severity of the malformation is that Caspase-9 may also activate other effector caspases such as Caspase-6 or Caspase-7. While Caspase-9^{-/-} mice exhibited a more pronounced phenotype than mice with a Caspase-3 null mutation, the most severe morphogenetic distortions were found in Apaf-1 KO mice (Cecconi et al., 1998; Yoshida et al., 1998). Apaf-1^{-/-} mice showed strong craniofacial abnormalities such as ossification defects, deficient midline fusion of the palatal shelves, as well as dramatic alterations of the lens and retina. Also cauliflower-like masses on the face present in Apaf-1^{-/-} mice were not observed in either Caspase-3 or Caspase-9 gene-targeted mice.

It has been suggested that Caspase-8 can physically interact with Apaf-1 in overexpression systems. A more detailed analysis, however, showed that Caspase-9 is the only Apaf-1 interacting protease in living cells (Slee et al., 1999). Thus, the idea that another caspase may substitute Caspase-9 is appealing, but currently none of the other known caspases appears to be activated by Apaf-1. Despite a normal development of the thymus, thymocytes from Caspase-9- and Apaf-1-deficient mice were resistant to a number of apoptotic stimuli. Nevertheless, both mouse models contained a comparable number to wild type mice of double-positive thymocytes, indicating that Apaf-1 and Caspase-9 are not involved in negative selection. In thymocytes and embryonic stem cells from KO mice, Cytochrome *c* was translocated into the cytosol, confirming that Apaf-1 and Caspase-9 act downstream of Cytochrome *c*. Thymocytes from *Apaf-1*^{-/-} mice were also resistant to a loss of mitochondrial transmembrane potential (Yoshida et al., 1998). It has been suggested that opening of the mitochondrial permeability pore and loss of transmembrane potential may be an initial event for Cytochrome *c* release and subsequent caspase activation (Kroemer, 1997). The results observed in KO mice, however, strongly suggest that the decrease of the transmembrane potential is downstream of Apaf-1-mediated caspase activation. This assumption is supported by the fact that in several apoptotic systems Cytochrome *c* release preceded mitochondrial membrane depolarization by many hours.

2-Proapoptotic proteins released from the mitochondria

2.1-Cytochrome *c*

Cytochrome *c*, a component of the mitochondrial electron transfer chain, initiates caspase activation when released from the mitochondria during apoptosis (Liu, Kim et al. 1996). Cytosolic Cytochrome *c* binds to Apaf-1, a protein containing a caspase recruitment domain (CARD), a nucleotide binding domain, and multiple WD-40 repeats (Zou, Henzel et al. 1997). The binding of Cytochrome *c* increases Apaf-1 affinity for dATP/ATP about 10 fold (X). The binding of nucleotide to the Apaf-1/Cytochrome *c* complex triggers its oligomerization to form the apoptosome, which subsequently recruits multiple Procaspase-9 molecules to the complex and facilitates their autoactivation. Only the caspase-9 bound to the apoptosome is able to efficiently cleave and activate downstream executioner caspases such as Casase-3 (Rodriguez and Lazebnik 1999). Murine embryos devoid of Cytochrome *c* die in utero by midgestation, but cell lines established from early *cytochrome c* null embryos are viable under conditions that compensate for defective oxidative phosphorylation. As compared to cell lines established from wild-type embryos, cells lacking Cytochrome *c* show reduced Caspase-3 activation and are resistant to the proapoptotic effects of UV irradiation, serum withdrawal, or staurosporine. In contrast, cells lacking Cytochrome *c* demonstrate increased sensitivity to cell death signals triggered by TNFalpha (Li, Li et al. 2000).

2.2-Smac/Diablo and Omi/HtrA2

Concurrent with Cytochrome *c*, smac/Diablo, a 25-kD mitochondrial protein, is released from mitochondria into cytosol during apoptosis (Du, Fang et al. 2000). Smac is a nuclear-encoded mitochondrial protein containing a 55-amino-acid mitochondrial targeting sequence at its N-terminus. This sequence is removed upon import into the mitochondria (Du, Fang et al. 2000). The four extra amino acids (at the N-terminus) of the mature Smac, Ala-Val-Pro-Ile (AVPI), bind to the BIR (baculovirus IAP (inhibitor of apoptosis protein) repeat) domain of IAPs (for details about IAPs see chapter 3.2) (Chai, Du et al. 2000) (Fig.7). The exposed N-terminal alanine of mature Smac is absolutely required for the binding of IAPs (Chai, Du et al. 2000; Liu, Sun et al. 2000; Wu, Chai et al. 2000). Because this alanine becomes exposed only when the signal peptide is cleaved after mitochondrial entry,

mitochondrial targeting becomes a critical step for Smac function. *smac*^{-/-} mice are viable, grow, and mature normally and they do not show any histological abnormalities (Okada, Suh et al. 2002). Although the cleavage *in vitro* of Procaspase-3 was inhibited in lysates of *smac*^{-/-} cells, all types of cultured *smac*^{-/-} cells tested responded normally to all apoptotic stimuli applied. There were also no detectable differences in Fas-mediated apoptosis in the liver *in vivo*. These results suggest that there may be a redundant molecule or molecules capable of compensating for a loss of Smac function (Okada, Suh et al. 2002). Such a molecule is Omi/HtrA2, a mammalian serine protease with high homology to bacterial HtrA chaperones. Omi/HtrA2 is localized in mitochondria and is released to the cytoplasm in response to apoptotic stimuli. Omi/HtrA2 induces cell death in a caspase-dependent manner by interacting with the inhibitor of apoptosis protein as well as in a caspase-independent manner that relies on its protease activity (Suzuki, Imai et al. 2001; Hegde, Srinivasula et al. 2002; Cilenti, Lee et al. 2003).

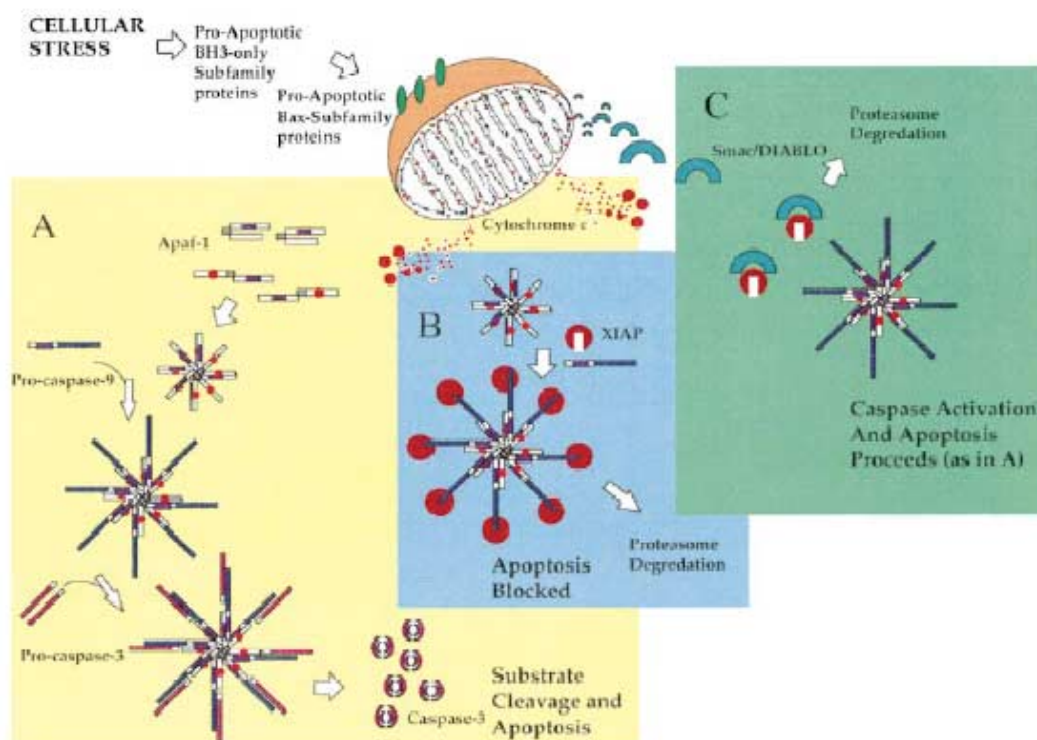


Fig.7: Smac inhibitory function (*Cell*, 2000 (Green 2000)).

A. Cytochrome *c* release and apoptosome formation. B. XIAP inhibits Caspase-9 activation by the apoptosome. C. Smac binds to XIAP and blocks its inhibitory activity, thereby promoting apoptosis.

In addition to the BIR3 domain of XIAP, Smac/Diablo has also been shown to form a stable complex with the BIR2 domain of XIAP (Chai, Shiozaki et al. 2001). The linker sequence immediately preceding the BIR2 domain is involved in XIAP-mediated binding and inhibition of Caspase-3 and Caspase-7 (Chai, Shiozaki et al. 2001) (Sun, Cai et al. 1999; Huang, Park et al. 2001; Riedl, Renatus et al. 2001). Smac/Diablo binds to the BIR2 domain and presumably disrupts its inhibition of

Caspase-3 and Caspase-7 by steric hindrance (Chai, Shiozaki et al. 2001). The ability of Smac/Diablo to counter the inhibition of apoptosis by IAPs at multiple levels provides a powerful way for mitochondria to ensure rapid execution of apoptosis. The direct competition and mutual exclusion between Smac and activated caspases suggest an interesting feedback system in cells (Fig.7 and 10).

In this regard, Omi resembles Smac/DIABLO. It also binds IAPs and as a result activates caspase-9 (Suzuki, Imai et al. 2001; Cilenti, Lee et al. 2003). Omi protein is synthesized as a precursor that is processed in the mitochondria to produce the mature protein. This processing exposes an internal tetrapeptide motif, AVPS, at the amino terminus (Martins 2002). Processing of the precursor Omi polypeptide is an intramolecular reaction and requires an intact protease domain. Omi can also induce apoptosis in a caspase-independent pathway that relies entirely on its ability to function as a serine protease (Hegde, Srinivasula et al. 2002).

2.3-Apoptosis-inducing factor (AIF)

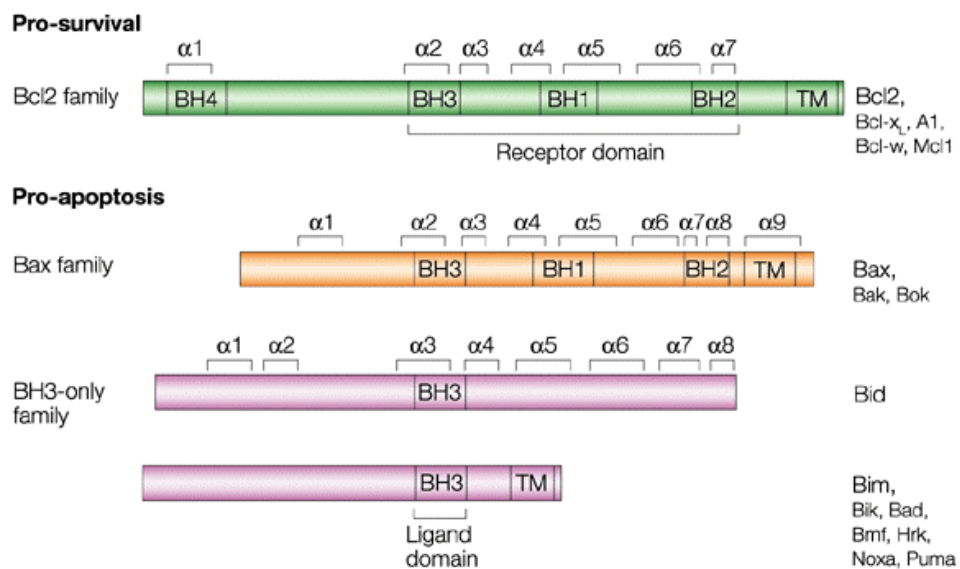
Apoptosis-inducing factor (AIF) is a 57-kD flavoprotein that resembles bacterial oxidoreductase and resides in the mitochondrial intermembrane space (Susin, Lorenzo et al. 1999). Upon induction of apoptosis, AIF translocates from the mitochondria to the nucleus and causes chromatin condensation and large-scale DNA fragmentation (Susin, Lorenzo et al. 1999). These effects are independent of caspases and the oxidoreductase activity of AIF (Miramar, Costantini et al. 2001). The mechanism by which AIF induces chromatin condensation and large-scale DNA fragmentation is not yet understood. Moreover AIF has not measurable DNase activity by itself, resulting in the possibility that AIF may work with another protein to cause such an effect (Susin, Lorenzo et al. 1999).

2.4-Endonuclease G

Endonuclease G (EndoG), a known 30-kD nuclease in the mitochondria, was purified recently from the supernatant of mouse mitochondria that was treated with Caspase-8-activated Bid (tBid), a condition that mimicked the initiation of cell death after activation of the cell surface death receptor CD95 (Li, Luo et al. 2001). EndoG is encoded by a nuclear gene, translated in the cytosol, and imported subsequently into the mitochondria. It has been described that Ca^{2+} -induces mitochondrial permeability transition and causes complete release of rat liver EndoG activity from its exclusive location within the mitochondrial intermembrane space (Davies, Hershman et al. 2003). Once released, EndoG is able to induce nucleosomal DNA fragmentation. EndoG activity is independent of caspase activation (Liu, Zou et al. 1997; Enari, Sakahira et al. 1998; Liu, Li et al. 1998; Li, Luo et al. 2001).

3-Induction of the mitochondria

The induction of the mitochondria usually takes place upon translocation of Bcl-2 family members to the mitochondria. Among them, the BH3-only family shares sequence homology with Bcl-2 only in the BH3 domain, an amphipathic helix required to interact with other Bcl-2 family members (Huang, Tschopp et al. 2000). At the mitochondria, they cause mitochondrial damage and release of apoptogenic proteins either by interacting with other members of the Bcl-2 family, or by relieving the inhibition exerted by anti-apoptotic Bcl-2 family members. In mammals, Bcl-2 has at least 20 relatives, all of which share at least one conserved Bcl-2 homology (BH) domain (Korsmeyer 1999) (Fig.8). The family includes four anti-apoptotic proteins: Bcl-x_L, Bcl-w, A1 (Wang, Guttridge et al. 1999) and Mcl1 (Leuenroth, Grutkoski et al. 2000), and two groups of proteins that promote cell death: Bax and Bak, and the BH3-only family.



Nature Reviews | Cancer

Fig.8: The three subfamilies of Bcl-2-related mammalian proteins (*Cancer Rev.*, 2002 (Cory and Adams 2002))

Moreover, the BH3-only family members are differently regulated. Some need proteolytic cleavage to be activated (Bid) (Li, Zhu et al. 1998), some are regulated through phosphorylation (Bad) (Wolf, Witte et al. 2001) or release from different cellular compartments (Bim, Bmf) (O'Connor, Strasser et al. 1998; Puthalakath, Huang et al. 1999) (Puthalakath, Villunger et al. 2001) (Fig.9), and some are transcriptionally regulated (Noxa, Puma) (Oda, Ohki et al. 2000; Nakano and Vousden 2001; Schuler, Maurer et al. 2003).

3.1-Cleavage of Bid

Bid is exclusively cytosolic in living cells. Upon activation of cell surface receptors like Fas/APO-1/CD95, TNFR1, DR-3, DR-4/TRAIL-R1 and DR-5/TRAIL-R2, Bid is cleaved by Caspase-8. The truncated Bid (tBid) translocates from cytosol to mitochondria and induces Cytochrome *c* release (Li, Zhu et al. 1998; Luo, Budihardjo et al. 1998). tBid targets mitochondria through its helices 4-6, the targeting specificity is provided by the binding to the mitochondria-specific lipid cardiolipin (Lutter, Fang et al. 2000). The targeting efficiency is dramatically enhanced by myristoylation at the N-terminal glycine residue of tBid that becomes exposed after Caspase-8 cleavage (Zha, Weiler et al. 2000) (Fig.1).

The ability to cleave and activate Bid may not be limited to Caspase-8. Other caspases, such as Caspase-3, as well as other proteases, like granzyme B and lysosomal proteases, have been shown to cleave and activate Bid (Li, Zhu et al. 1998; Heibei, Goping et al. 2000; Sutton, Davis et al. 2000; Alimonti, Shi et al. 2001; Stoka, Turk et al. 2001). Bid may therefore serve as a general integrator and amplifier for many apoptotic signals. Bid^{-/-} mice injected with an antibody directed against Fas that can activate the receptor, nearly all survive, whereas wild-type mice die from massive hepatocyte apoptosis and haemorrhagic necrosis. About half of the Bid-deficient animals have no apparent liver injury and show no evidence of activation of the effector Caspase-3 and -7, although the initiator Caspase-8 was activated. Other Bid-deficient mice survive with only moderate damage: all three caspases (-8, -3 and -7) are activated but their cell nuclei are intact and no mitochondrial Cytochrome *c* is released. In bid^{-/-} cultured cells treated with anti-Fas antibody (hepatocytes and thymocytes) or with TNF α (fibroblasts), mitochondrial dysfunction is delayed, Cytochrome *c* is not released, effector caspase activity is reduced and the cleavage of apoptosis substrates is altered. This loss-of-function model supports evidence that Bid is a critical substrate *in vivo* for signalling by death-receptor agonists, which mediates a mitochondrial amplification loop that is essential for apoptosis of certain cell types (Yin, Wang et al. 1999).

3.2-Phosphorylation of Bad

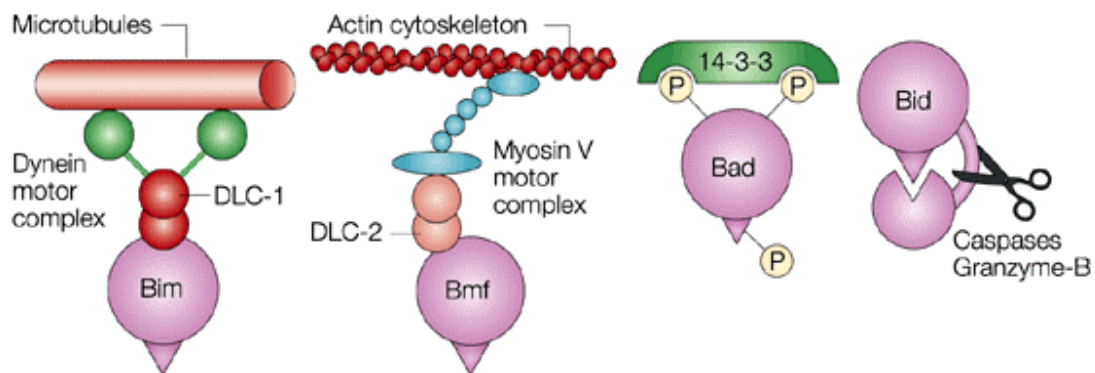
Bad, another BH3-only protein, is regulated primarily by phosphorylation and dephosphorylation. In the absence of survival signals, Bad is dephosphorylated. The BH3 domain of Bad binds to and inactivates the antiapoptotic members of the Bcl-2 family at the outer mitochondrial membrane, thereby promoting cell death. Conversely, in the presence of trophic factors, Akt a mitochondria-anchored protein kinase (del Peso, Gonzalez-Garcia et al. 1997) phosphorylate Bad, resulting in its binding to 14-3-3 proteins in the cytosol (Wolf, Witte et al. 2001). Several phosphatases, including calcineurin, protein phosphatase 1 α , and protein phosphatase 2A, have been shown to dephosphorylate Bad *in vitro* and to activate its pro-apoptotic activity (del Peso, Gonzalez-Garcia et al. 1997; Zundel and Giaccia 1998; Hinton and Welham 1999;

Scheid, Schubert et al. 1999; Datta, Katsov et al. 2000; Kuwahara, Saito et al. 2000; Springer, Azbill et al. 2000).

3.3-Dissociation of Bim and Bmf from the cytoskeleton

Bim and Bmf are further BH3-only proteins, which have been found to associate with cellular microtubule complexes by binding to dynein light chains (Fig.9). Early during apoptosis, Bim/LC8 dissociates from the microtubule complex (Puthalakath, Huang et al. 1999) and Bmf/LC2 dissociates from the actin cytoskeleton (Puthalakath, Villunger et al. 2001), and both translocate to the mitochondria. This dissociation seems to represent an independent starting point for apoptosis. Recombinant Bim alone is as efficient as tBid in releasing Cytochrome *c* and EndoG when incubated with mitochondria *in vitro*.

Mice lacking Bim show apoptosis defects in their immune system (Bouillet, Cory et al. 2001). Moreover, the abundance of Bim also seems to be critically regulated at the level of transcription during apoptosis (Biswas and Greene 2002). In healthy cells, Bmf is sequestered to myosin V motors by association with dynein light chain 2. Certain damage signals, such as loss of cell attachment (anoikis), unleash Bmf, allowing it to translocate and bind prosurvival Bcl-2 proteins (Puthalakath, Villunger et al. 2001).



Nature Reviews | Cancer

Fig.9: Diverse modes of post-translational regulation of BH3-only proteins (*Cancer Rev.*, 2002 (Cory and Adams 2002)).

In healthy cells, BH3-only proteins are held in check by a variety of strategies. Bim and Bmf are sequestered to the microtubules or cytoskeleton, respectively, via interaction with a dynein light chain (DLC). Phosphorylated Bad is bound by 14-3-3 scaffold proteins. Bid is synthesized as precursor, which requires proteolytic cleavage to be fully active.

3.4-The role of Bax and Bak

Once the BH3-only proteins reach the mitochondria, they need to cooperate with other mitochondrial proteins to induce the release of apoptogenic proteins. The proapoptotic members of the Bcl-2 family that contain BH1-BH3 but not BH4, such as Bax and Bak, are the likely mediators for the BH3-only proteins (Korsmeyer, Wei et al. 2000) (Fig.8). The important role of these proteins in apoptosis has been demonstrated dramatically in *bax* and *bak* double KO mice. MEF cells lacking both *bax* and *bak* are resistant to multiple apoptotic stimuli, including overexpression of the BH3-only proteins tBid, Bim and Bad (Wei, Zong et al. 2001). Concurrent with the translocation of the BH3-only proteins to the mitochondria, Bax and Bak undergo conformational changes and oligomerization, presumably induced by transient interaction with the BH3-only protein tBid (Korsmeyer, Wei et al. 2000; Nechushtan, Smith et al. 2001). The oligomerized Bax and Bak may form a pore big enough for the apoptogenic proteins to pass through or else destabilize the mitochondrial outer membrane through an unknown mechanism. So the common mechanism usually involves the inhibition of the Bcl-2/Bcl-X_L heterodimer by an activated BH3-only member, heterodimer that can inhibit Bax/Bak activity at the mitochondria (Hsu, Wolter et al. 1997; Lutter, Fang et al. 2000; Murphy, Ranganathan et al. 2000; Shimizu and Tsujimoto 2000; Wei, Zong et al. 2001; Thomenius, Wang et al. 2003).

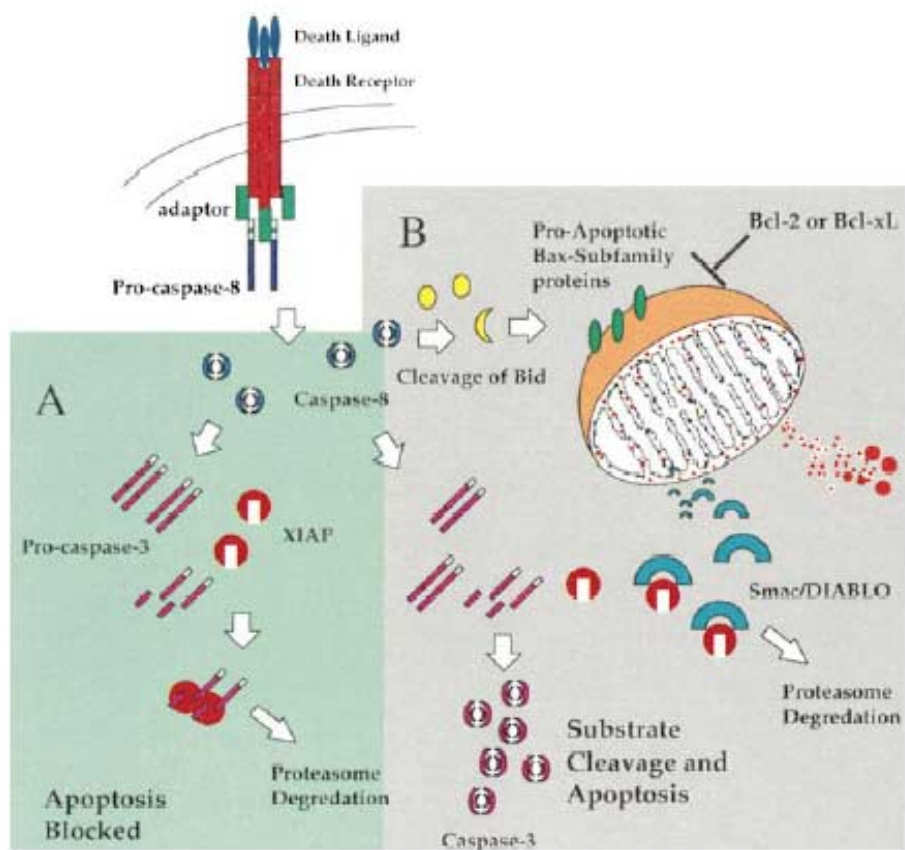


Fig.10: Bcl-2 family member activity and function during apoptosis (Cell, 2000 (Green 2000))

4-Apoptosis-inhibiting mechanisms

4.1-The Bcl-2 anti-apoptotic members

Bcl-2 and its closest homologues, Bcl-x_L and Bcl-w, inhibit apoptosis in response to many, but not all, cytotoxic insults (Chiou, Rao et al. 1994; Zha, Aime-Sempe et al. 1996; Furukawa, Estus et al. 1997; Badrichani, Stroka et al. 1999; Huang, Tschopp et al. 2000). Their hydrophobic carboxy-terminal domain helps to target them to the cytoplasmic face of three intracellular membranes: the outer mitochondrial membrane, the endoplasmic reticulum (ER) and the nuclear envelope (Akao, Otsuki et al. 1994; Thomenius, Wang et al. 2003). Bcl-2 is an intergral membrane protein, even in healthy cells (Janiak, Leber et al. 1994; Lee, Hoeflich et al. 1999), whereas Bcl-w and Bcl-x_L only become tightly associated with the membrane after a cytotoxic signal (Hsu, Wolter et al. 1997). This indicates an induced conformational change of these proteins. In bcl-2 deficient mice, extensive apoptosis occurs during abnormal nephrogenesis, and renal failure is found very quickly after birth (Gassler, Elger et al. 1998).

The less well studied proteins A1 and Mcl1 have a weaker survival activity and are more divergent in sequence, perhaps indicative of additional functions (Fujise, Zhang et al. 2000). The mechanism of their antiapoptotic activity is not yet absolutely clear, but it is generally acknowledged that they can form hetero-dimers with the proapoptotic members of Bcl-2 family and the BH3-only proteins, sequestering those and preventing their targeting to the mitochondria [Murphy, 2000 #199; Zha, 1996 #202; Priault, 1999 #200; Thomenius, 2003 #201].

Posttranslational modifications of Bcl-2 have also been proposed as regulatory mechanism of apoptosis. Phosphorylation of Bcl-2 has been reported, although it is still unclear whether phosphorylation is activating or inactivating the inhibitory function of this protein (May, Tyler et al. 1994; Haldar, Jena et al. 1995; Ito, Deng et al. 1997) and whether this is a general phenomenon since it appears to occur prominently in M-phase arrested cells (Ling, Tornos et al. 1998; Scatena, Stewart et al. 1998). More recently, Bcl-2 was reported to be a cleavage substrate for activated Caspase-3 with the carboxyl-terminal Bcl-2 cleavage product triggering apoptosis (Cheng, Kirsch et al. 1997).

Moreover, Bcl-XL was found to indirectly bind to Apaf-1 through a new protein called Aven, and disrupt the apoptosome formation (Chau, Cheng et al. 2000).

4.2-The IAPs

Another family of related proteins, the inhibitor of apoptosis proteins (IAPs), have been identified and described as caspases inhibitors (e.g. Caspase-9 and -3

(Deveraux, Takahashi et al. 1997; Roy, Deveraux et al. 1997)). IAPs contain at least one, but usually three, BIR (baculovirus IAP repeat) motifs that are capable of interacting with caspases and occluding their catalytic pockets (Hozak, Manji et al. 2000). Certain IAPs also possess C-terminal RING domains (Fig.11).

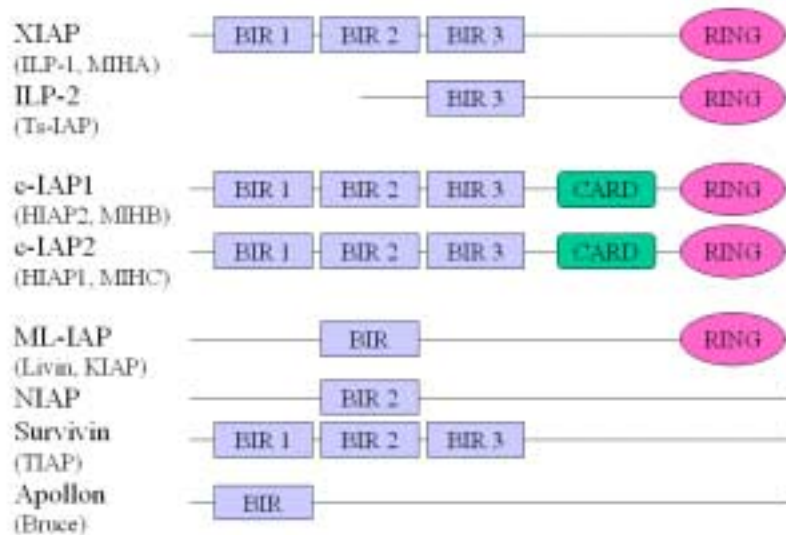


Fig.11: Mammalian IAPs/BIRPs.

Alternative designations are shown in brackets. The X-linked IAP (XIAP) is the best characterized member of this family. BIR, baculovirus IAP repeat; CARD, caspase-recruitment domain; ILP, IAP-like protein; MIHA, mammalian IAP homologue A; NAIP, neuronal apoptosis inhibitory protein.

Many proteins that contain the latter motif act as E3 ubiquitin ligases and can participate in reactions that culminate in the transfer of polyubiquitin chains to their target proteins (Hozak, Manji et al. 2000). Polyubiquitinated proteins are typically rapidly bound and destroyed by the proteasome. IAPs preferentially interact with active caspases, although evidence that they can promote polyubiquitination of the proteases *in vivo* has been lacking. However, numerous studies have shown that IAPs can impede caspase activity and delay the onset of apoptosis (Tran, Rak et al. 1999). Anti-apoptotic activity of IAPs can be relieved by competitive binding of Smac/Diablo when released from the mitochondria [Wu, 2000 #213] (see *Smac/Diablo and Omi/HtrA2*) (Fig.7 and 10).

4.3-Receptor-mediated survival pathway

Apoptosis can also be blocked by activation of survival receptors upon binding of the appropriate ligand. The best understood survival pathway is governed by the insulin-like growth factor 1 receptor (IGF-1R). Binding of IGF-1 to the receptor stimulates its tyrosine kinase activity, resulting in activation of the phosphatidyl

inositol 3' kinase (PI3 kinase) that in turn phosphorylates and activates protein kinase B (Pkb/Akt) (Kandel and Hay 1999). Pkb/Akt can inhibit the apoptotic pathway by its ability to phosphorylate the proapoptotic Bcl-2 family member Bad, thereby preventing the release of Cytochrome *c* and the activation of caspases (Lawlor and Alessi 2001) (see *Phosphorylation of Bad*).

D-Clinical implications of apoptotic pathways disruption

In the past years more and more diseases have been correlated to apoptotic dysfunction, like: cancer, AIDS, neurodegenerative disorders, meningitis, diabetes, transplant-rejection, etc.... Some models are developed in the following chapters as examples.

1-Cancer

Cancer is a widespread disease, causing about 20% of death in the developed world. Since decades, intense biomedical research has focused on the elucidation of the cause and etiology of this disease in pursuit of the development of more effective therapies. Due to mutations of certain genes, all cancer cells have escaped normal control mechanisms that restrain cell proliferation, and statistical analysis of epidemiological surveys suggest the necessity of 3 to 7 independent mutations for the formation of a malignant cancer cell (Hanahan and Weinberg 2000).

Mutations within several hundred of different genes have been linked to human cancer, indicating that possibly every cancer might carry its individual set of mutated genes. Most often, mutations that result in unrestrained proliferation affect either proto-oncogenes or tumour suppressor genes. Proto-oncogenes often act at many points along the pathway that stimulate cell proliferation, whereas the task of tumour suppressors are mainly confined to negatively regulating cell growth. Analyses of human cancer specimens revealed that mutations of tumour suppressor genes involved in apoptotic pathways are found in almost any kind of cancer, indicating that loss of the apoptotic function is a prerequisite for the development of cancer (Fig.12). Hence the therapeutic approaches that aim to re-establish the apoptotic pathway in cancer cells have gained immense interest, particularly because those therapies might achieve the complete elimination of cancer cells (Ehlert and Kubbutat 2001). Moreover, it is important to notice that until now, every cancer derived cell line studied is still able to undergo apoptosis by some kind of stimulus, even when some apoptotic pathways are blocked.

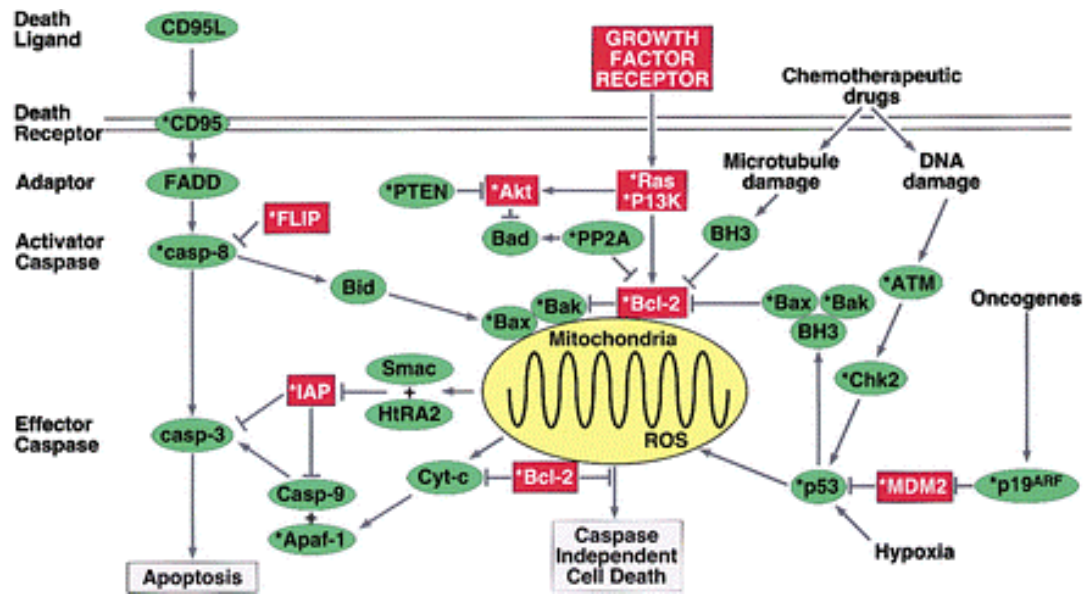
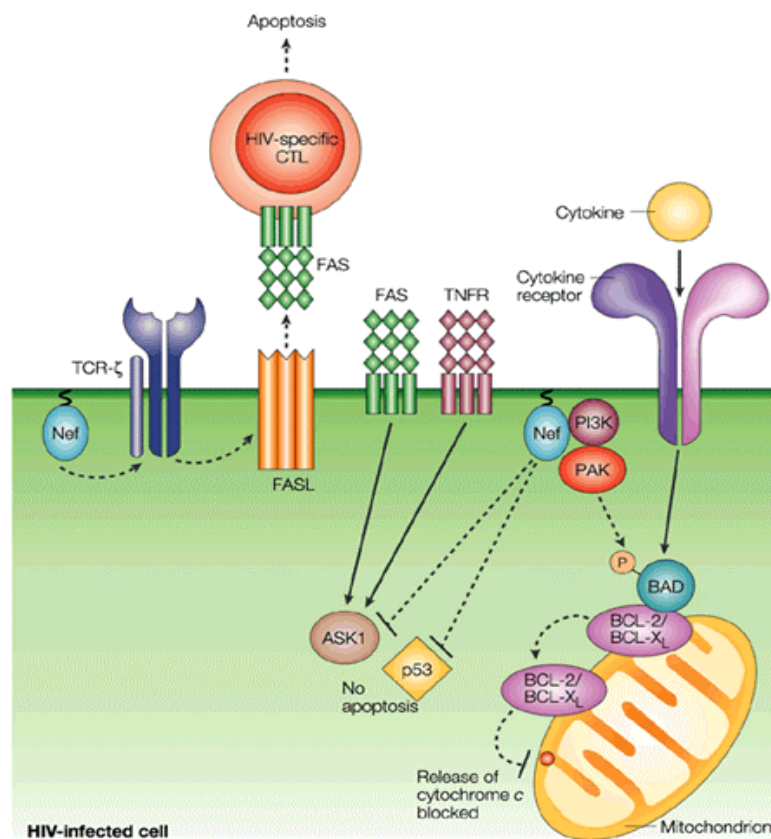


Fig.12: The integrated apoptotic pathways (*Cell*, 2002 (Johnstone, Ruefli et al. 2002))
 A schematic diagram showing some of the known components of the intrinsic and death receptor apoptotic programs that may modulate tumour development and therapy.

The cellular targets for different cytotoxic agents are diverse. Thus, anticancer drugs are classified as DNA-damaging agents (cyclophosphamide, cisplatin, doxorubicin), antimetabolites (methotrexate, 5-fluorouracil), mitotic inhibitors (vincristine), nucleotide analogues (6-mercaptopurine), or inhibitors of topoisomerase (etoposide). The common underlying mechanisms for chemotherapy-induced apoptosis might be damage to DNA, lipid components of cell membranes, and cellular proteins causing an imbalance of the cellular homeostasis commonly designated as cellular stress. The type and dose of stress within the cellular context appears to dictate the outcome of the cellular response, which is intimately converted to complex pathways mediating cell cycle control or cell death. Apoptosis seems to be induced if damage exceeds the capacity of repair mechanisms (Herr and Debatin 2001). Mutation of many genes involved in the regulation of apoptosis have been identified in human cancer, resulting in the development of novel therapeutic approaches such as activations of death receptors using recombinant ligand, inhibition of Bcl-2 expression by antisense reagents (Nicholson 2000) or induction of apoptosis through peptides derived from pro-apoptotic proteins like Smac or TRAIL (Yang, Mashima et al. 2003), (Fulda, Wick et al. 2002). Although based on different targets and delivery methods, all these approaches have the common goal to eliminate tumour cells by restoration of the apoptotic function (Ehlert and Kubbutat 2001).

2-AIDS

In vivo infection of lymphatic tissue with HIV is accompanied by enhanced apoptosis, which affects mainly bystander cells. Indeed, apoptosis is suspected (but it is not yet clear exactly how) to play an important role in the clinical development of the disease. It has been observed that 1/10⁵ cells dying by apoptosis are infected by HIV. This effect might result, at least in part, from the Nef-induced upregulation of expression of Fas-ligand on the surface of the infected cells, a phenomenon for which the mechanism remains unclear but seems to involve the T-cell receptor (TCR) pathway (Mueller, De Rosa et al. 2001) (Fig.13). FasL on the surface of HIV-infected cells could interact with Fas molecules displayed on the neighbouring cells, including virus-specific CTLs, thereby triggering their apoptosis. Furthermore, recent analyses of HIV-infected patients have shown that HIV-specific CTLs are more prone to Fas-mediated apoptosis than the HCMV-specific CTLs from the same individuals (Peterlin and Trono 2003).



Nature Reviews | Immunology

Fig.13: HIV and Apoptosis (*Nature Immunology*, 2003 (Peterlin and Trono 2003)). Nef protein can protect HIV-infected cells against HIV-specific CTLs killing.

Other Fas-related events contribute to HIV-induced cell death of bystander lymphocytes. For example, crosslinking of CD4 by the HIV envelope in the presence of the soluble Tat can induce the expression of FasL and the apoptosis of uninfected

cells. HIV can also protect its host cell from apoptosis through the Nef protein. Nef inactivates the proapoptotic Bad, thereby blocking the mitochondrial-induced apoptotic pathway (Wolf, Witte et al. 2001).

3-Neurodegenerative disorders

Neuronal cell death underlies the symptoms of many human neurological disorders, including Alzheimer's, Parkinson's and Huntington's diseases, stroke and amyotrophic lateral sclerosis (Mattson 2000). The identification of specific genetic and environmental factors responsible for these diseases has bolstered evidence for a shared pathway of neuronal death and neuronal apoptosis involving oxidative stress, perturbed calcium homeostasis, mitochondrial dysfunction and activation of caspases (Tab.1). For each of the disorders described below, analysis of post-mortem tissue from patients and studies of experimental animal and cell-culture models have implicated neuronal apoptosis. Studies of the pathogenic mechanisms of genetic mutations that cause early-onset autosomal dominant forms of Alzheimer's (Guenette and Tanzi 1999) and Huntington's (Sathasivam, Hobbs et al. 1999) diseases and amyotrophic lateral sclerosis (Borchelt, Wong et al. 1998) have been particularly valuable in implicating apoptosis in age-related neurological disorders.

Factors that may modulate apoptosis in neurodegenerative disorders

<i>Disorder</i>	<i>Genetic factors</i>	<i>Environmental factors</i>
Alzheimer's	APP, presenilin mutations, ApoE	Head trauma, low education, calorie intake
Parkinson's	A-synuclein, parkin mutations	Head trauma, toxins, calorie intake
Huntington's	Poly-CAG expansions in huntingtin	
ALS	Cu/Zn-SOD mutations	Toxins, autoimmune response
Stroke	Cadasil mutations	Smoking, dietary calories and fat

Table 1: Proteins implicated in neurodegenerative disorders.

In most of the neurodegenerative disorders considered here, the disease process lasts for years or even decades. It is therefore likely that, although individual neurons may be dysfunctional for extended periods in these disorders, they may die

rapidly once the apoptotic cascade is fully activated. In this view, the progressive deficits that occur in chronic neurodegenerative disorders are the result of progressive attrition of the individual neurons (Mattson 2000).

4-Autoimmune disease

The *in vivo* function of CD95/Fas was originally defined by the observation that the recessive mouse *lpr* mutation associated with systemic autoimmunity and lymphoproliferation is due to a transposable element insertion that inactivates Fas transcription. A similar mouse syndrome is caused by the recessive *gld* allele of the *FasL* gene (Watanabe-Fukunaga, Brannan et al. 1992). In humans, the autoimmune lymphoproliferative syndrome (ALPS), which has many similarities to *lpr*-associated disease in mice, is associated with dominant mutations in *Fas*, *FasL* or other genes in the Fas pathway (Siegel, Chan et al. 2000) (Fig. 14).

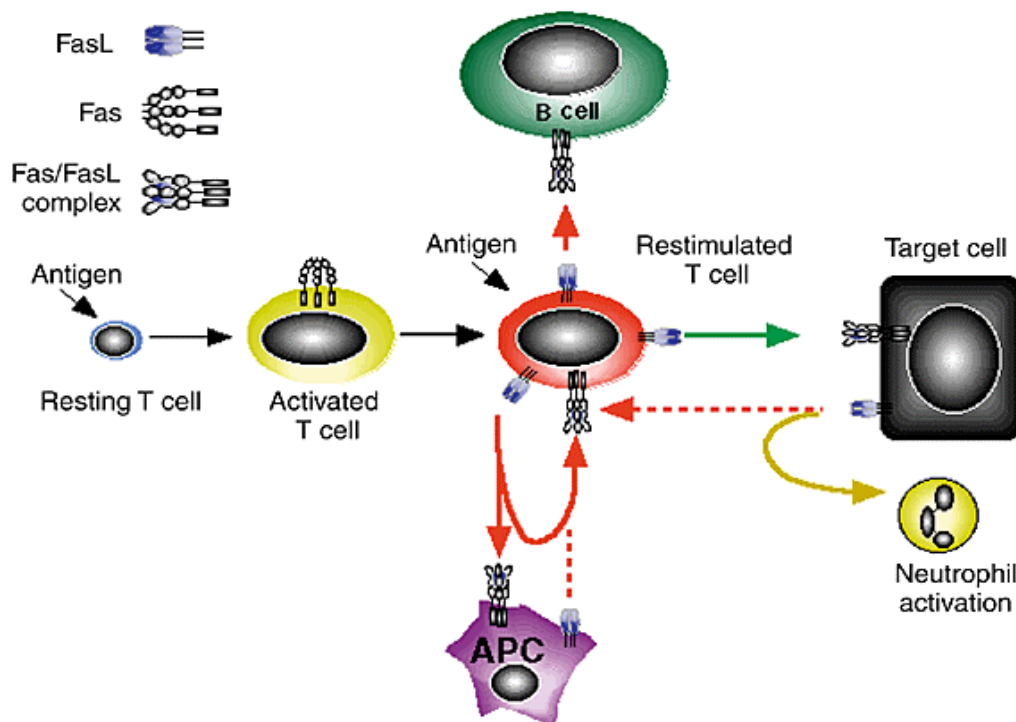


Fig. 14: Fas-FasL control of immune cell homeostasis (Nature Immunology, 2000 (Siegel, Chan et al. 2000))

Analysis of mutations from a large number of ALPS patients show that all dominantly interfering Fas mutants harbor mutations within the PLAD domain (preligand assembly domain), whereas not all encode the ligand-binding CRD2 region. Thus, preassociation is critical for the dominant-interfering effect of these mutations (Fisher, Rosenberg et al. 1995). Moreover, this paper suggests that CD95 might be “preassembled” in trimers and that the CD95L induces a conformational change rather than oligomerization.

E-The goal of the project

The previous chapter has made it clear that most of human diseases and disorders are related to the apoptotic pathway dysfunction. Unrevealing and understanding the complex crosstalks that take place during this process, as well as determining all the players involved in these multiple pathways leading to program cell death, has become an urgency, since it was clear that this could lead to more specific, more potent and less toxic clinical applications. The aim of this work was to identify new anti-apoptotic proteins and to understand their mechanistic function. Moreover, it is clear that the mitochondria play a central role in initiating, activating and amplifying nearly all apoptotic pathways. It therefore seems relevant to investigate all the blocking check-points of apoptosis downstream of mitochondria induction.

Because yeast systems are generally used and intensively optimised (Jurgensmeier, Krajewski et al. 1997; Xu and Reed 1998), I decided to perform a yeast survival screen to look for “anti-apoptotic proteins inhibiting downstream of Cytochrome *c* release”. Therefore, I used a cDNA library constructed from a pool of breast tumours (in order to increase the possible expression of anti-apoptotic proteins), to transform an HC4 *S. pombe* strain constructed by myself. This HC4 strain expresses the CED4 (*C. elegans* homologue of Apaf-1) under the control of the inducible promoter *nmt-1*. As CED4 (but not Apaf-1) can efficiently kill yeast *S. pombe* cells (James, Gschmeissner et al. 1997), I reasoned that this HC4 strain would be a good model to find new anti-apoptotic proteins capable of inhibiting CED4 and subsequently Apaf-1 induced apoptosis in yeast cells as well as in mammalian cells.

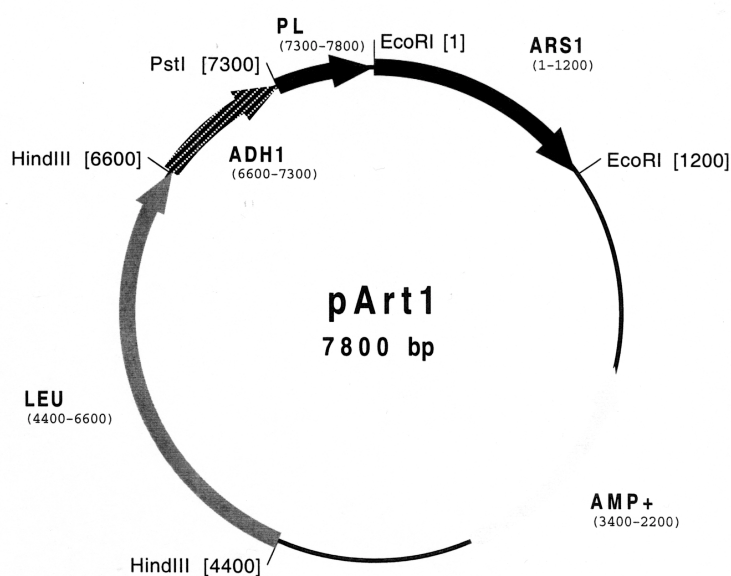
II-Material and methods

A-The yeast survival screen

1-cDNA libraries used for the yeast survival screen

1.1- 1 Human mammary carcinoma cDNA-library cloned into the yeast expression vector pART1b, without start codon provided by a linker.

The library was prepared in collaboration with *PROMEGA* and cloned into the pART 1b vector (pART 1 with an additional XhoI-site in the SmaI-site)



Pst I Sal I Bam HI Xho I

Multiple cloning site: gaa ttg ctg cag gtc gac tct aga gga tcc ccc ctc gag gcc tcg

The pART1 vector was kindly provided by Dr. Paul Nurse (ICRF, London) and modified further by *PROMEGA*.

5' : **PstI**-Adapter:

5'- g ggg cac gag-3'

3'- ac gtc ccc gtg ctc-5'

3' : poly(dT)-**XhoI**-linker:

5'-gag aga gag aga gag aga gaa cta gtc **agc agt** ttt ttt ttt ttt tt-3'

cDNA Size Fractionation: >0.5 kB

Recombination frequency (representing the percentage of plasmids containing a cDNA insert) : >50%.

Average Insert Size : 0.8 kB

Purified plasmid DNA containing the cDNA cloned into pART1b: 85µg/ml .

1.2- Human mammary carcinoma cDNA-library 2 cloned into the yeast expression vector pART1b, with a start codon provided by a linker.

The library was prepared in collaboration with *PROMEGA* and cloned into the pART 1b vector (pART 1 with an additional XhoI-site in the SmaI-site)

5' : PstI-ATG-HA-Adapter:

5'- **g** aaa **atg** gcc tac ccc tac gac gtg ccc gac tac gcc tcc ctc gga tcc-3'

3'- **ac gtc** ttt tac cgg atg ggg atg ctg cac ggg ctg atg cgg agg gag cct agg-5'

3' : poly(dT)-XhoI-linker:

5'-gag aga gag aga gag aga gaa cta **gtc tgc agt** ttt ttt ttt ttt tt-3'

cDNA Size Fractionation: >0.5 kB

Recombination frequency (representing the percentage of plasmids containing a cDNA insert) : >40%.

Average Insert Size : 0.75 kB

Purified plasmid DNA containing the cDNA cloned into pART1b: 400µg/ml .

2-Yeast transformation

150 ml of yeast culture in EMM medium (*Bio 101*) plus appropriate supplements (leucine, uracil, adenine (all *Bio 101*), thiamine (*Sigma*)) were grown to a density of 1×10^7 cells/ml ($O.D._{600} = 0.5$). Yeast cells were washed twice with water (centrifugation at 1,000 g for 5 min) and resuspended in 1.5 ml fresh 1xTE/1xLiAc (0.1 M) yielding competent cells. 100 ng plasmid DNA (yeast expression construct with appropriate selection marker) were mixed with 0.1 mg denaturated herring sperm DNA (*Bio 101*) and 100 µl competent yeast cell suspension. 600 µl 40% PEG 8000 (*Sigma*)/LiAc (0.1 M) were added and the mixture was vortexed for 10 seconds. The cells were incubated at 30°C for 30 minutes with mild shaking, then after adding 70 µl DMSO the suspension was heat shocked for 15 minutes at 42°C. Afterwards, yeast cells were chilled for 2 minutes on ice, washed, resuspended in 100 µl TE and plated on EMMA agar plates (*Bio 101*) containing appropriate supplements.

3-Buffers and solutions

0.1M Lithium acetate: 10.2 g in 1 L, pH 4.9

Tris/EDTA (TE): 200 mM Tris-base, 20 mM EDTA, ddH₂O.

B-Basic molecular biology

1-Mini-Prep.

1.1-QIAGEN column (according to manufacturer's protocol)

1.2-Alkaline Lysis Method.

1.5 ml of saturated overnight bacteria culture in a 1.5 ml Eppendorf reaction tube ("Eppi") was centrifuged 20sec at maximal speed in bevel centrifuge at 13,000 rpm. The supernatant was removed, and the pellet was resuspended in 100 µl GTE and incubated at room temperature for 5min. Then 200 µl of freshly prepared 0.2M NaOH/1% SDS were added and the mixture was shaken by inverting the tube. Then the mixture was incubate on ice for 5min. Add 150 µl of Potassium Acetate, vortex and incubated on ice 5min, spin 3min at maximal speed and the supernatant transfered to a fresh tube. 800 µl of 95% Ethanol were added and the mixture was incubated 2 min at room temperature. Then the mixture was spin 1min to pellet the plasmids and RNA, the supernatant was remove and the pellet washed with 600 µl of 70% Ethanol. Then the pellet was air-dried and resuspended it in 30-50 µl of water (or TE buffer) with 3 µl RNase (10 mg/ml).

1.3-Buffers and solutions

Glucose/Tris/EDTA pH 8.0 (GTE): 50 mM glucose, 25 mM Tris-Cl pH 8.0, 10 mM EDTA pH 8.0. Autoclave and store at 4°C.

Potassium acetate, 5 M, pH 4.8: 29.5 ml glacial acetic acid, KOH pellets to pH 4.8, H₂O to 100 ml.

2-Maxi-Prep.

2.1-QIAGEN column (according to manufacturer's protocol).

2.2-Lithium Chloride Method.

250 ml of saturated overnight bacteria culture were centrifuged at 5,000 rpm and 4°C for 20 min in sterile polypropylene 500 ml Beckman bottle in a J2-21 centrifuge (*Beckman*) equipped with an JA-10 rotor (*Beckman*). The pellet was resuspended in 10 ml GTE (0°C), add Lysosyme (*Roth*) and left 10 min on ice. 20 ml of freshly prepared 0.2 N NaOH/1%SDS were added, the tubes were gently inverted 3-6 times and left 10 min on ice. Then 15 ml of 5 M KO Ac, pH 4.8 was added, and the mixture was shaken gently and left 10 min on ice. It was then centrifuged 15 min at 5,000 rpm, 4°C and the supernatant was filtered through a tissue (or "Falten filter") in a 50 ml Falcon. 20 ml Isopropanol were added and the mixture was left 15 min at room temperature. It was then spin 10 min at 5,000 rpm. The pellet was resuspended in 4-ml water and 4 ml of 5 M LiCl were added to the mixture that was then left on ice 30 min at least. Then the mixture was spin 5 min at 5,000 rpm, at 4°C and the supernatant was transferred into a fresh 50 ml falcon. 18 ml 95% ethanol were added and the mixture was left 1 hour at -20°C. Then it was spin 15 min at 5,000 rpm, at 4°C, the pellet was resuspend in 0.5 ml TE pH 8.0 and transferred to a 1.5 ml Eppendorf reaction tube. 10 µl (10 mg/ml) RNase were added and the mixture was incubated at 56°C for 30 min, then 10 µl (10 mg/ml) proteinase K were added and the mixture was incubate at 37°C for 30 min. The DNA was extracted with an equal volume of 1: 1 Phenol-Chloroform and a centrifugation step of 2 min at 13,000g. The supernatant was transferred to a fresh tube and the procedure was repeated 2 times (until the protein interface has disappeared). 1.0 ml 95% Ethanol was added, the mixture was shaken and spin 10 min at maximal speed. Finally, the pellet was washed with 70% ethanol and resuspended in 200 µl TE pH8.0.

3-Mega-Prep for cDNA Library amplification (QIAGEN column).

4-DNA digestions, and DNA ligations

4.1- DNA digestion

In 20 µl total volume 1 µg DNA, 2 µl restriction enzyme (40 units), 2 µl reaction buffer 10x and if necessary 2 µl BSA 10x (*New England BioLabs*) were added. The mixture was incubated 1-2 hours at 37°C (overnight when a PCR insert was prepared for ligation).

4.2- DNA Phenol-extraction and DNA precipitation

To the DNA sample the same volume phenol/chlorophorm (1:1) was added. It was then vortexed and spin down 2 minutes at 13,000 rpm in microfuge. The water upper phase was transferred into a fresh 1.5 ml Eppendorf tube and 2x volume of 100% ethanol and 2 μ l 5M NaCl (end concentration is about 30 μ M) was added. The mixture was vortexed and kept 30 minutes at -20°C before spinning 20 minutes at 13,000 rpm in microfuge. The pellet was washed with 70% ethanol and air-dried. Then it was resuspended in an appropriate volume of H_2O . If the DNA sample was a cloning vector that needed dephosphorylation, it was resuspended in 88 μ l H_2O .

4.3- 3'-OH DNA dephosphorylation

To the 88 μ l DNA sample, 10 μ l 10x phosphatase buffer and 2 μ l Phosphatase Alkaline (CIP) were added. It was then incubated 1h at 37°C .

4.4- Gel extraction

DNA samples were loaded on 1% agarose gel and after migration, DNA samples were cut out of the gel with a scalpel (minimal amount of agarose) and the extraction was performed conforming to QIAGEN-gel extraction kit (*QIAGEN*), according to the manufacturer's protocol.

4.5- DNA ligation

In 10 μ l of total volume the cloning vector with digested DNA insert (ratio 1:3), 1 μ l 10x ligation buffer and 1 μ l ligase (400 unit) (*New England BioLabs*) were mixed, digested and dephosphorylated. The mixture was incubated overnight at 16°C and 2-4 μ l of the ligation mix were used for transformation of competent bacteria.

5-Bacterial transformation

5.1-Calcium chloride transformation

5.1.1-Preparation of calcium chloride competent cells.

One vial of frozen glycerol stock of the appropriate strain of *E. coli* (e.g. DH5 α *) was thawed and added to an Erlenmeyer flask containing 50 ml of pre-warmed LB medium, and incubated at 37°C with shaking at 250 rpm overnight. Then bacterial cells were diluted in LB medium to O.D₆₀₀ 0.2 and grown to O.D₆₀₀ 0.5-0.6 (about 1/2 hour). Then cells were transferred to a sterile polypropylene 500 ml Beckman bottle in a J2-21 centrifuge (*Beckman*) equipped with an JA-10 rotor (*Beckman*), and collected the cells by centrifugation at 3,000 rpm (1,600 g) for 8 minutes at 4° C in a J2-21 centrifuge (*Beckman*) equipped with an JA-10 rotor. After centrifugation, the supernatant was decanted and resuspended the cell pellet in one-half volume (250 ml) of cold, sterile 50 mM calcium chloride, incubated in an ice-water bath for 20 minutes, and centrifuged as before. The supernatant was decanted and the cell pellet was gently resuspended in one-tenth volume (25 ml) of cold, sterile 50 mM calcium chloride to yield the final competent cell suspension.

For stocks, 1 ml of the competent cell suspension was transferred to sterile Eppendorf 1.5 ml tubes. 300 μ l of sterile glycerol were added to the 1 ml aliquots of the final competent cell suspension prepared above, giving a final concentration of 23% glycerol. The competent cells were stored at -80°C indefinitely.

*DH5 α : F' 80dlacZ(lacZYA-argF)U169 deoR recA1 endA1 hsdR17(rK-, mK+) phoA supE44 - thi-1 gyrA96 r (*Biocompar*).

5.1.3-Transformation of competent bacteria with plasmid DNA.

To use competent cells for transformation, one stock vial was thawed on ice. Plasmid DNA was added and the mixture was incubated for 1/2 hour. Then it was heat shocked at 42°C for 90 seconds, 500 μ l of LB were added and the mix was incubated for 1 hour at 37°C with gentle shaking before spreading on plates with adequate selective LB-agarose medium.

5.2-Bacteria transformation by electroporation.

5.2.1- Preparation of electrocompetent Cells.

KC8* or BL21** cells were grown overnight at 37 °C while shaking with 250 rpm in LB-medium. Bacteria were diluted to O.D₆₀₀ 0.2 and grown to an O.D₆₀₀ of 0.5

(which typically required 1 hour of shaking at 250 rpm at 37 °C). The 1 litre of cells was distributed into four sterile polypropylene 500 ml Beckman bottle in a J2-21 centrifuge (*Beckman*) equipped with an JA-10 rotor (*Beckman*) and centrifuged at 5,000 rpm (4,500 g) at 4 °C for 10 minutes. Each pellet was resuspended in 100 ml of ice cold sterile double distilled water and combined into two Sorval centrifuge bottles (i.e each bottle then will contain 200 ml of resuspended pellet). The mixture was centrifuged at 5,000 rpm at 4 °C for 10 minutes in the JA-10 (*Beckman*) rotor and the pellets resuspended each in 100 ml of ice cold sterile double distilled water and then combined pellets into one Beckman centrifuge bottle and centrifuged at 5,000 rpm at 4 °C for 10 minutes in the JA-10 (*Beckman*) rotor once more. (Note: The purpose of all these centrifugation/resuspension/centrifugation steps is to insure that the cells are essentially "salt-free" as salt causes arching during the electroporation step). The pellet was resuspended in 100 ml of 10% ice cold sterile glycerol, centrifuged as above, and finally the pellet was resuspended in about the same volume of 10% ice cold sterile glycerol to give salt-free, concentrated electrocompetent cells. 40 µl of these electrocompetent cells were aliquoted into small snap cap tubes and immediately frozen by placing in crushed dry ice and then store at -80°C until needed.

* KC8 genotype: *hsdR*, *leuB600*, *trpC9830*, *pyrF::Tn5*, *hisB463*, *lacDX74*, *strA*, *galU,K*. Due to the *Tn5* transposon, KC8 is kanamycin resistant; in addition, it does not provide alpha-complementation of the beta-galactosidase gene (*Clontech*).

** BL21 : *hsdR*, *leuB600*, *trpC9830*, *pyr::Tn5*, *hisB463*, *lacDeltaX74*, *strA*, *galU*, *galK* Note: *Tn5* confers *kanr* Carries the *trpC*, *leuB*, and *hisB* mutations for complementation to yeast *TRP1*, *LEU2*, and *HIS3* wild-type genes, respectively. For selectively rescuing either the AD or DNA-BD vector from yeast after a GAL4 or LexA two-hybrid library screening. (*Amersham*).

5.2.2-Electroporation Protocol

The electrocompetent bacteria were thawed on ice for about one minute. 50-100 ng of the plasmid or 1-2 µl of the DNA ligation mix was added to the bacterial cells. 40 µl of the mix was transferred into Bio-Rad electroporation cuvettes (0.2 cm wide). The Bio-Rad Gene Pulser™ was turned on and the voltage set on 1.5 kV and capacity on 25 µF. After electroporation, the cells were immediately resuspended in 1 ml of SOC and transferred into an Eppendorf 1.5 ml tube. The cells were then incubated at 37 °C for 30 minutes with 250 rpm in a Thermomixer compact (*Eppendorf*). Finally cells were spin in a microfuge at 13,000 rpm for 20 seconds, resuspended in 200 µl fresh LB and plated on appropriate LB-agarose selective medium.

5.2.3-Buffers and solutions

SOC medium: 0.5% yeast extract, 2% tryptone (*Roth*), 10 mM NaCl, 2.5 mM KCl, 10 mM MgCl₂, 10 mM MgSO₄, 20 mM glucose.

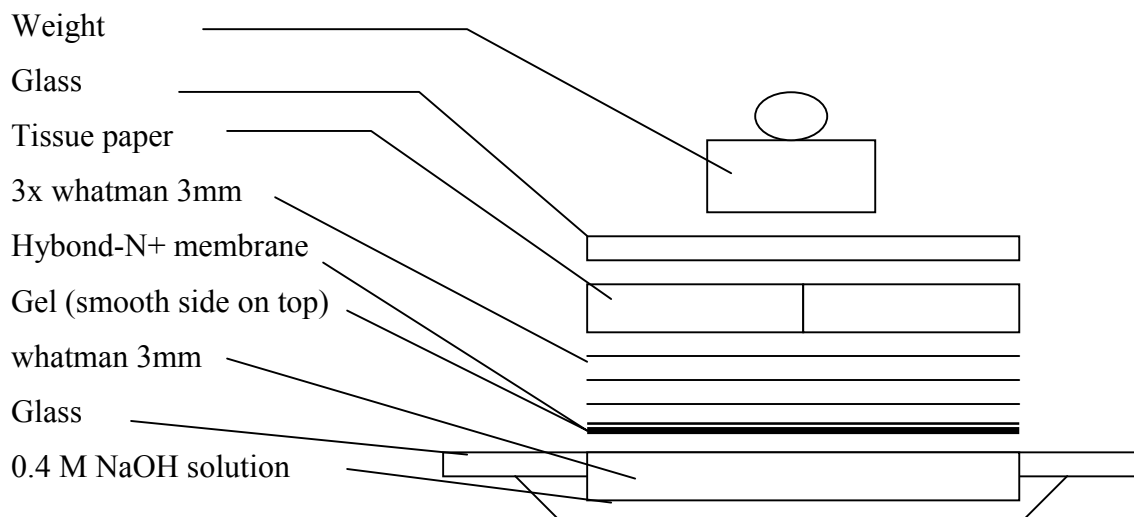
6-Southern Blot analysis.

6.1- Yeast genomic DNA extraction

Yeast genomic DNA was obtained by vortexing yeast cells in Phenol:Chlorophorm (volume 1:1) with glass beads (425-600 µm) from *Sigma* (1 volume beads per 1 volume yeast cell suspension). The mixture was centrifuged at 13,000 g and 4⁰C for 5 min. The supernatant was transferred into a fresh tube. DNA was precipitated by adding 2x the volume of 100% ethanol and spinning the mixed solution at 13,000 g for 20 min. The pellet was washed with 70% ethanol and resuspended in ddH₂O.

6.2- Protocol for the DNA transfer on the membrane, the insert radioactive labelling and the insert hybridization.

Genomic DNA samples were digested overnight with appropriate restriction enzymes and loaded on a 1% agarose gel. After electrophoresis (160 V), the gel was soaked in 0.2 M HCl solution and shacked gently for about 15 minutes until the marker colours change. The gel was then transferred to a 0.4 M NaOH solution and shacked gently until the colours return to their original shade. Hybond-N+ (*Amersham*) membrane is soaked in a 0.4 M NaOH solution and transfer was prepared as follows:



The DNA transferred overnight.

The DNA was then UV cross-linked on the membrane in a Stratelinker^R UV Crosslinker (*Stratagene*) with the “crosslink” mode. The membrane was rolled in a glass tube of appropriate size and incubated 1 hour in Church buffer at 65°C.

Radioactive labelling of DNA probes:

50 ng DNA in 21 µl H₂O was denatured at 100°C for 5 minutes and then put on ice. From a DNA labelling kit (*Amersham*), 4 µl dATP, 4 µl dTTP, 4 µl dGTP, 5 µl primer solution, 5 µl reaction buffer, 2 µl polymerase (klenow) and in the radioactive laboratory 5 µl [³²P]dCTP (*Amersham*) with 10 mCi/ml were added to the mixture. The mixture was incubate 1h at 37°C. A Nick column (SephadexTM G-50, *Amersham*) was equilibrated with TE buffer, and the radioactive sample was dropped on the filter of the Nick column. Then 400 µl TE were added, and the eliminated liquid was collected in an Eppendorf tube and discarded in appropriate trash. 400 µl TE were added and the radioactive sample was collected in a fresh Eppendorf tube. 1µl was kept to quantify radioactivity in the sample by scintillation counter. The sample was denatured at 100°C before being carefully pipetted it in the glass tube with the membrane. The membrane was then incubated with the radioactively labelled DNA probe on roller overnight at appropriate temperature (e.g 65°C). The membrane was washed with the high stringency 2x SSC/1% SDS buffer and the low stringency 20x SSC/1% SDS buffer, 20 minutes each at 65°C, check radioactivity levels and then washed last time with 0.2x SSC/1% SDS at room temperature. The membrane was exposed to a Hyperfilm MP (*Amersham*) overnight at -80°C.

6.3- Buffers and solutions

SSC 20x 3M NaCl, 0.3 M Na₃citrate·2H₂O adjust to pH 7.0 with 1 M HCl

CHURCH buffer: 1% BSA, 1mM EDTA, 0.5M Na₂HPO₄ pH 7.2, 7% SDS

1M Na₂HPO₄ pH 7.2 (500 ml): 134 g Na₂HPO₄·7H₂O or 71g anhydrous Na₂HPO₄, 4 mL 85% H₃PO₄

7-Northern Blot analysis

7.1- RNA extraction

Yeast RNA was obtained by vortexing yeast cells in Trizol reagent (*Life Technologies*) with glass beads (1 volume beads per 1 volume yeast cell suspension)

according to the Trizol reagent manufacturer's protocol (*Life Technologies*). The mixture was centrifuged at 13,000 g and 4°C. The supernatant (clear phase) was transferred into a fresh tube. RNA was precipitated by adding 2x the volume of 100% ethanol and spinning the mixed solution at 13,000 g. The pellet was washed with 70% ethanol and resuspended in ddH₂O.

7.2-Protocol for the RNA transfer on the membrane, the insert radioactive labelling and the insert hybridization.

RNA samples were loaded on a formaldehyde-containing agarose gel. After electrophoresis, RNA was transferred onto a Hybond N⁺ membrane (*Amersham*) and hybridized with 100 ng of a ³²[P]-labelled full length cDNA probe/250 µl Herring DNA* according to standard protocols (see: southern-blot). The membrane hybridization is done in STARK buffer or in Hybridization solution (*Clontech*) between 42°C and room temperature due to the weaker affinity of DNA/RNA.

7.3- Buffers and solutions

STARK solution: 5xSSC, 25 mM Sodium phosphate buffer, 1x Denhardt's solution, 50% v/v formamid, 0.5% w/v non fat dried milk, 4% w/v SDS

Sodium Phosphate buffer 25 mM in 100ml: 14.2 g Na₂HPO₄, 15.6 g NaH₂PO₄·2H₂O

*250 µg/ml Herring sperm DNA (250 µl/10ml STARK)

Denhardt 100x: 500ml, 10 g Ficoll 400, 10 g polyvinylpyrrolidone, 10 g bovine serum albumin, H₂O to 500 ml

Gel 1%: 150 ml, 126 ml H₂O, 1.5 g agarose (boil), 9 ml formaldehyde, 15 ml 10x MOPS (dry under a hood)

10x MOPS: 2 M MOPS pH 7.0, 5 M NaOH, 1 M EDTA pH 8.0 (Store in the dark).

8-Western Blot analysis

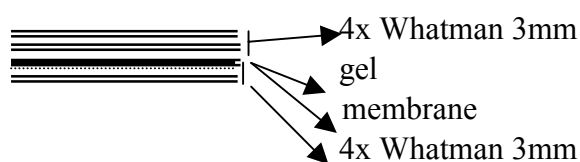
8-1-Protein extract

Yeast cell lysates were prepared by vortexing yeast cells for 5 min. in lysis buffer (TE buffer/1 mM PMSF, 1 tablet Complete-Mini protease inhibitor cocktail (*Roche*) per 10 ml buffer) and glass beads (425-600 µm) from *Sigma* (1 volume beads

per 1 volume yeast suspension). The mixture was centrifuged at 13,000 g, 4°C for 5 min. The supernatant was used for quantification of protein concentration and Western blot analysis.

8.2-Protocol

5-10 µg protein samples are loaded on 12% PAGE gel. Proteins are submitted to vertical electrophoresis for about 2 h in PAGE buffer, with 120 V.



Semidry transfer is set for 2 hours, with appropriate milli-Amperes (e.g. 40 cm² membrane with 40 mA).

Protein transfer was checked by incubating the membrane 2 minutes in Ponceau and washing the membrane with PBS/0.05% Tween. All subsequent steps were performed with constant shaking. The membrane was blocked in 5% low fat milk/PBS/0.05% Tween for minimum 1 hour. The primary antibody was incubated with the membrane in 5% low fat milk/PBS/0.05% Tween diluted in a suitable manner (usually 1/500 to 1/3,000) overnight at 4°C or 1-2 hours at room temperature. The membrane was then washed in PBS/0.05% Tween for 30 minutes with buffer changes every 10 minutes. The secondary antibody coupled to the HRP enzyme was incubated with the membrane 1-2 hours at room temperature diluted in 5% low fat milk/PBS/0.05% Tween (usually 1/2000 to 1/10 000 following instructions). Then the membrane was washed again for 30 minutes with buffer changes. ECL solution (*Amersham*) substrate to HRP was used to reveal the experiment result.

8.4-Stripping membrane for subsequent hybridizations.

1 µl β-mercapto-ethanol per 1ml stripping buffer was added to the stripping buffer, and the membrane was incubated in 10 ml stripping buffer at 56°C for 30 minutes. The membrane was washed with H₂O until the smell was not detectable any longer, then washed for 15 minutes in PBS/0.05% Tween.

8.4-Buffers and solutions

10 ml Migration gel (12%): 4.2 ml 30% Acrylamide, 2.5 ml Tris-HCl pH 8.8 (1.5 M), 3.2 ml H₂O, 100 µl 10% SDS, 7 µl TEMED, 70 µl 10% APS

5 ml Stacking gel (2,4%): 830 µl 30% Acrylamide, 1.2 ml Tris-HCl pH 6.8 (0,5 M), 2.8 ml H₂O, 50 µl 10% SDS, 3.3 µl TEMED, 70 µl 10% APS.

SDS-PAGE 10x, 5 l : 1% SDS (375 ml 20% stock solution), 300 g Tris, 750 g Glycin, H₂O to 5 l.

Stripping buffer 500 ml : 2% SDS (5 ml 20% stock solution), 62.5 mM Tris-HCl pH 6.0 (62.5 ml 0.5 M Tris), H₂O to 500 ml.

PBS 10x 137mM NaCl, 2.7 mM KCl, 4.3 mM Na₂HPO₄·7H₂O, 1.4 mM KH₂PO₄, pH 7.4

SDS/glycerol stock solution: 7.3% w/v SDS, 29.1% v/v glycerol, 83.3 mM Tris-base, tip of a small spatula of Bromophenol blue, dd H₂O.

9-GST-pulldowns

BL21* bacteria were grown as an overnight culture in 3ml selective LB medium. The next day, 2ml of the saturated culture were transferred in a 10ml selective (usually ampicilin) LB-culture and grown up to O.D₆₀₀. 0.5 at 37°C (1 or 2 h). The bacteria were induced with 1mM IPTG for 3h (30 or 37°C) and centrifuged at 4,500 g, 4°C for 10 min then resuspended in 1ml Lys-S buffer (with PMSF and anti-proteinase cocktail tablets) into an Eppendorf 1.5 ml tube. Bacteria were sonicated 3x 30 sec with a Branson SONIFIER 250 from *G.HEINEMANN* (90% duty cycle, output control 4) and left on ice for 30 min, they were inverted every 5 min. Centrifuge 30 min at 4°C with 13,000 rpm and supernatant was transferred into a fresh Eppendorf 1.5ml tube. 50µl Gluthation-agarose were added to the lysate and the mixture was put on a spinning wheel for 30 min at 4°C. Mixture was centrifuged 2 min at 5,000 rpm at 4°C, then washed 3 times with 1ml 0.5xLys-S and beads were resuspended in 50 µl 0.5xLys-S. The yield of GST fusion protein was estimated by running an aliquot on SDS PAGE gel.

* *E. coli* BL21: *E. coli* B F⁻, *ompT*, *hsdS* (r_B⁻, m_B⁻), *gal*, *dcm*. (Amersham)

Lys-S buffer 1x: 50 mM Tris pH 7.8, 0.4 M NaCl, 0.5 M EDTA, 10% Glycerol, 0.1NP40.

10-Immunoprecipitation

10.1-Protocol

Cells were lysed in 500 µl 1% Triton-buffer with 1 M PMSF and cocktail inhibitor (1 tablet/10 ml lysis buffer, *Roche*), then incubated on ice 10 minutes and

sonicated 3x 10 seconds with a Branson SONIFIER 250 from *G.HEINEMANN* (90% duty cycle, output control 4). The lysate was centrifuged at 13,000 rpm, 4°C for 30 minutes and the supernatant was transferred into a fresh eppendorf tube (50 µl were kept in a separate tube for the 10% input). All subsequent steps were performed at 4°C. 500 µl HNTG, 30 µl protein A/G coupled to agarose beads (*Santa Cruz Biotechnology*) and 5-10 µl antibody suitable for immunoprecipitation were added to the lysate. The mixture was shaken on a spinning wheel in eppendorf tubes at 4°C, 4 hours (or overnight) and then spin 2 minutes at 5,000 rpm, 4°C. Supernatant was discarded and beads washed by resuspending them in 1 ml HNTG. Washing steps were repeated twice and finally the mixture was centrifuged 2 minutes at 13,000 rpm, 4°C. 20 µl protein loading buffer were added and the mixture was boiled at 95°C for 5 minutes. After centrifuging 1 minute in a microfuge at 13,000 rpm, the supernatant was loaded on polyacrylamid/SDS gel.

10.2-Buffers and solutions

1% Triton: 1% triton-100, 0.1% SDS, 150 mM NaCl, 5 mM EDTA and 50 mM Tris-HCl pH 7.5 (keep at 4°C).

HNTG: 20 mM HEPES pH 7.5, 150 mM NaCl, 0.1% triton-100 and 10% glycerin (keep at 4°C).

11-PCR and RT-PCR

11.1- PCR

In a 1.5 ml eppendorf tube to 25 µl of total volume were added: 100 ng template DNA, 2.5 µl of 10x reaction buffer, 1 µl of MnSO₄ (50 nM stock solution), 3 µl of dNTP mix (2.5 mM stock solution), 2.5 µl of primer 1 (3 µM stock solution), 2.5 µl of primer 2 (3 µM stock solution), 0.5 µl (10 units) platinum polymerase (*Invitrogen*) and H₂O to total reaction volume. Then one drop of mineral oil was added on top to avoid evaporation. Samples were set in a PCR machine programmed as follow:

1x		94°C	5 minutes,

35x	-	94°C	30 seconds
	-	X°C	1min 30 sec
	-	68°C	1 min/kbp of insert to be amplified,

1x		68°C	10 min.

X°C = appropriate annealing temperature for the primers

11.2- RT-PCR

0.5 to 5 µg of total RNA and the RT-PCR kit from *Amersham* were used. In a PCR tube, 2 µg RNA in 11 µl H₂O were mixed with 0.2 µg hexanucleotides (1 µl). The mixture was incubated 5 min at 70°C, then laid on ice. 4 µl 5x RT-buffer, 2 µl 10 mM dNTPmix (dATP, dCTP, dTTP and dGTP), 0.5 µl RNAsin (20u) and 1.5 µl H₂O were added. Mixture was incubated 5 min at 25°C, then 1 µl RTCMulv Reverst Aid MBI/Zugatase (the reverse transcriptase) was added and the mixture was incubated 10 min at 25°C, 60 min at 42°C and 5 min at 70°C. 2-10 µl of the final mixture were used as a PCR template.

13-Plasmids maps and cloning strategies

13.1- pcDNA3.1+/- (*Invitrogen*)



Comments for pcDNA3.1/Zeo (+)
5015 nucleotides

CMV promoter: bases 209-863
T7 promoter priming site: bases 863-882
Multiple cloning site: bases 895-1010
BGH reverse priming site: bases 1022-1039
BGH polyadenylation signal: bases 1021-1235
fl origin: bases 1298-1711
SV40 promoter and origin: bases 1776-2101
EM7 promoter: bases 2117-2183
Zeocin™ resistance gene: bases 2184-2558
SV40 polyadenylation: bases 2688-2817
pUC origin: bases 3201-3874 (C)
bla promoter: bases 4880-4978 (C)
Ampicillin (bla) resistance gene: bases 4019-4879 (C)

The following genes were cloned into pcDNA3.1+

Δaven-pcDNA3.1+ (BamHI/XhoI)

Primer 1: Habam

5'-aca gga tcc aaa atg gcc tac ccc tac gac gtg ccc gac tac gcc-3'

Primer 2: pArt1 3', 5'-ttg gaa ttc gag ctc ggt ac-3'

A PCR reaction was set up with the above primers and clone B2 or *Δaven* (in part-1 *S. pombe* expression vector) as the template.

Δroret-pcDNA3.1+ (PstI/XhoI)

Primer 1: part 1 5'-ata gtg ggt ggt gga cag gt-3'

Primer 2: pArt1 3', 5'-ttg gaa ttc gag ctc ggt ac-3'

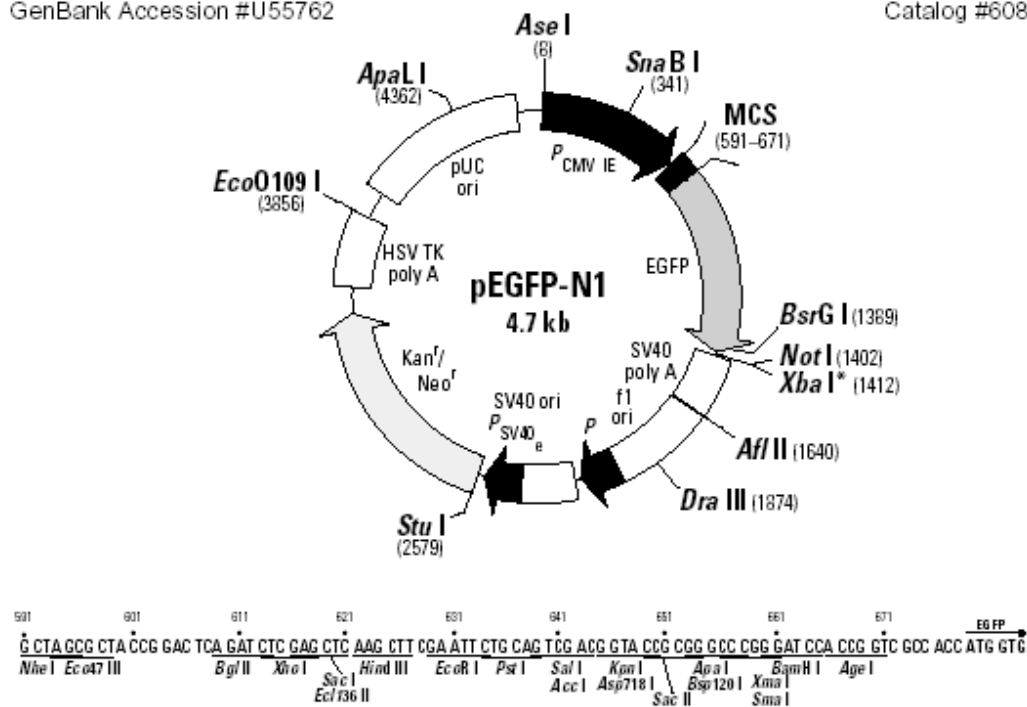
A PCR reaction was set up with the above primers and clone B1 or *Δroret* (in part-1 *S. pombe* expression vector) as the template.

13.2- In pEGFP-N1 (Clontech)

pEGFP-N1 Vector Information

GenBank Accession #U55762

PT3027-5
Catalog #6085-1



The following genes were cloned into pEGFP-N1:

ΔAven-pEGFP-N1(XhoI/XhoI)

Primer 1: *ΔAven* 5'-aca ctc gag atg agt gag tta ttg gtt cga gcc ctt caa gag-3'

Primer 2: *AvenX* 3'-Stop, 5'-aca ctc gag gga aat cat gct gtc caa cca gtc ttc-3'

A PCR reaction was set up with the above primers and *Aven*-pSG5 as the template.

Δroret- pEGFP-N1(XhoI/XhoI)

Primer 1: ΔRoretX 5'-aca ctc gag atg tcc aag ctt tac ttc gat gtg aag aaa atg-3'

Primer 2: RoRetX 3'-Stop,

5'-aca ctc gag gtc acc tgg ggg agg cag aaa caa agg-3'

A PCR reaction was set up with the above primers and Δroret-pcDNA3.1+ as the template.

roret(celera cDNA collection) (XhoI/XhoI)

Primer 1 : RoRetX 5'-aca ctc gag atg gcc tca acc acc agc acc aag aag atg-3'

Primer 2 : RoRetX 3'-Stop,

5'-aca ctc gag gtc acc tgg ggg agg cag aaa caa agg-3'

A PCR reaction was set up with the above primers and RoRet-pCMV.SPORT6 as the template.

roret(genestorm cDNA collection) (XhoI/XhoI)

Primer 1: RoRetX 5'-aca ctc gag atg gcc tca acc acc agc acc aag aag atg-3'

Primer 2: RoRetX 3'-Stop,

5'-aca ctc gag gtc acc tgg ggg agg cag aaa caa agg-3'

A PCR reaction was set up with the above primers and RoRet-pcDNA3.1/GS as the template.

fte-1- pEGFP-N1(XhoI/XhoI)

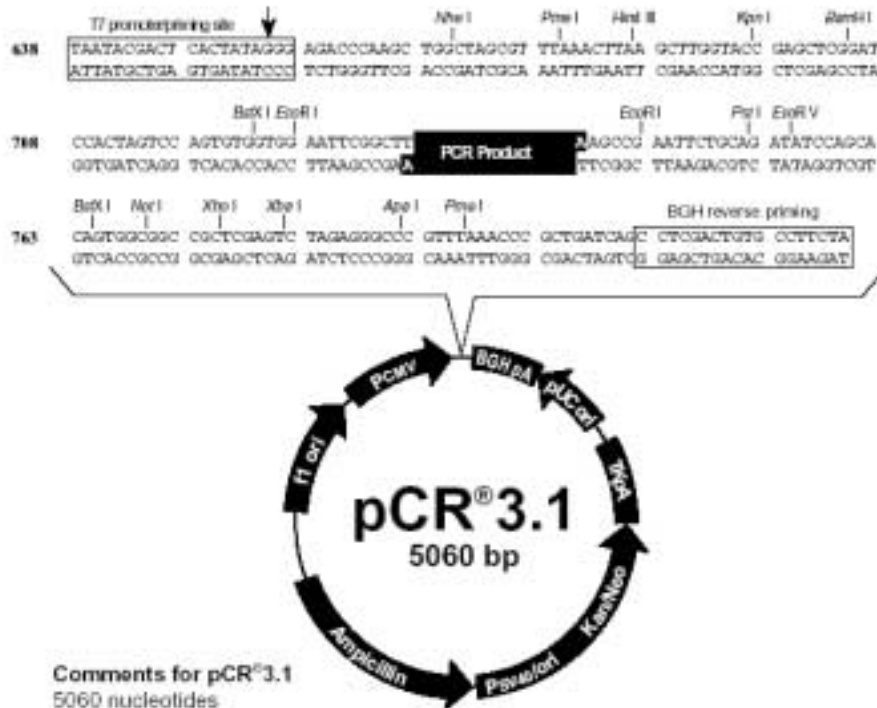
Primer 1: Fte-1X 5'-aca ctc gag atg gcg gtt ggc aag aac aag cgc ctt acg-3'

Primer 2: Fte-1X 3'-Stop, 5'-aca ctc gag aac aga ttc ttg gac tgg tgg ttc ata-3'

A PCR reaction was set up with the above primers and fte-1-pMEXneo as the template.

13.3- In pCR3.3-Gatway-compatible modified. (parental vector is pCR3.1 from *Invitrogen*)

The pCR3.3 vector was modified in a Gateway (*Invitrogen*) compatible system by Dr. Vladimir Kirchin (Georg-Speyer-Haus, Frankfurt).



The following genes were cloned in the Gateway compatible pCR3.3 vector:

Flag-Δroret (EcoRI/EcoRV)

Primer 1: dRoRet-EcoRI 5'-cag gaa ttc tcc aag ctt tac ttc gat gtg aag aaa atg-3'

Primer 2: RoRetEcoRV 3', 5'-cag gat atc tta gtc acc tgg ggg agg cag-3'

A PCR reaction was set up with the above primers and RoRet-pcDNA3.1/GS as the template.

Flag-roret(genestorm) (EcoRI/EcoRV)

Primer 1: RoRetEcoRI-ATG 5'-cag gaa ttc gcc tca acc acc agc acc aag-3'

Primer 2. RoRetEcRV 3', 5'-cag gat atc tta gtc acc tgg ggg agg cag-3'

A PCR reaction was set up with the above primers and RoRet-pcDNA3.1/GS as the template.

13.4- In pGADT7 (Clontech)

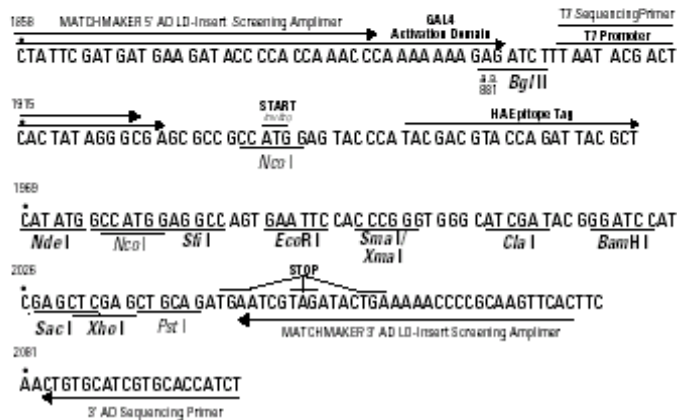
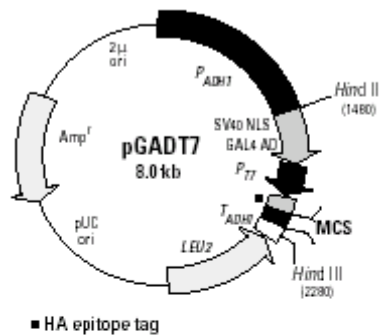
This vector is a two-hybrid vector for the prey (fusing the cDNA to the GAL4 activation domain).

pGADT7 Vector Information

GenBank Accession #: Submission in progress.

PT3249-5

Catalog # K1612-1



The following genes were cloned in pGADT7:

dAven-pGADT7 (BamHI/XhoI)

Primer 1: dAven-ATGBH

5'-acg gga tcc tgc agg cgg agc gag gag ctc ggg gag gcc-3'

Primer 2: AvenX 3', 5'-aca ctc gag tta gga aat cat gct gtc caa cca gtc ttc-3'

A PCR reaction was set up with the above primers and Aven-pSG5 as the template.

Δroret-pGADT7 (EcoRI/XhoI)

Primer 1: dRo-ATGEc 5'-agt gaa ttc tcc aag ctt tac ttc gat gtg aag aaa atg-3'

Primer 2: RoRetX 3', 5'-aca ctc gag tta gtc acc tgg ggg agg cag aaa caa agg-3'

A PCR reaction was set up with the above primers and ΔRoRet-pcDNA3.1+ as the template.

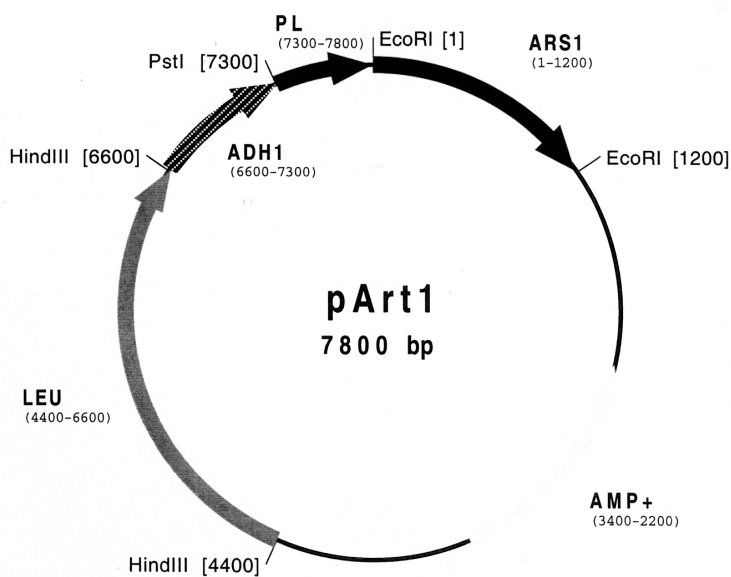
Fte-1-pGADT7 (BamHI/XhoI)

Primer 1: Fte-ATGBH 5'-acg gga tcc tgg cgg ttg gca aga aca agc gcc tta cga-3'

Primer 2: Fte-1X 3', 5'-aca ctc gag tta aac aga ttc ttg gac tgg tgg ttc ata-3'

A PCR reaction was set up with the above primers and fte-1-pMEXneo as the template.

13.5- In pArt1 (expression vector for *S. pombe* kindly provided by Dr. Paul Nurse, NCBR, London).



The following genes were cloned in pArt1:

HA-BclXL-pArt1(pstI/BamHI)

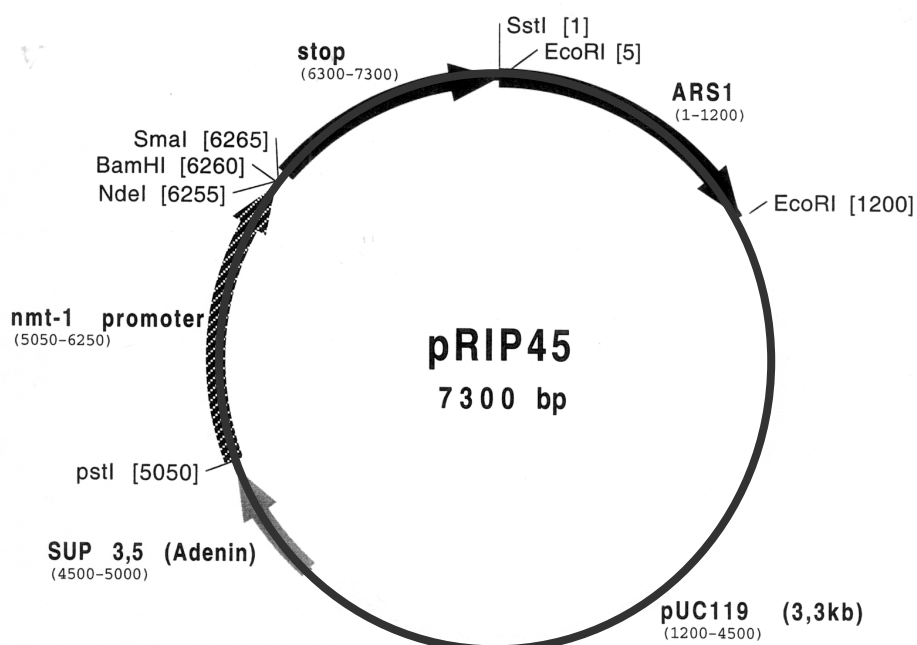
Primer 1: BclXLpArt1 5'-aca ctg cag aaa atg gcc tac ccc tac gac gtg ccc gac tac gcc tcc ctc gga tcc tct cag agc aac cgg gag ctg gtg gtt gac-3'

Primer 2: BclXLpArt1 3',

5'-aca gga tcc tea ttt ccg act gaa gag tga gcc cag cag-3'

A PCR reaction was set up with the above primers and BclXL-pcDNA3.1 as the template.

13.6- In pRIP 45 (expression vector for *S. pombe* kindly provided by Dr. Paul Nurse, NCBR, London).



The following genes were cloned in pRIP45:

HA-CED4-pRIP45 (SmaI/SmaI)

Primer 1: HA-ced4-Sma-5'- aca ccc ggg aaa atg gcc tac ccc tac gac gtg ccc gac tac gcc tcc ctc gga tcc ctc tgc gaa atc gaa tgc cgc gct ttg agc-3'

Primer 2: HA-ced4-3',

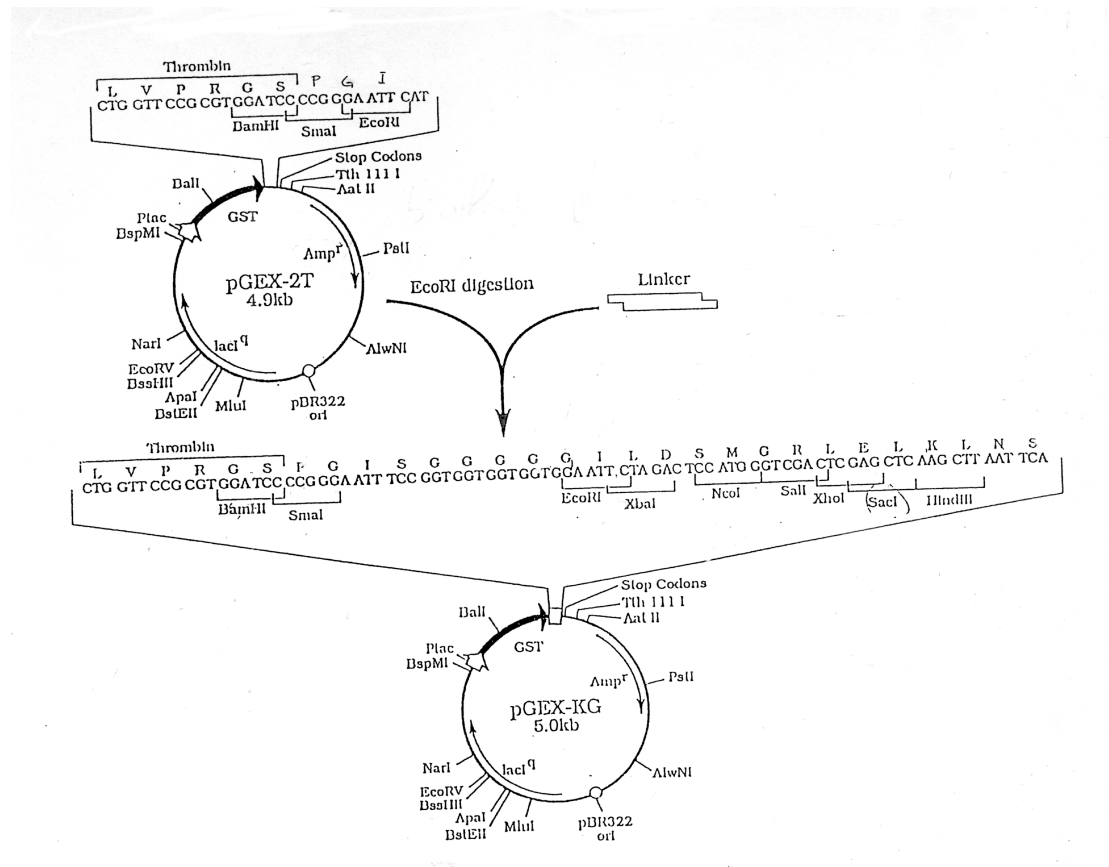
5'-aca ccc ggg tta aca gca tgc aaa att ttt gag gga gtc ata-3'

A PCR reaction was set up with the above primers and Rep 45-CED4

as the template.

13.7- In pGEX-AHK (expression vector for GST-fusion proteins in BL21 *E. coli*, fusing gene to GST).

The parental vector is pGEX-2T from *Clontech* and the pGEX-AHK was kindly provided by Dr. Thorsten Heinzl, Georg-Speyer-Haus, Frankfurt)



pGEX-AHK:

Kinase cleavage site BamHI SmaI

CTG GTT CCG CGT GGA TCT CGT CGT GCA TCT GTT GGA TCC CCG GGA
 L V P R G S R R A S V G S P G

EcoRI Sall XbaI

ATT TCC GGT GGT GGT GGT GGA ATT GAA TTC GTC GAC TCT AGA
 I S G G G G G I E F

NotI NcoI XhoI HindIII

GCG GCC GCT CCA TGG CTC GAG CTC AAG CTT AAT TCA

The following genes were cloned in pGEX-AHK:

Δ aven- pGEX-AHK (XhoI/XhoI)

Primer 1: dAvenX-ATG 5'-aca ctc gag agt gag tta ttg gtt cga gcc ctt caa gag-3'

Primer 2: AvenX 3', 5'-aca ctc gag tta gga aat cat gct gtc caa cca gtc ttc-3'

A PCR reaction was set up with the above primers and Aven-pSG5 as the template.

Δ roret- pGEX-AHK (XhoI/XhoI)

Primer 1: dRoRetX-ATG 5'-aca ctc gag tcc aag ctt tac ttc gat gtg aag aaa atg-3'

Primer 2: RoRetX 3', 5'-aca ctc gag tta gtc acc tgg ggg agg cag aaa caa agg-3'

A PCR reaction was set up with the above primers and Δ RoRet-pcDNA3.1+ as the template.

Fte-1- pGEX-AHK (XhoI/XhoI)

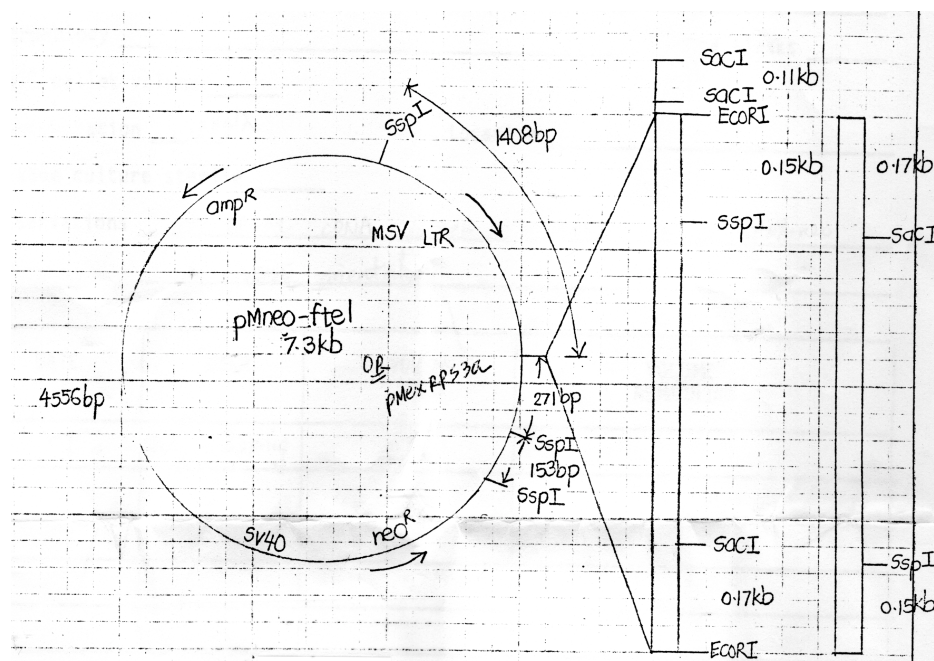
Primer 1: Fte1X-ATG 5'-aca ctc gag gcg gtt ggc aag aac aag cgc ctt acg-3'

Primer 2: Fte-1X 3', 5'-aca ctc gag tta aac aga ttc ttg gac tgg tgg ttc ata-3'

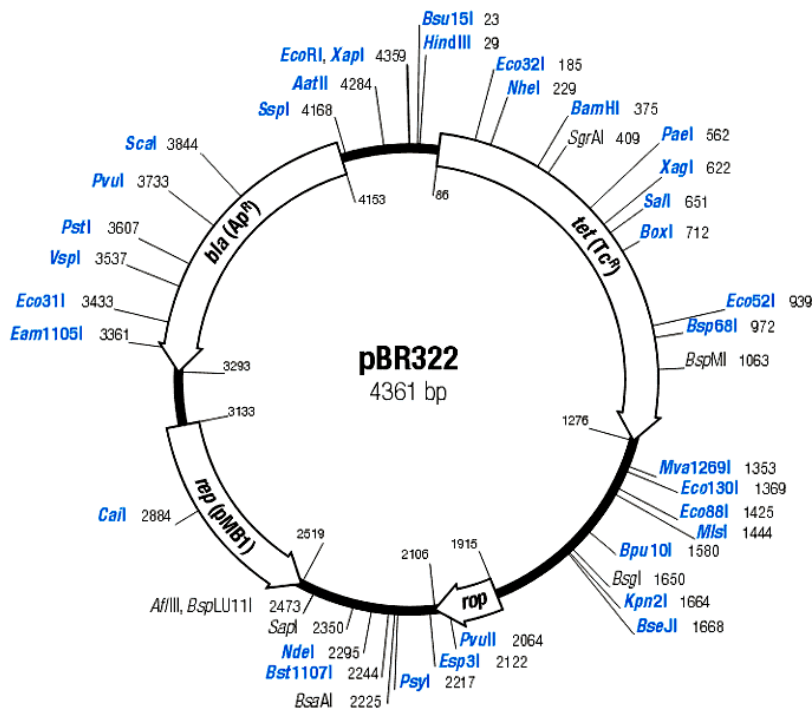
A PCR reaction was set up with the above primers and fte-1-pMEXneo as the template.

13.8- Constructs provided by other research groups

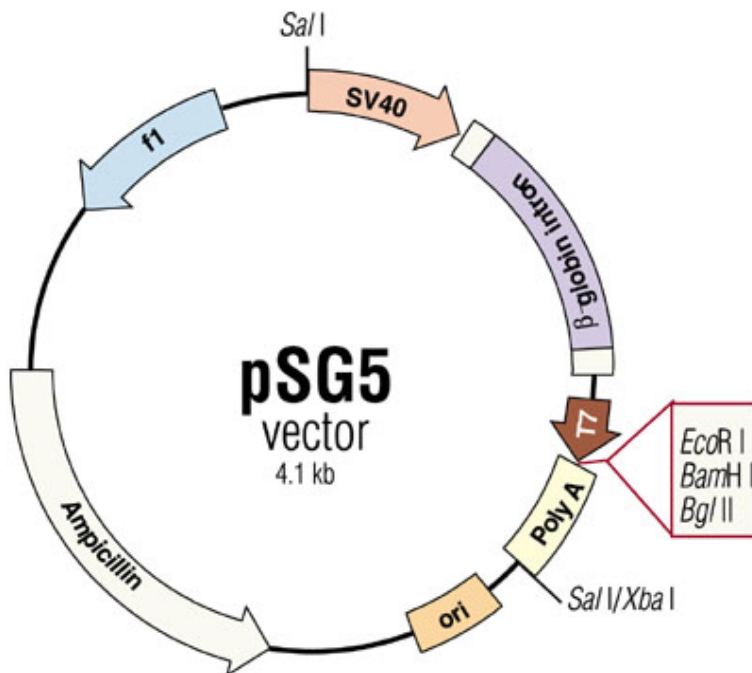
fte-1-pMEXneo (from Dr. Helmut Zarbl, Fred Hutchinson cancer research centre, Seattle, WA, USA)



hSAA1.1-pBR322 (from Dr. Barbara Kluve-Beckerman, Dep. Path. And lab. Medicine, Indianapolis, US)



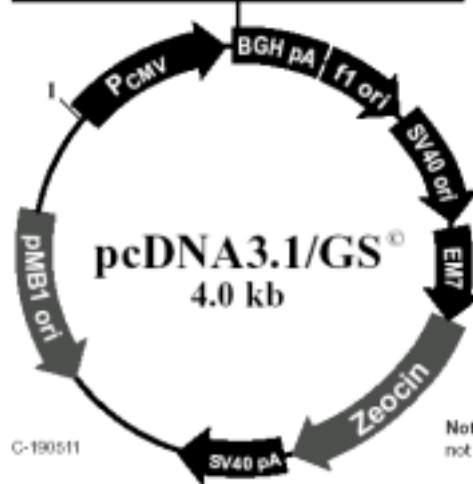
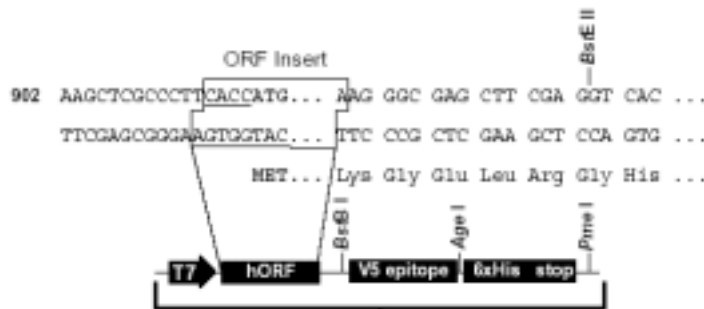
Aven-pSG5 (from Dr. Marie Harwick, Johns Hopkins University, Baltimore, US)



RoRetpcDNA3.1/GS genestorm cDNA collection (*Resgen, Invitrogen*)

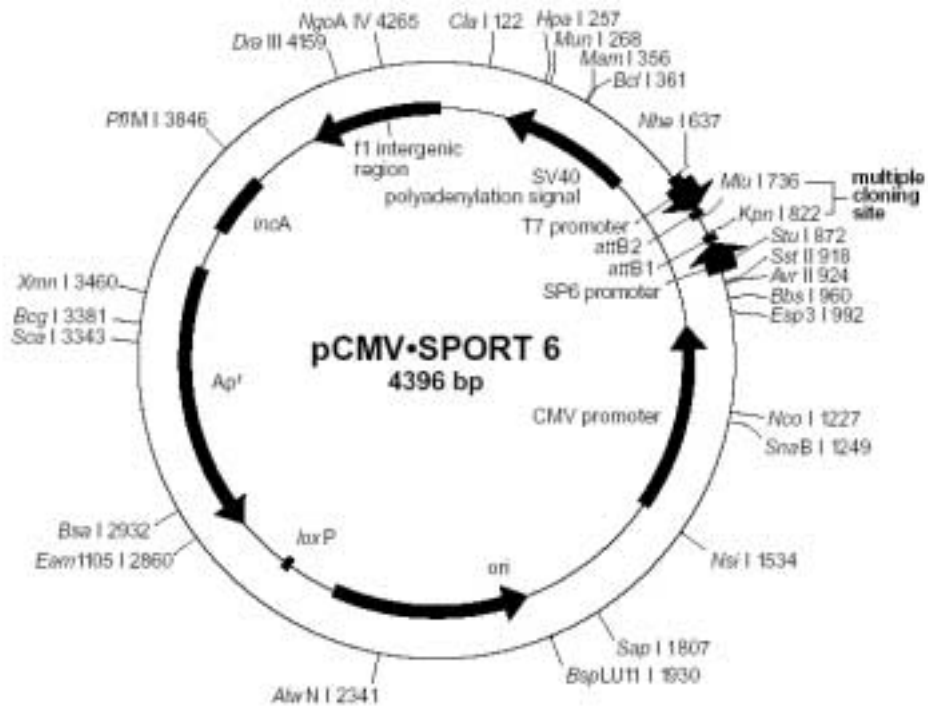
Comments for pcDNA3.1/GS (no insert)
4020 nucleotides

CMV promoter: bases 209-863
T7 promoter priming site: bases 863-882
yORF cloning site: between base 914 and 915
V5 epitope: bases 944-985
Polyhistidine tag: bases 995-1012
pcDNA3.1/BGH Reverse priming site: bases 1035-1052
BGH polyadenylation signal: bases 1034-1248
f1 origin: bases 1311-1724
SV40 promoter and origin: bases 1789-2114
EM-7 promoter: bases 2130-2196
Zeocin™ resistance gene: bases 2197-2571
SV40 polyadenylation: bases 2590-2782
pMB1 origin (pUC-derived): bases 3214-3887 (opposite strand)



Note: The underlined sequence CACC is not found in all clones.

RoRetpCMV.SPORT6 celera cDNA collection (*Resgen, Invitrogen*)



pCMV-SPORT 6 multiple cloning site and primer binding regions: 941-917 (The sequence listed here is the (+) strand.)



* This MluI restriction site is contained within the SalI adapter introduced into the vector upon ligation of the cDNA insert.

14-Yeast Two-Hybrid (Y2H) assay.

14.1- β -galactosidase assay.

AH109 or CG-1945* yeast cells are co-transformed with the GAL4 DNA-binding domain fused to the prey gene and the GAL4 activation domain fused to the bait gene. They were plated on selective medium (DOBA, -uracil, -tryptophane and -leucine). When colonies were large enough, a Whatman filter (90 mm Dia, No.5) was pressed on the plate until humidity diffuses into the filter. Then the filter was gently removed with the yeast colonies now attached to it and thrown in liquid nitrogen for 10 sec to break membrane wall. Then filter was allowed to thaw and placed on a filter paper soaked in Z buffer/X-gal solution. The yeast colonies hosting interacting partners turned blue within the next 8 hours.

*AH109 and CG-1945. (can be purchased from *Clontech*).

Strain	Genotype	References
AH109	MAT α , <i>trp1-901, leu2-3, 112, ura3-52, his3-200, gal4Δ, gal80Δ, LYS2 :: GAL1_{UAS}-GAL1_{TATA}-HIS3, GAL2_{UAS}-GAL2_{TATA}-ADE2, URA3 :: MEL1_{UAS}-MEL1_{TATA}-lacZ</i>	James et al., 1996; A. Holtz, unpublished
Y187	MAT α , <i>ura3-52, his3-200, ade2-101, trp1-901, leu2-3, 112, gal4Δ, mef⁻, gal80Δ, URA3 :: GAL1_{UAS}-GAL1_{TATA}-lacZ</i>	Harper et al., 1993
CG-1945	MAT α , <i>ura3-52, his3-200, ade2-101, lys2-801, trp1-901, leu2-3, 112, gal4-542, gal80-538, cyf12, LYS2 :: GAL1_{UAS}-GAL1_{TATA}-HIS3, URA3 :: GAL4_{17-mer(q2)}-CYC1_{TATA}-lacZ</i>	Feilbter et al., 1994; C. Giroux, pers. comm.

14.2-Buffers and solutions.

Z buffer: 16.1 g/l Na₂HPO₄·7H₂O/5.5 g/L NaH₂PO₄·H₂O/0.75 g/l KCl/0.246 g/l MgSO₄·H₂O adjust to pH 7.0 and autoclave.

Z buffer/X-gal solution: 100 ml Z buffer/0.27 ml β -mercaptoethanol/1.67 ml X-gal stock solution.

X-gal stock solution: dissolve 5-bromo-4-chloro-3-indolyl- β -D-galacto-pyranoside (X-gal; #8060-1) in N,N-dimethylformamide (DMF) at a concentration of 20 mg/ml. Store in the dark at -20°C.

C-Cell culture

1-Basic handling

Cells were trypsinized and resuspended in DMEM (*LIFE TECH*) complete medium and passaged one to eight them just before confluency is reached. Normal

culture medium was 10% FCS/10 ml glutamine/5 ml Pen-strep (penicillin and streptomycin) from *Bio*Whittaker* in 500 ml DMEM or RMPI from *LifeTech*. Trypsinization required prior washing of the cells in PBS. They were then incubated 5 min with 2 ml Trypsin (*Bio*Whittaker*) in a 9 cm diameter plate at 37°C. Some cell lines needed scrapping to detach them (e.g. Kim-2)

For stocks:

Cells were centrifuged at 1,400 rpm and the supernatant was removed. The pellet was resuspended in 90% FCS/10% DMSO and the cells were transferred immediately on dry ice in cryotubes. Then the cells were stored overnight at -80°C before being transferred into the liquid nitrogen tank for years.

2-Transfection

RKO* and 293T** cells were transfected using the PEI method. Briefly, 13.5µl of a polyethyleneimine solution (10mM in PBS, high molecular weight PEI from *Aldrich*) were diluted with 150µl of PBS. In parallel, 5µl of DNA solution were diluted with 150 µl of PBS and both solutions were mixed and vortexed. After 10 minutes of incubation at room temperature, the DNA/PEI mixture was added to the cells (1x10⁶ cells/10 cm plate) in serum-free medium. 4 hours later, the medium was replaced with FCS-containing medium.

*RKO: human colorectal carcinoma cells (*Invitrogen*).

**293T: human embryonic kidney cells, transformed with large T antigen (*Invitrogen*).

3- Apoptosis quantification by LIVE/DEAD assay

Apoptotic cell death was measured using the LIVE/DEAD Viability/Cytotoxicity kit from *Molecular Probes* according to the supplier's protocol. Cells were washed with PBS and resuspended in 40 µl of 4 µM EthD-1/2 µM Calcein for 30 min in the dark at room temperature. In this assay, living cells are distinguished by the presence of ubiquitous intracellular esterase activity, determined by the enzymatic conversion of the virtually nonfluorescent cell-permeant calcein AM to the intensely green fluorescent calcein (ex/em 495 nm/515 nm). Ethidium homodimer-1 enters cells with damaged membranes and undergoes a 40-fold enhancement of fluorescence upon binding to nucleic acids, thereby producing a bright red fluorescence in dead cells (ex/em 495 nm/635 nm). EthD-1 is excluded by the intact plasma membrane of living cells. For each experiment, at least 200 green and red cells were counted using a *Nicon* fluorescence microscope (TE300).

4- Caspase activity assay.

Cells were washed in PBS, centrifuged at 2,000 rpm, and the pellet was frozen immediately in liquid nitrogen then stored at -80°C . The *BioVision* “Mch6 Fluorometric Protease Assay Kit” was used for the following steps. The pellet was resuspended in 50 μl of chilled cell lysis buffer. The mixture was incubated on ice 10 min then transferred in a 96 well plate. 50 μl 2x reaction buffer/10 mM DTT was added to the mixture with 5 μl LEHD-AFC substrate (50 μM final concentration). The mixture was incubate 2 hours at 37°C and the reaction result was read out at 505 nm.

5- KIM-2 cells.

5.1-Cell culture

Kim-2 cells were cultured and treated as describe in [MacLaren, 2001 #9112; Gordon, 2000 #9113; Clarkson, 2000 #9114] to induce differentiation and apoptosis. Cells were maintained in “maintenance medium” and passaged by scrapping 1/5 when they reached near confluency. To differentiate them, they were cultured in “maintenance medium” up to complete confluency, then the medium was exchanged with “differentiation medium”. Cells were kept in this medium for about two weeks, changing medium every second day until they formed multiple layer and structures similar to tubules (differentiated pattern). To induce apoptosis, differentiated cells were incubated overnight in “apoptosis medium”. About 30% of the cells were apoptotic.

5.2-Buffers and solutions

KIM-2 Maintenance medium: 250ml DMEM (*LIFE TECH*), 250 ml F-12 nutrient mix (*LIFE TECH*), 50 ml Foetal calf serum (10%) (*LIFE TECH*), 6 ml L-Glutamine (5%)(*LIFE TECH*), 500 μl Insulin (5 mg/ml stock solution) (*SIGMA*), 500 μl EGF (5 $\mu\text{g}/\text{ml}$ stock solution) (*SIGMA*), 250 μl Linoleic acid (10 mg/ml stock solution) (*SIGMA*). Optional, 500 μl Gentamicin (50 mg/ml stock solution) (*LIFE TECH*).

KIM-2 Differentiation medium: 250ml DMEM (*LIFE TECH*), 250 ml F-12 nutrient mix (*LIFE TECH*), 50 ml Foetal calf serum (10%) (*LIFE TECH*), 6 ml L-Glutamine (*LIFE TECH*), 500 μl Insulin (5 mg/ml stock solution) (*SIGMA*), 500 μl Dexamethosone (40 $\mu\text{g}/\text{ml}$ stock solution) (*SIGMA*), 500 μl Prolactin (1 mg/ml stock solution) (*SIGMA*), 250 μl Linoleic acid (10 mg/ml stock solution) (*SIGMA*).

KIM-2 Apoptosis medium: 250ml DMEM (*LIFE TECH*), 250 ml F-12 nutrient mix (*LIFE TECH*), 50 ml Foetal calf serum (10%) (*LIFE TECH*), 6 ml L-Glutamine (*LIFE*

TECH), 500 µl Insulin (5 mg/ml stock solution) (*SIGMA*), 250 µl Linoleic acid (10 mg/ml stock solution) (*SIGMA*).

Collagen coating solution: 5 ml collagen type 1 (*SIGMA*), 2.8 ml 10% acetic acid (filtered), 42.2 ml ddH₂O.

D-FACS analysis

1-Propidium Iodide staining of fixed cells

1.1-Fixation

Cells were centrifuged at 1,400 rpm at 4°C for 5 minutes, supernatant and 500 µl ice cold 70% ethanol was pipetted drop by drop while vortexing. Adherent cells had to be trypsinized and washed with PBS. Fixed cells can be conserved at 4°C for several days.

1.2-PI staining

The cells were washed with 2 ml 38 mM Na-Citrate pH 7.4 and spin with 1400 rpm 5 minutes at 4°C. The supernatant was removed and 500 µl 38mM Na-Citrate pH 7.4, 50 mM propidium iodide (1/50 of 2.5 mg/ml stock), 5 mM RNase (1/2000 of 10mg/ml stock solution) were added. The cells were then incubated for 20 minutes at 37°C in the dark. The samples were handled immediately. The cell suspension was analyzed with a FACScalibur (*Becton Dickinson*). The “Cell Quest Pro” software was used and PI stained cells were detected in the FL2 fluorescence. Cells with hypoploid DNA content (represented in the sub-G₁ peak of the cell cycle profile) were considered apoptotic.

3-Buffers and solutions

FACS Flow, FACS rinse, Cell WASH were purchased at *Becton Dickinson*.

E-Confocal laser scanning microscopy

1-Fixation and antibody staining of cells

293T cells were grown in appropriate thin bottom 2.2 cm diameter plates (25/22 mm. Serie 3500, *WillcoWells B.V.*), and transfected as described previously.

All subsequent steps were done at room temperature. The supernatant was gently removed and cells were washed with 1 ml PBS/1 mM CaCl₂/0.5 mM MgCl₂. Then cells were fixed with 500 µl 3% Formaldehyde/PBS for 10 min and washed twice with 1 ml PBS, 5 min each. Then cells were permeabilized with 500 µl 0.1% Triton-100/PBS for 5 min and washed twice 5 min with 3% BSA/PBS. Cells were incubated with gentle shaking 1-3 hours with 150 µl primary antibody 1/100 in 3% BSA/PBS. The cells were washed twice with PBS and incubated 1 hour with 150 µl of the species specific secondary antibody 1/1000 in 3% BSA/PBS. As a last step, cells were washed twice with PBS, and one drop of Vectashield (mounting medium for fluorescence, with DAPI) from *LINARIS* was used with 100 µl PBS to avoid dehydration of the cells. It was possible to keep them up to one week at 4°C.

F- Cancer profiling array with tumours cDNA

To analyze mRNA expression levels in normal and tumour tissue the Cancer Profiling Array from *Clontech* was used (catalog No. #7841-1). This array contains many cDNA pairs of tumour and normal tissue, each from the same patient. The membrane was hybridized with [³²P]-labelled cDNA probes of human *ubiquitin* (supplied by *Clontech*), human *c-myc*, human *Δaven*, human *Δroret*, human *fte-1* and mouse *Δhmgbl* (which recognises the human *hmgbl* transcript) according to the supplier's protocol. Hybridization signals were detected and quantified with a *BIO RAD* phosphoimager (Molecular Imager FX) and the Quantity One software.

G-Preparation of protein lysates from tumour samples for Western Blot analysis.

1-Protein lysate preparation.

All primary human mammary carcinoma samples (kindly provided by Dr. Christine Solbach, Frauenklinik, Universitätsklinikum, Frankfurt) were collected directly after surgery, frozen in liquid nitrogen and stored at -80⁰ C. They were classified as follows:

Tu.-No.	TNM	Grading	ER/PR	Her2/neu
83	pT3 pN1 M0	3	pos./neg.	neg.
167	pT4 pN0 M0	3	pos./neg.	neg.
249	pT2 pN0 M0	2	pos./neg.	neg.
250	pT2 pN0 M0	3	neg./neg.	neg.
256	pT1 pN0 M0	2	pos./pos.	neg.
611	pT3 pN1	3	neg./neg.	nd
876	pT2 pN0	3	pos./neg.	nd
1096	pT3 pN1	nd	neg./pos.	nd
1132	pT3 pN1	3	nd	nd

Another seven samples were human breast carcinomas passaged in nude mice for several years and tested for human origin. 0.5 cm³ tumour material was crushed in a 12.0/75 mm *Greiner* tube using a homogenizer (Ultra-Turrax T25, *Janke & Kunkel, IKA Labortechnik*) in 1ml lysis buffer and centrifuged at 4⁰C. The supernatant was used for quantification of protein concentration and subsequent Western blot analysis with 40 µg protein per sample.

2-Buffers and solutions

Lysis buffer: 30 mM Tris-HCL (pH7.5), 150 mM NaCl, 1% Triton X-100, 10% Glycerol, 1 mM PMSF, 1 tablet Complete protease inhibitor cocktail (*Roche*) per 10 ml buffer

H-Mouse mammary glands mRNA, northern blot analysis.

A mouse mammary gland Northern Blot from *RNWAY Laboratories* (Catalog No. NeverFailTM m106) was hybridized with 100 ng [³²P]-labelled *Δhmgbl*, *β-actin* and *gapdh* mouse cDNA probes following the manufacturer's instructions. The membrane contains mouse mammary gland mRNA preparation from non-pregnant and pregnant mice as well as from lactating and involuting animals.

I- Common Drugs and companies

Agarose ultra pure (*Life Technologies, Gibco BRL*)
Bromophenol blue (*Roth*)
Dimethylsulfoxid, DMSO, C₂H₆SO (*Roth*)
ECL western blotting detection reagent (*AmershamPharmacia*)
EGTA (*Sigma*)
Ethanol 100% (*Roth*)
Formaldehyde 37% (*Sigma*)
Formamid (*Roth*)
Glass beads, 425-600 µm (*Sigma*)
Glycerol (*Roth*)
G-418 sulfate (*CalBiochem*)
HEPES (*Roth*)
Hydrochloric acid 1 M, HCl (*Roth*)
Lithium Chloride, LiCl (*Roth*)
Lysosym (*Roth*)
Methanol (*Roth*)

MOPS, C₇H₁₅NO₄S (*Roth*)
Nonfat dried milk powder (*AppliChem*)
Phenol and buffer pH 10.5 for saturated Phenol (*Sigma*)
Phosphatase alkaline, AP, (*Roche*)
PMSF (*Aldrich*)
Potassium acetate, C₂H₃KO₂ (*Roth*)
Potassium dihydrogen phosphate, KH₂PO₄ (*Roth*)
2-Propanol, Isopropanol (*Roth*)
Proteinase cocktail tablets (*Roche*)
Proteinase K (*Roche*)
RNase (*Roche*)
Rotiphorese Gel 30, polyacrylamid (*Roth*)
SDS ultra pure 20% (*Roth*)
Sodium acetate, C₂H₃NaO₂·3H₂O (*Roth*)
Sodium hydroxide, NaOH (*Roth*)
TEMED p.a. (*Roth*)
Tri reagent (*Sigma*)
Trichloromethan/Chloroform (*Roth*)
Tris, C₄H₁₁NO₃ (*Roth*)
Tris hydrochlorid, C₄H₁₁NO₃HCl (*Roth*)
Tween^R 20 (*Roth*)

Other more specific reagents and drugs are mentioned in the protocol text with companies of purchase.

J- Tools and equipments

Bench tools: _ Biofuge *pico* (*Heraeus*)
_ Vortex REAXcontrol (*Heidolph*)
_ Pipetus^R-akku (*Hirschmann Laborgeräte*)
_ Electrophoresis power supply- EPS 301
(*Amersham pharmaciabiotech*)
_ Hoefer Semiphor, semidry transfer unit
(*Pharmacia Biotech*)
_ Hoefer HE33, mini horizontal submarine unit
(*Pharmacia Biotech*)
_ GNA 200, for big gels (*Pharmacia Biotech*)
_ MV120, mini vertical gel system (*LTF*)
_ Rocking table "Rocky", to wash membranes
(*Fröbel Labortechnik*)
_ Thermomixer compact, for 1.5 ml tubes (*Eppendorf*)
_ Dri-Block^R DB-2D (*Techne*)

Centrifuges: _ Biocentrifuge/J2-21 centrifuge with rotor JA-10 and JA-20
(*Beckman*)

_ Ultracentrifuge TL-100 (*Beckman*)
_ SIGMA 2K15 (*Laborcentrifugen*)
_ Heraeus Typ. Nr.4400, minifuge GL Heraeus Christ (*Heraeus*)

TE300, Fluorescent microscope (*Nicon*)
FACSCalibur (*Becton Dickinson*)
LEICA DMIRBE, Confocal microscope (*LEICA*)
iCycler PCR machine (*Bio-RAD*)
Branson SONIFIER 250 (*G.HEINEMANN*)
1500 TR-CARB^R, liquid scintillation analyser (*PACKARD*)

III-Results.

A-The screens

1- The Yeast survival screen

The HC4 strain was derived from wild type *S. pombe* yeast stably transformed with the HA-CED4-pRIP45 vector, containing the adenine selection makers that allows growth on medium without adenine. This vector has an *nmt-1* inducible promoter allowing expression of *CED4* when thiamine is removed from the medium. When thiamine is present, gene expression is repressed. A stable HC4 yeast strain with the HA-CED4-pRIP45 vector integrated in the chromosomal DNA was obtained by culturing a *CED4* expressing colony in non-selective liquid yeast medium for 2-3 passages. Then, an aliquot was plated on non-selective agar plates including leucin, uracil, adenine, thiamine. Growing colonies were then replica-plated on successively selective (containing leucin, uracil, thiamine, and without adenine) and non-selective medium (including adenine), the second being important for the survival of the later chosen clone colony. During the incubation in non-selective medium, the Ade-containing plasmid will be lost if it is not stably integrated in the genome. Colonies still inducible for *CED4* expression and efficient cell killing on agar plates lacking adenine were considered stably transformed. It was important to obtain a yeast strain that would give the minimal background of colonies surviving *CED4* expression, and such a strain was chosen and called HC4.

The HC4 *S. pombe* strain was cultured overnight in 1l of liquid yeast medium containing leucin, uracil and thiamine up to O.D₆₀₀ 0.6, and transformed using the LiAc method with 320 µg of a human breast carcinoma library cDNA with the ATG containing 5'-linker and with 64µg of library cDNA without a linker-encoded start codon. The total amount of transformed cDNA was therefore 384 µg. The efficiency of the transformation was determined as $2,5 \cdot 10^3$ colonies/µg cDNA, resulting in $9,6 \cdot 10^5$ of clones which were eventually screened.

After replica-plating twice on uracil and phloxin-containing medium, the surviving *CED4*-expressing colonies were scrapped on uracil media to test their regrowth potential. Phloxin is a red dye that penetrates damaged yeast cell membrane walls and which allows to determine by its reddish colour if a yeast colony is dying (red) or still alive (cream). This "regrowth" test was important because some yeast colonies are feeding themselves from the nutrients provided by surrounding dead yeast cells, and can survive regardless of the selective medium based on starvation of essential nutrients. In my screen 473 clones regrew. These 473 clones were pooled in liquid medium, incubated for 4 hours and the library cDNA plasmids were extracted together with the chromosomal DNA. 1/4 of the amount of DNA was used for a second round of selection (transformation of HC4, replica plating twice and regrowth test on uracil medium). After this second round of survival selection, 22 clones remained.

Plasmid cDNA were isolated and sequenced. The result is listed below:

- B1: Human RoRet / or zinc finger protein 15..
- B2: Homo sapiens cell death regulator AVEN.
- B3/5: Similar to mus musculus early blastocyst cDNA clone, similar to the L36 ribosomal protein.
- B9/10/11/13/18: Expression vector Beta-lactamase and beta-propylmalate dehydrogenase genes.
- B12: Human v-fos transformation effector protein (Fte-1)/ 40S ribosomal protein S3A (human)
- B15: Human tumor necrosis factor/ Lysosome-associated membrane glycoprotein 1 precursor .
- B17: PPAR γ -cofactor 2
- B19: Peptidyl-prolyl cis-trans isomerase A (human)/ or Cyclophilin A.
- B20: Serum amyloid A (SAA1-2) beta gene.
- B21: Human fuse binding protein.
- B22: Mitochondrial DNA control region sequence.

B-Selection of candidate genes for future investigations

The screen came up with potentially interesting anti-apoptotic cDNA candidates, but the number of genes excluded the possibility to analyse them all. I decided to select only some of them for further investigation. The criteria by which I selected them were the maintenance of CED4 expression in HC4 yeast cells expressing the library plasmids (to avoid isolation of transcriptional down regulators of CED4 expression), the interest of published information about the particular clones and their potential to inhibit apoptosis in a mammalian system.

1-CED-4 expression

I cultured the clones in selective medium (devoid of thiamine to induce CED4 expression) for 48 hours and extracted protein lysate. These protein extracts were used in a Western Blot to test the presence or absence of the killer-protein CED4 (see Fig. 15)

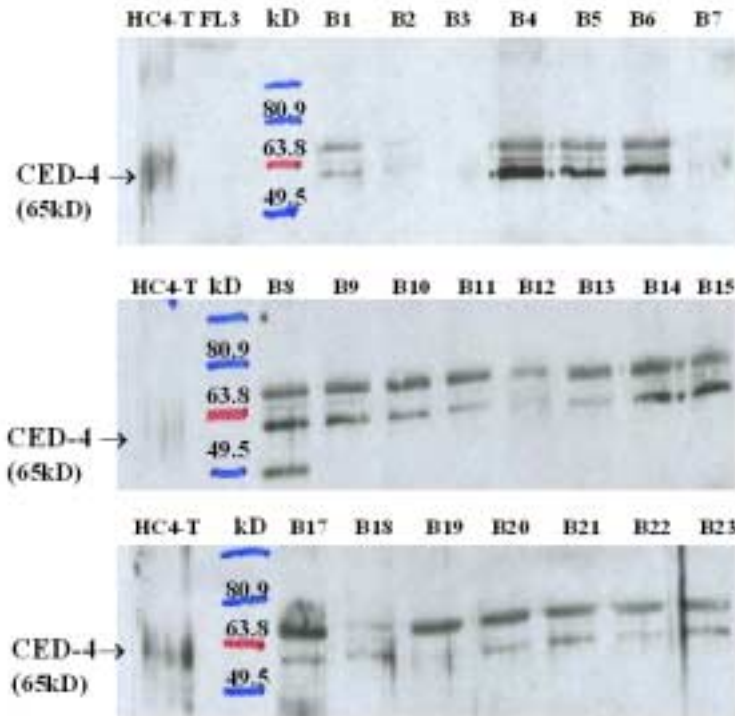


Fig. 15 : The isolated 23 HC4 clones transformed with the tumour library (B1-B23) were grown in medium plus thiamine to O.D₆₀₀ 0.5, then washed twice with water, diluted to O.D. 0.03 and cultured in medium without thiamine overnight to induce Ced-4 expression. Protein extracts were prepared and Western Blot was performed with an anti-CED4 antibody obtained from Dr. Horwitz (Howard Hughes Medical Institute, Department of Biology, Massachusetts Institute of Technology, Cambridge 02139, USA). The expected size of the protein is 65 kD. CED4 expression had to be confirmed to exclude transcriptional downregulation by the protecting library plasmid. I was not interested to isolate and analyse transcriptional regulators downregulating the *CED4* gene expression.

All clones I had obtained in the survival screen were still expressing detectable amounts of CED4 except B3 (where the protein concentration was too low to allow interpretation, and B19).

2-Literature analysis of the clones encoding for a protein

The sequencing results were blasted in HUSAR (from the webDKFZ site) and NIH blast (from the webPubMed site). I determined the clones length, the contained coding or non-coding sequence in the clones and the published roles of each protein encoded by my cDNAs.

Clones	Article	cDNA part found in the screen	properties	cloning
1-1A9RoRet	J.N.Fisher et al Genom Res 1997	830-1398 (nt)	Homology to ZNF RoGSA (type and structure cyclohex anti-antigen and the Ret finger protein.	4RoRet pCDNA3.1+ 4RoRet pRES2
2-AVEN	J.M.Hendrich et al Molecular Cell Apr 2000	591-1039 (nt)	Inhibitor of Caspase activation binds to Bcl-XL and Apaf-1	Avan p305 4Avan pCDNA3.1+
3-Tigressin beta 4	M.Nach et al Cell Mol. Com 2000, Vol 7	+/- sense	Increase resistance to apoptosis in adherent fibroblasts. Ret +/- DNA strand.	
12 Fte-1 human v-fos transformation effector	C.J.DuBois et al Proc. Natl. Acad. Sci. USA March 1992, Vol 89	1-793 (full length)	Encodes the mammalian homologue for a yeast gene involved in protein import into mitochondria.	Pte-1 pVEEneo
13-L-lysosome associated membrane glycoprotein-1 precursor	No publication	300 bp	3' untranslated region	h13 pCDNA3.1+
17-PPAR-γ2 (Fgf2) Peroxisome proliferator activator receptor-γ	B.M.Spiegelman et al EMBO 1992, Vol 11	3-429 (full length -6 bp)	PPAR-γ cofactor 2 binds to the AF-1 region of PPARγ and to the estrogen receptor. It causes a dramatic increase in fat cell differentiation.	4Fgf2 pCDNA3.1+
20-SAA1 beta gene serum amyloid A	J.Jgerard et al Ann. Rheum. Dis 2001, Vol 40	282-369 (nt)	Involved in the atherosclerosis and amyloidosis	SAA1.1 pRR322 4SAA1 pCDNA3.1+
21-FBP human fibronectin binding protein	D.Lavie et al Mol. Cell 2003, Feb	1731-1933 (nt)	Low of function leads to arrest of proliferation and c-myc expression. Identified as an apoptosis associated protein in human Burkitt lymphoma cell line.	FBP pCDNA1 RSP-ORF 4FBP pCDNA3.1+
22-Mitochondrial DNA control region	No publication	300 bp	??? no apparent reading frame	M2 pCDNA3.1

Tab.2 : Details about the cDNA clones found in the CED4 yeast survival screen. The name and the gene fragments are coupled with the published data and informations.

From the literature and the CED4 expression test, I decided to carry on with the analysis of the following genes:

Human RoRet/zinc finger protein 15.

(accession number: U90547)

Homo sapiens cell death regulator AVEN.

(accession number: AF283508)

Human v-fos transformation effector protein (Fte-1)/

40S ribosomal protein S3a (human)

(accession number: M84711)

PPAR γ -cofactor 2

(similar to the mus musculus PGC2 with accession number: AF220501)

Serum amyloid A (SAA1-2) beta gene.

(accession number: M23698)

Human fuse binding protein.
(accession number: U05040)

3-Anti-apoptotic potential of the candidate clones in mammalian cells

We obtained several full length gene constructs from the laboratories that have either identified these proteins or are further studying them: the full length human *aven* cDNA in the CMV expression vector pSG5 (*aven*-pSG5) from Dr. Marie Harwick (Johns Hopkins University, Baltimore, US), the full length human *fte-1/s3a* cDNA in the MSV expression vector pMEXneo (*fte-1*-pMEXneo) from Dr. Helmut Zarbl (Fred Hutchinson cancer research centre, Seattle, WA, USA), the full length human *SAA1.1 β* cDNA in the cloning vector pBR322 (*SAA1.1 β* -pBR322) from Dr. Barbara Kluge-Beckerman (Dep. Path. And lab. Medicine, Indianapolis, US) and the human *FBP* cDNA in the CMV expression vector pcDNA1/amp from Dr. David L. Levens (NCI, DCS, Bethesda, MD, USA). Δ *roret*, Δ *aven*, *PGC2*, Δ *SAA1.1 β* and Δ *FBP* were cloned in the pcDNA3.1+ mammalian expression vector (*Invitrogen*). Then two functional tests were performed: analysis of the protecting potential of the clones against Bak-GFP induced apoptosis in 293T cells (human embryonic kidney cells, transformed with large T antigen) and against FasL/ α Flag/cycloheximide-induced apoptosis in RKO cells (human colorectal carcinoma cells).

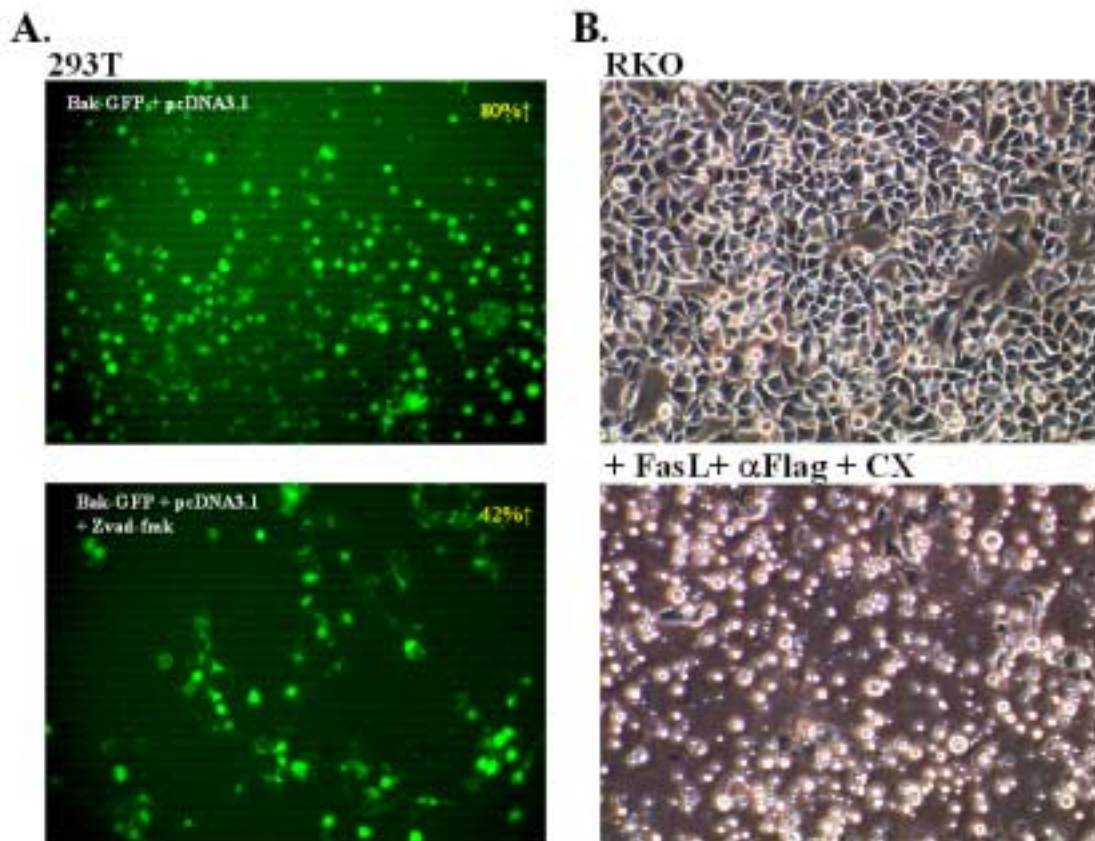
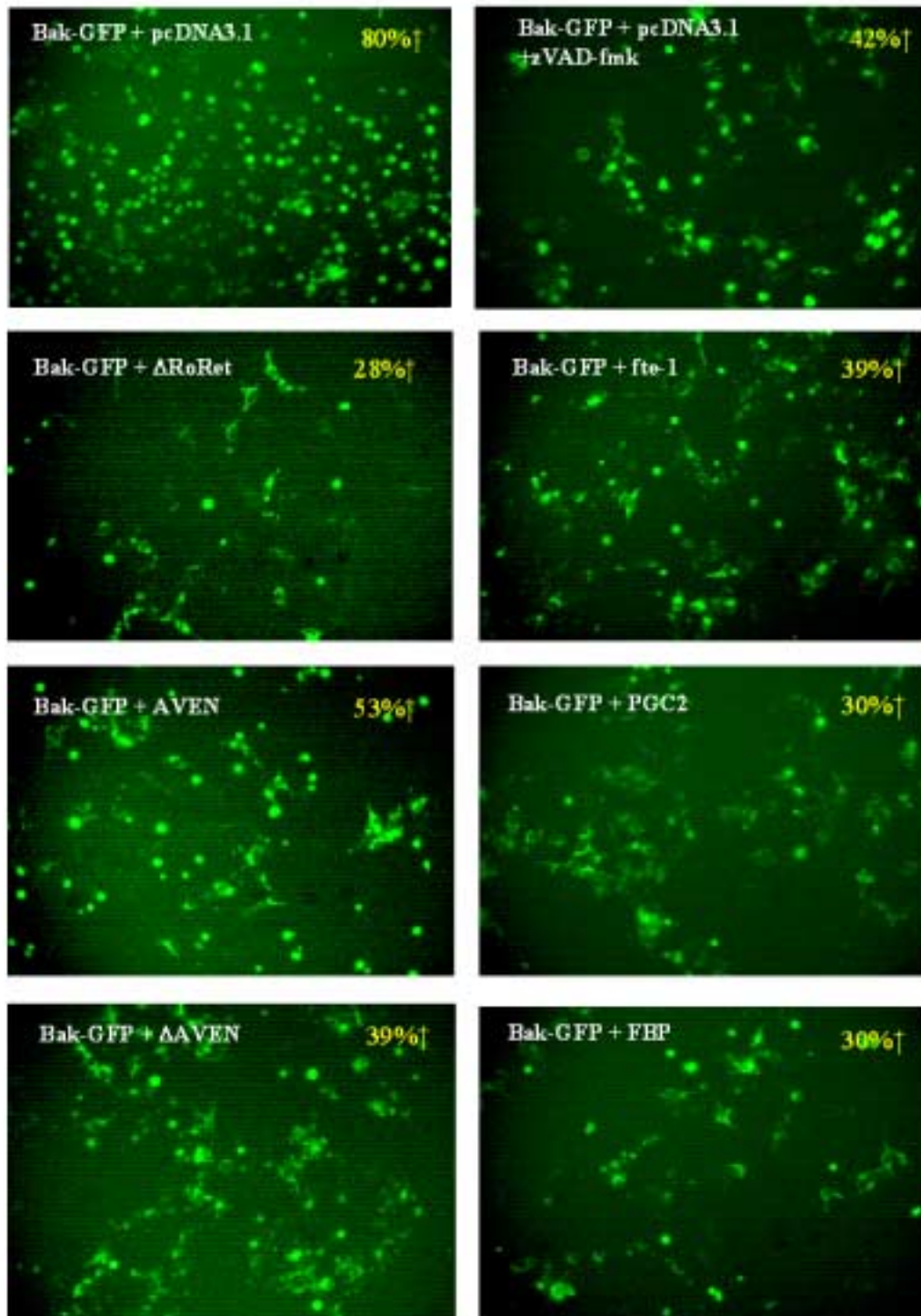


Fig.16: Two different model systems to study apoptosis inhibition by the cDNA clones isolated in the yeast survival screen.

(A) 293T cells were transfected with 0.5 μg *bak-gfp* plus 1.5 μg pcDNA3.1+ and treated (or not) with 10 μM zVAD-fmk. The next day (16 h later) dying cells (round bright green cells) were distinguished from living cells (spread living cells with no GFP in the nucleus) using a fluorescent microscope. (B) RKO cells were transfected with 1 μg pcDNA3.1+ and the next day treated with 10 ng/ml FasL, 1 mg/ml anti-FLAG antibody and 0.1 $\mu\text{g}/\text{ml}$ cycloheximide with or without zVAD-fmk. The next day (16 h later) cells were collected and the percentage of apoptotic cells was determined by FACS analysis of propidium iodide stained fixed cells and by the LIVE/DEAD assay from *Molecular Probes*.

These model systems were used to test the protection efficiency of the isolated clones in mammalian cells and to allow us to select the most potent apoptosis inhibitors.

A.



B.

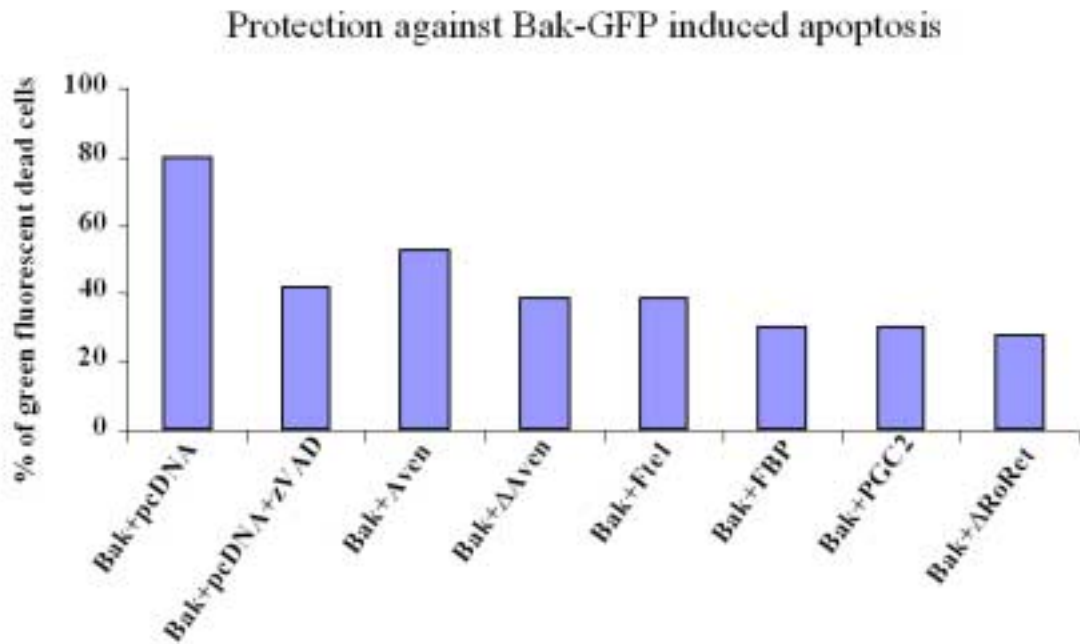


Fig.17: 293T cells were transfected with 0.5 μg *bak-gfp* plus 1.5 μg $\Delta\text{rotet-pcDNA3.1+}$, 1.5 μg *aven-pGS5*, 1.5 μg $\Delta\text{aven-pcDNA3.1+}$, 1.5 μg *fte-1-pMEXneo*, 1.5 μg *pgc2-pcDNA3.1+* or *fbp-pcDNA3*. The next day (16 h later) dying cells (round bright green cells) were distinguished from living cells (spread living cells with no GFP in the nucleus) by fluorescent microscopy. (A) Picture of Bak-GFP expression in the 293T cells. (B) Graphic presentation of green fluorescent dead cells. The experiment was repeated twice with similar results.

Unfortunately, the experiment with ΔSAA1 was unsuccessful (the cell morphology not permitting any real distinction between dead and living cells) and no conclusion about the protective capacity of ΔSAA1 could be obtained by this particular assay.

Fig.18: RKO cells were transfected with either 1 μ g pcDNA3.1+, 1 μ g *aven*-pGS5, 1 μ g Δ *aven*-pcDNA3.1+, 1 μ g *fte-1*-pMEXneo, 1 μ g *fbp*-pcDNA3, 1 μ g Δ *fbp*-pcDNA3.1+, 1 μ g Δ *saal*-pcDNA3.1+, 1 μ g Δ *pgc2*-pcDNA3.1+ or 1 μ g Δ *roret*-pcDNA3.1+. The next day, cells were treated with 10 ng/ml FasL, 1 mg/ml anti-FLAG antibody and 0.1 μ g/ml cycloheximide with or without zVAD-fmk. The next day (16 h later) cells were collected and the percentage of apoptotic cells was determined by FACS analysis of propidium iodide stained fixed cells (blue bars) and by the LIVE/DEAD assay from *Molecular Probes* (brown bars).

The readout of these various experiments was that most clones (full length or Δ deletion mutants as identified in the screen) were efficiently inhibiting apoptosis induced by Bak and FasL, some of them as efficient as the general caspase-inhibitor zVAD. While experimental results with FasL-induced apoptosis gave variable protection potential depending of the experiment (Fig.18 represents one example), the outcome with Bak-induced apoptosis was constant (as shown later by the arrow bars of the Bak protection and caspase activity assays).

3-Computational analysis of Aven, Fte-1 and RoRet.

Computational analysis was done with HUSAR (from webDKFZ site) and NIH-blast (from webPubMed site). The results are represented below as the schematic representations of the proteins (with NIH-blast program) with their predicted domains and additional informations published about the particular protein.

3.1-Aven:



Fig.19: Graphic representation of Aven obtained with NIH-blast. The protein comprise 362 amino-acids. The program could define no homology to any known domain.

BC010488. Homo sapiens, cell death regulator Aven,

CDS 1..1089
 codon_start=1
 product=cell death regulator aven

protein_id=AAH10488.1

translation=MQAERGARGGRGRRPGRGRRPGGDRHSERPGAAA AVARGGGGGG
 GGDGGGRRRGRGRGRGFRGARGGRGGGAPRGSRRREP GGWGAGASAPVEDD
 SDAETYGEENDEQGNYSKRKIVSNWDYQDIEKEVNNESGESQRGTD FSVLL
 SSAGDSFSQFRFAEKEKWDSEASCPKQNSAFYVDSELLV RALQELPLCLRLNV
 AAELVQGTVPLEVPQVKPKRTDDGKGLGMQLKGPLGPGGRGPIFELKS VAA
 GCPVLLGKDNPSGPSRDSQKPTSPLQSAGDHLEEELDLLLNLD APIKEGDNIL
 PDQTSQDLKSKEDGEVVQEEEVCAKPSVTEEKNMEPEQPSTSKNVTEEELED
 WLDSMIS

nucleotide sequence, coding region=1 atgcaggcgg agcaggagc tcggggaggc
 cgtgggaggc ggccaggcgg cggccggcct ggcggagatc gccacagcga gcggccccga gccgcagcgg
 cggtagccag aggcggcggc ggaggcggcg gcggggacgg aggcggacgc cggggccgtg gccgtggccc
 gggcttccgc ggcgctcgcg gaggccgagg aggaggaggc gccccgcgag gcagccgccc ggagccggga
 ggctggggcg caggggccag cgcgccggtt gaagatgaca gcgatgcaga gacctatgga gaagagaatg
 atgaacaggg aaattattct aaaagaaaga ttgtctctaa ctgggatcga tatcaagata ttgaaaaaga
 ggtcaataat gaaagtggag agtcacagag gggaacagat ttcagtgtcc tccttagctc tgcaggggac
 tcattctcac agttccggtt tgctgaggag aaagaatggg atagtgaagc ttctgtcca aacagaatt cagcattta
 tgtgatagt gattattgg ttcgagcct tcaagagctg cctctctgcc tccgactcaa cgttctgcc
 gaactgttcc agggtagct tcttttagag gttcctcagg tgaacccaaa gagaactgat gatggcaagg
 gattagggat gcagttaaag gggcccttgg ggctggagg aagggggccc atctttgagc tgaatctgt
 ggctgtggc tgcctgtgt tgctgggcaa agacaacca agcccgggtc ctcaaggga ttctcagaaa
 cccacttccc cactgcagtc agcaggagac catttgaag aagaactaga tctgttctt aatttagatg
 cacataaaa agagggat aacatctac cagatcagac gtctcaggac ctgaaatcca aggaagatgg
 ggaggtgtgc caagaggaag aagttgtgc aaaaccatct gtgactgaag aaaaaacat ggaacctgag
 caaccaagta cctcaaaaaa tgttaccgag gaagagctgg aagactgggt ggacagcatg atttctaa 1081

3.2-Fte-1/S3a:



Fig.20: Graphic representation of Fte-1/S3a obtained with NIH-blast. The protein comprise 264 amino-acids. The blue regions represent so called low complexity regions. The program could define a domain with homology to the Ribosomal_S3ae domain and homology to the Ribosomal protein S1a (RPS1A).

M84711. Human v-fos transformation effector protein (Fte-1),

AUTHORS Kho,C.J. and Zarbl,H.

TITLE Fte-1 encodes a gene that is highly conserved during evolution

JOURNAL Unpublished (1992)

```

gene      1..795
          gene=Fte-1
CDS      1..795
          codon_start=1
          product=v-fos transformation effector protein
          protein_id=AAA58487.1
  
```

```

translation=MAVGKNKRLTKGGKKGAKKKVVDPFSKGDWYDVKAPAMFNIR
NIGKTLVTRTQGTKIASDGLKGRVFEVSLADLQNDEVAFRKFKLITEDVQ GK
NCLTNFHGMDLTRDKMCSMVKKWQTMIEAHVDVKTTDGYLLRLFCVGF TK
KRNNQIRKTSYAQHQQVRQIRKKMMEIMTREVQTNDLKEVVNKLIPDSIGKD
IEKACQSIYPLHDVFVRKVKMLKKPKFELGKLMELHGEGSSSGKATGDETGA
KVERADGYEPPVQESV
  
```

```

nucleotide sequence, coding region=1 atggcggttg gcaagaacaa ggcgcttacg aaagcgggca
aaaagggagc caagaagaaa gtgggtgac catttctaa gaaagattgg tatgatgtga aagcacctgc
tatgttcaat ataagaata ttgaaagac gctcgtcacc aggaccaag gaacaaaat tgcattgat
ggtctcaagg gtcgtgtgtt tgaagtgagt ctgctgatt tgcagaatga tgaagtgca ttagaaaat tcaagctgat
tactgaagat gttcagggtg aaaactgcct gactaactc catggcatgg atcttaccg tgacaaaatg
tgttccatgg tcaaaaatg gcagacaatg attgaagctc acgttgatgt caagactacc gatggttact tgcctcgtc
gttctgtgtt ggtttacta aaaaacgcaa caatcagata cggaagacct cttatgctca
gcaccaacaggtccgcaaaa tccggaagaa gatgatggaa atcatgacc gagaggtgca gacaaatgac
ttgaaagaag tggtaataa attgattcca gacagcattg gaaaagacat agaaaaggct tgccaatcta tttatcctc
ccatgatgtc ttcgttagaa aagtaaaaat gctgaagaag cccaagttg aattgggaaa gctcatggag
cttcattgtg aaggcagtag ttctggaaa gccactgggg acgagacagg tgctaaagt gaacgagctg
atggatatga accaccagtc caagaatctg ttaa 781
  
```

3.3-RoRet:

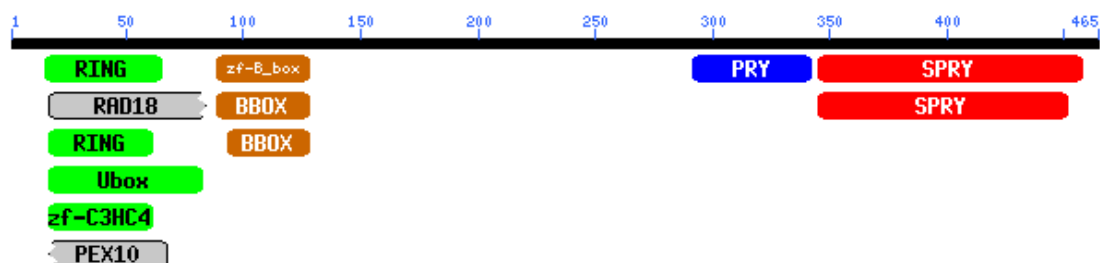


Fig.21: Graphic representation of RoRet obtained with NIH-blast. The protein comprise 362 amino-acids. The program could define several domains with homology to known protein domains (SPRY, PRY, BBOX, RING and zf-C3HC4 which are explained in the discussion).

U90547 Human Ro/SSA ribonucleoprotein homolog (RoRet)

Chromosomal Locus HSU90547 REGION: 22..1419

AUTHORS Ruddy,D.A., Kronmal,G.S., Lee,V.K., Mintier,G.A., Quintana,L.,
Domingo,R. Jr., Meyer,N.C., Irrinki,A., McClelland,E.E., Fullan,A.,
Mapa,F.A., Moore,T., Thomas,W., Loeb,D.B., Harmon,C.,
Tsuchihashi,Z., Wolff,R.K., Schatzman,R.C. and Feder,J.N.

TITLE A 1.1-Mb transcript map of the hereditary hemochromatosis locus

JOURNAL Genome Res. 7 (5), 441-456 (1997)

PUBMED 9149941

chromosome=6

map=6p21.3

gene 1..1398

gene=RoRet

CDS 1..1398

product=Ro/SSA ribonucleoprotein homolog

protein_id=AAB53425.1

translation=MASTTSTKMMEEATCSICLSLMTNPVSINCGHSYCHLCITDFFKN
PSQKQLRQETFCPPQCRAFPFHMDSLRPNKQLGSLIEALKETDQEMSCEEHGE
QFHLFCEDQGLICWRCERAPQHKGHTTALVEDVCQGYKEKLQKAVTKLKQ
LEDRCTEQKLSTAMRITKWKEKVQIQRQKIRSDFKNLQCFLHEEEKSYLWRL
EKEEQQTLRRLRDYEAGLGLKSNELKSHILELEEKCOGSAQKLLQNVNDTSL
RSWAVKLETSEAVSLELHTMCNVSKLYFDVKKMLRSHQVSVTLDPDTAHHE
LILSEDRRQVTRGYTQENQDTSSRRFTAFCVVGCEGFTSGRRYFEVDVGEFT
GWDLVGCMENVQRGTGMKQEPQSGFWTLRLCCKKGYVALTSPPTSLHLHE
QPLLVGIFLDYEAGVVSFYNGNTGCHIFTFPKASFSDTLRPYFQVYQYSPLFLP
PPGD

nucleotide sequence, coding region=1 atggcctcaa ccaccagcac caagaagatg atggaggaag
ccacctgctc catctgcctg agcctgatga cgaacccagt aagcatcaac tgtggacaca gctactgcca
cttgtgtata acagacttct ttaaaaacce aagccaaaag caactgaggc aggagacatt ctgctgtccc
cagtgtcggg ctccatttca tatggatagc ctccgacca acaagcagct gggaagcctc attgaagccc
tcaaagagac ggatcaagaa atgtcatgtg aggaacacgg agagcagttc cacctgttct gcgaagacga
ggggcagctc atctgtggc gctgtgagcg ggcaccacag cacaagggc acaccacagc tctgttgaa
gacgtatgcc agggctacaa ggaaaagctc cagaaagctg tgacaaaact gaagcaact gaagacagat
gtacggagca gaagctgtcc acagcaatgc gaataactaa atggaaagag aaggtacaga ttcagagaca
aaaaatccgg tctgacttta agaatctcca gtgttctca catgaggaag agaagtctta tctctggagg
ctggagaaag aagaacaaca gactctgagt agactgaggg actatgaggc tggctgggg ctgaagagca
atgaactcaa gagccacatc ctggaactgg aggaaaaatg tcagggctca gccagaaat tgtctcagaa
tgtaatgac actttgagca ggagttgggc tgtgaagctg gaaacatcag aggtgtctc ctggaact
catactatgt gcaatgttc caagctttac ttcgatgtga agaaaatgtt aaggagtcat caagttagtg tgactctgga
tccagataca gctcatcacg aactaattct ctctgaggat cggagacaag tgactcgtgg atacaccag
gagaatcagg acacatcttc caggagattt actgccttc cctgtgtctt gggtttgaa ggcttcacct
caggaagacg ttactttgaa gtggatgtg gcgaaggaac cggatgggat ttaggagttt gtatggaaaa
tgtcagagg ggcactggca tgaagcaaga gcctcagctt ggattctgga ccctcaggct gtgcaaaaag
aaaggctatg tagcacttac ttctcccca acttccttc atctgcatga gcagcccctg cttgtgggaa ttttctgga
ctatgaggcc ggagttgat cctttataa cgggaatact ggctgccaca tctttacttt cccgaaggct tcttctctg
atactctccg gcctatttc caggtttatc aatattctcc ttgtttctg cctccccag gtgactaa 1381

Since I only isolated the 548 last nucleotides of RoRet cDNA, we obtained two full length cDNAs from *ResGen* (*Invitrogen corporation*): one cDNA from the *Celera* library (RoRet-pCMV.SPORT6) and one cDNA from the *Genestorm* library (RoRet-pcDNA3.1/GS).

C-Results in S. pombe

1-The protection potential against Bak- and CED4- induced yeast cell death.

To test the specificity of the protection I assessed the inhibitory potential of the clones B1(RoRet), B2(Aven) and B12(Fte-1) against CED4- and Bak- induced yeast cell death. DSI is an *S. pombe* strain which expresses Bak under control of the *nmt-1* promoter (as the strain HC4 expresses CED4 under control of the same promoter). I transformed DSI and HC4 with either the empty expression vector pArt1 as a control, Δ roret-pArt1 (B1), Δ aven-pArt1 (B2) or *fte-1*-pArt1 (B12). When colonies appeared, yeasts were replica-plated twice on selective medium without thiamine to induce Bak and CED4 expression (Fig. 22).

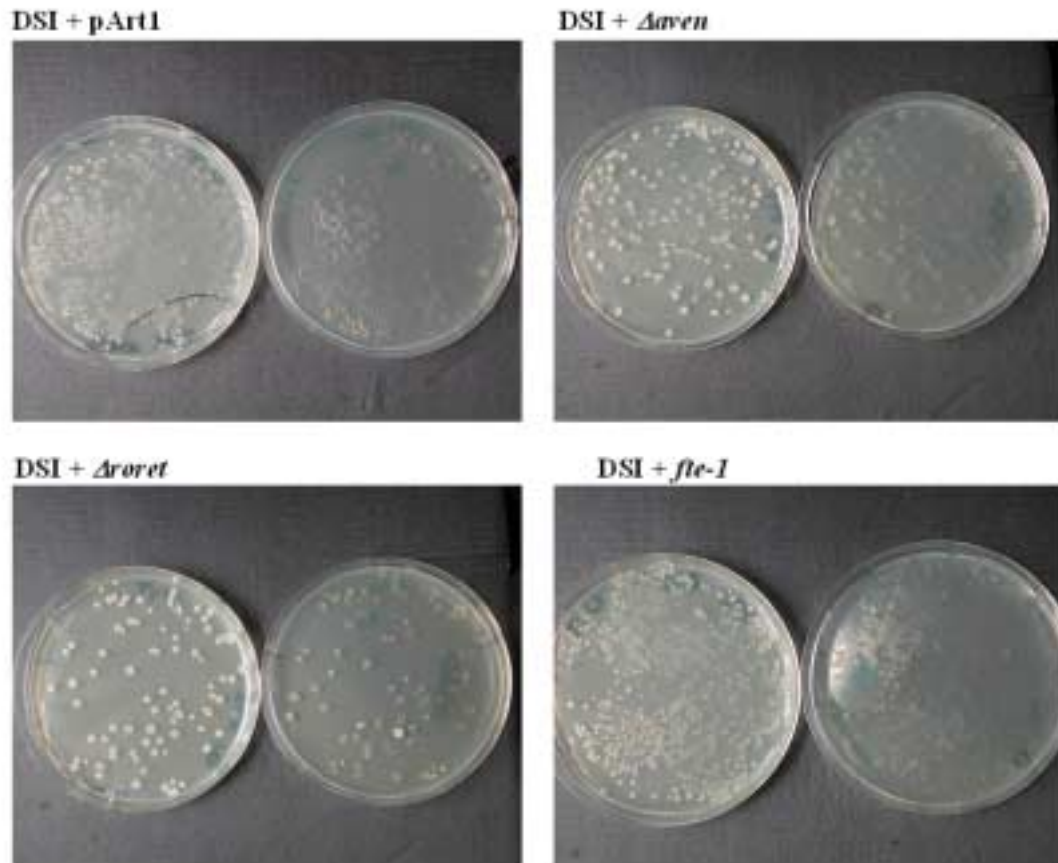


Fig. 22: (Left of each picture) DSI yeast cells were transformed with 1 μ g *pArt1*, Δ *roret*-*pArt1* (B1), Δ *aven*-*pArt1* (B2) or *fte-1*-*pArt1* (B12) and plated on agar plates containing uracil and thiamine. (left plate in each picture) When the colonies had appeared, they were replica-plated in absence of thiamine to allow induction of Bak expression (right plate in each picture).

The yeast cells died very efficiently on all plates, and none of the clones was able to confer protection against Bak-induced killing in *S. pombe*.

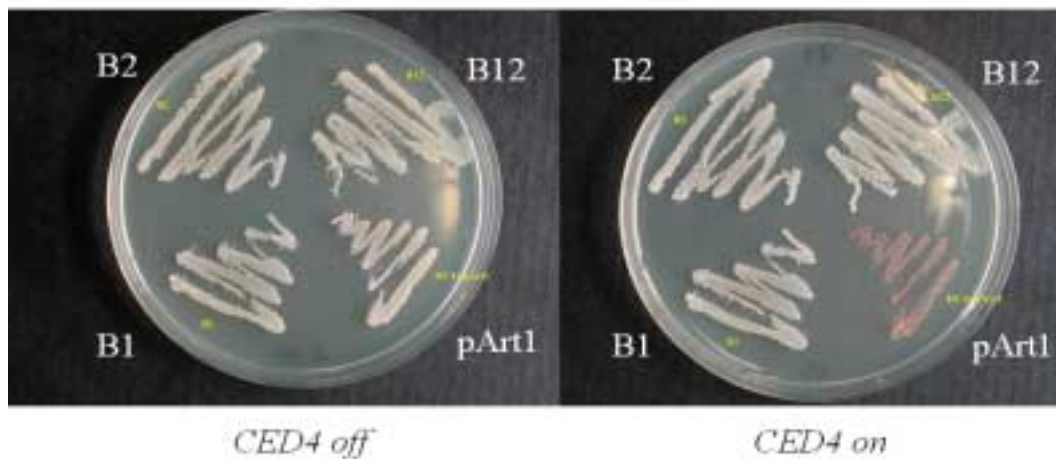


Fig.23: Left: HC4 yeast were transformed with 1 μ g *pArt1*, Δ *roret*-*pArt1* (B1), Δ *aven*-*pArt1* (B2) or *fte-1*-*pArt1* (B12) and plated on uracil and thiamine containing agar plates. The yeast colonies were growing in the absence of CED4 expression. Right: when colonies appeared, they were replica-plated twice on agar plates lacking thiamine to allow induction of CED4 expression. Dead yeast cells appear dark red after uptake of phloxin.

HC4 transformed with empty *pArt1* vector became phloxin-red and died, whereas HC4 transformed with Δ *roret*, Δ *aven* or *fte-1* continued to grow which proves protection by these cDNAs against CED4-induced cell death in *S. pombe*.

2-CED4 induces cell death rather than growth arrest in *S. pombe* and Aven, RoRet and Fte-1 confer protection against CED4 yeast killing

To distinguish whether CED4 induces cell death or growth arrest in *S. pombe*, I set up the following experiment: HC4 transformed with *pArt1*, Δ *roret*-*pArt1*, Δ *aven*-*pArt1* or *fte-1*-*pArt1* were cultured in liquid culture medium containing uracil and thiamine up to O.D.₆₀₀ 0.5. They were then incubated in selective medium inducing CED4 expression for 16h, 24h, 40h, 48h and 64h. When the yeast cultures reached an O.D.₆₀₀ of 0.8 they were again diluted to 0.2. At each time point mentioned, an aliquot of the same number of yeast cells (calculated using the O.D.₆₀₀) was plated on agar plates containing uracil and thiamine to repress again expression of CED4 and to test if the yeast cells were able to regrow. We reasoned that if colonies appeared, the yeasts would have only been blocked in growth. Otherwise the yeast cells would have been killed by CED4 expression.

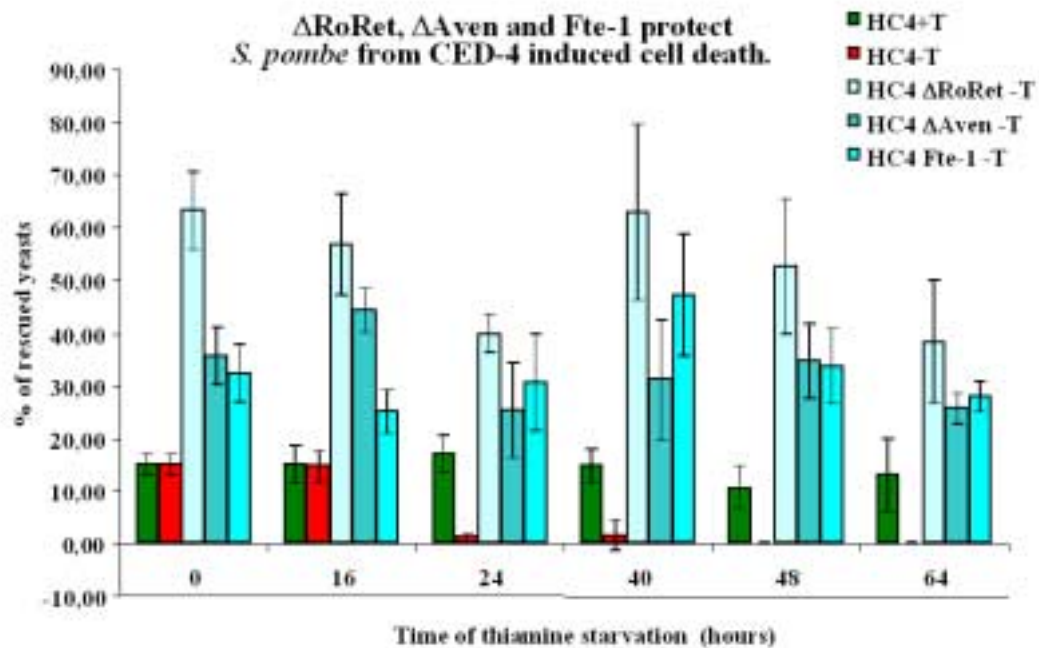


Fig. 24: HC4 containing Δ roret, Δ aven and *fte-1* were starved of thiamine for different lengths of time. 200 yeast cells each were plated on thiamine-containing agar plates to repress again CED4 expression. After 2 days colony number were counted and presented as percentage of rescued yeast colonies.

Fig. 26 shows that CED4 not only induces growth arrest but rather kills *S. pombe* yeast cells, and that Δ RoRet, Δ Aven and Fte-1 can protect against CED4 killing.

3-Yeast protection assay in liquid medium

To further investigate the protection efficiency of the clones in *S. pombe*, I measured growth curves of HC4 transformed with pArt1, Δ roret-pArt1, Δ aven-pArt1 or *fte-1*-pArt1. Transformed yeasts were cultured in liquid culture medium containing uracil and thiamine up to O.D.₆₀₀ 0.5. They were then washed twice with water before diluting them in medium containing uracil at O.D.₆₀₀ 0.05 and incubating them in selective medium without thiamine for 20h, 40h, 60h and 80h. When yeasts reached an O.D.₆₀₀ of 0.8 they were again diluted to 0.05 to prevent growth arrest because of too low yeast cell concentrations.

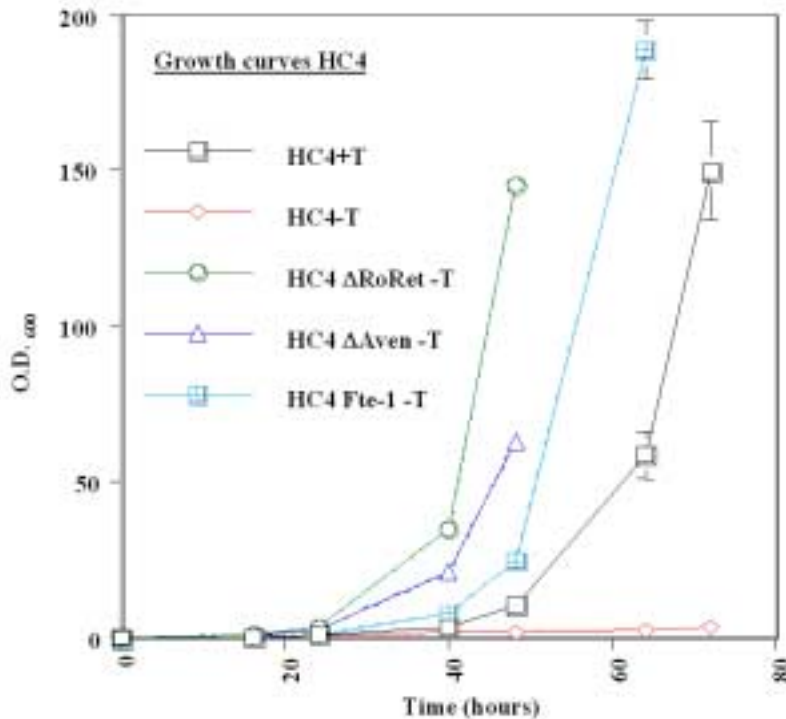


Fig.25: The transformed HC4 yeast strains containing the protecting library plasmids were cultured for 24h in yeast medium plus thiamine, which represses CED4 transcription. The cells were then washed with H₂O twice and diluted to approximately 0.05 O.D. ₆₀₀, in medium with (+T, -CED4) or without thiamine (-T, +CED4). Cell expansion was quantified by measuring the O.D. ₆₀₀.

The results showed that $\Delta roret$ was the most efficient cDNA to protect yeast cells against CED4 induced cell death. $\Delta Aven$ and Fte-1 were also protecting CED4-expressing yeast cells.

D-Functional assays

1- Apoptosis assays quantified by FACS analysis

It was now important to quantify the protection effect of Aven, RoRet and Fte-1 in mammalian systems (293T and RKO cells) and their efficiency *in vivo* against different apoptotic stimuli (are they general apoptosis inhibitors or do they inhibit only specific killing stimuli). Therefore I cloned *roret*, $\Delta roret$ and $\Delta aven$ in mammalian expression vectors: *Flag-roret*-pCR33, *roret*-pEGFP, $\Delta roret$ -pcDNA3.1+, *Flag-Δroret*-pCR33, $\Delta roret$ -pEGFP, $\Delta aven$ -pcDNA3.1+, $\Delta aven$ -pEGFP and *fte-1*-pEGFP. Further constructs were obtained either from other laboratories or they were purchased commercially: *aven*-pSG5, *roret*-pcDNA3.1/GS and *fte-1*-pMEXneo (for further details about these constructs, see *Material and methods, Plasmids maps and cloning strategies*).

Because I had screened for inhibitors downstream of apoptosome formation, I first looked at the apoptosis-inhibiting potential of Aven, RoRet and Fte-1 against caspase-9-induced apoptosis [Rodriguez, 1999 #6714]. I co-transfected RKO cells with the constitutively active *apaf-1* M368L kindly provide by Dr. Gabriel Núñez (University of Michigan Medical School, Ann Arbor, MI, USA), *caspase-9* and either pcDNA3.1+, Δ *roret*-pcDNA3.1+, *roret*-pcDNA3.1/GS, Δ *aven*-pcDNA3.1+, *aven*-pSG5, *fte-1*-pMEXneo or *bcl-x_L*-pcDNA3.1. Apaf-1 M368L is an Apaf-1 mutant that can bind and activate Caspase-9 without Cytochrome *c* induced conformational change [Hu, 1999 #3617]. I analysed by FACS the influence of Aven, RoRet and Fte-1 on apoptotic cell death.

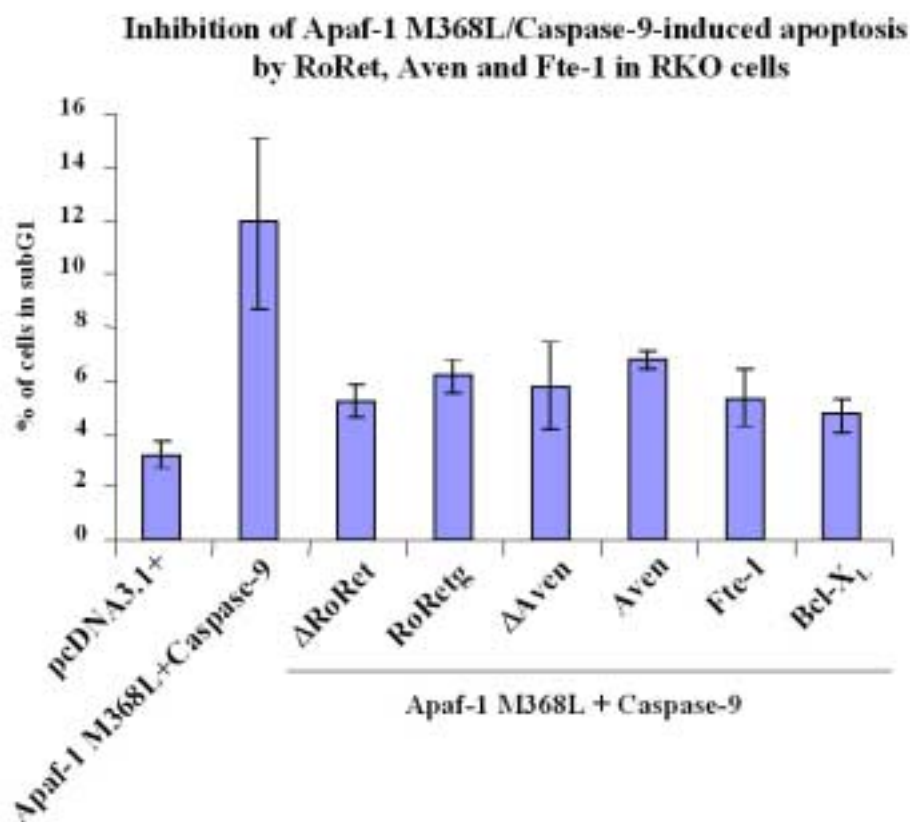


Fig.26: 1×10^6 RKO cells were transfected by *Fugene* with pcDNA3.1+, or *apaf-1* M368L/*caspase-9* with either pcDNA3.1+, or Δ *roret*-pcDNA3.1+, *roret*-pcDNA3.1/GS (RoRetg), Δ *aven*-pcDNA3.1+, *aven*-pSG5, *fte-1*-pMEXneo or *bcl-x_L*-pcDNA3.1. The next day, cells were fixed, stained with PI and analysed by FACS. The experiment was done three times in triplicates. One of the three similar results is shown above and the error bars indicate the variation between the three samples of the triplicate in one experiment.

RoRet, Aven, Fte-1 and their deletion mutants were efficient in inhibiting DNA fragmentation and cell death in a reproducible manner. The low percentage of dead cells was certainly due to the poor transfection efficiency in RKO cells.

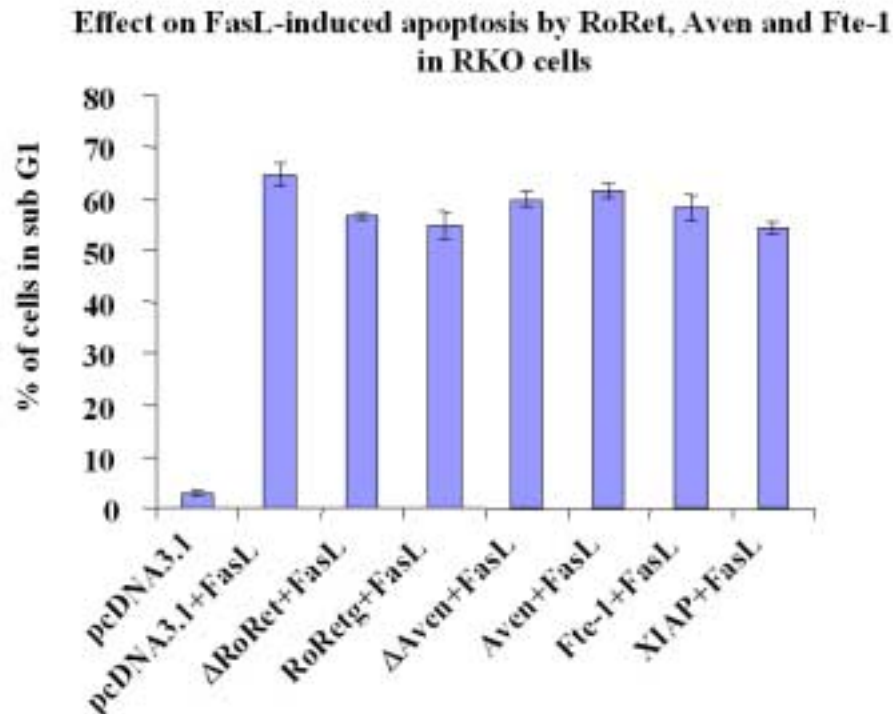


Fig. 27: 1×10^6 RKO cells were transfected with 1 μ g pcDNA3.1+, 1 μ g Δ roret-pcDNA3.1+, 1 μ g *roret*-pcDNA3.1/GS, 1 μ g Δ aven-pcDNA3.1+, 1 μ g *aven*-pGS5, 1 μ g *fte-1*-pMEXneo or *xiap*-pEBB. XIAP-pEBB was kindly provided by Dr. Colin S Duckett (University of Michigan Medical School, Ann Arbor, MI, USA) and contains an EF-1 α promoter. 16 hours later, cells were treated with 10 ng/ml FasL, 1 mg/ml anti-FLAG antibody and 0.1 μ g/ml cycloheximide with or without zVAD-fmk. 8 hours later cells were collected and the percentage of apoptotic cells was determined by FACS analysis of propidium iodide stained fixed cells. The experiment was done three times in triplicates. One of the three similar results is shown above and the error bars indicate the variation between the three samples of the triplicate in one experiment.

The protection efficiency observed was barely visible when measured by FACS, but the control was not very convincing either, suggesting that technical problems like the transfection efficiency, may obscure the obtained results.

I then tested whether RoRet, Aven, Fte-1 and the Δ -deletion mutants protect against UV-induced apoptosis.

Inhibition of UV-induced apoptosis by RoRet, Aven and Fte-1 in RKO cells

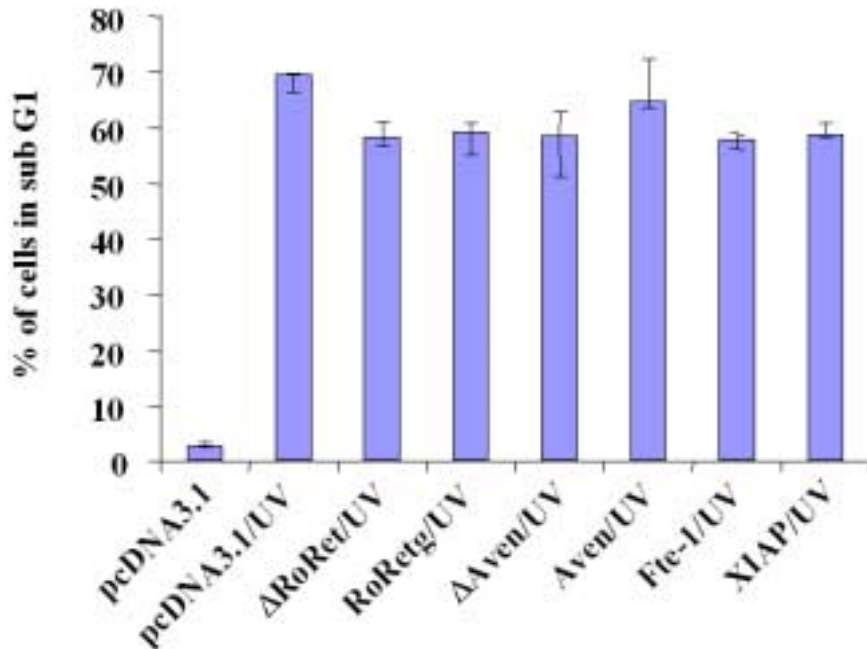


Fig. 28: 1×10^6 RKO cells were transfected with 1 μ g pcDNA3.1+, 1 μ g Δ roret-pcDNA3.1+, 1 μ g *roret*-pcDNA3.1/GS (RoRetg), 1 μ g Δ aven-pcDNA3.1+, 1 μ g *aven*-pGS5, 1 μ g *fte-1*-pMEXneo or *xiap*-pEBB. 16 hours later, cells were treated with 20 sec UV light. The next day (16 h later) cells were collected and the percentage of apoptotic cells was determined by FACS analysis of propidium iodide-stained fixed cells. The experiment was done three times in triplicates. One of the three similar results is shown above and the error bars indicate the variation between the three samples of the triplicate in one experiment.

As for the CD95 killing the protection efficiency against UV-induced apoptosis was not very convincing. Only about 10-15% protection was observed. The low transfection efficiency of RKO cells (20-30%) at best (with the XIAP control) was a serious problem and therefore I decided to change model.

2- Apoptosis quantified by the LIVE/DEAD assays

In the first experiment I tested the specific protection efficiency of RoRet, Aven and Fte-1 against Apaf-1 M368L/Caspase-9 induced apoptosis. Again I used the mutated form of Apaf-1 (Apaf-1 M368L) that does not need Cytochrome *c* release to bind Caspase-9 and to trigger its cleavage and activation.

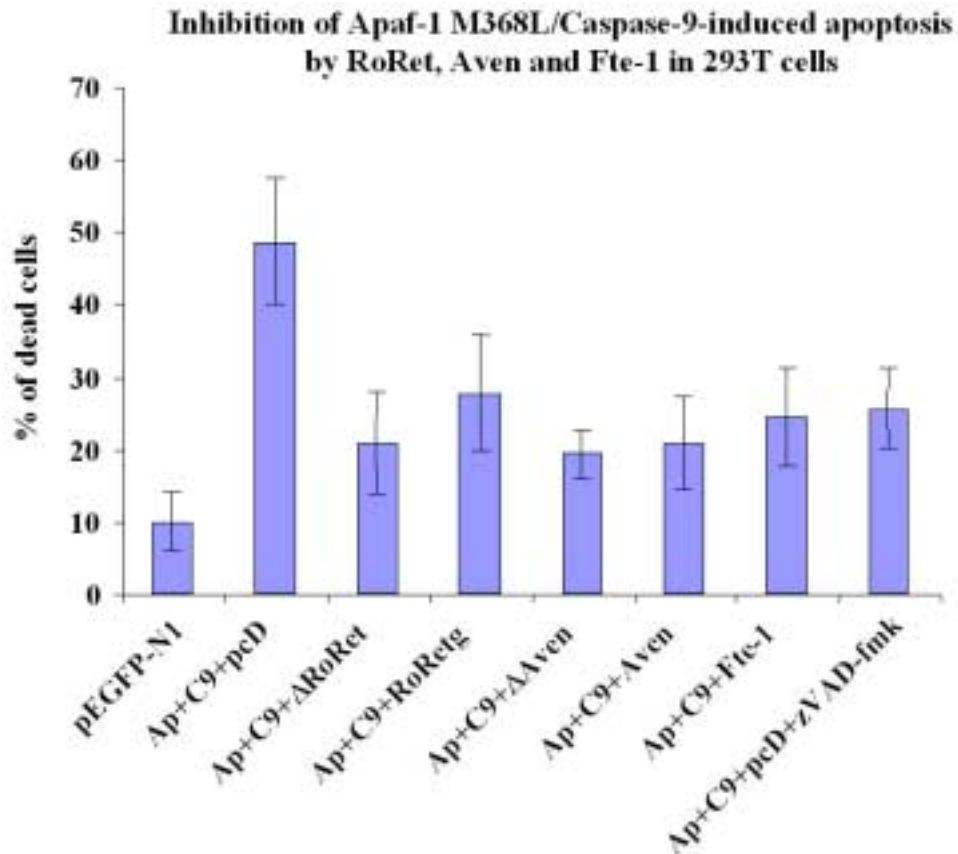


Fig. 29: 1×10^6 293T cells were transfected with $0,3 \mu\text{g}$ *apaf-1M368L* (Ap)+ $0,3 \mu\text{g}$ *caspase-9* (C9)+ $1,2 \mu\text{g}$ protector plasmid DNA by PEI. The following day cells were stained, and red dead cells and green living cells were both counted in a fluorescence microscope using UV-light. The figure represents one of three similar experiments done in triplicates. For each sample 200 cells were counted. The error bars represent the variation between the three sample of a triplicate.

In this assay RoRet, Aven and Fte-1 inhibit Apaf-1/caspase-9 -induced apoptosis in human 293T cells as they do in RKO cells (see Fig. 26)

The pro-apoptotic Bcl-2 family member Bak is known to trigger mitochondrial induction and to induce apoptosis. I was interested to test whether RoRet, Aven and Fte-1 inhibit Bak-induced apoptosis in mammalian cells, as they protect against yeast killing by Bak.

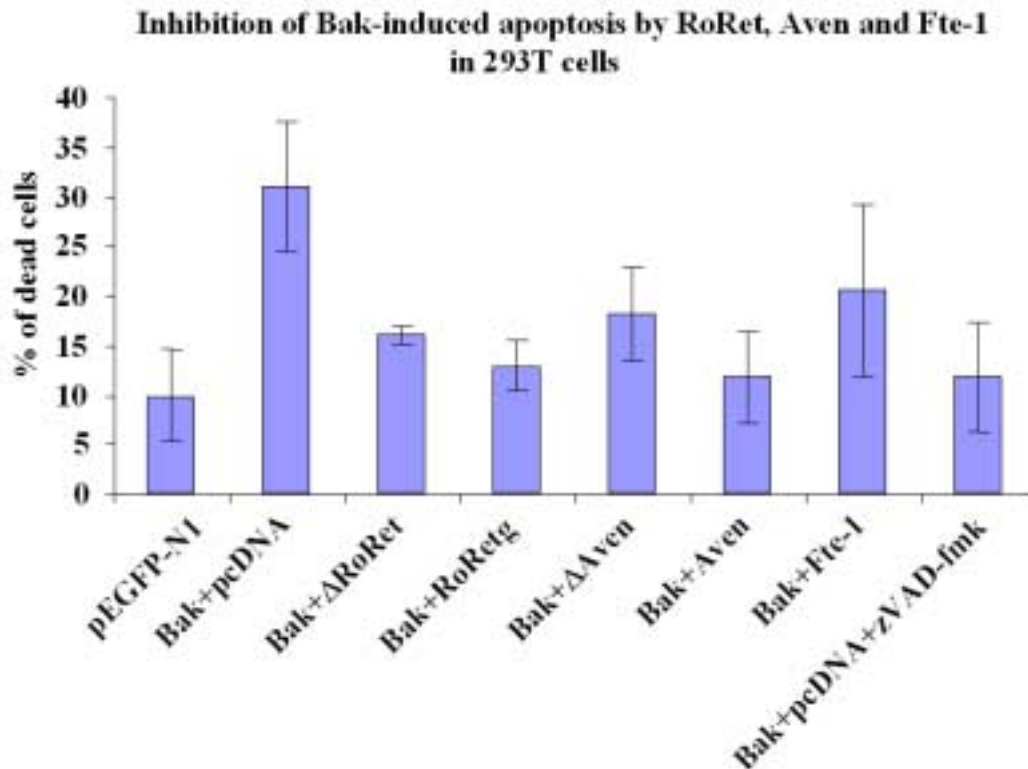


Fig.30: 1×10^6 293T cells were transfected with $0,5 \mu\text{g}$ *bak-gfp* + $1,5 \mu\text{g}$ protector plasmid DNA (*roret*, *aven*, *fte-1*) by the PEI method. The next day cells were stained and red dead cells versus green living cells in UV light were counted using a fluorescent microscope. The figure represents one of three similar experiments done in triplicates. For each sample 200 cells were counted. The error bars represent the variation between the three sample of a triplicate.

RoRet, Aven, Fte-1 and their deletion mutants could efficiently inhibit Bak-induced apoptosis.

E- Analysis of the molecular pathways by which RoRet, Aven and Fte-1 may inhibit apoptosis

One way to analyse at which level of the apoptotic programme a certain protein is inhibiting cell death is to look for caspase cleavage and activation.

1- Analysis of Caspase-9 and -3 cleavage by Western Blot

In a set of different experiments I looked at Caspase-9 and -3 cleavage. I transfected 293T cells with either pcDNA3.1+, or *apaf-1* M368L/*caspase-9* with

pcDNA3.1+, $\Delta roret$ -pcDNA3.1+, $\Delta aven$ -pcDNA3.1+, *aven*-pSG5 or *fte-1*-pMEXneo. The next day I lysed the cells and looked in Western Blot for procaspase-9 cleavage. The results of the three Western Blots shown below lack data about RoRet full length, because at this time the full length cDNA was not available.

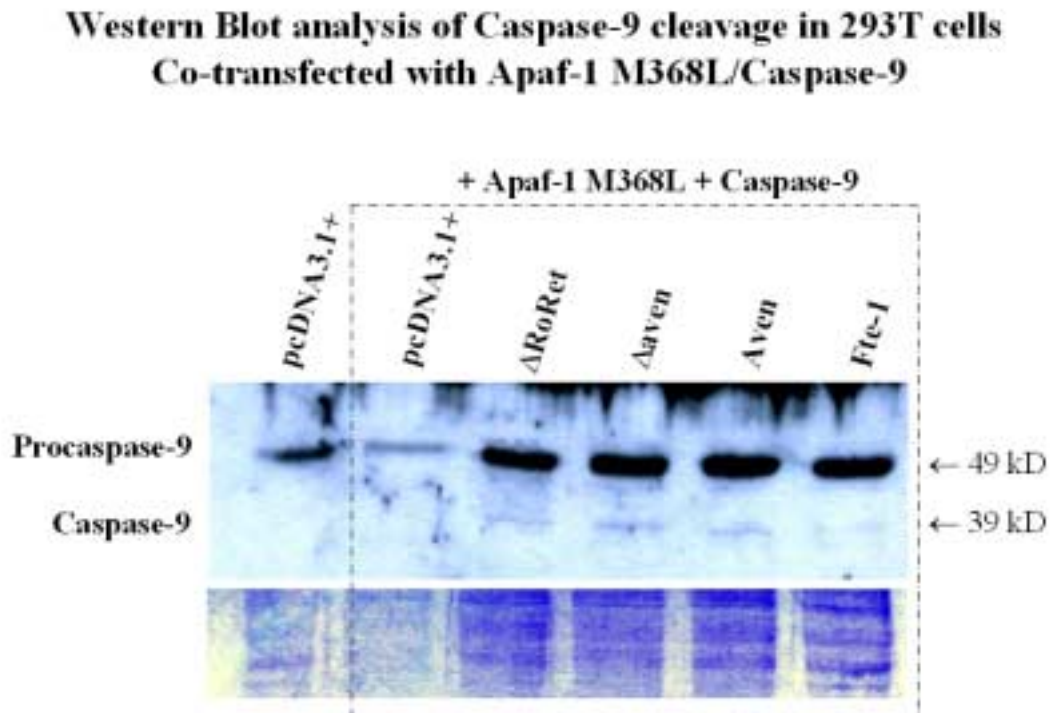


Fig. 31: 1×10^6 293T cells were transfected with $0,3 \mu\text{g}$ *apaf-1M368L* + $0,3 \mu\text{g}$ *caspase-9* + $1,2 \mu\text{g}$ protector plasmid DNA (*aven*, *fte-1* and $\Delta roret$) by the PEI method. The following day cells were lysed and procaspase-9 cleavage was analysed by Western Blot with an anti-Caspase-9 antibody (1/1000) from Pharmingen, and anti-rabbit secondary antibody (1/2000) from Amersham.

I observed that pro-Caspase-9 was disappearing when cells over-express Apaf-1 M368L and Caspase-9. The levels of procaspase-9 were maintained like in healthy cells when the protecting proteins (*Aven*, *Fte-1* and $\Delta RoRet$) were overexpressed together with Apaf-1 M368L and Caspase-9, even though a faint band at the correct size of the large subunit of Caspase-9 (p39) was still visible, suggesting that the inhibition was not complete. It is unclear why this p39 band was not visible in the cells transfected with *apaf-1 M368L/caspase-9* only cells. A possibility would be that the cells are completely dead and that the proteins are already partly degraded.

I then looked at endogenous Caspase-3 cleavage by Western Blot. In this experiment I used RKO cells because they are sensitive to FasL-induced apoptosis and have a detectable amount of endogenous Caspase-3. Therefore, they need to be

transfected only with the protector gene, while in the previous experiment it was important to reach a high transfection efficiency which is possible in 293T cells but not in RKO cells.

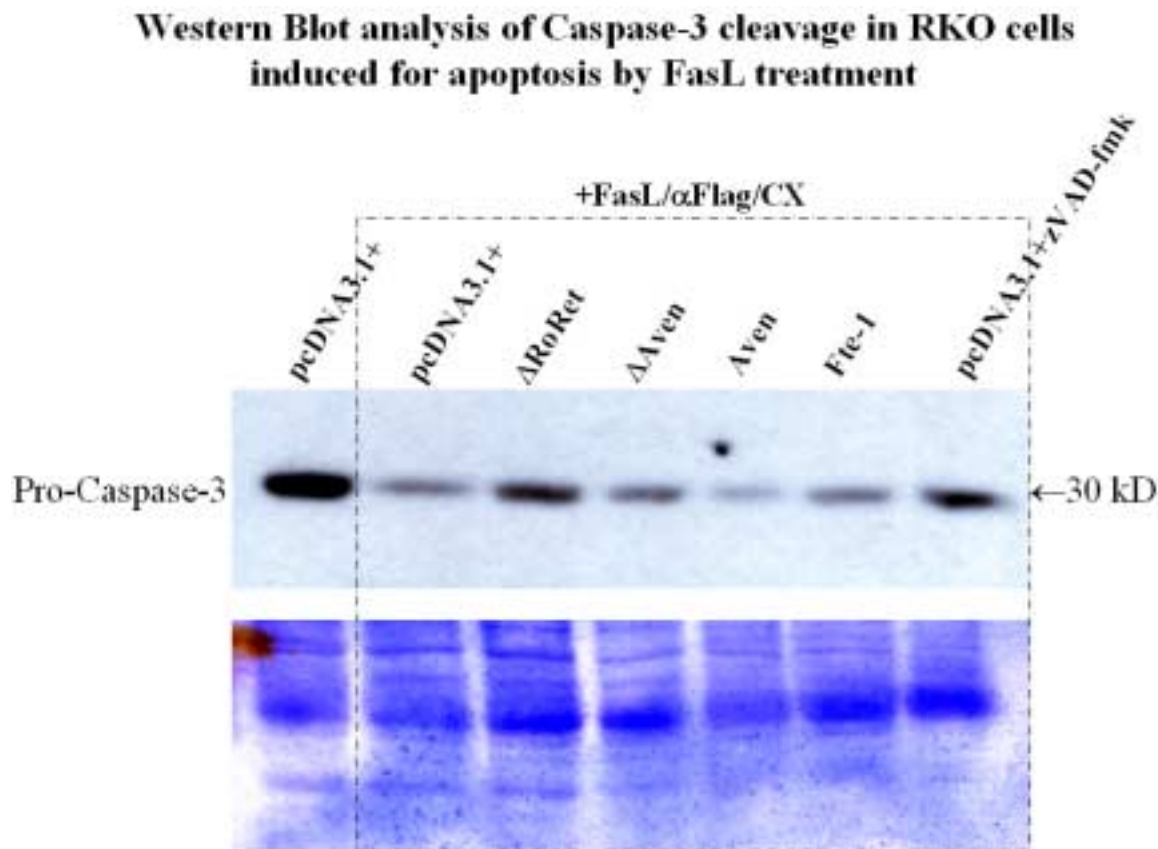


Fig. 32: 1×10^6 RKO cells were transfected with 1 μ g pcDNA3.1+, 1 μ g Δ roret-pcDNA3.1+, 1 μ g Δ aven-pcDNA3.1+, 1 μ g *aven*-pGS5, or 1 μ g *fte-1*-pMEXneo. The next day, cells were treated with 10 ng/ml FasL, 1 mg/ml anti-FLAG antibody and 0.1 μ g/ml cycloheximide with or without zVAD-fmk. 16 h later the cells were collected and lysed. Cell lysates were analysed for Caspase-3 cleavage by Western Blot using anti-Caspase-3 antibody (1/1000) from *Santa Cruz* (and anti-rabbit antibody (1/2000) from *Amersham*).

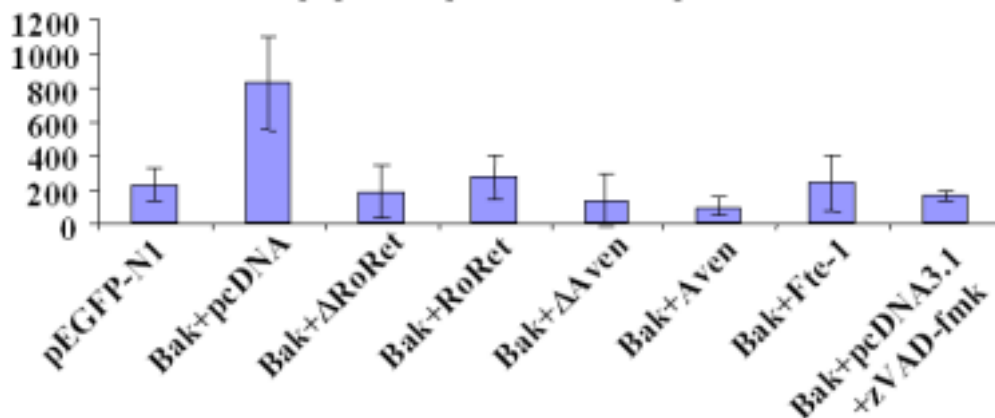
In this experiment the disappearance of the pro-Caspase-3 band was taken as a measure for pro-Caspase-3 cleavage. As can be seen in Fig. 32, Δ RoRet and Δ Aven could inhibit in part procaspase-3 cleavage, whereas Aven and Fte-1 were ineffective to do so when killed by FasL-induced apoptosis.

2- Inhibition of Caspase-9 and – 3 activity by Aven, RoRet and Fte-1

Caspases are enzymes whose activity can be inhibited either by preventing their cleavage and subsequent activation, or by inhibiting the activity of the already

active enzyme. The difficulty to assess a real difference in the amount of cleaved Caspase-9 or -3 lead to the hypothesis that the inhibition may take place after the cleavage, and would affect enzyme activity. Therefore, I looked for caspase activity inhibition in 293T cells. I transfected 293T cells with pEGFP-N1, or *bak-gfp* with pcDNA3.1+, Δ *roret*-pcDNA3.1+, *roret*-pcDNA3.1/GS, Δ *aven*-pcDNA3.1+, *aven*-pSG5 or *fte-1*-pMEXneo. The next day I lysed the cells and measured Caspase-9 and -3 activity using fluorescent peptides as specific substrates.

A. Inhibition of Caspase-9 activity in 293T cells induced to undergo apoptosis upon Bak overexpression



B. Inhibition of Caspase-3 activity in 293T cells induced to undergo apoptosis upon Bak overexpression

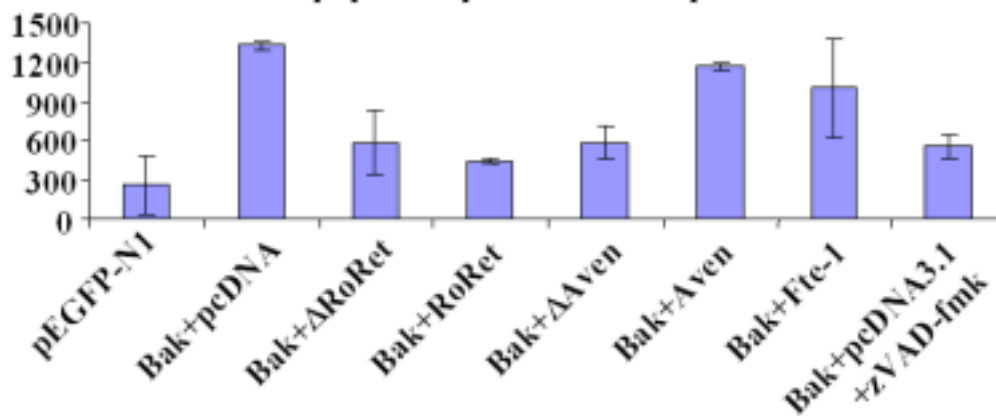


Fig. 33: 1×10^6 293T cells were transfected with $0,5 \mu\text{g}$ *bak-gfp* + $1,5 \mu\text{g}$ protector plasmid DNA by the PEI method. The following day cells were pelleted and lysed to perform Caspase-9 (A) and Caspase-3 (B) activity assays. The error bars represent the variability between three independent experiments.

I observed that Δ RoRet, RoRet, Δ Aven, Aven and Fte-1 inhibited Caspase-9 activity. Caspase-3 activity could only be efficiently blocked by Δ RoRet, RoRet and Δ Aven, while Aven and Fte-1 gave different results in different experiments permitting no definitive conclusion. Moreover, I observed that only RoRet was inhibiting caspase-9 and -3 activity in RKO cells treated with FasL (data not shown).

Δ Aven and Aven were sometimes inhibiting UV-induced Caspase-3 activity, but the variability of the outcome in these experiments did not permit a conclusive analysis of these data.

Taken together, the protection assays, the Western Blots analysis and the caspase activity results suggest that while RoRet seems to inhibit apoptosis induced by a wider range of stimuli (Bak, Apaf-1/Caspase-9, FasL and sometimes UV). Aven inhibits only Bak- and Apaf-1/Caspase-9-induced apoptosis at the level of Caspase-9 activity. Moreover Δ Aven is always more potent in inhibiting apoptosis than the full length Aven, while Δ RoRet and RoRet seem to be equally capable to inhibit apoptosis. Strangely, despite inhibition of apoptosis and Caspase-9 activity, no inhibition of Caspase-3 activity could be seen with Aven full length (not explainable).

Fte-1 can also inhibit apoptosis at the level of Caspase-9 activation, induced by Bak or Apaf-1 M368L/Caspase-9 expression.

F- Cellular localization of RoRet, Aven and Fte-1, and analysis of their possible interaction with Apaf-1.

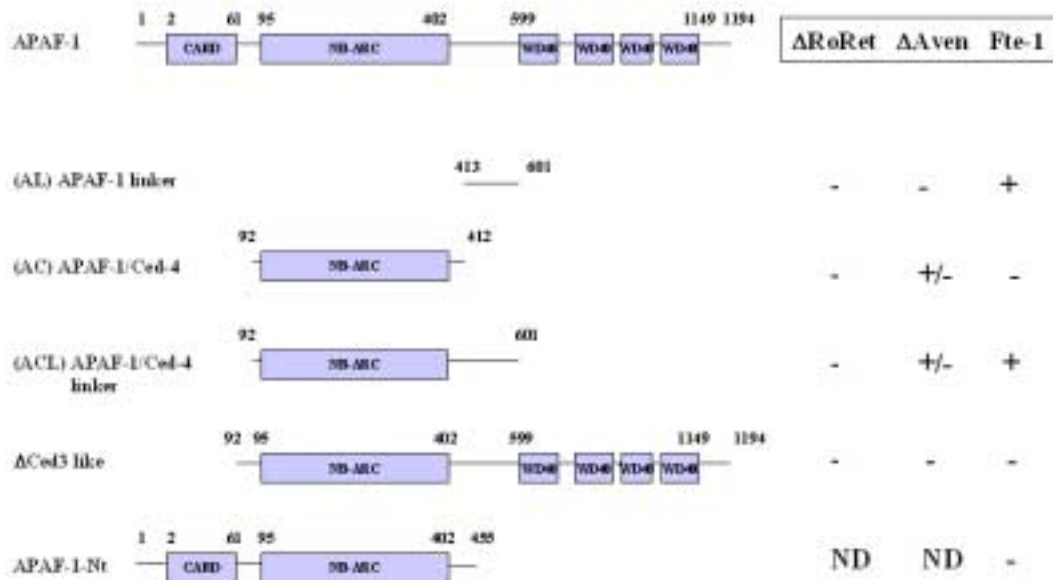
The next interesting question was to determine how RoRet, Aven and Fte-1 can inhibit apoptosis mechanistically. The clones were isolated during a survival screen using CED4 as the “killer protein”. CED4 is homologous to the activated form of Apaf-1, therefore one possibility is that the protecting proteins might interact with Apaf-1, thereby blocking apoptosome activation.

1- Apaf-1 interaction studies of RoRet, Aven and Fte-1 in a Two-hybrid system.

One method to study direct interaction between two proteins is to use the Two-Hybrid assay. This method is based on the fusion of one protein to the DNA binding domain of a transcription factor and of the fusion of the other protein to the transactivation domain of the same transcription factor, in this case deletion mutants of Apaf-1 on one side and Δ roret, Δ aven and fte-1 on the other side. If the two proteins bind to each other, the transcription factor is reconstituted and transcription of specific reporter genes can take place. Here I cloned Δ roret, Δ aven and fte-1 in pGADT7 yeast expression vector fusing the proteins to the activation domain of the Gal4. Separately I obtained different deletion mutants of Apaf-1 fused to the DNA binding domain of the Gal4. These constructs had been cloned into the pAS2-1 yeast expression vector (kindly provided by Dr. Seamus Martin, National University of Ireland, Maynooth, Co. Kildar, Ireland). These Apaf-1-deletion mutants contained in different combinations-(shown below in Fig. , A) the important domains of Apaf-1: the CARD domain that binds to Caspase-9, the CED4 homology domain NB-ARC, the linker stretch between the CED4 homolog domain and the WD40 repeat domain, and finally the WD40 repeat domain. I then co-transformed by the LiAc method AH-109 *S. cerevisiae* with my protecting prey constructs together with the different Apaf-

1 mutants, and tested protein-protein interaction by growth on DOBA, -His, -Trp, -Leu selective medium. In addition, I performed a β -galactosidase assay. Histidine and β -galactosidase served as reporter genes activated by the potentially reconstituted Gal4 transcription factor. A positive interaction can be translated by growth on -His medium and detection of β -galactosidase activity.

A.



B.

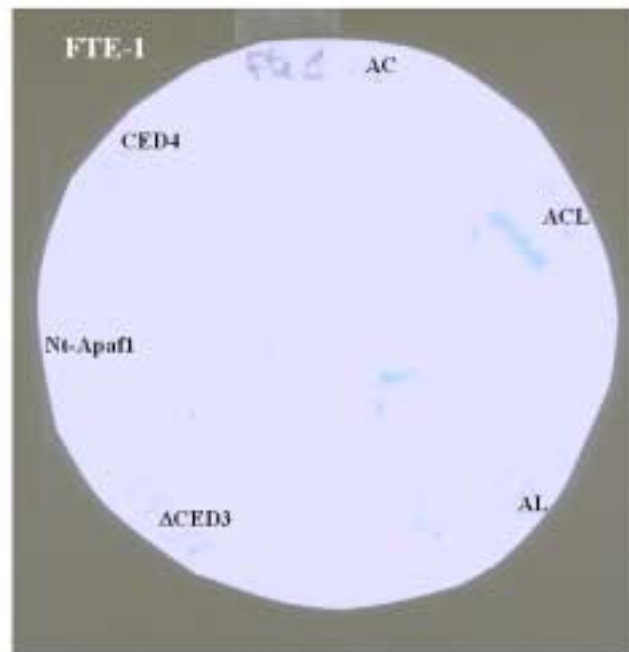


Fig. 34: (A) The yeast two-hybrid system was used to look for binding of Δ Aven and Δ RoRet to Apaf-1 and to map the region of the putative Apaf-1 binding site. Δ aven, Δ roret and *fte-1* were co-transfected with several Apaf-1 deletion mutants into the yeast strain AH109. Protein interactions were assayed by growth on yeast medium lacking histidin and by β -galactosidase activity. The table summarizes the different Apaf-1-deletion mutant constructs. (B) The picture show Fte-1 interaction with two deletion mutants (AC and ACL).

From these results in yeast I conclude that only Fte-1 shows direct binding to Apaf-1 in the region between the CED4 like domain and the WD40 repeat domain. Nevertheless, Fte-1 showed no binding with the deletion mutant containing the linker together with the WD40 repeat region, suggesting that this domain which may prohibit binding of Fte-1 to the linker by steric hinderance. Δ RoRet showed no binding to Apaf-1 in the yeast two-hybrid assay. Δ Aven shows weak binding to the CED4-like domain of Apaf-1, yeast cells grew slowly and the β -galactosidase activity assay was positive in one out of two experiments, the filter turning blue after a long time (more than 10 hours). It is altogether possible that Δ Aven binds to Apaf-1, but this binding in yeast cells is very weak (+/-), suggesting that some post-translational modifications take place in mammal cells that are necessary for this interaction and which are missing in yeast.

2- Analysis of the potential interaction of RoRet, Aven and Fte-1 with Apaf-1 using the GST-pull down method

One possibility is that Aven and RoRet are not directly binding to Apaf-1, but require an intermediate protein which would explain the negative results obtained in the yeast-two-hybrid system. This can be tested using a GST-pull down assay by incubating GST-fusion proteins with adequate cell lysate (with activated Apaf-1). Therefore, I cloned *Δroret*, *Δaven* and *fte-1* into the pGEX-AHK vector, fusing them to the GST coding sequence. I then expressed the GST-fusion proteins in BL21 bacteria (mini-GST expression). Upon IPTG treatment, these bacteria can be induced to express the GST-fusion proteins, which are later used for the pull down.

GST-fusion protein expression and pull down assay

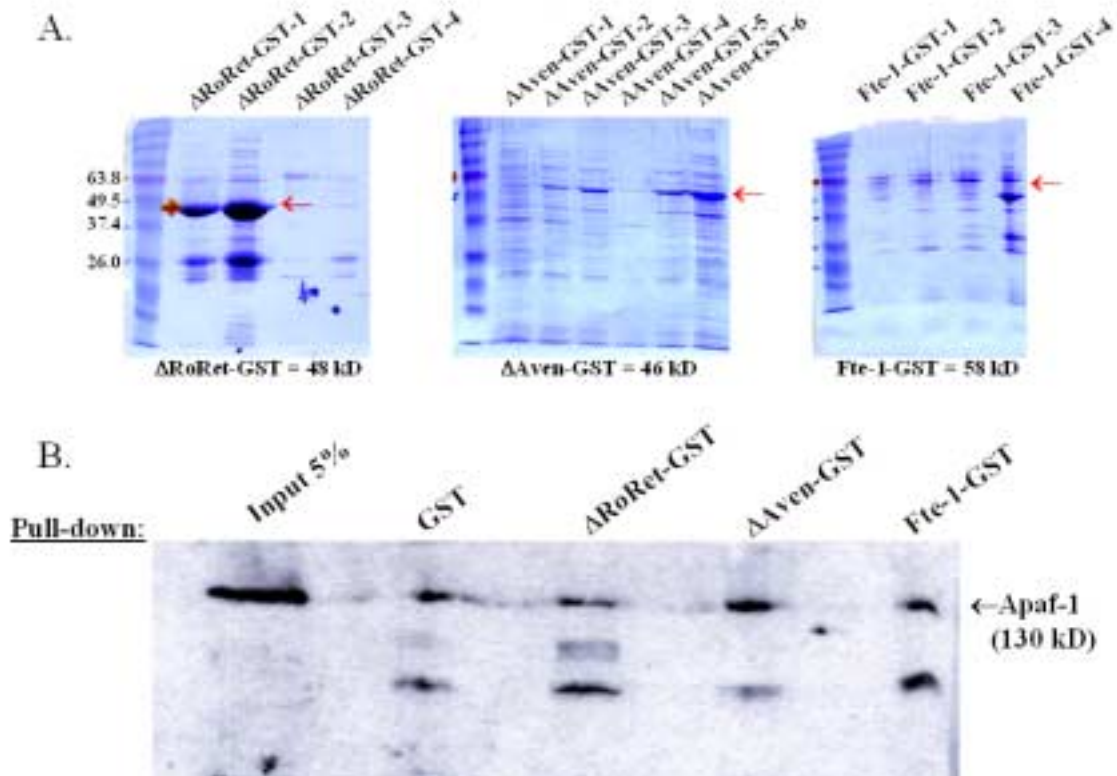


Fig.35: (A) Δ roret-pGEX-AHK, Δ aven-pGEX-AHK and *fte-1*-pGEX-AHK were transformed into the BL21 bacterial strain by electroporation. Four to six colonies of each construct were chosen for protein expression. GST-fusion proteins were then purified using GST coupled agarose beads, and an aliquot of the purified proteins was loaded on a polyacrylamid/SDS gel to verify protein expression levels. (B) GST-fusion proteins were used for a pull down experiment with 293T cells lysate. After several washing steps, beads were loaded on a polyacrylamid/SDS gel to perform a Western Blot analysis and to look for binding of endogenous Apaf-1 to Δ RoRet, Δ Aven et Fte-1 (anti-Apaf-1 from *Pharmingen*) presence.

GST-fusion proteins expression was sufficient for Δ RoRet-GST and Δ Aven-GST (Fig. 35, A), but Fte-1-GST could only be poorly expressed and gave high amounts of smaller proteins that may be explained by protein degradation or cleavage. In figure (Fig. 35, B) I show a representative blot for the GST pull down with Δ RoRet-GST, Δ Aven-GST and Fte-1-GST. Δ Aven and Fte-1 may bind to Apaf-1, while the background band obtained with Δ RoRet is quite fainter and the negative control shows a high background band, as a result of Apaf-1 binding to GST alone.

3- Co-immunoprecipitation of RoRet, Aven and Fte-1 with Apaf-1.

The next step was to try a mammalian co-immunoprecipitation system. I decided to clone *roret*, *aven* and *fte-1* in the pEGFP-N1 vector (see material and methods) fusing them to the Green Fluorescent Protein (GFP) at their C-terminal end. I tried to co-immunoprecipitate the GFP-fused proteins with Apaf-1 by either using an anti-GFP antibody or the other way round by using an anti-Apaf-1 antibody.

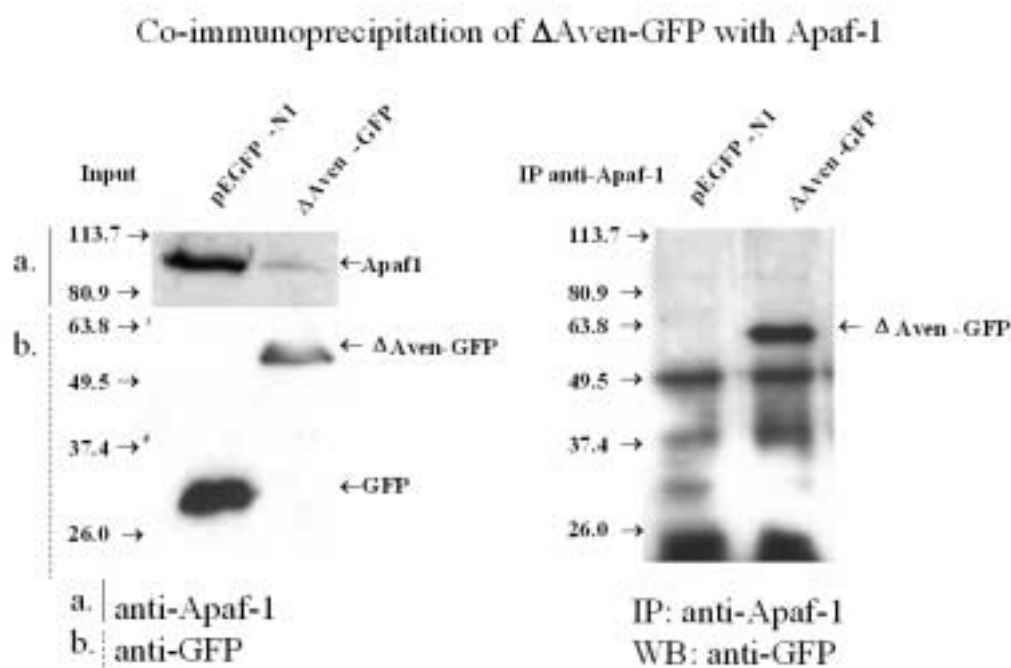


Fig. 36: 293T cells were transfected with 3 μ g *apaf-1* plus 9 μ g Δ aven-pEGFP-N1 by the PEI method, 24 hours later cells were lysed and Δ Aven-GFP was co-immunoprecipitated with anti-Apaf-1 antibody from *Santa Cruz*. The GFP antibody used in the blot was purchased from *Roche*.

As shown in Fig. 36, I could co-immunoprecipitate Δ Aven-GFP together with Apaf-1 with an anti-Apaf-1 antibody, but I could not co-immunoprecipitate either Δ RoRet-GFP, RoRet-GFP or Fte-1-GFP with Apaf-1 (data not shown). Another experiment when I tried to co-immunoprecipitate FLAG- Δ RoRet and FLAG-RoRet with Apaf-1 (with anti-FLAG antibody or with anti-Apaf-1 antibody) was not successful either, but led to the hypothesis that RoRet may be cleaved in the cell (data not shown). It is still possible that RoRet may interact with Apaf-1, but the conditions under which this interaction would be detectable still have to be determined. The results from the yeast Two-Hybrid assay suggest that Fte-1 and Apaf-1 are interacting directly.

4- Cellular localization of RoRet, Aven, Fte-1 and their deletion mutants, and co-localization studies with Apaf-1 and Caspase-9 by confocal microscopy

4.1-Co-localization of RoRet, Aven, Fte-1 with Apaf-1 or Caspase-9

I decided to look for co-localization of RoRet, Aven and Fte-1 with Apaf-1 and with Caspase-9 using confocal laser scanning microscopy, as well as define the cellular localization of RoRet, Aven, Fte-1 using the GFP-tagged versions of them. All the subsequent analysis were done using the sequential mode of channel detection. As a control I stained the cells with the secondary antibody only and in this case a very weak background could be detected that was easily distinguishable from the much stronger specific signals.

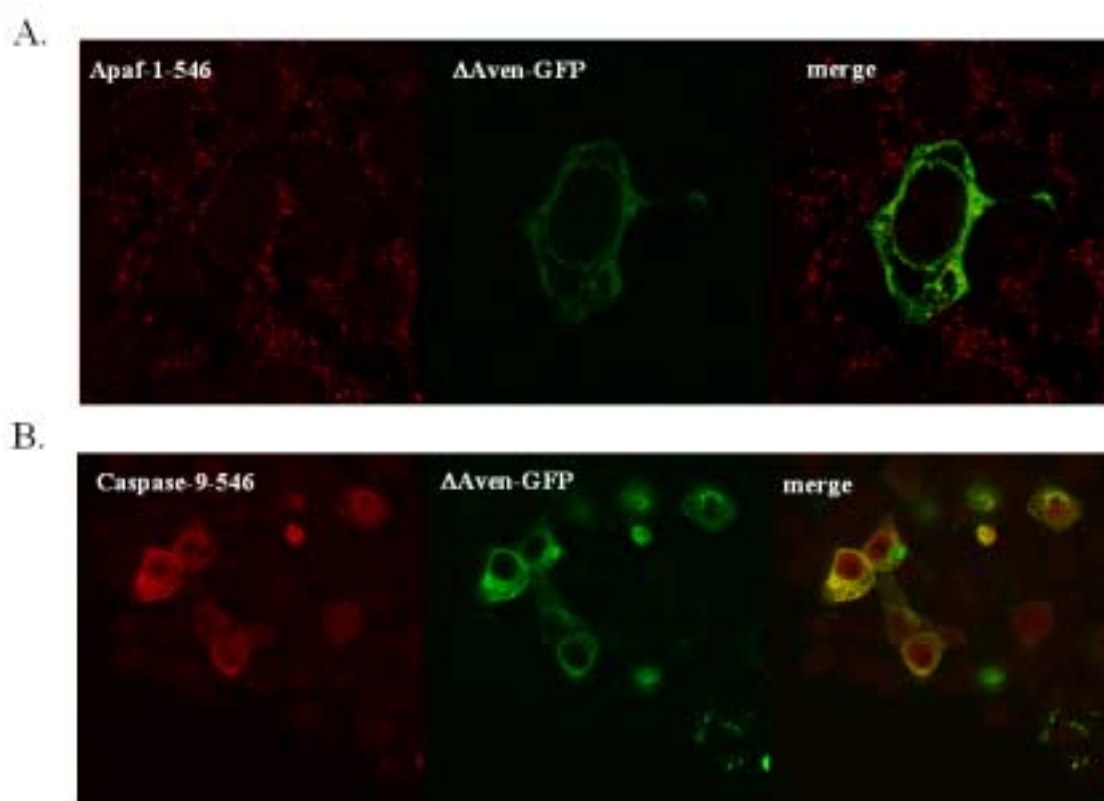


Fig. 37: 1×10^6 293T cells (grown on thin-bottom plates) were transfected with $\Delta Aven-GFP$ by the PEI method. The following day, cells were fixed with formaldehyde and stained with anti-Apaf-1 (*Pharmingen*) and anti-rabbit-546 (*Molecular Probes*) (A) or with anti-Caspase-9 (*Pharmingen*) and anti-rabbit-546 (*Molecular Probes*) (B). I then looked for co-localization by confocal laser scanning microscopy. The two images obtained were combined (merged) and co-localization was detected by the change of colour (here yellow).

$\Delta Aven$ is located in the cytoplasm in a spotted fashion, suggesting some aggregates or organelle location (see Fig. 37). No $\Delta Aven$ was detected in the nucleus. Apaf-1 showed also a cytoplasmic profile, again spotted rather than diffused. Apaf-1

concentration increased around the nucleus and in a compact area near the nucleus. Caspase-9 was found in the cytoplasm and in some cells in the nucleus. It is important to point out that Apaf-1 and Caspase-9 detected in these experiments are the endogenous proteins. The merged pictures for Δ Aven and Apaf-1 showed yellow spots suggesting that Δ Aven and Apaf-1 are partly co-localizing, whereas the merging picture for Δ Aven and Caspase-9 show a clear co-localization of both proteins.

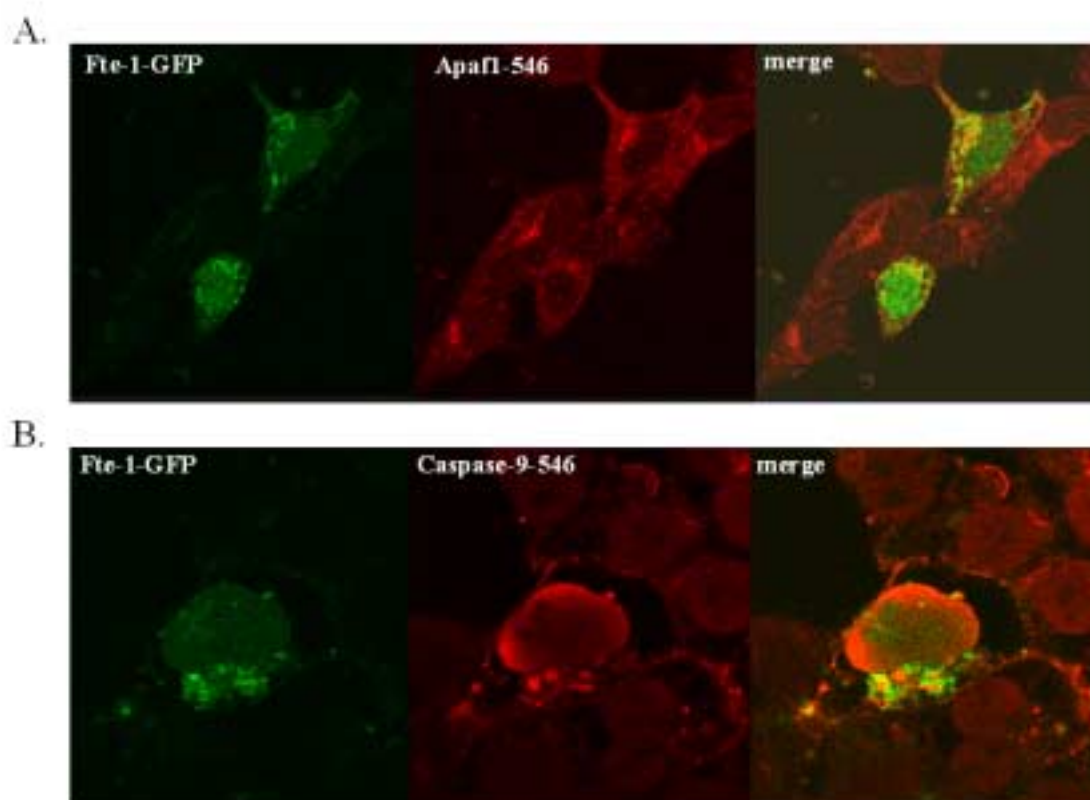


Fig. 38: 1×10^6 293T cells (grown on thin-bottom plates) were transfected with *fte-1-gfp* by the PEI method. The following day, cells were fixed with formaldehyde and stained with anti-Apaf-1 (*Pharmingen*) and anti-rabbit-546 (*Molecular Probes*) (A) or with anti-Caspase-9 (*Pharmingen*) and anti-rabbit-546 (*Molecular Probes*) (B). I then looked for co-localization of Fte-1 with Apaf-1 and Caspase-9 using confocal laser scanning microscopy. The two images obtained were combined (merged) and co-localization was detected by the change of colour towards yellow.

Fte-1-GFP can be detected in a well-defined compartment that looks like the endoplasmic reticulum or the Golgi (see Fig. 38). The specific staining of these compartments in future experiments will tell which organelle these structures really represent. In this experiment, yellow areas indicating co-localization could be detected at the compartment described above in the merged picture for Fte-1 and Apaf-1 (see Fig. 38, A), whereas no clear co-localization could be detected for fte-1 and Caspase-9 (see Fig. 38, B). Martinez-A et al., described Apaf-1 localizing at the

Golgi but not the ER in cells expressing Bcl-2, whereas in cells without Bcl-2 (from knockout mice) Apaf-1 was diffused in the cytoplasm (Ruiz-Vela, Albar et al. 2001).

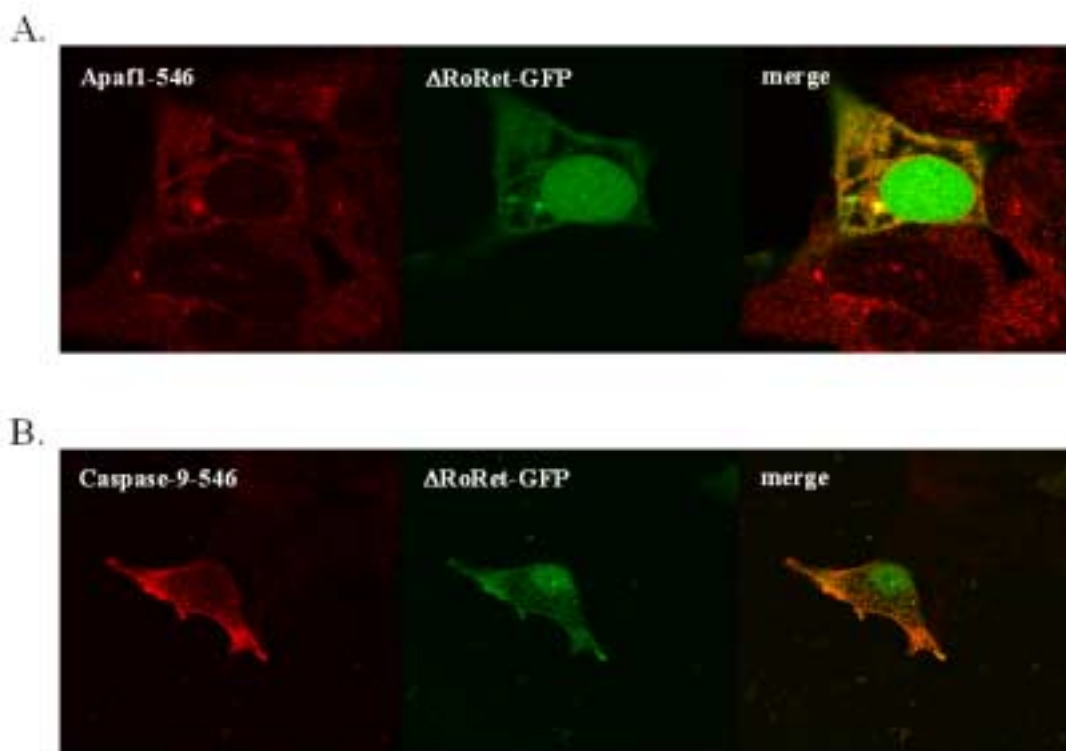


Fig. 39: 1×10^6 293T cells (grown on thin-bottom plates) were transfected with $\Delta roret-gfp$ by the PEI method. The following day, cells were fixed and stained like in the previous experiment (see e.g. Fig. 37) I then looked for co-localization by using confocal laser scanning microscopy.

$\Delta RoRet-GFP$ shows a diffuse cytoplasmatic and a clear nuclear localization. Nevertheless, the merged picture is ambiguous and no conclusion about $\Delta RoRet$ localization with either Apaf-1 or Caspase-9 can be drawn.

4.2- Are Aven, RoRet and Fte-1 localized in the apoptosome ?

I investigated whether Aven, RoRet and Fte-1 co-localize simultaneously with Apaf-1 and Caspase-9 in the apoptosome complex which is formed after Cytochrome *c* release during the apoptotic process. For this purpose I used the sequential scanning mode (that measure the different fluorescence channels sequentially) in confocal laser scanning microscopy. I stained 293T cells co-transfected with the *gfp*-fusion constructs, *caspase-9* and *apaf-1 M368L* with antibodies suitable for immunohistochemistry.

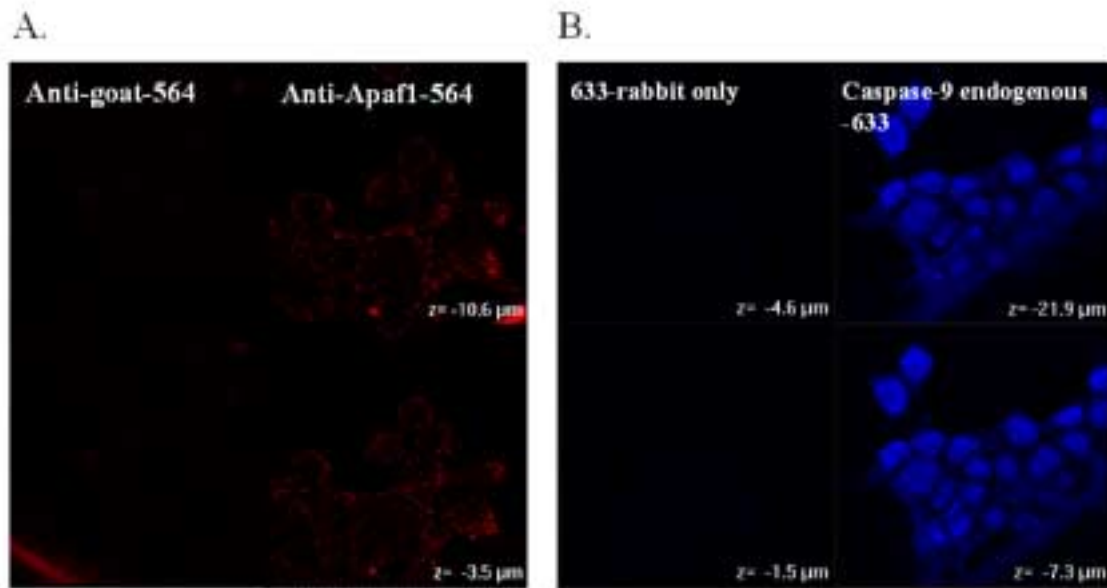


Fig. 40: (A) 293T cells were stained for endogenous Apaf-1 with an anti-Apaf-1 antibody from *Santa Cruz* and anti-goat-564 antibody from *Molecular Probes*. (B) 293T cells were stained for endogenous Caspase-9 with anti-Caspase-9 antibody from *Pharmingen* and anti-rabbit-633 antibody from *Molecular Probes*.

The experiment shown in Fig. 40 proves the specificity of the anti-Apaf-1 and anti-Caspase-9 antibodies used. Moreover, the localization of both Apaf-1 (cytosolic) and Caspase-9 (cytosolic and nuclear) were in accordance with the published observations of other groups (Ritter, Marti et al. 2000; Ruiz-Vela, Albar et al. 2001). The colour code in the following experiments is as follows: green for the GFP fusion proteins (Δ RoRet-GFP, Δ Aven-GFP and Fte-1-GFP), red for Apaf-1, blue for Caspase-9, yellow for co-localization of the GFP fusion proteins with Apaf-1, light-blue for co-localization of the GFP fused proteins with Caspase-9, lila for co-localization of Apaf-1 with Caspase-9 and white for simultaneous co-localization of the GFP fusion protein with Apaf-1 and Caspase-9.

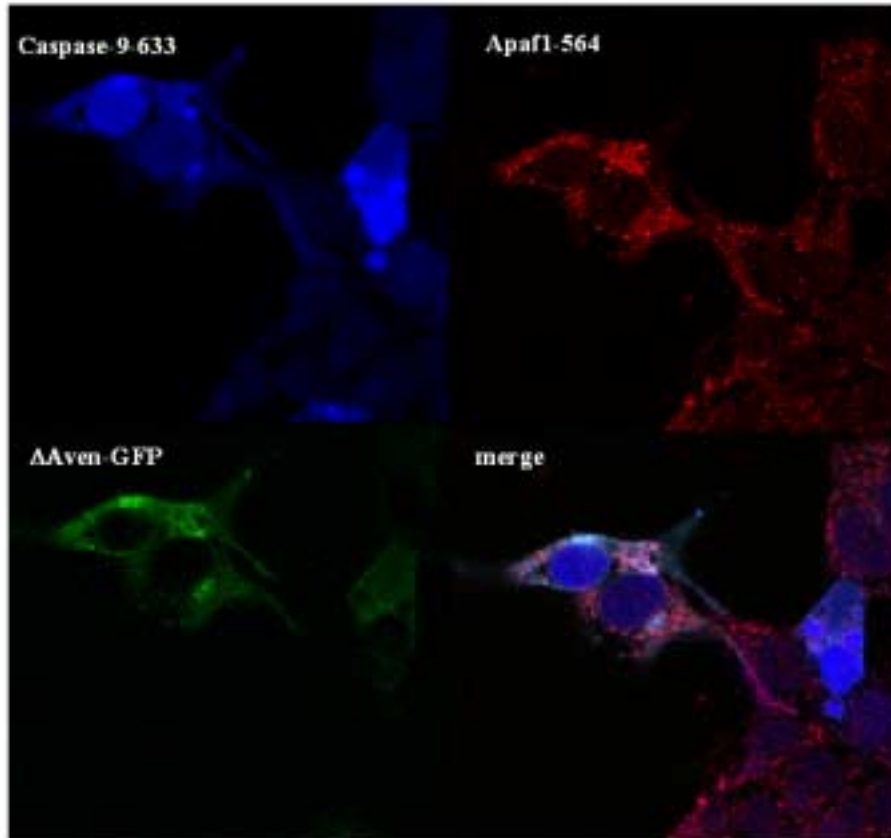


Fig. 41: 1×10^6 293T cells, grown on thin-bottom culture plates, were transfected with *Apaf-1M368L* plus *caspase-9* plus $\Delta Aven-gfp$ by the PEI method. The following day, cells were fixed with formaldehyde and stained with anti-Caspase-9 antibody (*Pharmingen*) plus anti-rabbit-633 antibody (*Molecular Probes*), or anti-Apaf-1 antibody (*Santa Cruz*) plus anti-goat-564 antibody (*Molecular Probes*). We then looked for co-localization (merged picture) by using confocal laser scanning microscopy (sequential scanning mode).

Co-localization of Apaf-1 with Caspase-9 was detectable (lila colour) only in those cells with Apaf-1 and Caspase-9 overexpression. In such cells that also expressed $\Delta Aven-GFP$, white streaks were detectable in the cytoplasm suggesting co-localization of all three proteins (see Fig. 41).

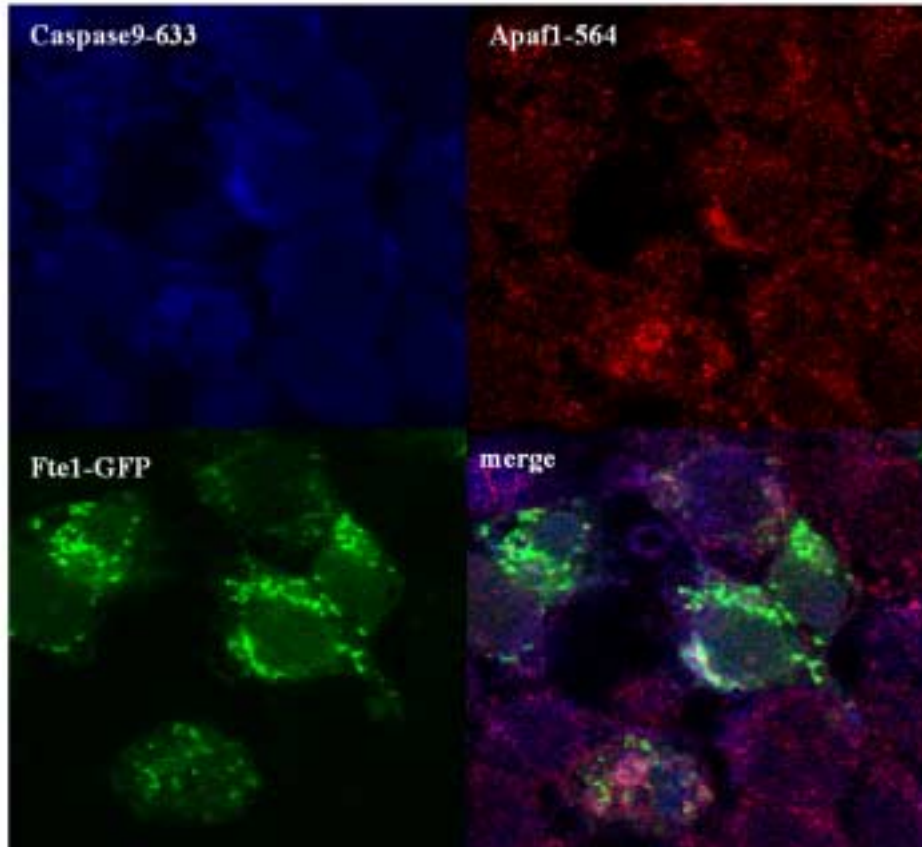


Fig. 42: 1×10^6 293T cells, grown on thin-bottom culture plates, were transfected with *Apaf-1M368L + caspase-9 + fte-1-gfp* by the PEI method. Subsequently, cells were fixed and stained as before with anti-Caspase-9 antibody (*Pharmingen*) plus anti-rabbit-633 antibody (*Molecular Probes*), or anti-Apaf-1 antibody (*Santa Cruz*) plus anti-goat-564 antibody (*Molecular Probes*), and analysed for co-localization (merged picture) by using confocal laser scanning microscopy (sequential scanning mode).

In the experiment shown in Fig. 42 the result was less clear. In some cells white areas (Fte-1-GFP, Apaf-1 and Caspase-9 co-localization) could be detected, in others (not shown) only yellow areas (co-localization of Fte-1-GFP with Apaf-1) was observed. Moreover, the white areas co-exist with green ones within some cells, suggesting that only a specific pool of Fte-1-GFP co-localizes with Apaf-1 and/or with Caspase-9. Numerous lila areas confirm the expected Apaf-1 and Caspase-9 co-localization.

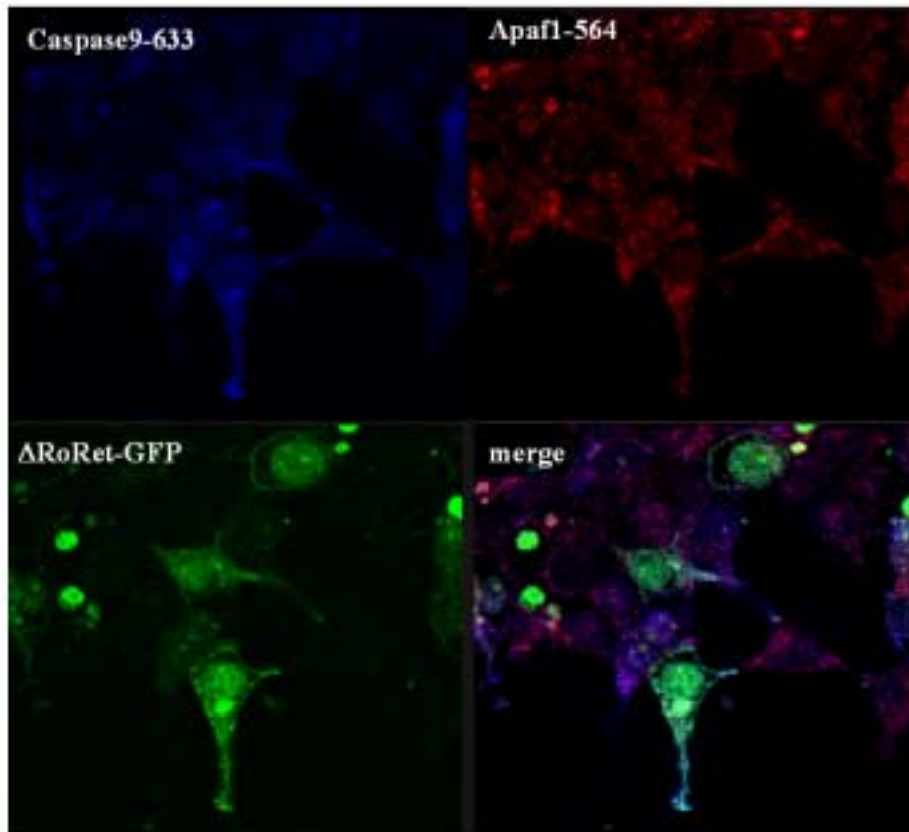
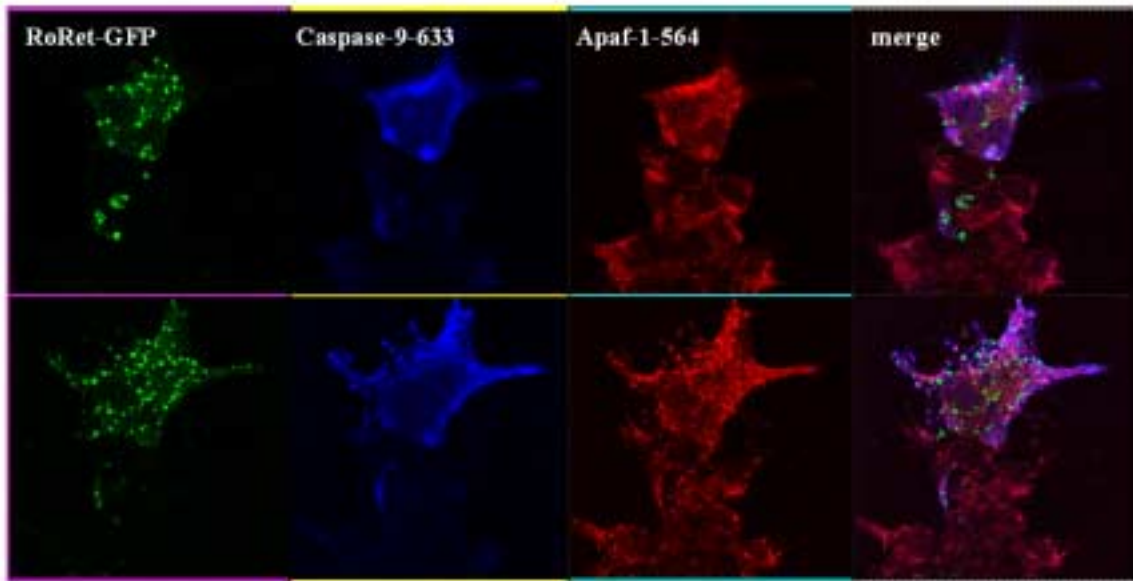


Fig. 43: 1×10^6 293T cells, grown on thin-bottom culture plates, were transfected with *Apaf-1M368L+ caspase-9 + Δroret-gfp* by the PEI method. Subsequently, cells were fixed and stained as before with anti-Caspase-9 antibody (*Pharmingen*) plus anti-rabbit-633 antibody (*Molecular Probes*), or anti-Apaf-1 antibody (*Santa Cruz*) plus anti-goat-564 antibody (*Molecular Probes*). They were analysed for co-localization (merged picture) using confocal laser scanning microscopy (sequential scanning mode).

Δ RoRet-GFP seems to co-localize with caspase-9 (light blue areas) but not with Apaf-1 (yellow areas were rarely detected only in dying cells). No white areas could be detected (see Fig. 45).

Full length RoRet-GFP showed a largely punctuated pattern that looks similar to some vesicular structure (see Fig. 43). Further characterization of these organelles should tell what they exactly are. RoRet-GFP could also be detected in the nucleus of a few cells. The dramatically different localization pattern of Δ RoRet-GFP and RoRet-GFP (data not shown), suggesting the presence of a cytoplasmic localization signal in the amino-acid sequence of RoRet that must be deleted in the Δ RoRet mutant.

A.



B.

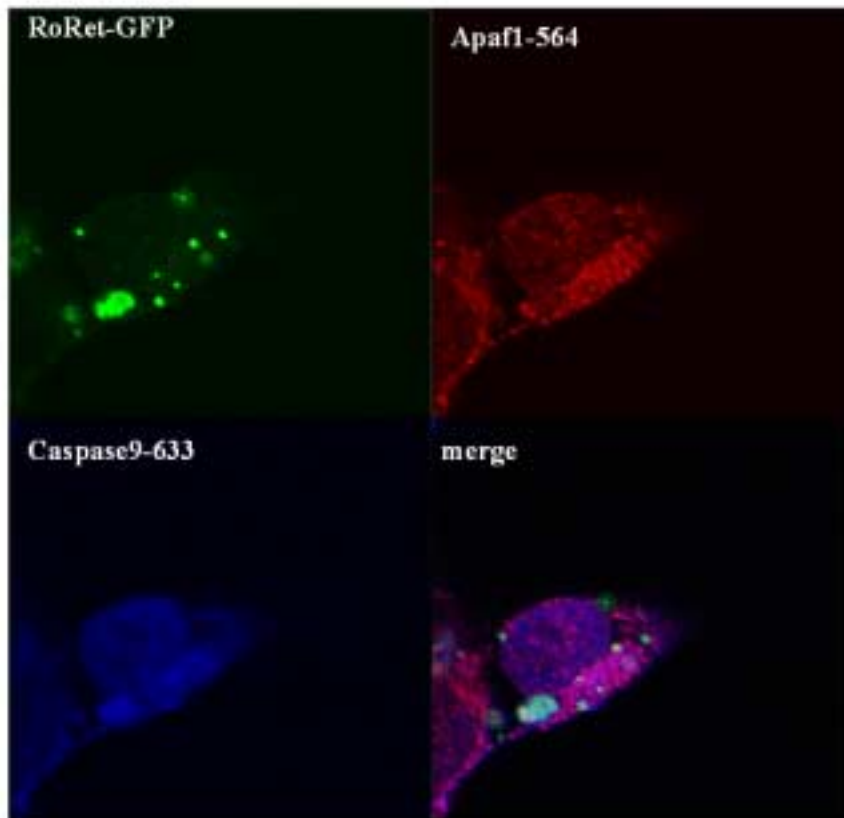


Fig. 44: (A) 1×10^6 293T cells, grown on thin-bottom culture plates, were transfected with *Apaf-1M368L* + *caspase-9* + *roret-gfp* by the PEI method. Subsequently, cells

were fixed and stained as before with anti-Caspase-9 antibody (*PharMingen*) plus anti-rabbit-633 antibody (*Molecular Probes*), or anti-Apaf-1 antibody (*Santa Cruz*) plus anti-goat-564 antibody (*Molecular Probes*), and analysed for co-localization (merged picture) using confocal laser scanning microscopy (sequential scanning mode). (B) The same experiment as shown in A presented with a larger magnification.

As for Δ RoRet-GFP, light blue areas show co-localization of RoRet-GFP with Caspase-9, but no white areas could be detected, which would indicate simultaneous co-localization of RoRet-GFP with Caspase-9 and Apaf-1 (see Fig. 44). Lila areas show again that Apaf-1 and Caspase-9 co-localize. It is also to note that some remaining green spots in the merged picture show that only a certain pool of RoRet-GFP co-localizes with Caspase-9.

G-Possible involvement of Aven, Fte-1 and RoRet in mammary gland development and/or tumourigenesis

1-Mammary gland development

Aven, RoRet and Fte-1 were indentified in a breast tumour cDNA library, which may indicate that these genes are involved in mammary gland development. I first looked for Aven expression during mouse mammary gland development. For this purpose, I used a mRNA Northern Blot from Clontech with RNA samples prepared from female mouse mammary glands during different developmental stages.

Mouse Aven regulation during mammary gland development

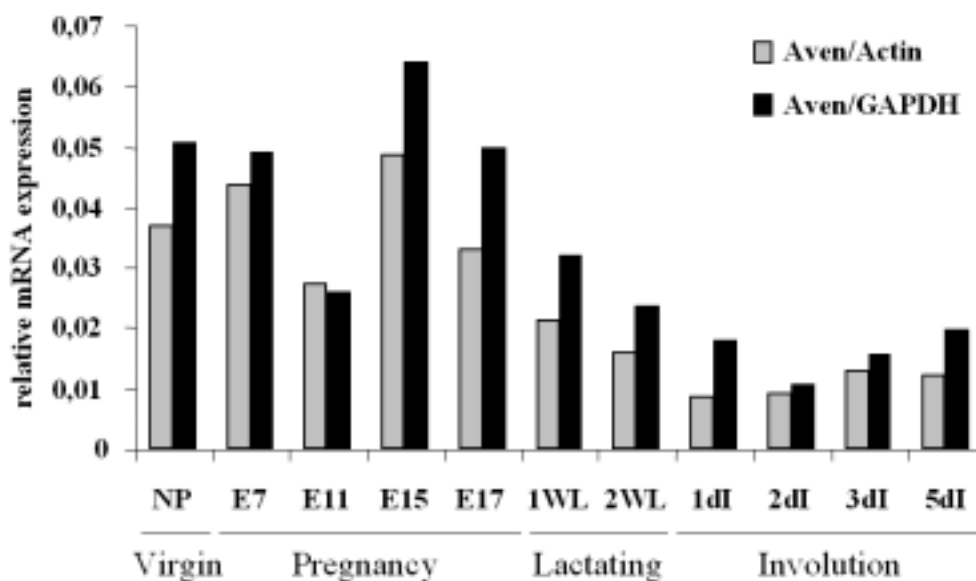


Fig. 45: Different mRNA preparations of mammary glands from non-pregnant (NP), pregnant (E7-E17), lactating (1WL, 2WL) and involuting (1dI-5dI) mice were used for Northern Blot analysis. The membrane was hybridized sequentially with cDNA probes for mouse *Aven*, *β -actin* and *gapdh*. *aven* RNA expression was normalized to *β -actin* (grey bars) or *gapdh* (black bars) RNA levels. Hybridization signals were quantified with a *BIO RAD* phosphoimager.

Down regulation of *aven* mRNA was clearly visible during lactation and during the time of involution, when the glands undergo apoptosis. *aven* expression levels show a tendency to increase again during the late days of involution (day 5). The same experiment is planned for Fte-1 and RoRet.

2- Kim-2 cells as an *in vitro* model for differentiation and apoptosis induction in the mammary gland

I used the published model system of KIM-2 cells to mimic differentiation and apoptosis induction in mammary gland (Gordon, Binas et al. 2000). I cultured Kim-2 cells in differentiating medium for two weeks and then drove them into apoptosis by removing the lactogenic hormones. Then I studied *Aven* expression during these different steps (undifferentiated, differentiated and apoptotic) by Western Blot.

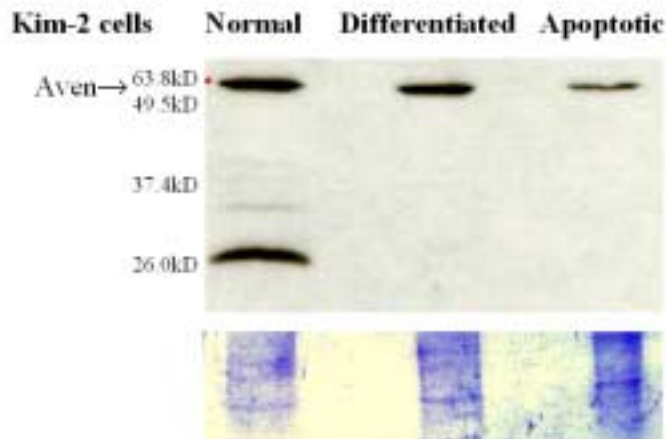


Fig. 46: Kim-2 cells were grown in normal medium, differentiated for two weeks in differentiation medium and driven into apoptosis by removal of cytokines as published [Gordon, 2000 #9113]. At each step of differentiation, cell lysates were prepared, and *Aven* expression was studied in western blot.

I found that Aven slightly decreases in differentiating cells, and significantly decreases in apoptotic cells. A lower band that seems to be specific appears only in undifferentiated cells. As it is described that only about 30% of the cells undergo apoptosis, it is also possible that the remaining Aven comes from the non-apoptotic cells

2-Aven, Fte-1 and RoRet expression in tumours

2.1- The cancer profiling arrays

Aven, Fte-1 and RoRet were isolated during a survival screen using a breast cancer cDNA library. The idea was that in such a library some anti-apoptotic genes important for tumorigenesis and survival of the tumours would be overexpressed (gain-of-function). As number of anti-apoptotic proteins have been correlated with tumorigenesis, I tested the possible implication of my clones in this context. For this I analysed the expression levels of my clones in tumour versus the normal tissue.

To analyse mRNA expression levels in normal and tumour tissue I used the Cancer Profiling Array from *Clontech*. This array contains many cDNA pairs of tumour and normal tissue of a single patient. The membrane was hybridized with ³²[P]-labelled cDNA probes of human *ubiquitin* (supplied by *Clontech*), human Δ aven, human *c-myc*, human Δ roret and human *fte-1* according to the supplier's protocol.

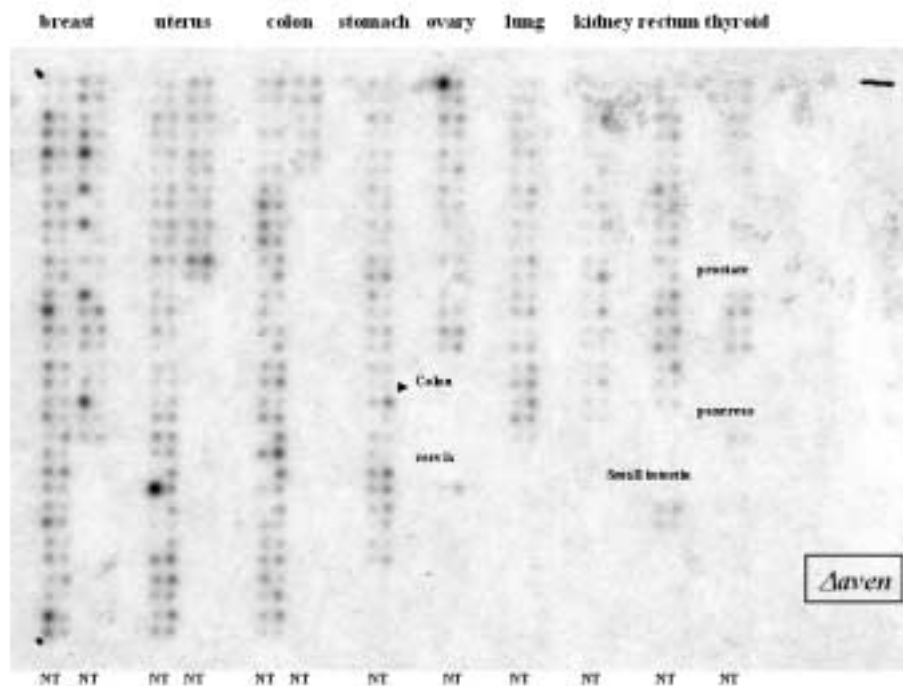
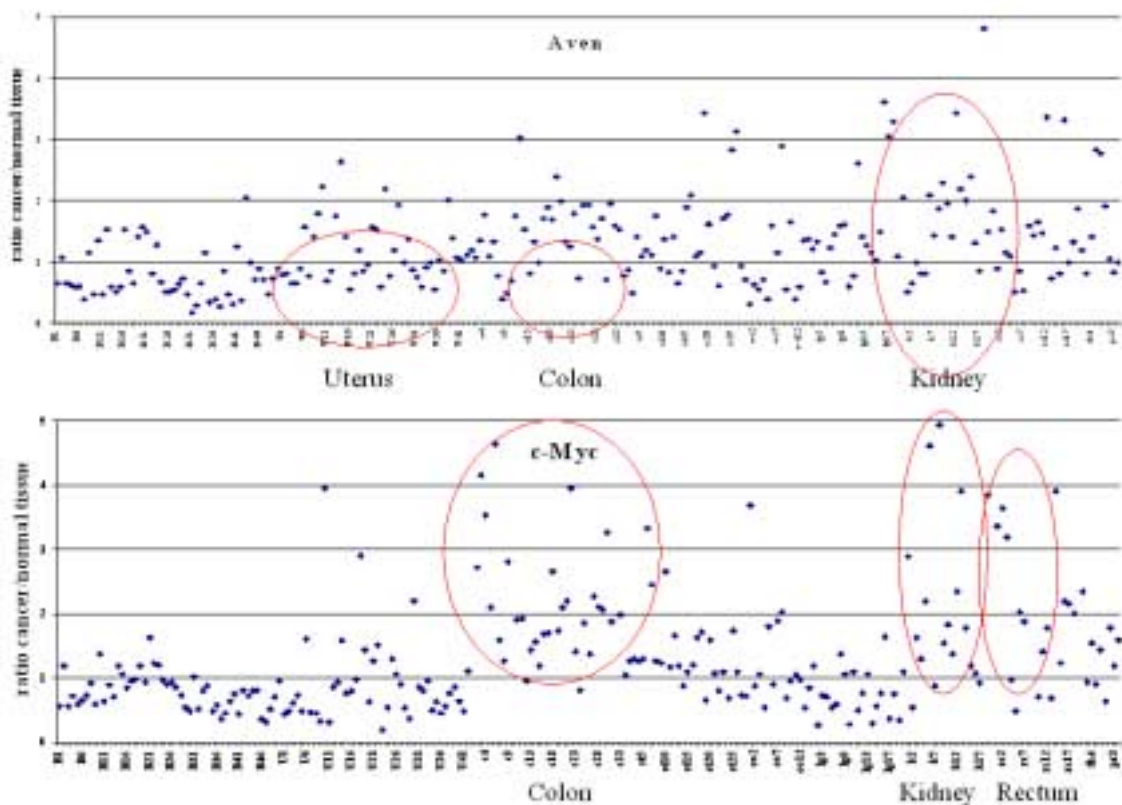


Fig.47: A Cancer Profiling Array from *Clontech* was hybridized with a ^{32}P -labelled *Aven* probe. cDNA synthesized from different tumour RNAs was spotted pairwise on the array together with cDNA derived from corresponding normal tissue of the same patient. In total, 42 tumours of the uterus, 35 colon cancers, 27 stomach cancers, 14 tumours of the ovary, 1 cervix carcinomas, 21 lung carcinomas, 20 renal carcinomas, 18 adenocarcinomas of the rectum, 2 tumours of the small intestine, 6 thyroid gland carcinomas, 4 prostate carcinomas and 1 pancreas carcinoma were screened for potential upregulation.

The same membrane was stripped and re-hybridized up to three times with a different cDNA probe. Radioactive intensity was then quantified each time with a *BIO RAD* phosphoimager and I calculated for each sample the ratio between the signal strength for the intensity for the tumour and the normal tissue. The results are pictured below as *EXEL* graphs.



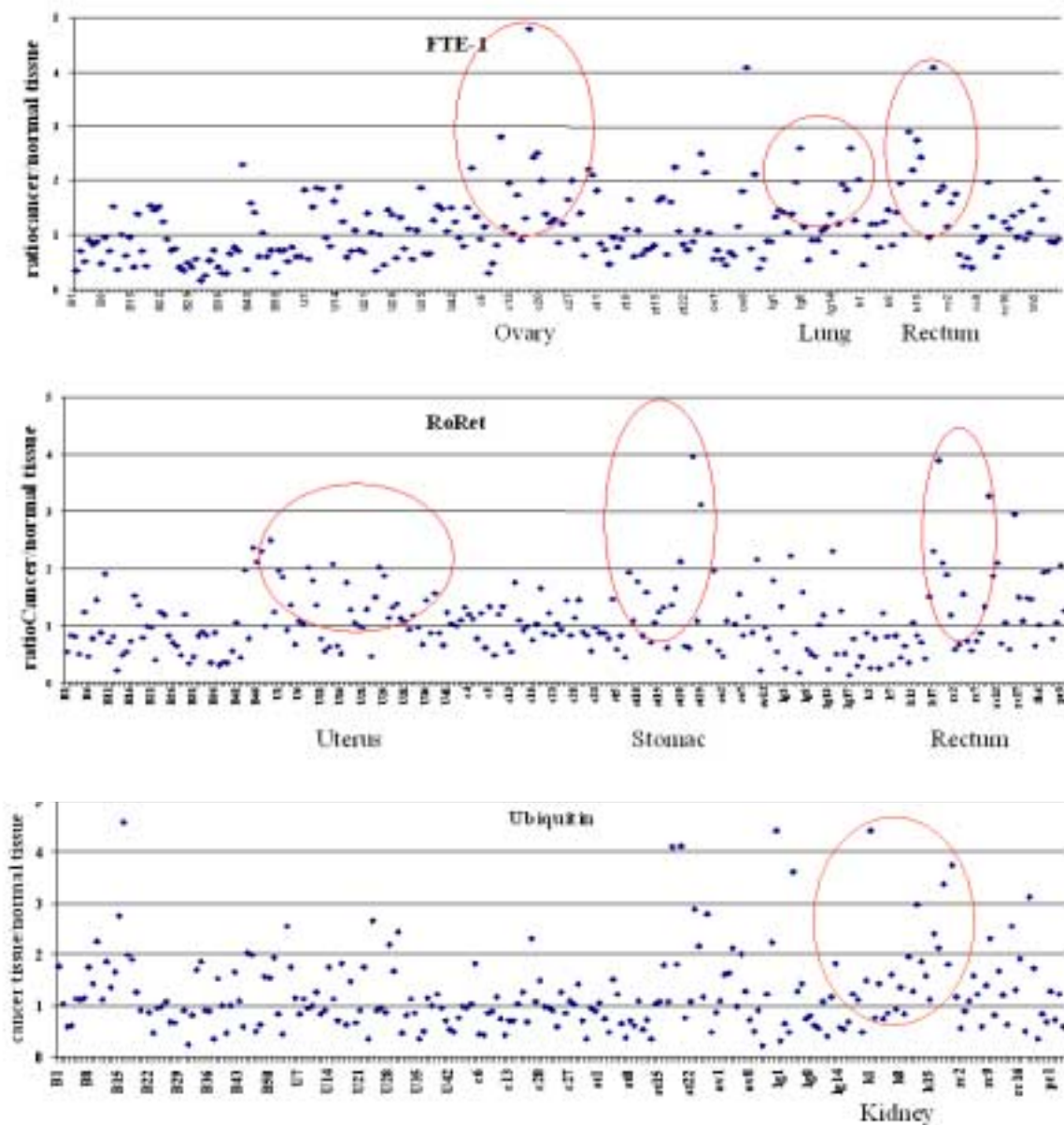


Fig. 48: A Cancer Profiling Array from *Clontech* was hybridized with a ^{32}P -labelled *Avan*, *c-myc*, *Aroret*, *fte-1* and *ubiquitin* probe. cDNA synthesized from different tumour RNAs was spotted pairwise on the array together with cDNA derived from corresponding normal tissue of the same patient. Hybridization signals were quantified with a *BIO RAD* phosphoimager. Represented in the figure are the ratios between the signal strength of tumour and normal tissue. Values greater than one indicate *aven* tumour overexpression. For additional controls the array was re-hybridized with probes for the *bona fide* oncogene *c-myc* and *ubiquitin* as house keeping gene.

I observed upregulation of *aven* in tumours of the uterus, colon and kidney. *fte-1* mRNA levels were upregulated in colon, lung and kidney cancers and *roret* mRNA in uterus, stomach and kidney cancers. These data have to be confirmed at the protein level in tumour samples by Western Blotting. *c-myc* is as expected

upregulated for example in colon cancer (Russo, Arzani et al. 2003), but it was a surprise to observe some regulation in the *ubiquitin* levels as well (e.g. upregulation in kidney tumours). These results are of course only indicative which tumour entities might be worth of further analysis on the protein level. For this reason I started to collect samples of normal tissue/tumour pairs of breast, colon and kidney.

2.2- Western Blots analysis of tumour lysates

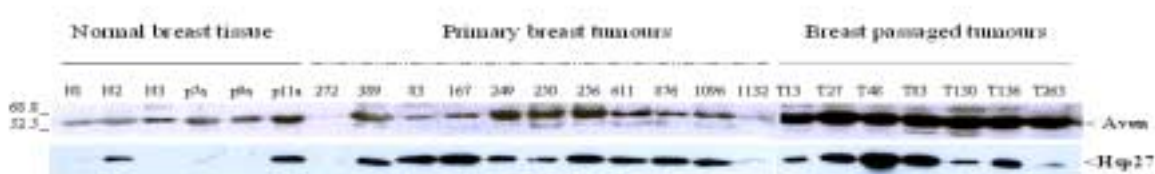


Fig. 49: Aven protein expression in human mammary carcinomas. 40 µg of protein lysates from normal breast tissue (p7a, p9a, p11a, N1, N2, N3) from breast reductions, primary breast tumours (83, 167, 249, 250, 256, 611, 876, 1096, 1132) and breast tumours passaged in nude mice (T13, T27, T48, T83, T130, T136, T236) were analysed in a Western blot experiment with an anti-Aven B antibody kindly provided by Dr. Marie Harwick (Johns Hopkins University, Baltimore, USA). As a loading control, the membrane was rehybridized with an anti-HSP27 antibody. For more detail about the sample provenance see *Material and methods, Protein lysates from tumour samples*.

An upregulation of Aven could be detected in the breast tumours passaged in nude mice. No real difference could be seen in the Aven expression level of normal tissue and primary mammary carcinoma. Hsp 27 was used as a loading control, but showed variations in its expression. Actin and tubulin (data not shown) also showed variations in their expression level.

IV-Identification of HMGB1 in a yeast survival screen as an apoptosis-inhibiting protein.

1-A yeast survival screen with Bak as the “killer” protein led to isolation of HMGB1

We wanted to employ functional yeast survival screens to identify new anti-apoptotic mammalian genes out of tumour-derived libraries as described in the previous part of my work. To test the system, we originally used an inducible Bak

expression system in *S. pombe* to screen a cDNA library prepared from exponentially growing NIH3T3 mouse fibroblasts. Altogether 5×10^4 transformed yeast clones were tested for Bak-resistance in a non-saturated library screen. One of the *S. pombe* colonies surviving Bak expression after library transformation contained a truncated deletion mutant of the mouse *Hmgb1* gene lacking the C-terminal 33 amino acids. This $\Delta Hmgb-1$ deletion mutant does not represent a naturally occurring mRNA variant but was rather generated in the cloning process when the oligo-dT primer annealed within the *Hmgb1* coding sequence during reverse transcription of the RNA. $\Delta HMGB1$ still contains the two HMG-boxes identified in the full length HMGB-1 while the highly acidic C-terminal tail is deleted. I cloned mouse $\Delta hmgb-1$ and mouse full length *Hmgb1* in a constitutive *S. pombe* expression vector and further analyzed $\Delta HMGB1$ -conferred protection in Bak expressing yeasts. When Bak expression is induced in the *S. pombe* yeast strain DSI growing on agar plates, the yeast cells die within 48 hours. Co-expression of either $\Delta HMGB1$ or full length HMGB1 protects the yeast colonies from Bak-induced cell death (Fig.50 , A).

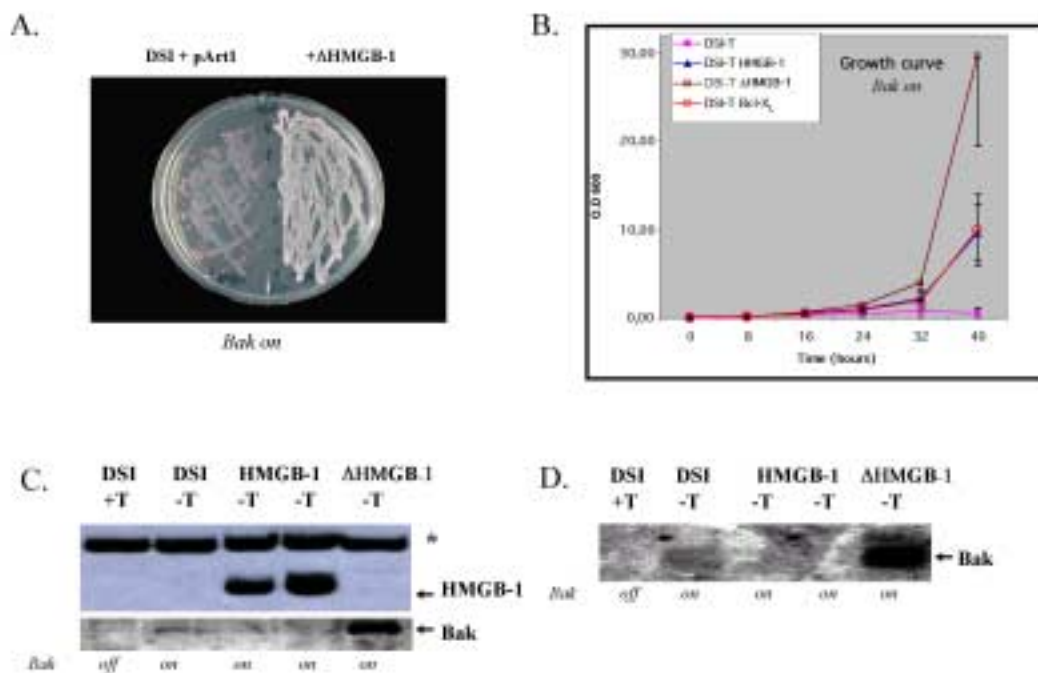


Fig. 50: Functional *S. pombe* yeast survival screen with inducible *bak* expression. A: Principle of the screen: The *S. pombe* yeast strain DSI was transformed with an NIH 3T3 mouse fibroblast-derived cDNA library and plated on thiamine-containing agar plates to allow growth of the colonies (*bak* off). Replica-plating onto thiamine-free agar plates induced *bak* and library *cDNA* expression. Only those yeast colonies which were protected against Bak-induced cell death survived. Untransformed or *pArt1* empty vector-transformed DSI yeast colonies, when replica-plated onto thiamine-free agar plates, died upon induction of *bak*. B: A *Hmgb-1* deletion mutant

lacking the C-terminal 33 amino acids ($\Delta Hmgb1$) was identified in the screen and - like full length *Hmgb1* - protects DSI yeast cells against Bak-induced cell death.

I also measured growth curves of the different yeast strains in liquid culture. *S. pombe* cells cease growth upon Bak expression (DSI, -T) (Fig. 50, B). When co-expressing Δ HMGB1 or full length HMGB1 the Bak transformed yeasts continued to grow exponentially, as they do when the Bak-antagonist Bcl-x_L is co-expressed. I then performed Western- and Northern blot analysis to confirm expression of HMGB-1 and Bak in the yeast strains we had used for the experiments (Fig. 50, C and D). I could detect full length HMGB1 protein in the transformed yeasts but the anti-HMGB1 antibody did not recognize Δ HMGB1 due to the C-terminal deletion. Induction of *bak* transcription in the DSI *S. pombe* strain leads to the production of small amounts of *bak* mRNA and protein sufficient to kill the DSI strain. In DSI cells co-transformed with $\Delta Hmgb1$ a much higher amount of Bak RNA and protein is detectable and - in the presence of Δ HMGB1 - tolerated by the yeast cells. Interestingly, I was unable to detect Bak expression in DSI yeast colonies co-transformed with full length *Hmgb1*.

These results show that full length HMGB1 and Δ HMGB1 protect *S. pombe* cells against Bak-induced yeast killing. While we cannot rule out that the protective effect of full length HMGB1 involves transcriptional downregulation of the Bak yeast expression construct, the largely increased amount of Bak in $\Delta hmgb-1$ co-transformed yeast cells indicates protection by Δ HMGB1 against the Bak protein by another mechanism. Moreover, yeast transformed with *HMGB1* and *bak-gfp* are still green (data not shown) suggesting that the mechanism of protection does not involved transcriptional downregulation of *bak* mRNA.

2-HMGB1 protects mammalian cells against Bak-induced apoptosis

Next I wanted to investigate whether HMGB1 is able to suppress cell death upon Bak overexpression not only in yeast but also in mammalian cells. For this experiment I used the human colon carcinoma cell line RKO. Transient transfection of RKO cells with Bak alone induced apoptosis which was blocked by co-transfection of either $\Delta Hmgb1$ or full length *Hmgb1*. The percentage of dead cells was measured with the LIVE/DEAD assay in fluorescent microscopy (Fig. 51, A) and by PI staining in FACS (Fig. 51, B).

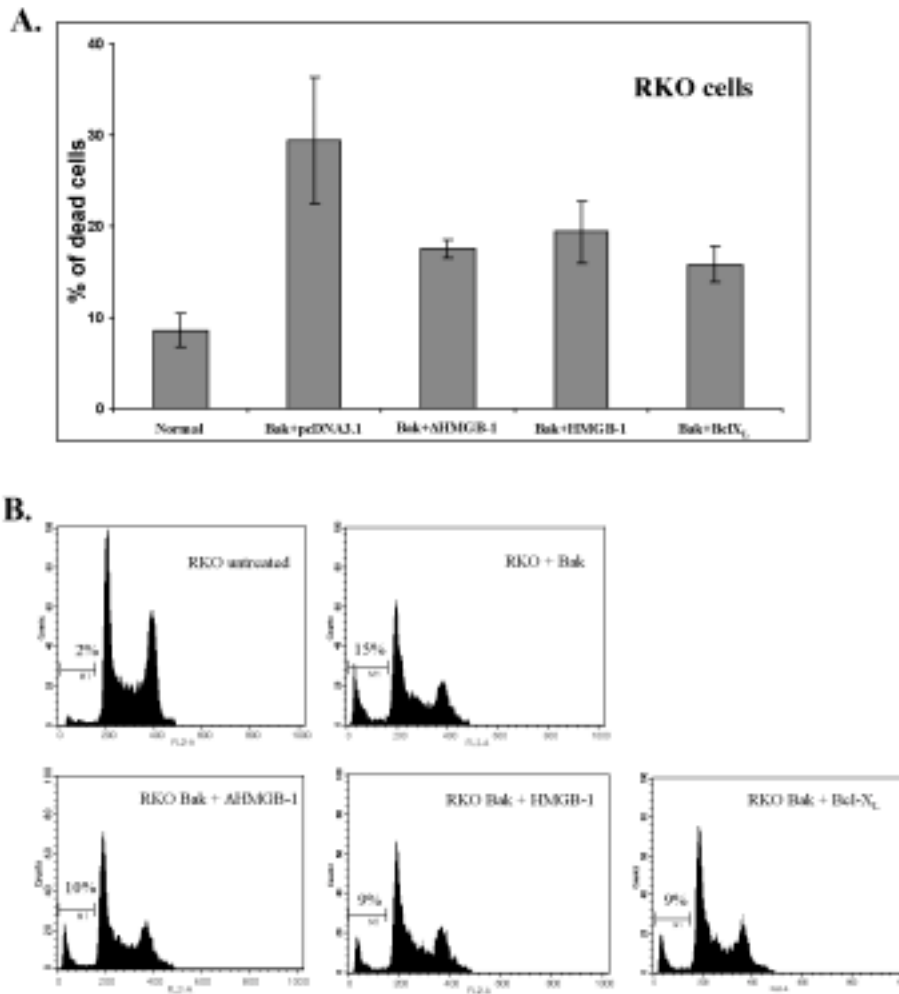


Fig. 51: HMGB1 and Δ HMGB1 inhibit Bak-induced apoptosis in RKO cells. A: RKO cells were seeded in 6-well plates at 1×10^6 cells/well. The next day $0.5 \mu\text{g}$ *gfp-bak* cDNA together with $1.5 \mu\text{g}$ of either empty vector pcDNA3.1, *Hmgb1*, Δ *Hmgb1* or *bcl-x_L* cDNA were transfected using FUGENE (Roche). 16 hours later cells were collected (including floating cells) and the percentage of dead cells was determined using the LIVE/DEAD Viability/Cytotoxicity kit from Molecular Probes. Co-transfection of both *Hmgb1* and Δ *Hmgb1* reduced the level of apoptosis to the same extent as did transfection of the *bona fide* inhibitor of Bak-killing, *bcl-x_L*. B: Quantification of a similar experiment as shown in A by a different method. Dead cells were counted by FACS analysis after ethanol fixation and propidium iodide staining. Apoptotic cells appear in the hypoploid sub-G₁ peak. Results shown in A are from 3 independent experiments, and results shown in B represent one of three experiments with similar results.

HMGB1 was as effective in inhibiting Bak killing as was Bcl-x_L in control co-transfections (see Fig. 51). The experiment was repeated with a different method to detect apoptotic cell death and the results were confirmed. Interestingly, endogenous HMGB1 is expressed at a relatively high level in RKO cells (data not shown), yet

further elevation of the HMGB1 level rescued RKO cells from apoptosis induced by *bak* transfection.

These data indicate that the protection conferred by HMGB1 in yeast against Bak-induced cell death is a general phenomenon observable also in mammalian cells. The overall low numbers of apoptotic cells in the experiment shown in Fig. 51, B are probably due to the poor transfection efficiency obtained in RKO cells.

3-Correlation between HMGB1 expression and tumourigenesis

Mutational activation of anti-apoptotic proteins is one possible mechanism through which transformed cells evade apoptosis and propagate to form tumours. Since HMGB1 protects against Bak-induced cell death in mammalian cells I analyzed HMGB1 protein levels in normal breast and in primary breast carcinoma material by performing Western blot experiments (Fig.52). I examined six different samples derived from normal breast tissue and they showed hardly any detectable HMGB1 protein (first six lanes). In comparison, of nine primary breast carcinomas tested, all expressed HMGB1, six of them in high amounts. I also examined seven human breast carcinomas which were passaged for a long time in nude mice. Such passaging of tumour cells in mice is regarded as an artificial model for tumour metastasis, i.e. genes important for metastasis become upregulated.

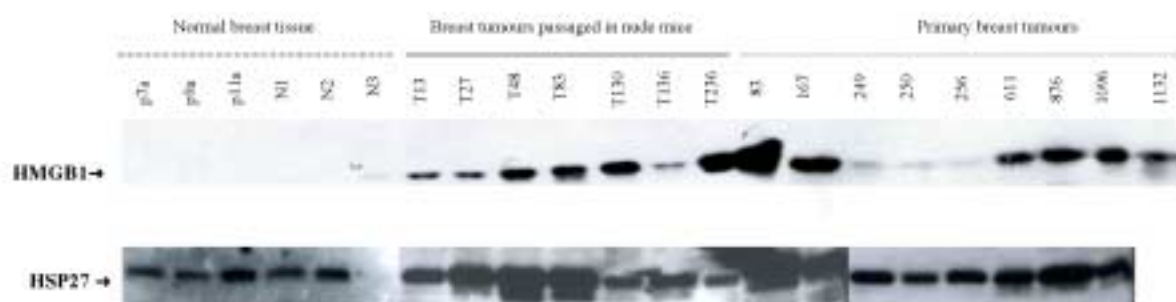


Fig. 52: HMGB1 protein overexpression in human mammary carcinomas. 40 μ g of protein lysates from normal breast tissue (p7a, p9a, p11a, N1, N2, N3), primary breast tumours (83, 167, 249, 250, 256, 611, 876, 1096, 1132) and breast tumours passaged in nude mice (T13, T27, T48, T83, T130, T136, T236) were analyzed in a Western blot experiment with an anti-HMGB1 antibody (*PharmMingen*). As a loading control, the membrane was rehybridized with an anti-HSP27 antibody (*Santa Cruz*).

All seven passaged breast tumours expressed high HMGB1 protein levels.

These expression data suggest that the HMGB1 protein is indeed upregulated in human breast carcinomas and that it is expressed constantly at a high level in a tumour transplantation model.

Since HMGB1 protein levels were elevated in breast carcinomas compared to normal breast tissue, I examined other tumour entities for *HMGB1* mRNA upregulation. For this purpose I hybridized a human cancer array with a ^{32}P -labelled *Hmgb1* cDNA probe (Fig. 53). Onto this cancer array equal amounts of cDNAs prepared from human tumour and corresponding normal tissue of the same patient were spotted in a pairwise fashion. The array represented a large collection of different tumours that were screened for *HMGB1* upregulation (for detail on the tumour types, see *The cancer profiling array*). To quantify expression levels, hybridization intensities were measured with a phosphoimaging system and to indicate up- or downregulation of a particular gene in a certain tumour the ratio between the arbitrary intensity values of a tumour and of the corresponding normal tissue were obtained. A ratio of greater than one would represent a tumour with an upregulated mRNA level compared to normal tissue while values smaller than one indicate mRNA downregulation in a certain tumour.

Fig. 53: Elevated *HMGB1* mRNA levels in tumours of the uterus, colon and stomach. A Cancer Profiling Array from *Clontech* was hybridized with a 32 [P]-labelled $\Delta Hmgb1$ probe. cDNA synthesized from different tumour RNAs was spotted pairwise on the array together with cDNA derived from corresponding normal tissue of the same patient. Hybridization signals were quantified with a *BIO RAD* phosphoimager. Represented in the figure are the ratios between the signal strength of tumour and normal tissue. Values greater than one indicate *HMGB1* tumour overexpression. For additional controls the array was re-hybridized with probes for the *bona fide* oncogene *c-myc* and for *ubiquitin*. A: Mean values of the signal strength ratio for each tumour entity. Uterus-, colon- and stomach-derived carcinomas show *HMGB1* overexpression. B: Expression ratios for each individual tumour. In some of the tumours *HMGB1* mRNA is expressed up to six times higher than in the corresponding normal tissue.

Fig. 53 summarizes the results for *HMGB1*, *c-myc* and *ubiquitin* in tumours of uterus, colon and stomach. For each gene, the mean ratio between several tumour/normal tissue pairs is represented for every tumour entity. *c-myc* as a *bona fide* oncogene is upregulated in tumours of the stomach and, even more prominently, in colon cancers. *c-myc* levels in tumours of the uterus appear normal. *Ubiquitin* expression in uterus and colon cancers seems to be unchanged. *HMGB1* mRNA on the other hand is upregulated in tumours of the uterus, colon and stomach. In further tissues represented on the tumour array but not shown in Fig. 53 I could not detect significant mean upregulation of *HMGB1* in the corresponding tumours although several individual tumours showed an obvious increase in the amount of *HMGB1* mRNA. While Fig. 53, A shows the mean ratio for each gene and tumour entity, Fig. 53, B displays the ratio of *HMGB1* mRNA expression levels between tumour and normal tissue for every single cancer represented on the array. Within individual tumours *HMGB1* mRNA is upregulated up to sixfold compared to the corresponding normal tissue.

In summary, these data imply that, in addition to HMGB-1 protein overexpression in breast carcinomas, *HMGB1* mRNA is upregulated in tumours derived from uterus, colon and stomach.

Dr. Kirsten Völp from Dr. Martin Zörnig laboratory (Georg-Speyer-Haus, Frankfurt) and Dr. Stephan Joos from Dr. Peter Lichter (DKFZ, Heidelberg) performed complementary experiments to this work. Their working results combined with mine allowed acceptance of the manuscript **“HMGB1 inhibits cell death in yeast and mammalian cells and is abundantly expressed in human breast carcinoma”** in *FASEB Journal* (*in press*). See Index.

V-Discussion

A-The survival screen and the selection of the isolated cDNA clones

Most of human diseases and disorders are related to the apoptotic pathway dysfunction. The aim of this work was to identify new anti-apoptotic proteins and understand their mechanistic function in order to provide new targets for therapies. I performed a yeast survival screen to look for “anti-apoptotic proteins inhibiting downstream of Cytochrome *c* release (Jurgensmeier, Krajewski et al. 1997; Xu and Reed 1998). For the screen I used as a “killer” gene, CED4, the *C. elegans* homologue of Apaf-1 that is inducing cell death in *S. pombe* (James, Gschmeissner et al. 1997). After two rounds of selection I isolated 22 cDNA that did confer protection against CED4 induced yeast cell death and verified that CED4 was still expressed in these clones under selective conditions (Fig.15), thus preventing the isolation of false positive clones mutated in their genome-integrated *nmt-1-CED4*. They were all sequenced and analysed by biocomputing whereas their name, the part of the protein encoded and the published data records. Particularly interesting were: the human RoRet / or zinc finger protein 15, the homo sapiens cell death regulator AVEN, the human thymosin beta 4, the human v-fos transformation effector protein (Fte-1)/or 40S ribosomal protein S3a, the human tumor necrosis factor/ or Lysosome-associated membrane glycoprotein 1 precursor , the PPAR γ -cofactor 2 (PGC2), the Serum amyloid A (SAA1-2) beta gene and the human fuse binding protein (FBP). Most of the cDNA clones were truncated, encoding only for a more or less extensive C-terminal part. This was due to the fact that very often the reverse polymerase transcribes only partly from 3' end to 5'end of the mRNA. Moreover some of the cDNAs were not in frame due to a base pair insertion disturbing the reading frame. Nevertheless some reports state that the yeast transcription machinery some times slips on the chromatine, permitting the transcription of a coding transcript. This frame-shift was later corrected by PCR.

Because none of the identified clones were typical antiapoptotic proteins, even though later some would be published as displaying antiapoptotic activity like Fte-1 and PPAR γ , I made extensive literature research to determine all the known data about each found protein (Tab.2). I decided to discard the Thymosin beta 4, because it encoded for the antisense DNA strand (-/+ strand) of the gene. Even though it would have been interesting to know how the antisense Thymosin beta 4 may have antiapoptotic activity, I decided to look for real potential antiapoptotic proteins. The same reason made me discard the human tumor necrosis factor/ or Lysosome-associated membrane glycoprotein 1 precursor, because the cDNA isolated encoded for a sequence in the 3'-untranslated, and the mitochondrial DNA control region. 3'-untranslated regions by controlling the specific decay of a mRNA have been found regulating cell fate (Bevilacqua, Ceriani et al. 2003; Stoecklin, Lu et al. 2003), but it was not the purpose of my work. I was interested in antiapoptotic proteins. From the literature and the CED4 expression test, I decided that the interesting clones to analyse would be: the RoRet, zinc finger protein 15, the homo sapiens cell death regulator AVEN, the v-fos transformation effector protein (Fte-1/ S3a), the PPAR γ -

cofactor 2 (PGC2), the Serum amyloid A (SAA1-2) beta gene and the fuse binding protein (FBP).

Indeed, Aven (Fig. 19) was just published to be antiapoptotic (Chau, Cheng et al. 2000) and act by binding to Apaf-1 and Bcl-X_L. The article was stating that its activity was derived from it's bringing Bcl-X_L and Apaf-1 together. But in my screening system only CED4 (or activated Apaf-1) was expressed with the C-terminal region of Aven. This was suggesting that Aven could by itself inhibit activated-Apaf-1-induced apoptosis and that the deleted protein contained the inhibitory activity of Aven. The deletion mutant encoded by the cDNA isolated in my screen is corresponding to the 183 last amino-acids of Aven where the putative Apaf-1 binding domain was define by Harwick and Al.

Fte-1/S3a (Fig. 20) was by then only described as encoding for a mammalian homologue for a yeast gene involved in protein import into mitochondria (Kho and Zarbl 1992) and as overexpressed in some tumour types(Kho, Wang et al. 1996). It was later published to have antiapoptotic (Song, Sakamoto et al. 2002) activity, even though the data produced in this paper were not very convincing concerning the mechanism proposed (that it may bind PARP and inhibit its DNase activity).

PGC2 is a PPAR γ cofactor found up to now only in fat tissue, and which function is still unknown. It was lately published that the PPAR γ receptor could play a role in modulating apoptosis(Padilla, Kaur et al. 2000; Goetze, Eilers et al. 2002), and the mechanism was shown to involve FLIP for the antiapoptotic activity (Okada, Yan et al. 2002).

The serum amyloid 1 beta gene is involved in rheumatoid arthritis and amyloidosis (Moriguchi, Terai et al. 2001). FBP (fuse binding protein) was identified during another screen for antiapoptotic proteins using a different method, mentioned in the publication, but not further investigated in its mechanism (Brockstedt, Rickers et al. 1998).

And finally RoRet (Fig. 21), was just a predicted protein, but its numerous and complex domains (a ring domain, a SPRY domain and a B-Box) suggested some very interesting functions like E3-ubiquitine ligase potential, DNA binding potential, and other undefined functions for the SPRY and B-Box domains. It was identified during the sequencing of the 1.1-Mb Transcript Map of the Hereditary Hemochromatosis Locus, and was named *RoRet* for its homology to the 52-kD *Ro/SSA* lupus and Sjogren's syndrome auto-antigen and the *RET* finger protein (Ruddy, Kronmal et al. 1997). The cDNA isolated during my screen corresponds to the PRY-SPRY domain.

To increase the stringency of the selection, I then decided to test these clones in a mammalian system, against Bax induced apoptosis in 293T cells and FasL induced apoptosis in RKO cells. I cloned the deletion part of each gene (corresponding to the cDNA isolated during the survival screen) in pcDNA3.1+, a mammalian expressing vector, and obtained most full length genes in mammalian expressing vectors from various groups. The only missing clone was RoRet, which was later purchased from *Invitrogen Corporation, ResGen*. The readout of these various experiments was that most clones full length or deletion mutants were

efficient in inhibiting apoptosis induced by Bak and FasL with an efficiency of 30% to 50% reduction of the dead cells (Fig.16-18).

For practical reasons I decided to reduce the number to three candidate clones. Based on the literature and the computational analyses, I finally decided to follow Aven as a new promising anti-apoptotic molecule in collaboration with Dr. M. Harwick (Johns Hopkins University, Baltimore, US) who first isolated and characterized the gene. I also chose Fte-1, because ribosomal proteins have revealed along the years to be implicated in more mechanisms than just protein translation, and RoRet because even though nothing else than its gene sequence is published, it contains very interesting domains. Two cDNA encoding for the full length gene were purchased by *ResGen*: RoRetg from the genestorm cDNA library contained the predicted DNA sequence, but RoRetc from the celera cDNA library contained a TTA stop codon in frame after 762 bp and should have led to the expression of a shorter protein. Intriguingly, cloning of this cDNA in the pEGFP-N1 vector that fused GFP to the C-terminal end of RoRetc, resulted in a protein migrating at the same height as RoRetg protein fused to GFP. The cellular localization looked the same as well. We are not able to explain this result. One possibility would be that the translation machinery is somehow slipping over the stop codon without recognizing it.

B-Analysis of RoRet, Aven and Fte-1 protection in yeast *S. pombe* and mammalian cells against apoptosis induction by different stimuli .

1-RoRet, Aven and Fte-1 protect mammalian cells against cells death induced by Bak and Apaf-1 M368L/Caspase-9 overexpression, but protect *S.pombe* only against CED4 induced cell death.

The different killing assays in *S. pombe* and in 293T and RKO cells had two goals. First I wanted to determine the protection efficacy against apoptosis induction by different stimuli, and second, I wanted to define if there is some similarity in the apoptotic pathway taking place in *S. pombe* and in mammalian cells. Indeed, some lately published work report of a yeast caspase existence (Madeo, Herker et al. 2002), and yeast cell death similar to apoptosis has long been observed without identification of the yeast homologues to the proteins able to induce these cell deaths (Bak, Bax, CED4...) (Jurgensmeier, Krajewski et al. 1997), (James, Gschmeissner et al. 1997).

The first experiments in yeast showed that Δ RoRet, Δ Aven and Fte-1 can protect *S. pombe* against CED4 but not Bak induced cell death (Fig. 22-25). The rescuing experiment of HC4 cells confirmed that CED-4 not only induces growth arrest but rather kills *S. pombe* yeast cells actively, and that Δ RoRet, Δ Aven and Fte-1 can protect against CED4 killing (Fig. 24). The low percentage of yeast cells reappearing when cultured only in non selective medium suggests that the *nmt-1* promoter may be leaky, allowing a certain amount of CED4 to be expressed in non selective medium as well. The growth curve (Fig. 25) showed the effect of Δ RoRet, Δ Aven and Fte-1 expression in *S. pombe* cells on their growth when CED4 is

induced (Fig. 23). The results showed that Δ RoRet was the most efficient to protect yeast cells against CED4 induced cell death. Δ Aven and Fte-1 were also efficient in their protection. And interestingly, the HC4 yeast cells transformed with the protective cDNAs were growing faster than the HC4 yeast cells growing in non selective medium, suggesting again that the *nmt-1* promoter may be leaky and allow a certain amount of CED4 to be expressed in non selective medium. This would explain the apparent slow growth of these HC4 *S. pombe* yeast cells in non selective medium. In *S. pombe*, CED4 induces cell death by translocating from the cytoplasm to the nucleus and inducing chromatin condensation. When co-expressed with CED9 its anti-apoptotic partner, it relocates at the endoplasmic reticulum and outer mitochondrial membrane (James, Gschmeissner et al. 1997). This suggests several possibilities of inhibitory mechanisms for RoRet, Aven and Fte-1. They could either block CED4 translocation to the nucleus, or block its binding to the chromatin, or sequester CED4 to some other compartment (mitochondria, ER, Golgi...). Nevertheless, all those mechanisms suggest direct or indirect binding to CED4.

The experiments aiming at testing the protective effect of Aven, Fte-1 and RoRet were first performed in RKO cells, which are suitable for FACS analysis. The propidium iodide staining and FACS cell cycle analysis is a convenient way to quantify apoptotic cell death. I co-transfected RKO cells with *apaf-1 M368L* and *caspase-9* and pcDNA3.1+, Δ *roret*-pcDNA3.1+, *roret*-pcDNA3.1/GS, Δ *aven*-pcDNA3.1+, *aven*-pSG5, *fte-1*-pMEXneo or *bcl-x_L*-pcDNA3.1. Apaf-1 M368L is an Apaf-1 mutant which doesn't need Cytochrome *c* release to activate Caspase-9, it can self-associated and bind procaspase-9 independently of the conformational change induced by Cytochrome *c*, but still requiring dATP/ATP [Hu, 1999 #3617]. Even though the induction of apoptosis was not strikingly high, certainly due to the transfection efficiency always quite low in RKO cells (20% to 30%), it was nevertheless obvious that RoRet, Aven, Fte-1 and their deletion mutants were efficient in inhibiting DNA fragmentation and cell death in a reproducible manner (Fig. 26).

Because RKO cells are probably type II cells, which means that their apoptotic onset needs mitochondrial activation and can be blocked by Bcl-2 overexpression (data obtained in our laboratory), I tested the protection efficiency of RoRet, Aven and Fte-1 against FasL induced apoptosis (Fig. 27). The protection effect was never exceeding 10% inhibition of cell death. But the transfection efficiency in RKO cells is ranging between 20% to 30% (determined by the number of cells expressing GFP when transfected with the pEGFP-N1) so in the end a 10% protection could still be significant if related to the amount of cells effectively overexpressing RoRet, Aven and Fte-1. FACS or MACS-sorting could have probably solved this problem, but our FACSCalibur (*Becton Dickinson*) didn't possessed this mode.

I also tested RoRet, Aven and Fte-1 protection efficiency against UV-induced apoptosis (Fig. 28). UV is known to induce p53 which in turn induces Bak targeting to the mitochondria [Degenhardt, 2002 #2212][Pohl, 1999 #6427] and Bax transcription (Kugu, Ratts et al. 1998). But again the protection efficiency was not very striking. It is possible that RoRet, Aven and Fte-1 protect only at the level of Caspase-9 activation, and that FasL and UV are inducing more than only one

apoptotic pathway. It was also obvious that the transfection efficiency was a problem, so I decided to change the system with cells easier to transfect like the 293T human embryonic kidney cells. But when tested in FACS, I observed that 293T cells do not fragment their DNA when induced into apoptosis by UV, Bak or Apaf-1 M368L/Caspase-9 overexpression. Thus I also had to change the readout system. As it is published in many papers and not necessary to prove anymore, Bak and Apaf-1/Caspase-9 overexpression induce apoptosis in mammalian cells. I decided to choose a system where I would only have to distinguish between dead and living cells. I found such a system provided by *Molecular Probes*: the LIVE/DEAD assay.

I co-transfected again RoRet, Aven, Fte-1 and their deletion mutants with Apaf-1 M368L and Caspase-9, in 293T cells (Fig. 29). This time I could reach 70% to 80% transfection efficiency, and apoptosis induction ranged between 40% and 60%. In this case an inhibition from 50% apoptosis to 20%-30% could be judged as significant. In this assay RoRet, Aven and Fte-1 inhibit Apaf-1/caspase-9 -induced apoptosis in efficiently in 293T cells. Furthermore, as Bak is known to trigger the mitochondrial pathway for apoptosis, I tested RoRet, Aven and Fte-1 potential to inhibit Bak induced apoptosis. The co-transfection experiment of Bak-GFP with RoRet, Aven, Fte-1 and their deletion mutants showed that RoRet, Aven, Fte-1 and their deletion mutants could efficiently inhibit Bak induced apoptosis, or with other words, mitochondrial activation induced apoptosis (Fig. 30). Taken together, these results point to the hypothesis that RoRet, Aven and Fte-1 inhibit apoptosis at the level of the apoptosome formation and Caspase-9 activation.

Because the results in *S. pombe* showed no inhibition of RoRet, Aven or Fte-1 Bak-induced cell death (Fig. 22), but inhibition of CED4 induced cell death (Fig. 23), I concluded that the pathways inducing cell death by CED4 or Bak expression were different and separated in yeast *S. pombe*, whereas in mammalian cells Bak activates the mitochondria and leads to activation of Apaf-1 downstream of Cytochrome *c* release. This hypothesis of separate death pathways induced in yeast would account for the different morphological features described for Bak, Bax or CED4 induced cell death. Bax causes growth arrest of yeast cells accompanied by cytochrome *c* release from mitochondria to cytosol, but in this case Cytochrome *c* is not necessary to induce cell death, it seems to be only a side effect of Bax killing (Manon, Chaudhuri et al. 1997), this cell death can be blocked by Bcl-2 coexpression. Bak is able to induce yeast cell lethality that can be antagonized by the mammalian anti-apoptotic protein Bcl-x_L. In this case cell death is accompanied by morphological feature resembling apoptosis like loss of nuclear membrane integrity, vacuolisation and chromatin condensation and fragmentation (Ink, Zornig et al. 1997). And CED-4 could induce active Cell Death in *S. pombe*, that was accompanied by the translocation of CED-4 from the ER and mitochondria to the nucleus (James, Gschmeissner et al. 1997). All these feature belong to the described morphological changes occurring during mammalian cells apoptosis, but none of the cell death inducers (Bak, Bax or CED4) was able to result in all these morphological changes at once. This suggest that yeast is still a simple organism, and the complicated pathway cross-talks occurring in mammalian cells do not exist into yeast.

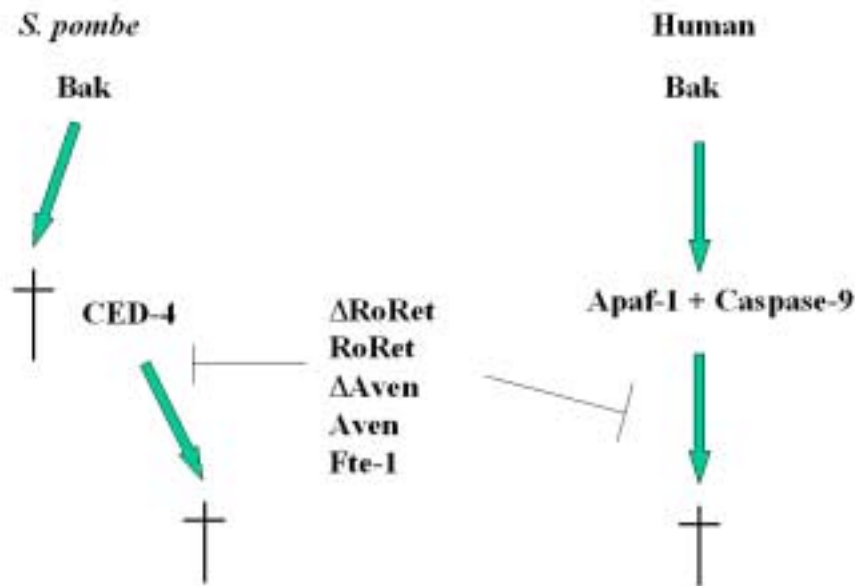


Fig. : Schematic representation of the obtained results about the protection capacity of RoRet, Aven and Fte-1.

2-RoRet, Aven and Fte-1 protect differently against apoptosis in mammalian cells.

RoRet, Aven and Fte-1 are inhibiting downstream of apoptosome formation as shown in the previous chapter. There are nevertheless, several possible inhibiting roles they can exert. They can block Caspase-9 cleavage, or only inhibit its activity. They could also act downstream of Caspase-9 activation by inhibiting Caspase-3 cleavage or activity. To test these different hypothesis, I co-transfected 293T cells with Apaf-1 M368L, Caspase-9 and RoRet, Aven, Fte-1 and their deletion mutants. I then looked by Western Blot for procaspase-9 cleavage. The data did not include results about RoRet full length, because at this time I had not obtained yet the full length cDNA. I could observe that procaspase-9 was disappearing when cells were overexpressing Apaf-1 M368L and Caspase-9 (Fig. 31). The levels of Procaspase-9 were maintained when the protecting proteins were over expressed together with Apaf-1 M368L and Caspase-9, even though a faint band at the correct size of Caspase-9 (p39) was still visible, suggesting that the inhibition was not complete. This would confirmed the protection data showing only 30% to 50% apoptosis inhibition. I then tried to look at Caspase-3 cleavage (Fig. 32). The result was not conclusive, due again perhaps to the low transfection efficiency of RKO cells. Nevertheless, ΔRoRet and ΔAven could inhibit in part procaspase-3 cleavage, whereas Aven and Fte-1 were quite ineffective. Again, FasL induced apoptosis in

RKO cells may also act through activation of other caspases. Unfortunately no clear data could be obtained with 293T cells.

The next step in the unravelling of the molecular pathway was to test caspase activity inhibition. The rather strong specificity of RoRet, Aven and Fte-1 protection in mind, I looked for inhibition of caspases activity (Fig. 33) focussing on Caspase-9 and -3 only by mitochondrial activation induced apoptosis in 293T cells. In these experiments, it was obvious that Δ RoRet, RoRet, Δ Aven, Aven and Fte-1 could inhibit Caspase-9 activity. When Caspase-3 activity could only be efficiently blocked by Δ RoRet, RoRet and Δ Aven, while Aven and Fte-1 give different results in different experiments permitting no definitive conclusion. Similar results, if somewhat less striking (again due to the transfection efficiency limits) were observed in RKO cells (data not shown).

The western blots data and the caspases activity data taken together, I can conclude that Δ RoRet, RoRet and Δ Aven are efficient inhibitors of Caspase-9 and Caspase-3 activity. In contrast, Aven full length and Fte-1 can only partly inhibit Caspase-9 activity. It is interesting to note again that the deleted forms are as if not more efficient than the full length protein, one possible explanation would be that the active inhibitory part of the protein must be activated through conformational changes or cleavage, whereas the deletion mutant already exhibit this inhibitory function without further activation necessary. I could conclude from this that the inhibition activity of both RoRet and Aven was situated in the deletion part isolated in the survival screen. The unpublished data from Dr. Marie Harwick about Aven confirm the last assumption for Aven. The deletion mutants of Aven without the domain define by my work had no inhibitory activity when they tested them for Caspase-9 activation.

A protein can inhibit the activity of another by binding directly or indirectly to it and blocking its activation or its catalytic activity. Because I isolated RoRet, Aven and Fte-1 in a screen against CED4 (activated Apaf1 homologue) induced cell death, I wanted to see if they could bind to Apaf-1. I had thus tested this hypothesis by “Yeast two-hybrid” for the possibility of direct binding. I also looked at potential interaction by “GST-pull down” of Apaf-1 from 293T cell lysate with RoRet, Aven and Fte-1 or “Co-immunoprecipitation” of Apaf-1 from 293T cell lysate with RoRet, Aven and Fte-1. The last two methods were interesting if the binding of Apaf-1 to one of the clones was indirect, or would require some post-translational modification and activation, that would be provided by the cell lysate components.

The results of the Yeast two-hybrid (Fig. 34) showed that only Fte-1 could binding to Apaf-1 in the region between the CED4 like domain and the WD40 repeat domain, from amino-acid 412 to amino-acid 601. Moreover, it is interesting to notice that Fte-1 do not bind to this region of Apaf-1 if the WD40 repeat region is present, suggesting that normally this region is masked, and when Apaf-1 is activated by binding to Cytochrome *c* it undergo a conformational change that would expose this domain to where Fte-1 can bind. Δ RoRet and Δ Aven showed no binding, in the two-hybrid, meaning that if there is interaction, it is not direct interaction, or it needs post-

translational modification that do not occur in *S. cerevisiae*. The results from the GST-pull down (Fig. 35) couldn't be analysed because Apaf-1 M368L did bind to the GST protein alone, if some what less strongly, still well enough to disturb the outcome of the experiment.

I also tried co-immunoprecipitation of my clones tagged to GFP, using either anti-GFP antibody, or anti-Apaf-1 antibody. I could co-immunoprecipitate Δ Aven together with Apaf-1 (Fig. 36), but I couldn't co-immunoprecipitate either Δ RoRet, RoRet or Fte-1 with Apaf-1. The result was quite puzzling for Fte-1 because the former data suggested that Apaf-1 and Fte-1 do interact. Maybe the interaction occurs under specific conditions not yet determined. It is also possible that the presence of the GFP protein (28 kD) at the C-terminal end of the protein disturb the interaction. Therefore I planned the repetition of these co-immunoprecipitation with FLAG-tagged proteins. Further studies will also try to detect these proteins within the apoptosome in collaboration with Sebastian Wesselborg by gel size chromatography and Western Blot analysis.

In further studies, I used confocal scanning microscopy to determine the cellular localization of RoRet, Aven, Fte-1 and their deletion mutants in order to verify if interaction can happen *in vivo* and to confirm co-localization. And following the previous experiments, it seemed relevant to try to look if Δ Aven and Fte-1 may co-localize with Apaf-1. It was also interesting to study the cellular localization of RoRet, which until now was completely unknown. Moreover, because it wasn't clear from the previous experiments, whether there is interaction with Apaf-1, and if this interaction is direct or indirect, I decided to look also for co-localization with Caspase-9. Caspase-9 and Apaf-1 bind to one another during the apoptosome formation (Li, Nijhawan et al. 1997; Srinivasula, Ahmad et al. 1998; Rodriguez and Lazebnik 1999), and RoRet and Aven could bind to Apaf-1 through Caspase-9. And as the issue of their maybe protection at the apoptosome level was still open, it was interesting to investigate if Aven, RoRet and Fte-1 could co-localize simultaneously with Apaf-1 and Caspase-9 in the apoptosome complex. For this purpose I have used the sequential scanning mode in confocal laser scanning microscopy. I have specifically stained 293T cells co-transfected with the GFP fusion constructs, Caspase-9 and Apaf-1 M368L. The specific Apaf-1 mutant was used in order to trigger Caspase-9/Apaf-1 complex formation without any other stimuli than protein over-expression (Hu, Benedict et al. 1999). The first thing that I could say is that co-localization of Apaf-1 with Caspase-9 was detectable only in these cells showing Apaf-1 over-expression. This was logical if we assume that only the mutant form of Apaf-1 can bind and activate Caspase-9 without further stimuli as protein over-expression.

Δ Aven-GFP showed a localization pattern similar to the one published for Aven (Chau, Cheng et al. 2000) (Fig. 41). Δ Aven is located in the cytoplasm in a spotted fashion, suggesting some aggregates or organelles location. No Δ Aven was detected in the nucleus. Apaf-1 showed also a cytoplasmic profile, and again spotted and not diffuse. Apaf-1 concentrations increase around the nucleus and in a compact area near the nucleus (Fig. 37-44). Former reported data observed that Apaf-1

localizes at the Golgi in cells expressing Bcl-2 and in the cytoplasm in cells lacking Bcl-2 (Ruiz-Vela, Albar et al. 2001). Caspase-9 was found in the cytoplasm and sometimes the nucleus (Fig. 37-44). These results are also confirming published the data about its cellular localization (Hausmann, O'Reilly et al. 2000; Shikama, U et al. 2001). The overlay pictures of Δ Aven and Apaf-1 showed that Δ Aven and Apaf-1 are partly co-localizing, whereas the overlay picture of Δ Aven and Caspase-9 show a clear co-localization of these two proteins (Fig. 37). Moreover, in cells over expressing Apaf-1 M368L the overlay picture of Δ Aven, Apaf-1 and Caspase-9 suggests the presence of all three proteins in a complex (Fig. 41). It would be interesting to look for co-immunoprecipitation of Aven with Caspase-9, and check if it's interacting with pro-caspase-9 or the cleaved activated form.

Fte-1-GFP could be detected in a well define compartment that looks like the endoplasmic reticulum or the Golgi (Fig. 38), specific staining of these compartments are planned and should confirm this guess. In this experiment, the overlay of Fte-1 and Apaf-1 could detect co-localization at the compartment described above, whereas the overlay of Fte-1 and Caspase-9 could detect co-localization areas surrounding this compartment. I could say that Fte-1 and Apaf-1 partly co-localize, but the result with Caspase-9 was not clear (Fig. 38). In the experiment with Fte-1-GFP, Apaf-1 M368L and Caspase-9 showed that in some cells co-localization of all three proteins could be detected, whereas in others only areas where Fte-1-GFP co-localizes with Apaf-1 M368L but not Caspase-9 could be seen (Fig. 42). Moreover, these co-localization of all three proteins areas co-exist with still free Fte-1-GFP, suggesting that only a specific pool of Fte-1-GFP co-localizes with Apaf-1 and/ or with Caspase-9. The exact conditions in which this co-localization would take place are not yet determined. One hypothesis is that Fte-1 would be the unknown protein that encores Apaf-1 to the Golgi in those cells expressing Bcl-2 (Ruiz-Vela, Albar et al. 2001).

Δ RoRet-GFP shows a diffuse cytoplasmatic and nuclear cellular localization (Fig. 39). The merged picture of Δ RoRet-GFP and Apaf-1 or Caspase-9 was not clear enough to really suggest a co-localization with either Apaf-1, either Caspase-9 (Fig. 39). But in the experiment where I tried to look for all three protein colocalization, Δ RoRet-GFP seem to co-localize with caspase-9 but not really with Apaf-1 M368L (Fig. 43). No co-localization of all three proteins could be detected, suggesting a more probable interaction with Caspase-9 that with Apaf-1. It is altogether possible that Δ RoRet-GFP protect the cell against apoptosis by binding to Caspase-9 and preventing its recruitment to Apaf-1. Such a hypothesis will be investigated in the future by co-immunoprecipitation attempts of Δ RoRet-GFP with Caspase-9. Full length RoRet was also cloned in pEGFP-N1 and the fusion GFP construct was used for detection in confocal laser scanning microscopy (Fig. 44). The cellular localization of the full length protein showed a largely punctuated pattern that looks similar to some kind of vesicles suggesting that the deletion mutant protein lack some targeting signal in its sequence. Further characterization of these organelles should tell us what they are exactly. RoRet-GFP could also sometimes (not shown because not significantly frequent) be detected into the nucleus. And, like for Δ RoRet, I saw co-localization of RoRet with Caspase-9, but not with Apaf-1 together with Caspase-9, even though Apaf-1 and Caspase-9 obviously co-localized. It suggests that two different pools of Caspase-9 interact with either RoRet either Apaf-1. This could join

the hypothesis emitted for Δ RoRet, that RoRet would bind Caspase-9 and preventing it from being recruited at the apoptosome.

C-Analysis of the In vivo relevance of these inhibitors of apoptosis: their possible implication in tissue homeostasis, regulation or tumourigenesis.

It was important to investigate the physiological relevance of these proteins function. It was not possible to look for RoRet protein because of the absence of antibodies (we are in the process of raising and purifying them). Nevertheless, it was still possible to analyse expression levels of this gene at the mRNA level. On the other side, Aven and Fte-1 could be investigated on both protein and mRNA levels. The functional and physiological aspects were investigated by studying the expression of Aven in a highly regulated tissue: the mammary gland, and secondly by investigating the different expression levels of Aven, Fte-1 and RoRet in tumour tissues versus healthy tissues.

To look for Aven regulation in morphologically changing tissue, the choice of the mammary glands tissue was relevant. Indeed, during pregnancy the mammary glands are the siege of multiple changes: epithelial mammary cells differentiate and form branching tubules and small alveoli. Then during lactation the differentiation continues and the alveoli produce milk proteins. After birth, these alveoli undergo apoptosis, the mammary tissue undergo involution and returns to its state before pregnancy. For this purpose I analysed the expression of *aven* on a Northern Blot (from *Clontech*) where equal amounts of mRNA from the different differentiated stages of the mammary gland were spotted (Fig. 45). I could observe downregulation of Aven during lactation and during involution. What was more surprising was that if we consider the lactation state as highly differentiated for the mammary gland cells, then there is the question, why don't we observe down regulation already during the pregnancy when the cells are differentiating? It is possible that during the pregnancy the cells need a higher proliferation potential and not so much differentiating capacity. It may imply that Aven is important during proliferation and would be downregulated during differentiation. It is also possible that Aven is downregulated during lactation to prepare the cells for apoptosis during involution. It was nevertheless reassuring to observe the lowest expression levels of Aven (which is anti-apoptotic) during involution time which witnesses high apoptosis within the mammary gland cells. RT-PCR studies (data not shown) showed a tendency of down regulation already during pregnancy, and already an up-regulation to normal levels during day 5 of involution.

I tried to go one step further by using the published model of KIM-2 cells. This mouse mammary epithelial cell line can be induce to differentiate and after differentiation further induced into apoptosis (Gordon, Binas et al. 2000). I studied Aven expression at the different differentiated stages of this cell line: undifferentiated, differentiated and apoptotic by Western Blot (Fig. 46). I found that Aven slightly decreases in differentiating cells, and significantly decreases in apoptotic cells. As it is described that only about 30% of the cells undergo apoptosis, it is also possible that the remaining Aven comes from the non-apoptotic cells. This question will be

answered in further studies involving *aven* anti-sense RNA and siRNA. Nevertheless, the results are consistent with the described anti-apoptotic activity of Aven that will suppose downregulation or rapid degradation of the protein to allow apoptosis. Furthermore, the decrease in the protein level during the differentiated stage suggest again that Aven may also be important during proliferation.

To investigate the possible role of Aven, RoRet or Fte-1 in cancerogenesis I analyse mRNA expression levels in normal and tumour tissue. For this I used the Cancer Profiling Array from *Clontech*. This array contains many cDNA pairs of tumour and normal tissue, each from a single patient (Fig. 47). This array was intend to screen a large panel of tumour types an allow us to determine in what possible tumour type our apoptosis inhibitors could play a role. It was interesting to observe a tendency to up regulation of *aven* in uterus, colon and especially in kidney tumours. *fte-1* showed a tendency to be up regulated in colon cancers and *roret* in uterus cancers. Moreover, the specific tumours where *c-myc* was up-regulated, like colon and rectum, showed that the array screen should be accurate. Indeed some published data already state that *c-myc* play an important role in colon cancer-genesis (Funato, Kozawa et al. 2001; Wilson, Velcich et al. 2002). The *ubiquitin* was mend as a negative control, and not surprisingly was only found slightly up-regulated in kidney cancer. Zarbl and Al. have already studied the role of Fte-1 in transformed mouse fibroblasts, they observed that Fte-1 is not sufficient to induce cell transformation, but the suppression of Fte-1 could suppress the transformed phenotype (Kho, Wang et al. 1996) (Fig. 48). This would suggest that Fte-1 is necessary if not enough for cell transformation. But of course these data have to be confirmed at the protein level in tumour samples by western blotting. And for this reason I have started to collect samples of normal tissue/tumour pairs of breast, colon and kidney. Further investigations are also pursue in collaboration with Dr. Stephan Joos (DKFZ, Heidelberg, Germany), that will allow the testing of tumour tissue arrays with the anti-aven and the anti-Fte-1 antibody.

D-HMGB1 inhibits cell death in yeast and mammalian cells and is overexpressed in certain human tumours.

HMGB1 was identified during a different screen where we set up an inducible Bak expression system in *S. pombe*. When we transformed Bak expressing *S. pombe* yeast cells with a cDNA library synthesized from mouse NIH 3T3 fibroblasts, we found the chromosomal protein HMGB1 as a protector against Bak-induced yeast cell death. The deletion mutant Δ HMGB1, which we isolated in the screen and which lacks the C-terminal 33 amino acids, is even more potent in inhibiting Bak-killing in yeast than the full length protein (Fig. 50). Since we only tested 5×10^4 transformed yeast colonies for Bak-resistance, screening of the NIH 3T3 library was by far not complete. This probably explains why we did not isolate well-known inhibitors of Bak cytotoxicity like Bcl-x_L.

If protected against Bak-killing by overexpression of Δ HMGB1, *S. pombe* cells grow exponentially while expressing a large amount of Bak (which is much higher than the amount of Bak necessary to kill untransformed yeast cells). These data rule out the possibility that Δ HMGB1 downregulates Bak-transcription from the *nmt-1* promoter used to express Bak in the yeast.

I could show that both Δ HMGB1 and full length HMGB1 are able to suppress Bak-induced apoptosis in mammalian cells (Fig.51). HMGB1 is an abundant nuclear protein with roughly 1×10^6 molecules per nucleus (Bianchi and Beltrame 1998). Yet despite its abundance the protein may be limiting within cells: transient overexpression of HMGB1 enhances the transcriptional activity of factors such as P53 and steroid hormone receptors. Similarly, an increase of HMGB1 protein levels in mammalian cells by transfection leads to inhibition of Bak-killing. Since we have identified HMGB1 in a yeast screen for anti-apoptotic genes and because we have shown HMGB1's anti-apoptotic capacity in mammalian cells, we investigated whether the protein is overexpressed in human tumours. Our analysis revealed profound HMGB1 protein expression in human primary breast carcinomas (Fig.52). We also observed strong HMGB1 expression in human breast carcinomas transplanted into nude mice. In contrast, we could not detect significant amounts of HMGB1 protein in normal breast tissue arguing that the protein is overexpressed in mammary carcinomas. We also detected overexpression of *HMGB1* RNA in human tumours of the uterus, colon and stomach (Fig.53).

Elevated *HMGB1* mRNA levels have already been reported in human gastrointestinal adenocarcinomas compared to corresponding non-cancerous mucosa. The authors had suggested a correlation between *HMGB1* mRNA expression and differentiation /staging of the carcinomas. Furthermore, a strong intertumoural variation of *HMGB1* mRNA expression within 13 breast cancer samples was published by Flohr *et al.* (Flohr, Rogalla *et al.* 2001). The authors argue that this variation may contribute to the different response of estrogen receptor-positive breast tumours to endocrine therapy. This argument is based on the observation that HMGB-1 increases binding of the estrogen receptor to its DNA target sequence (Boonyaratanakornkit, Melvin *et al.* 1998). HMGB1 binds with high affinity to DNA damaged by cisplatin, and it is speculated that HMGB1 contributes to cisplatin cytotoxicity by shielding damaged DNA from repair (Pasheva, Ugrinova *et al.* 2002). Paradoxically, HMGB1 overexpression has also been correlated with cisplatin-resistance in cell lines (Imamura, Izumi *et al.* 2001) which could be explained by our data demonstrating anti-apoptotic properties for HMGB1. Both HMGB1 and HMGB-2 contain two similar, but distinct "HMG boxes" (A and B), and a long acidic C-terminal tail, which is deleted in the Δ HMGB1 protein identified in our yeast screen (reviewed in (Travers 2000)). The HMG box consists of approximately 80 amino acids and has a characteristic, twisted, L-shaped fold formed by three α -helical segments (Read, Cary *et al.* 1993). It binds to DNA through the minor groove and induces site-specific DNA deformations. HMGB proteins recognize and bind to altered DNA conformations, such as stem-loop, four-way-junction, kinked or underwound DNA ((Travers 2000) and references herein). Although they possess little or no sequence preference, HMGB1 interacts with proteins like P53 or steroid

hormone receptors and increases the apparent DNA binding affinity of these transcription factors (Jayaraman, Moorthy et al. 1998). Lack of the protein in *Hmgb1* knockout mice did not disrupt cell growth but rather caused lethal hypoglycaemia in the newborn mice, possibly due to impaired transcriptional glucocorticoid receptor activity (Calogero, Grassi et al. 1999). Such a role for HMGB1 as a regulator of transcription may influence the apoptotic behaviour of a cell. It has for example been shown that HMGB1 inhibits both P73 α/β - and P53-dependent transactivation from the *bax* gene promoter in *p53*-deficient SAOS-2 cells (Stros, Ozaki et al. 2002). Although this does not explain HMGB1's ability to suppress cell death upon Bak overexpression, it is certainly possible that HMGB1 transcriptionally regulates a downstream component of the Bak- triggered apoptosis pathway.

VII-Summary and outlooks

The aim of this work was to identify new anti-apoptotic proteins and to understand their mechanistic function in order to provide new potential targets for molecular therapies. I performed a yeast survival screen to identify anti-apoptotic proteins inhibiting apoptosis downstream of Cytochrome *c* release (Jurgensmeier, Krajewski et al. 1997; Xu and Reed 1998). For the screen I used as a “killer” protein, CED4, the *C. elegans* homologue of Apaf-1, to induce cell death in *S. pombe* (James, Gschmeissner et al. 1997). Six proteins were isolated that inhibit CED4-induced yeast cell death. Overexpression of these proteins also prevents induction of apoptosis by Caspase-9 activation through the apoptosome formation. Those six molecules were RoRet (Ruddy, Kronmal et al. 1997), Aven (Chau, Cheng et al. 2000), Fte-1/S3a (Kho, Wang et al. 1996), PGC2 (Padilla, Kaur et al. 2000; Goetze, Eilers et al. 2002), SAA1-2 β (Moriguchi, Terai et al. 2001) and FBP (Brockstedt, Rickers et al. 1998) of which I selected RoRet, Aven and Fte-1/S3a for further analysis.

RoRet is a new anti-apoptotic molecule that can inhibit the mitochondrial pathway via its PRY-SPRY domain. Its intracellular localization seems to vary depending of the cells. It can be either nuclear or localize in organelles which nature remains to be determined. The PRY-SPRY domain when expressed alone is located in the cytoplasm and into the nucleus. Whether it binds to Caspase-9 and prevents its recruitment to the apoptosome still has to be proven, but I did not obtain evidence that RoRet binds to Apaf-1. I also does not co-localize with the activated Apaf-1/Caspase-9 complex. The future production and analysis of knockout mice should help to better understand the *in vivo* functions of RoRet.

Aven was published to act as an anti-apoptotic protein and suggested to function via the recruitment of Bcl-X_L to Apaf-1. I could show that its C-terminal domain can bind to Apaf-1 and has a strong anti-apoptotic activity by itself. Moreover, I could show that Aven co-localizes with the activated Apaf-1/Caspase-9 complex suggesting that it is a component of the apoptosome. I could also show that the expression of Aven is regulated in mammary glands during the pregnancy cycle. Here again the production of knockout mice should help to unravel the complex activity of this protein.

Fte-1/S3a has been already implicated in increased transformation capacity of v-Fos in fibroblasts (Kho and Zarbl 1992; Kho, Wang et al. 1996). I could confirm in my work that it has anti-apoptotic activity and can protect against Bak- and Apaf-1-induced apoptosis. I could also show that it binds directly to activated Apaf-1 at the linker domain between the WD40 repeats and the CED4-like domain, suggesting that it may protect by sequestering the activated Apaf-1 to some organelles whose nature remains to be determined (Golgi, ER or even mitochondria). Moreover, expression studies on mRNA and protein level showed upregulation of Fte-1/S3a in colon, lung and kidney carcinoma. A larger panel of colon tumour samples is currently tested for expression, and should allow us to validate these data.

Hmgb1 (Flohr, Rogalla et al. 2001; Pasheva, Ugrinova et al. 2002; Stros, Ozaki et al. 2002) was identified during a survival screen performed with a NIH 3T3 mouse fibroblast cDNA library in a Bak-expressing yeast *S. pombe* strain. HMGB1 displays a broader anti-apoptotic activity, it can protect against Bak-, but also UV-, FasL- and TRAIL-induced apoptosis. I detected significant over expression of HMGB1 in breast and colon cancer, and elevated *HMGB1* mRNA amounts in uterus, colon and stomach tumours. The mechanism by which HMGB1 may protect remains nevertheless unclear, but doesn't involve binding of HMGB1 for example to Bak or downregulation of *bak* transcription (Brezniceanu et al; 2003).

Finally, these results show as a proof of principle that the survival screen in *S. pombe* was successful in identifying new and already known anti-apoptotic proteins that act downstream of Cytochrome *c* release during apoptosis and which might act as death-inhibiting oncogenes.

References:

- Acehan, D., X. Jiang, et al. (2002). "Three-dimensional structure of the apoptosome: implications for assembly, procaspase-9 binding, and activation." Mol Cell **9**(2): 423-32.
- Adams, J. M. and S. Cory (2002). "Apoptosomes: engines for caspase activation." Curr Opin Cell Biol **14**(6): 715-20.
- Ahmad, M., S. M. Srinivasula, et al. (1997). "CRADD, a novel human apoptotic adaptor molecule for caspase-2, and FasL/tumor necrosis factor receptor-interacting protein RIP." Cancer Res **57**(4): 615-9.
- Akao, Y., Y. Otsuki, et al. (1994). "Multiple subcellular localization of bcl-2: detection in nuclear outer membrane, endoplasmic reticulum membrane, and mitochondrial membranes." Cancer Res **54**(9): 2468-71.
- Alimonti, J. B., L. Shi, et al. (2001). "Granzyme B induces BID-mediated cytochrome *c* release and mitochondrial permeability transition." J Biol Chem **276**(10): 6974-82.
- Ameisen, J. C. (1994). "Programmed cell death (apoptosis) and cell survival regulation: relevance to AIDS and cancer." Aids **8**(9): 1197-213.
- Ameisen, J. C. (1996). "The origin of programmed cell death." Science **272**(5266): 1278-9.

- Ameisen, J. C., J. Estaquier, et al. (1994). "From AIDS to parasite infection: pathogen-mediated subversion of programmed cell death as a mechanism for immune dysregulation." Immunol Rev **142**: 9-51.
- An, B. and Q. P. Dou (1996). "Cleavage of retinoblastoma protein during apoptosis: an interleukin 1 beta-converting enzyme-like protease as candidate." Cancer Res **56**(3): 438-42.
- Arnoult, D., I. Tatischeff, et al. (2001). "On the evolutionary conservation of the cell death pathway: mitochondrial release of an apoptosis-inducing factor during Dictyostelium discoideum cell death." Mol Biol Cell **12**(10): 3016-30.
- Ashton-Rickardt, P. G., L. Van Kaer, et al. (1993). "Peptide contributes to the specificity of positive selection of CD8+ T cells in the thymus." Cell **73**(5): 1041-9.
- Badrichani, A. Z., D. M. Stroka, et al. (1999). "Bcl-2 and Bcl-XL serve an anti-inflammatory function in endothelial cells through inhibition of NF-kappaB." J Clin Invest **103**(4): 543-53.
- Baehrecke, E. H. (2002). "How death shapes life during development." Nat Rev Mol Cell Biol **3**(10): 779-87.
- Bennett, M., K. Macdonald, et al. (1998). "Cell surface trafficking of Fas: a rapid mechanism of p53-mediated apoptosis." Science **282**(5387): 290-3.
- Berger, T., M. Brigl, et al. (2000). "The apoptosis mediator mDAP-3 is a novel member of a conserved family of mitochondrial proteins." J Cell Sci **113**(Pt 20): 3603-12.
- Bevilacqua, A., M. C. Ceriani, et al. (2003). "Bcl-2 protein is required for the ARE-dependent degradation of its own messenger." J Biol Chem **17**: 17.
- Bianchi, M. E. and M. Beltrame (1998). "Flexing DNA: HMG-box proteins and their partners." Am J Hum Genet **63**(6): 1573-7.
- Biswas, S. C. and L. A. Greene (2002). "Nerve growth factor (NGF) down-regulates the Bcl-2 homology 3 (BH3) domain-only protein Bim and suppresses its proapoptotic activity by phosphorylation." J Biol Chem **277**(51): 49511-6.
- Boonyaratanakornkit, V., V. Melvin, et al. (1998). "High-mobility group chromatin proteins 1 and 2 functionally interact with steroid hormone receptors to enhance their DNA binding in vitro and transcriptional activity in mammalian cells." Mol Cell Biol **18**(8): 4471-87.
- Borchelt, D. R., P. C. Wong, et al. (1998). "Transgenic mouse models of Alzheimer's disease and amyotrophic lateral sclerosis." Brain Pathol **8**(4): 735-57.
- Bouillet, P., S. Cory, et al. (2001). "Degenerative disorders caused by Bcl-2 deficiency prevented by loss of its BH3-only antagonist Bim." Dev Cell **1**(5): 645-53.
- Brockstedt, E., A. Rickers, et al. (1998). "Identification of apoptosis-associated proteins in a human Burkitt lymphoma cell line. Cleavage of heterogeneous nuclear ribonucleoprotein A1 by caspase 3." J Biol Chem **273**(43): 28057-64.
- Brodsky, M. H., W. Nordstrom, et al. (2000). "Drosophila p53 binds a damage response element at the reaper locus." Cell **101**(1): 103-13.
- Calogero, S., F. Grassi, et al. (1999). "The lack of chromosomal protein Hmg1 does not disrupt cell growth but causes lethal hypoglycaemia in newborn mice." Nat Genet **22**(3): 276-80.
- Cerretti, D. P., C. J. Kozlosky, et al. (1992). "Molecular cloning of the interleukin-1 beta converting enzyme." Science **256**(5053): 97-100.
- Chai, J., C. Du, et al. (2000). "Structural and biochemical basis of apoptotic activation by Smac/DIABLO." Nature **406**(6798): 855-62.

- Chai, J., E. Shiozaki, et al. (2001). "Structural basis of caspase-7 inhibition by XIAP." *Cell* **104**(5): 769-80.
- Chau, B. N., E. H. Cheng, et al. (2000). "Aven, a novel inhibitor of caspase activation, binds Bcl-xL and Apaf-1." *Mol Cell* **6**(1): 31-40.
- Cheng, E. H., D. G. Kirsch, et al. (1997). "Conversion of Bcl-2 to a Bax-like death effector by caspases." *Science* **278**(5345): 1966-8.
- Chin, Y. E., M. Kitagawa, et al. (1997). "Activation of the STAT signaling pathway can cause expression of caspase 1 and apoptosis." *Mol Cell Biol* **17**(9): 5328-37.
- Chiou, S. K., L. Rao, et al. (1994). "Bcl-2 blocks p53-dependent apoptosis." *Mol Cell Biol* **14**(4): 2556-63.
- Christensen, S. T., J. Chemnitz, et al. (1998). "Staurosporine-induced cell death in *Tetrahymena thermophila* has mixed characteristics of both apoptotic and autophagic degeneration." *Cell Biol Int* **22**(7-8): 591-8.
- Cikala, M., B. Wilm, et al. (1999). "Identification of caspases and apoptosis in the simple metazoan Hydra." *Curr Biol* **9**(17): 959-62.
- Cilenti, L., Y. Lee, et al. (2003). "Characterization of a novel and specific inhibitor for the pro-apoptotic protease Omi/HtrA2." *J Biol Chem* **278**(13): 11489-94.
- Clarke, P. G. (1990). "Developmental cell death: morphological diversity and multiple mechanisms." *Anat Embryol* **181**(3): 195-213.
- Clarke, P. G. and S. Clarke (1996). "Nineteenth century research on naturally occurring cell death and related phenomena." *Anat Embryol (Berl)* **193**(2): 81-99.
- Cohen, G. M. (1997). "Caspases: the executioners of apoptosis." *Biochem J* **326**(Pt 1): 1-16.
- Cohen, J. J. (1993). "Apoptosis." *Immunol Today* **14**(3): 126-30.
- Cory, S. and J. M. Adams (2002). "The Bcl2 family: regulators of the cellular life-or-death switch." *Nat Rev Cancer* **2**(9): 647-56.
- Cowan, W. M., J. W. Fawcett, et al. (1984). "Regressive events in neurogenesis." *Science* **225**(4668): 1258-65.
- Cryns, V. and J. Yuan (1998). "Proteases to die for." *Genes Dev* **12**(11): 1551-70.
- Datta, S. R., A. Katsov, et al. (2000). "14-3-3 proteins and survival kinases cooperate to inactivate BAD by BH3 domain phosphorylation." *Mol Cell* **6**(1): 41-51.
- Davies, A. M., S. Hershman, et al. (2003). "A Ca²⁺-induced mitochondrial permeability transition causes complete release of rat liver endonuclease G activity from its exclusive location within the mitochondrial intermembrane space. Identification of a novel endo-exonuclease activity residing within the mitochondrial matrix." *Nucleic Acids Res* **31**(4): 1364-73.
- del Peso, L., M. Gonzalez-Garcia, et al. (1997). "Interleukin-3-induced phosphorylation of BAD through the protein kinase Akt." *Science* **278**(5338): 687-9.
- Deveraux, Q. L., R. Takahashi, et al. (1997). "X-linked IAP is a direct inhibitor of cell-death proteases." *Nature* **388**(6639): 300-4.
- Ding, H. F., G. McGill, et al. (1998). "Oncogene-dependent regulation of caspase activation by p53 protein in a cell-free system." *J Biol Chem* **273**(43): 28378-83.
- Dorstyn, L., P. A. Colussi, et al. (1999). "DRONC, an ecdysone-inducible *Drosophila* caspase." *Proc Natl Acad Sci U S A* **96**(8): 4307-12.
- Dorstyn, L., S. Read, et al. (2002). "The role of cytochrome c in caspase activation in *Drosophila melanogaster* cells." *J Cell Biol* **156**(6): 1089-98.

- Du, C., M. Fang, et al. (2000). "Smac, a mitochondrial protein that promotes cytochrome c-dependent caspase activation by eliminating IAP inhibition." Cell **102**(1): 33-42.
- Duan, H. and V. M. Dixit (1997). "RAIDD is a new 'death' adaptor molecule." Nature **385**(6611): 86-9.
- Ehlert, J. E. and M. H. Kubbutat (2001). "Apoptosis and its relevance in cancer therapy." Onkologie **24**(5): 433-40.
- Ellis, H. M. and H. R. Horvitz (1986). "Genetic control of programmed cell death in the nematode *C. elegans*." Cell **44**(6): 817-29.
- Ellis, R. E., J. Y. Yuan, et al. (1991). "Mechanisms and functions of cell death." Annu Rev Cell Biol **7**: 663-98.
- Enari, M., H. Sakahira, et al. (1998). "A caspase-activated DNase that degrades DNA during apoptosis, and its inhibitor ICAD." Nature **391**(6662): 43-50.
- Erhardt, P., K. J. Tomaselli, et al. (1997). "Identification of the MDM2 oncoprotein as a substrate for CPP32-like apoptotic proteases." J Biol Chem **272**(24): 15049-52.
- Evan, G. and T. Littlewood (1998). "A matter of life and cell death." Science **281**(5381): 1317-22.
- Evans, E. K., T. Kuwana, et al. (1997). "Reaper-induced apoptosis in a vertebrate system." Embo J **16**(24): 7372-81.
- Fantuzzi, G., A. J. Puren, et al. (1998). "Interleukin-18 regulation of interferon gamma production and cell proliferation as shown in interleukin-1beta-converting enzyme (caspase- 1)-deficient mice." Blood **91**(6): 2118-25.
- Finkel, E. (2001). "The mitochondrion: is it central to apoptosis?" Science **292**(5517): 624-6.
- Fisher, G. H., F. J. Rosenberg, et al. (1995). "Dominant interfering Fas gene mutations impair apoptosis in a human autoimmune lymphoproliferative syndrome." Cell **81**(6): 935-46.
- Flanagan, J. G. (1999). "Life on the road." Nature **401**(6755): 747-8.
- Flohr, A. M., P. Rogalla, et al. (2001). "Variation of HMGB1 expression in breast cancer." Anticancer Res **21**(6A): 3881-5.
- Fu, W. N., S. M. Kelsey, et al. (2001). "Apaf-1XL is an inactive isoform compared with Apaf-1L." Biochem Biophys Res Commun **282**(1): 268-72.
- Fuchs, S. Y., V. Adler, et al. (1998). "JNK targets p53 ubiquitination and degradation in nonstressed cells." Genes Dev **12**(17): 2658-63.
- Fujise, K., D. Zhang, et al. (2000). "Regulation of apoptosis and cell cycle progression by MCL1. Differential role of proliferating cell nuclear antigen." J Biol Chem **275**(50): 39458-65.
- Fulda, S., W. Wick, et al. (2002). "Smac agonists sensitize for Apo2L/TRAIL- or anticancer drug-induced apoptosis and induce regression of malignant glioma in vivo." Nat Med **8**(8): 808-15.
- Funato, T., K. Kozawa, et al. (2001). "Modification of the sensitivity to cisplatin with c-myc over-expression or down-regulation in colon cancer cells." Anticancer Drugs **12**(10): 829-34.
- Furukawa, K., S. Estus, et al. (1997). "Neuroprotective action of cycloheximide involves induction of bcl-2 and antioxidant pathways." J Cell Biol **136**(5): 1137-49.
- Garcia-Calvo, M., E. P. Peterson, et al. (1998). "Inhibition of human caspases by peptide-based and macromolecular inhibitors." J Biol Chem **273**(49): 32608-13.

- Gassler, N., M. Elger, et al. (1998). "Oligonephronia, not exuberant apoptosis, accounts for the development of glomerulosclerosis in the bcl-2 knockout mouse." Nephrol Dial Transplant **13**(10): 2509-18.
- Ghayur, T., S. Banerjee, et al. (1997). "Caspase-1 processes IFN-gamma-inducing factor and regulates LPS-induced IFN-gamma production." Nature **386**(6625): 619-23.
- Giaccia, A. J. and M. B. Kastan (1998). "The complexity of p53 modulation: emerging patterns from divergent signals." Genes Dev **12**(19): 2973-83.
- Goetze, S., F. Eilers, et al. (2002). "PPAR activators inhibit endothelial cell migration by targeting Akt." Biochem Biophys Res Commun **293**(5): 1431-7.
- Goldrath, A. W. and M. J. Bevan (1999). "Selecting and maintaining a diverse T-cell repertoire." Nature **402**(6759): 255-62.
- Gordon, K. E., B. Binas, et al. (2000). "A novel cell culture model for studying differentiation and apoptosis in the mouse mammary gland." Breast Cancer Res **2**(3): 222-35.
- Goyal, L. (2001). "Cell death inhibition: keeping caspases in check." Cell **104**(6): 805-8.
- Goyal, L., K. McCall, et al. (2000). "Induction of apoptosis by Drosophila reaper, hid and grim through inhibition of IAP function." Embo J **19**(4): 589-97.
- Green, D. R. (2000). "Apoptotic pathways: paper wraps stone blunts scissors." Cell **102**(1): 1-4.
- Gross, A., J. M. McDonnell, et al. (1999). "BCL-2 family members and the mitochondria in apoptosis." Genes Dev **13**(15): 1899-911.
- Gu, Y., K. Kuida, et al. (1997). "Activation of interferon-gamma inducing factor mediated by interleukin-1beta converting enzyme." Science **275**(5297): 206-9.
- Guenette, S. Y. and R. E. Tanzi (1999). "Progress toward valid transgenic mouse models for Alzheimer's disease." Neurobiol Aging **20**(2): 201-11.
- Haldar, S., N. Jena, et al. (1995). "Inactivation of Bcl-2 by phosphorylation." Proc Natl Acad Sci U S A **92**(10): 4507-11.
- Hanahan, D. and R. A. Weinberg (2000). "The hallmarks of cancer." Cell **100**(1): 57-70.
- Haupt, Y., S. Rowan, et al. (1995). "Induction of apoptosis in HeLa cells by trans-activation-deficient p53." Genes Dev **9**(17): 2170-83.
- Hausmann, G., L. A. O'Reilly, et al. (2000). "Pro-apoptotic apoptosis protease-activating factor 1 (Apaf-1) has a cytoplasmic localization distinct from Bcl-2 or Bcl-x(L)." J Cell Biol **149**(3): 623-34.
- Hays, R., L. Wickline, et al. (2002). "Morgue mediates apoptosis in the Drosophila melanogaster retina by promoting degradation of DIAP1." Nat Cell Biol **4**(6): 425-31.
- Hegde, R., S. M. Srinivasula, et al. (2002). "Identification of Omi/HtrA2 as a mitochondrial apoptotic serine protease that disrupts inhibitor of apoptosis protein-caspase interaction." J Biol Chem **277**(1): 432-8.
- Heibein, J. A., I. S. Goping, et al. (2000). "Granzyme B-mediated cytochrome c release is regulated by the Bcl-2 family members bid and Bax." J Exp Med **192**(10): 1391-402.
- Hengartner, M. O. (2000). "The biochemistry of apoptosis." Nature **407**(6805): 770-6.
- Hengartner, M. O. and H. R. Horvitz (1994). "C. elegans cell survival gene ced-9 encodes a functional homolog of the mammalian proto-oncogene bcl-2." Cell **76**(4): 665-76.

- Herr, I. and K. M. Debatin (2001). "Cellular stress response and apoptosis in cancer therapy." Blood **98**(9): 2603-14.
- Hinton, H. J. and M. J. Welham (1999). "Cytokine-induced protein kinase B activation and Bad phosphorylation do not correlate with cell survival of hemopoietic cells." J Immunol **162**(12): 7002-9.
- Hoepfner, D. J., M. O. Hengartner, et al. (2001). "Engulfment genes cooperate with ced-3 to promote cell death in *Caenorhabditis elegans*." Nature **412**(6843): 202-6.
- Horvitz, H. R. (1999). "Genetic control of programmed cell death in the nematode *Caenorhabditis elegans*." Cancer Res **59**(7 Suppl): 1701s-1706s.
- Horvitz, H. R., S. Shaham, et al. (1994). "The genetics of programmed cell death in the nematode *Caenorhabditis elegans*." Cold Spring Harb Symp Quant Biol **59**: 377-85.
- Hozak, R. R., G. A. Manji, et al. (2000). "The BIR motifs mediate dominant interference and oligomerization of inhibitor of apoptosis Op-IAP." Mol Cell Biol **20**(5): 1877-85.
- Hsu, Y. T., K. G. Wolter, et al. (1997). "Cytosol-to-membrane redistribution of Bax and Bcl-X(L) during apoptosis." Proc Natl Acad Sci U S A **94**(8): 3668-72.
- Hu, Y., M. A. Benedict, et al. (1999). "Role of cytochrome c and dATP/ATP hydrolysis in Apaf-1-mediated caspase-9 activation and apoptosis." Embo J **18**(13): 3586-95.
- Huang, D. C., J. Tschopp, et al. (2000). "Bcl-2 does not inhibit cell death induced by the physiological Fas ligand: implications for the existence of type I and type II cells." Cell Death Differ **7**(8): 754-5.
- Huang, Y., Y. C. Park, et al. (2001). "Structural basis of caspase inhibition by XIAP: differential roles of the linker versus the BIR domain." Cell **104**(5): 781-90.
- Hueber, A.-O., M. Zornig, et al. (2000). "A Dominant Negative Fas-associated Death Domain Protein Mutant Inhibits Proliferation and Leads to Impaired Calcium Mobilization in Both T-cells and Fibroblasts." J. Biol. Chem. **275**(14): 10453-10462.
- Imamura, T., H. Izumi, et al. (2001). "Interaction with p53 enhances binding of cisplatin-modified DNA by high mobility group 1 protein." J Biol Chem **276**(10): 7534-40.
- Ink, B., M. Zornig, et al. (1997). "Human Bak induces cell death in *Schizosaccharomyces pombe* with morphological changes similar to those with apoptosis in mammalian cells." Mol Cell Biol **17**(5): 2468-74.
- Inohara, N. and G. Nunez (2000). "Genes with homology to mammalian apoptosis regulators identified in zebrafish." Cell Death Differ **7**(5): 509-10.
- Ito, T., X. Deng, et al. (1997). "Bcl-2 phosphorylation required for anti-apoptosis function." J Biol Chem **272**(18): 11671-3.
- James, C., S. Gschmeissner, et al. (1997). "CED-4 induces chromatin condensation in *Schizosaccharomyces pombe* and is inhibited by direct physical association with CED-9." Curr Biol **7**(4): 246-52.
- Janiak, F., B. Leber, et al. (1994). "Assembly of Bcl-2 into microsomal and outer mitochondrial membranes." J Biol Chem **269**(13): 9842-9.
- Janicke, R. U., P. A. Walker, et al. (1996). "Specific cleavage of the retinoblastoma protein by an ICE-like protease in apoptosis." Embo J **15**(24): 6969-78.
- Jayaraman, L., N. C. Moorthy, et al. (1998). "High mobility group protein-1 (HMG-1) is a unique activator of p53." Genes Dev **12**(4): 462-72.

- Johnson, T. M., Z. X. Yu, et al. (1996). "Reactive oxygen species are downstream mediators of p53-dependent apoptosis." Proc Natl Acad Sci U S A **93**(21): 11848-52.
- Johnstone, R. W., A. A. Ruefli, et al. (2002). "Apoptosis: a link between cancer genetics and chemotherapy." Cell **108**(2): 153-64.
- Juo, P., C. J. Kuo, et al. (1998). "Essential requirement for caspase-8/FLICE in the initiation of the Fas- induced apoptotic cascade." Curr Biol **8**(18): 1001-8.
- Jurgensmeier, J. M., S. Krajewski, et al. (1997). "Bax- and Bak-induced cell death in the fission yeast *Schizosaccharomyces pombe*." Mol Biol Cell **8**(2): 325-39.
- Kandel, E. S. and N. Hay (1999). "The regulation and activities of the multifunctional serine/threonine kinase Akt/PKB." Exp Cell Res **253**(1): 210-29.
- Kane, D. J., T. A. Sarafian, et al. (1993). "Bcl-2 inhibition of neural death: decreased generation of reactive oxygen species." Science **262**(5137): 1274-7.
- Kerbel, R. S. (1997). "A cancer therapy resistant to resistance." Nature **390**(6658): 335-6.
- Kerr, J. F., A. H. Wyllie, et al. (1972). "Apoptosis: a basic biological phenomenon with wide-ranging implications in tissue kinetics." Br J Cancer **26**(4): 239-57.
- Kho, C. J., Y. Wang, et al. (1996). "Effect of decreased fte-1 gene expression on protein synthesis, cell growth, and transformation." Cell Growth Differ **7**(9): 1157-66.
- Kho, C. J. and H. Zarbl (1992). "Fte-1, a v-fos transformation effector gene, encodes the mammalian homologue of a yeast gene involved in protein import into mitochondria." Proc Natl Acad Sci U S A **89**(6): 2200-4.
- Kishimoto, H. and J. Sprent (1997). "Negative selection in the thymus includes semimature T cells." J Exp Med **185**(2): 263-71.
- Kissil, J. L., O. Cohen, et al. (1999). "Structure-function analysis of an evolutionary conserved protein, DAP3, which mediates TNF-alpha- and Fas-induced cell death." Embo J **18**(2): 353-62.
- Korsmeyer, S. J. (1999). "BCL-2 gene family and the regulation of programmed cell death." Cancer Res **59**(7 Suppl): 1693s-1700s.
- Korsmeyer, S. J., M. C. Wei, et al. (2000). "Pro-apoptotic cascade activates BID, which oligomerizes BAK or BAX into pores that result in the release of cytochrome c." Cell Death Differ **7**(12): 1166-73.
- Krammer, P. H. (2000). "CD95's deadly mission in the immune system." Nature **407**(6805): 789-95.
- Kroemer, G. and J. C. Reed (2000). "Mitochondrial control of cell death." Nat Med **6**(5): 513-9.
- Kugu, K., V. S. Ratts, et al. (1998). "Analysis of apoptosis and expression of bcl-2 gene family members in the human and baboon ovary." Cell Death Differ **5**(1): 67-76.
- Kuida, K., T. S. Zheng, et al. (1996). "Decreased apoptosis in the brain and premature lethality in CPP32- deficient mice." Nature **384**(6607): 368-72.
- Kuwahara, K., Y. Saito, et al. (2000). "Cardiotrophin-1 phosphorylates akt and BAD, and prolongs cell survival via a PI3K-dependent pathway in cardiac myocytes." J Mol Cell Cardiol **32**(8): 1385-94.
- Lawlor, M. A. and D. R. Alessi (2001). "PKB/Akt: a key mediator of cell proliferation, survival and insulin responses?" J Cell Sci **114**(Pt 16): 2903-10.
- Lee, S. T., K. P. Hoeflich, et al. (1999). "Bcl-2 targeted to the endoplasmic reticulum can inhibit apoptosis induced by Myc but not etoposide in Rat-1 fibroblasts." Oncogene **18**(23): 3520-8.

- Leuenroth, S. J., P. S. Grutkoski, et al. (2000). "The loss of Mcl-1 expression in human polymorphonuclear leukocytes promotes apoptosis." J Leukoc Biol **68**(1): 158-66.
- Levine, A., B. Belenghi, et al. (2001). "Vesicle-associated membrane protein of Arabidopsis suppresses Bax- induced apoptosis in yeast downstream of oxidative burst." J Biol Chem **276**(49): 46284-9.
- Levine, A. J. (1997). "p53, the cellular gatekeeper for growth and division." Cell **88**(3): 323-31.
- Lewis, K. (2000). "Programmed death in bacteria." Microbiol Mol Biol Rev **64**(3): 503-14.
- Li, H., L. Bergeron, et al. (1997). "Activation of caspase-2 in apoptosis." J Biol Chem **272**(34): 21010-7.
- Li, H., H. Zhu, et al. (1998). "Cleavage of BID by caspase 8 mediates the mitochondrial damage in the Fas pathway of apoptosis." Cell **94**(4): 491-501.
- Li, K., Y. Li, et al. (2000). "Cytochrome c deficiency causes embryonic lethality and attenuates stress-induced apoptosis." Cell **101**(4): 389-99.
- Li, L. Y., X. Luo, et al. (2001). "Endonuclease G is an apoptotic DNase when released from mitochondria." Nature **412**(6842): 95-9.
- Li, P., D. Nijhawan, et al. (1997). "Cytochrome c and dATP-dependent formation of Apaf-1/caspase-9 complex initiates an apoptotic protease cascade." Cell **91**(4): 479-89.
- Li, P. F., R. Dietz, et al. (1999). "p53 regulates mitochondrial membrane potential through reactive oxygen species and induces cytochrome c-independent apoptosis blocked by Bcl-2." Embo J **18**(21): 6027-36.
- Ling, Y. H., C. Tornos, et al. (1998). "Phosphorylation of Bcl-2 is a marker of M phase events and not a determinant of apoptosis." J Biol Chem **273**(30): 18984-91.
- Liu, X., C. N. Kim, et al. (1996). "Induction of apoptotic program in cell-free extracts: requirement for dATP and cytochrome c." Cell **86**(1): 147-57.
- Liu, X., P. Li, et al. (1998). "The 40-kDa subunit of DNA fragmentation factor induces DNA fragmentation and chromatin condensation during apoptosis." Proc Natl Acad Sci U S A **95**(15): 8461-6.
- Liu, X., H. Zou, et al. (1997). "DFP, a heterodimeric protein that functions downstream of caspase-3 to trigger DNA fragmentation during apoptosis." Cell **89**(2): 175-84.
- Liu, Z., C. Sun, et al. (2000). "Structural basis for binding of Smac/DIABLO to the XIAP BIR3 domain." Nature **408**(6815): 1004-8.
- Lockshin, R. A. and Z. Zakeri (2001). "Programmed cell death and apoptosis: origins of the theory." Nat Rev Mol Cell Biol **2**(7): 545-50.
- Los, M., S. Wesselborg, et al. (1999). "The role of caspases in development, immunity, and apoptotic signal transduction: lessons from knockout mice." Immunity **10**(6): 629-39.
- Ludovico, P., M. J. Sousa, et al. (2001). "Saccharomyces cerevisiae commits to a programmed cell death process in response to acetic acid." Microbiology **147**(Pt 9): 2409-15.
- Luo, X., I. Budihardjo, et al. (1998). "Bid, a Bcl2 interacting protein, mediates cytochrome c release from mitochondria in response to activation of cell surface death receptors." Cell **94**(4): 481-90.
- Lutter, M., M. Fang, et al. (2000). "Cardiolipin provides specificity for targeting of tBid to mitochondria." Nat Cell Biol **2**(10): 754-61.

- Madeo, F., S. Engelhardt, et al. (2002). "Apoptosis in yeast: a new model system with applications in cell biology and medicine." Curr Genet **41**(4): 208-16.
- Madeo, F., E. Frohlich, et al. (1997). "A yeast mutant showing diagnostic markers of early and late apoptosis." J Cell Biol **139**(3): 729-34.
- Madeo, F., E. Frohlich, et al. (1999). "Oxygen stress: a regulator of apoptosis in yeast." J Cell Biol **145**(4): 757-67.
- Madeo, F., E. Herker, et al. (2002). "A caspase-related protease regulates apoptosis in yeast." Mol Cell **9**(4): 911-7.
- Manon, S., B. Chaudhuri, et al. (1997). "Release of cytochrome c and decrease of cytochrome c oxidase in Bax- expressing yeast cells, and prevention of these effects by coexpression of Bcl-xL." FEBS Lett **415**(1): 29-32.
- Martin, D. A., R. M. Siegel, et al. (1998). "Membrane oligomerization and cleavage activates the caspase-8 (FLICE/MACHalpha1) death signal." J Biol Chem **273**(8): 4345-9.
- Martinou, J. C. and D. R. Green (2001). "Breaking the mitochondrial barrier." Nat Rev Mol Cell Biol **2**(1): 63-7.
- Martins, L. M. (2002). "The serine protease Omi/HtrA2: a second mammalian protein with a Reaper- like function." Cell Death Differ **9**(7): 699-701.
- Mattson, M. P. (2000). "Apoptosis in neurodegenerative disorders." Nat Rev Mol Cell Biol **1**(2): 120-9.
- May, W. S., P. G. Tyler, et al. (1994). "Interleukin-3 and bryostatin-1 mediate hyperphosphorylation of BCL2 alpha in association with suppression of apoptosis." J Biol Chem **269**(43): 26865-70.
- McCall, K. and H. Steller (1998). "Requirement for DCP-1 caspase during Drosophila oogenesis." Science **279**(5348): 230-4.
- Mehmet, H. (2000). "Caspases find a new place to hide." Nature **403**(6765): 29-30.
- Meier, P., A. Finch, et al. (2000). "Apoptosis in development." Nature **407**(6805): 796-801.
- Migliaccio, E., M. Giorgio, et al. (1999). "The p66shc adaptor protein controls oxidative stress response and life span in mammals." Nature **402**(6759): 309-13.
- Mihara, M., S. Erster, et al. (2003). "p53 Has a Direct Apoptogenic Role at the Mitochondria." Mol Cell **11**(3): 577-90.
- Miramar, M. D., P. Costantini, et al. (2001). "NADH oxidase activity of mitochondrial apoptosis-inducing factor." J Biol Chem **276**(19): 16391-8.
- Mittl, P. R., S. Di Marco, et al. (1997). "Structure of recombinant human CPP32 in complex with the tetrapeptide acetyl-Asp-Val-Ala-Asp fluoromethyl ketone." J Biol Chem **272**(10): 6539-47.
- Moon, H., D. Baek, et al. (2002). "Soybean ascorbate peroxidase suppresses Bax-induced apoptosis in yeast by inhibiting oxygen radical generation." Biochem Biophys Res Commun **290**(1): 457-62.
- Morgenbesser, S. D., B. O. Williams, et al. (1994). "p53-dependent apoptosis produced by Rb-deficiency in the developing mouse lens." Nature **371**(6492): 72-4.
- Moriguchi, M., C. Terai, et al. (2001). "A novel single-nucleotide polymorphism at the 5'-flanking region of SAA1 associated with risk of type AA amyloidosis secondary to rheumatoid arthritis." Arthritis Rheum **44**(6): 1266-72.
- Mueller, Y. M., S. C. De Rosa, et al. (2001). "Increased CD95/Fas-induced apoptosis of HIV-specific CD8(+) T cells." Immunity **15**(6): 871-82.

- Muller, M., S. Strand, et al. (1997). "Drug-induced apoptosis in hepatoma cells is mediated by the CD95 (APO-1/Fas) receptor/ligand system and involves activation of wild-type p53." *J Clin Invest* **99**(3): 403-13.
- Muller, M., S. Wilder, et al. (1998). "p53 activates the CD95 (APO-1/Fas) gene in response to DNA damage by anticancer drugs." *J Exp Med* **188**(11): 2033-45.
- Munsch, D., R. Watanabe-Fukunaga, et al. (2000). "Human and mouse Fas (APO-1/CD95) death receptor genes each contain a p53-responsive element that is activated by p53 mutants unable to induce apoptosis." *J Biol Chem* **275**(6): 3867-72.
- Murphy, K. M., V. Ranganathan, et al. (2000). "Bcl-2 inhibits Bax translocation from cytosol to mitochondria during drug-induced apoptosis of human tumor cells." *Cell Death Differ* **7**(1): 102-11.
- Muzio, M., A. M. Chinnaiyan, et al. (1996). "FLICE, a novel FADD-homologous ICE/CED-3-like protease, is recruited to the CD95 (Fas/APO-1) death-inducing signaling complex." *Cell* **85**(6): 817-27.
- Muzio, M., B. R. Stockwell, et al. (1998). "An induced proximity model for caspase-8 activation." *J Biol Chem* **273**(5): 2926-30.
- Nagata, S. (2000). "Apoptotic DNA fragmentation." *Exp Cell Res* **256**(1): 12-8.
- Nagata, S. and P. Golstein (1995). "The Fas death factor." *Science* **267**(5203): 1449-56.
- Nakano, K. and K. H. Vousden (2001). "PUMA, a novel proapoptotic gene, is induced by p53." *Mol Cell* **7**(3): 683-94.
- Nechushtan, A., C. L. Smith, et al. (2001). "Bax and Bak coalesce into novel mitochondria-associated clusters during apoptosis." *J Cell Biol* **153**(6): 1265-76.
- Newton, K., A. W. Harris, et al. (1998). "A dominant interfering mutant of FADD/MORT1 enhances deletion of autoreactive thymocytes and inhibits proliferation of mature T lymphocytes." *Embo J* **17**(3): 706-18.
- Newton, K. and A. Strasser (2000). "Ionizing radiation and chemotherapeutic drugs induce apoptosis in lymphocytes in the absence of Fas or FADD/MORT1 signaling. Implications for cancer therapy." *J Exp Med* **191**(1): 195-200.
- Nguyen, M., P. E. Branton, et al. (1998). "E1A-induced processing of procaspase-8 can occur independently of FADD and is inhibited by Bcl-2." *J Biol Chem* **273**(50): 33099-102.
- Nicholson, D. W. (2000). "From bench to clinic with apoptosis-based therapeutic agents." *Nature* **407**(6805): 810-6.
- Nicholson, D. W. and N. A. Thornberry (1997). "Caspases: killer proteases." *Trends Biochem Sci* **22**(8): 299-306.
- O'Connor, L., A. W. Harris, et al. (2000). "CD95 (Fas/APO-1) and p53 signal apoptosis independently in diverse cell types." *Cancer Res* **60**(5): 1217-20.
- O'Connor, L., A. Strasser, et al. (1998). "Bim: a novel member of the Bcl-2 family that promotes apoptosis." *Embo J* **17**(2): 384-95.
- Oda, E., R. Ohki, et al. (2000). "Noxa, a BH3-only member of the Bcl-2 family and candidate mediator of p53-induced apoptosis." *Science* **288**(5468): 1053-8.
- Oda, K., H. Arakawa, et al. (2000). "p53AIP1, a potential mediator of p53-dependent apoptosis, and its regulation by Ser-46-phosphorylated p53." *Cell* **102**(6): 849-62.
- Okada, H., W. K. Suh, et al. (2002). "Generation and characterization of Smac/DIABLO-deficient mice." *Mol Cell Biol* **22**(10): 3509-17.

- Okada, M., S. F. Yan, et al. (2002). "Peroxisome proliferator-activated receptor-gamma (PPAR-gamma) activation suppresses ischemic induction of Egr-1 and its inflammatory gene targets." *Faseb J* **16**(14): 1861-8.
- Oppenheim, R. W. (1991). "Cell death during development of the nervous system." *Annu Rev Neurosci* **14**: 453-501.
- Owen-Schaub, L. B., W. Zhang, et al. (1995). "Wild-type human p53 and a temperature-sensitive mutant induce Fas/APO-1 expression." *Mol Cell Biol* **15**(6): 3032-40.
- Padilla, J., K. Kaur, et al. (2000). "PPAR-gamma-mediated regulation of normal and malignant B lineage cells." *Ann N Y Acad Sci* **905**: 97-109.
- Pandey, P., A. Nakazawa, et al. (2000). "Requirement for caspase activation in monocytic differentiation of myeloid leukemia cells." *Oncogene* **19**(34): 3941-7.
- Pasheva, E. A., I. Ugrinova, et al. (2002). "The binding affinity of HMG1 protein to DNA modified by cis-platin and its analogs correlates with their antitumor activity." *Int J Biochem Cell Biol* **34**(1): 87-92.
- Peterlin, B. M. and D. Trono (2003). "Hide, shield and strike back: how HIV-infected cells avoid immune eradication." *Nat Rev Immunol* **3**(2): 97-107.
- Polyak, K., Y. Xia, et al. (1997). "A model for p53-induced apoptosis." *Nature* **389**(6648): 300-5.
- Priault, M., N. Camougrand, et al. (1999). "Comparison of the effects of bax-expression in yeast under fermentative and respiratory conditions: investigation of the role of adenine nucleotides carrier and cytochrome c." *FEBS Lett* **456**(2): 232-8.
- Prives, C. (1998). "Signaling to p53: breaking the MDM2-p53 circuit." *Cell* **95**(1): 5-8.
- Puthalakath, H., D. C. Huang, et al. (1999). "The proapoptotic activity of the Bcl-2 family member Bim is regulated by interaction with the dynein motor complex." *Mol Cell* **3**(3): 287-96.
- Puthalakath, H., A. Villunger, et al. (2001). "Bmf: a proapoptotic BH3-only protein regulated by interaction with the myosin V actin motor complex, activated by anoikis." *Science* **293**(5536): 1829-32.
- Raff, M. C. (1992). "Social controls on cell survival and cell death." *Nature* **356**(6368): 397-400.
- Ravi, R., G. C. Bedi, et al. (2001). "Regulation of death receptor expression and TRAIL/Apo2L-induced apoptosis by NF-kappaB." *Nat Cell Biol* **3**(4): 409-16.
- Read, C. M., P. D. Cary, et al. (1993). "Solution structure of a DNA-binding domain from HMG1." *Nucleic Acids Res* **21**(15): 3427-36.
- Reddien, P. W., S. Cameron, et al. (2001). "Phagocytosis promotes programmed cell death in *C. elegans*." *Nature* **412**(6843): 198-202.
- Rich, T., R. L. Allen, et al. (2000). "Defying death after DNA damage." *Nature* **407**(6805): 777-83.
- Riedl, S. J., M. Renatus, et al. (2001). "Structural basis for the inhibition of caspase-3 by XIAP." *Cell* **104**(5): 791-800.
- Ritter, P. M., A. Marti, et al. (2000). "Nuclear localization of procaspase-9 and processing by a caspase-3-like activity in mammary epithelial cells." *Eur J Cell Biol* **79**(5): 358-64.
- Rodriguez, A., P. Chen, et al. (2002). "Unrestrained caspase-dependent cell death caused by loss of Diap1 function requires the *Drosophila* Apaf-1 homolog, Dark." *Embo J* **21**(9): 2189-97.

- Rodriguez, A., H. Oliver, et al. (1999). "Dark is a Drosophila homologue of Apaf-1/CED-4 and functions in an evolutionarily conserved death pathway." Nat Cell Biol **1**(5): 272-9.
- Rodriguez, J. and Y. Lazebnik (1999). "Caspase-9 and APAF-1 form an active holoenzyme." Genes Dev **13**(24): 3179-84.
- Rotonda, J., D. W. Nicholson, et al. (1996). "The three-dimensional structure of apopain/ CPP32, a key mediator of apoptosis." Nat Struct Biol **3**(7): 619-25.
- Roy, N., Q. L. Deveraux, et al. (1997). "The c-IAP-1 and c-IAP-2 proteins are direct inhibitors of specific caspases." Embo J **16**(23): 6914-25.
- Ruddy, D. A., G. S. Kronmal, et al. (1997). "A 1.1-Mb transcript map of the hereditary hemochromatosis locus." Genome Res **7**(5): 441-56.
- Ruiz-Vela, A., J. P. Albar, et al. (2001). "Apaf-1 localization is modulated indirectly by Bcl-2 expression." FEBS Lett **501**(1): 79-83.
- Russo, P., D. Arzani, et al. (2003). "c-myc Down-Regulation Induces Apoptosis in Human Cancer Cell Lines Exposed to RPR-115135 (C(31)H(29)NO(4)), a Non-Peptidomimetic Farnesyltransferase Inhibitor." J Pharmacol Exp Ther **304**(1): 37-47.
- Ryoo, H. D., A. Bergmann, et al. (2002). "Regulation of Drosophila IAP1 degradation and apoptosis by reaper and ubcD1." Nat Cell Biol **4**(6): 432-8.
- Salmena, L., B. Lemmers, et al. (2003). "Essential role for caspase 8 in T-cell homeostasis and T-cell-mediated immunity." Genes Dev **17**(7): 883-95.
- Sansome, C., A. Zaika, et al. (2001). "Hypoxia death stimulus induces translocation of p53 protein to mitochondria. Detection by immunofluorescence on whole cells." FEBS Lett **488**(3): 110-5.
- Sathasivam, K., C. Hobbs, et al. (1999). "Transgenic models of Huntington's disease." Philos Trans R Soc Lond B Biol Sci **354**(1386): 963-9.
- Saunders, J. W., Jr. (1966). "Death in embryonic systems." Science **154**(749): 604-12.
- Savill, J. and V. Fadok (2000). "Corpse clearance defines the meaning of cell death." Nature **407**(6805): 784-8.
- Scaffidi, C., S. Fulda, et al. (1998). "Two CD95 (APO-1/Fas) signaling pathways." Embo J **17**(6): 1675-87.
- Scaffidi, C., P. H. Kramer, et al. (1999). "Isolation and analysis of components of CD95 (APO-1/Fas) death-inducing signaling complex." Methods **17**(4): 287-91.
- Scaffidi, C., I. Schmitz, et al. (1999). "The role of c-FLIP in modulation of CD95-induced apoptosis." J Biol Chem **274**(3): 1541-8.
- Scatena, C. D., Z. A. Stewart, et al. (1998). "Mitotic phosphorylation of Bcl-2 during normal cell cycle progression and Taxol-induced growth arrest." J Biol Chem **273**(46): 30777-84.
- Scheid, M. P., K. M. Schubert, et al. (1999). "Regulation of bad phosphorylation and association with Bcl-x(L) by the MAPK/Erk kinase." J Biol Chem **274**(43): 31108-13.
- Schuler, M., U. Maurer, et al. (2003). "p53 triggers apoptosis in oncogene-expressing fibroblasts by the induction of Noxa and mitochondrial Bax translocation." Cell Death Differ **10**(4): 451-460.
- Schulze-Osthoff, K., D. Ferrari, et al. (1998). "Apoptosis signaling by death receptors." Eur J Biochem **254**(3): 439-59.
- Sheikh, M. S., T. F. Burns, et al. (1998). "p53-dependent and -independent regulation of the death receptor KILLER/DR5 gene expression in response to genotoxic stress and tumor necrosis factor alpha." Cancer Res **58**(8): 1593-8.

- Shi, Y. (2002). "Mechanisms of caspase activation and inhibition during apoptosis." Mol Cell **9**(3): 459-70.
- Shikama, Y., M. U, et al. (2001). "Comprehensive studies on subcellular localizations and cell death- inducing activities of eight GFP-tagged apoptosis-related caspases." Exp Cell Res **264**(2): 315-25.
- Shimizu, S., T. Ide, et al. (2000). "Electrophysiological study of a novel large pore formed by Bax and the voltage-dependent anion channel that is permeable to cytochrome c." J Biol Chem **275**(16): 12321-5.
- Shimizu, S., Y. Shinohara, et al. (2000). "Bax and Bcl-xL independently regulate apoptotic changes of yeast mitochondria that require VDAC but not adenine nucleotide translocator." Oncogene **19**(38): 4309-18.
- Shimizu, S. and Y. Tsujimoto (2000). "Proapoptotic BH3-only Bcl-2 family members induce cytochrome c release, but not mitochondrial membrane potential loss, and do not directly modulate voltage-dependent anion channel activity." Proc Natl Acad Sci U S A **97**(2): 577-82.
- Siegel, R. M., F. K. Chan, et al. (2000). "The multifaceted role of Fas signaling in immune cell homeostasis and autoimmunity." Nat Immunol **1**(6): 469-74.
- Smith, K. G., A. Strasser, et al. (1996). "CrmA expression in T lymphocytes of transgenic mice inhibits CD95 (Fas/APO-1)-transduced apoptosis, but does not cause lymphadenopathy or autoimmune disease." Embo J **15**(19): 5167-76.
- Soengas, M. S., R. M. Alarcon, et al. (1999). "Apaf-1 and caspase-9 in p53-dependent apoptosis and tumor inhibition." Science **284**(5411): 156-9.
- Song, D., S. Sakamoto, et al. (2002). "Inhibition of poly(ADP-ribose) polymerase activity by Bcl-2 in association with the ribosomal protein S3a." Biochemistry **41**(3): 929-34.
- Song, Z., K. McCall, et al. (1997). "DCP-1, a Drosophila cell death protease essential for development." Science **275**(5299): 536-40.
- Springer, J. E., R. D. Azbill, et al. (2000). "Calcineurin-mediated BAD dephosphorylation activates the caspase-3 apoptotic cascade in traumatic spinal cord injury." J Neurosci **20**(19): 7246-51.
- Srinivasula, S. M., M. Ahmad, et al. (1998). "Autoactivation of procaspase-9 by Apaf-1-mediated oligomerization." Mol Cell **1**(7): 949-57.
- Steller, H. (1995). "Mechanisms and genes of cellular suicide." Science **267**(5203): 1445-9.
- Stoecklin, G., M. Lu, et al. (2003). "A Constitutive Decay Element Promotes Tumor Necrosis Factor Alpha mRNA Degradation via an AU-Rich Element-Independent Pathway." Mol Cell Biol **23**(10): 3506-15.
- Stoka, V., B. Turk, et al. (2001). "Lysosomal protease pathways to apoptosis. Cleavage of bid, not pro- caspases, is the most likely route." J Biol Chem **276**(5): 3149-57.
- Strasser, A. and K. Newton (1999). "FADD/MORT1, a signal transducer that can promote cell death or cell growth." Int J Biochem Cell Biol **31**(5): 533-7.
- Stros, M., T. Ozaki, et al. (2002). "HMGB1 and HMGB2 cell-specifically down-regulate the p53- and p73- dependent sequence-specific transactivation from the human Bax gene promoter." J Biol Chem **277**(9): 7157-64.
- Sun, C., M. Cai, et al. (1999). "NMR structure and mutagenesis of the inhibitor-of-apoptosis protein XIAP." Nature **401**(6755): 818-22.
- Susin, S. A., H. K. Lorenzo, et al. (1999). "Molecular characterization of mitochondrial apoptosis-inducing factor." Nature **397**(6718): 441-6.

- Sutton, V. R., J. E. Davis, et al. (2000). "Initiation of apoptosis by granzyme B requires direct cleavage of bid, but not direct granzyme B-mediated caspase activation." *J Exp Med* **192**(10): 1403-14.
- Suzuki, H., T. I. Guinter, et al. (1998). "Positive selection of CD4⁺ T cells by TCR-specific antibodies requires low valency TCR cross-linking: implications for repertoire selection in the thymus." *Eur J Immunol* **28**(10): 3252-8.
- Suzuki, Y., Y. Imai, et al. (2001). "A serine protease, HtrA2, is released from the mitochondria and interacts with XIAP, inducing cell death." *Mol Cell* **8**(3): 613-21.
- Teodoro, J. G. and P. E. Branton (1997). "Regulation of apoptosis by viral gene products." *J Virol* **71**(3): 1739-46.
- Thomas, A., T. Giesler, et al. (2000). "p53 mediates bcl-2 phosphorylation and apoptosis via activation of the Cdc42/JNK1 pathway." *Oncogene* **19**(46): 5259-69.
- Thomenius, M. J., N. S. Wang, et al. (2003). "Bcl-2 on the Endoplasmic Reticulum Regulates Bax Activity by Binding to BH3-only Proteins." *J Biol Chem* **278**(8): 6243-50.
- Thornberry, N. A. and Y. Lazebnik (1998). "Caspases: enemies within." *Science* **281**(5381): 1312-6.
- Thornberry, N. A., T. A. Rano, et al. (1997). "A combinatorial approach defines specificities of members of the caspase family and granzyme B. Functional relationships established for key mediators of apoptosis." *J Biol Chem* **272**(29): 17907-11.
- Tran, J., J. Rak, et al. (1999). "Marked induction of the IAP family antiapoptotic proteins survivin and XIAP by VEGF in vascular endothelial cells." *Biochem Biophys Res Commun* **264**(3): 781-8.
- Travers, A. (2000). "Recognition of distorted DNA structures by HMG domains." *Curr Opin Struct Biol* **10**(1): 102-9.
- Umansky, S. R. (1982). "The genetic program of cell death. Hypothesis and some applications: transformation, carcinogenesis, ageing." *J Theor Biol* **97**(4): 591-602.
- Uren, A. G., K. O'Rourke, et al. (2000). "Identification of paracaspases and metacaspases: two ancient families of caspase-like proteins, one of which plays a key role in MALT lymphoma." *Mol Cell* **6**(4): 961-7.
- Vander Heiden, M. G. and C. B. Thompson (1999). "Bcl-2 proteins: regulators of apoptosis or of mitochondrial homeostasis?" *Nat Cell Biol* **1**(8): E209-16.
- Varfolomeev, E. E., M. Schuchmann, et al. (1998). "Targeted disruption of the mouse Caspase 8 gene ablates cell death induction by the TNF receptors, Fas/Apo1, and DR3 and is lethal prenatally." *Immunity* **9**(2): 267-76.
- Vaux, D. L. (1993). "Toward an understanding of the molecular mechanisms of physiological cell death." *Proc Natl Acad Sci U S A* **90**(3): 786-9.
- Vaux, D. L., G. Haeccker, et al. (1994). "An evolutionary perspective on apoptosis." *Cell* **76**(5): 777-9.
- Vaux, D. L. and S. J. Korsmeyer (1999). "Cell death in development." *Cell* **96**(2): 245-54.
- Vaux, D. L., I. L. Weissman, et al. (1992). "Prevention of programmed cell death in *Caenorhabditis elegans* by human bcl-2." *Science* **258**(5090): 1955-7.
- Venot, C., M. Maratrat, et al. (1998). "The requirement for the p53 proline-rich functional domain for mediation of apoptosis is correlated with specific PIG3

- gene transactivation and with transcriptional repression." *Embo J* **17**(16): 4668-79.
- Walker, K. K. and A. J. Levine (1996). "Identification of a novel p53 functional domain that is necessary for efficient growth suppression." *Proc Natl Acad Sci U S A* **93**(26): 15335-40.
- Walker, N. P., R. V. Talanian, et al. (1994). "Crystal structure of the cysteine protease interleukin-1 beta- converting enzyme: a (p20/p10)₂ homodimer." *Cell* **78**(2): 343-52.
- Walsh, C. M., B. G. Wen, et al. (1998). "A role for FADD in T cell activation and development." *Immunity* **8**(4): 439-49.
- Wang, C. Y., D. C. Guttridge, et al. (1999). "NF-kappaB induces expression of the Bcl-2 homologue A1/Bfl-1 to preferentially suppress chemotherapy-induced apoptosis." *Mol Cell Biol* **19**(9): 5923-9.
- Wang, J., J. P. Silva, et al. (2001). "Increased in vivo apoptosis in cells lacking mitochondrial DNA gene expression." *Proc Natl Acad Sci U S A* **98**(7): 4038-43.
- Wang, S. L., C. J. Hawkins, et al. (1999). "The Drosophila caspase inhibitor DIAP1 is essential for cell survival and is negatively regulated by HID." *Cell* **98**(4): 453-63.
- Watanabe-Fukunaga, R., C. I. Brannan, et al. (1992). "Lymphoproliferation disorder in mice explained by defects in Fas antigen that mediates apoptosis." *Nature* **356**(6367): 314-7.
- Wei, M. C., W. X. Zong, et al. (2001). "Proapoptotic BAX and BAK: a requisite gateway to mitochondrial dysfunction and death." *Science* **292**(5517): 727-30.
- White, K., M. E. Grether, et al. (1994). "Genetic control of programmed cell death in Drosophila." *Science* **264**(5159): 677-83.
- Wiens, M., B. Diehl-Seifert, et al. (2001). "Sponge Bcl-2 homologous protein (BHP2-GC) confers distinct stress resistance to human HEK-293 cells." *Cell Death Differ* **8**(9): 887-98.
- Williams, G. T. (1991). "Programmed cell death: apoptosis and oncogenesis." *Cell* **65**(7): 1097-8.
- Williams, G. T. (1994). "Programmed cell death: a fundamental protective response to pathogens." *Trends Microbiol* **2**(12): 463-4.
- Wilson, A. J., A. Velcich, et al. (2002). "Novel detection and differential utilization of a c-myc transcriptional block in colon cancer chemoprevention." *Cancer Res* **62**(21): 6006-10.
- Wilson, K. P., J. A. Black, et al. (1994). "Structure and mechanism of interleukin-1 beta converting enzyme." *Nature* **370**(6487): 270-5.
- Wilson, R., L. Goyal, et al. (2002). "The DIAP1 RING finger mediates ubiquitination of Dronc and is indispensable for regulating apoptosis." *Nat Cell Biol* **4**(6): 445-50.
- Wolf, D., V. Witte, et al. (2001). "HIV-1 Nef associated PAK and PI3-kinases stimulate Akt-independent Bad- phosphorylation to induce anti-apoptotic signals." *Nat Med* **7**(11): 1217-24.
- Woo, M., R. Hakem, et al. (1998). "Essential contribution of caspase 3/CPP32 to apoptosis and its associated nuclear changes." *Genes Dev* **12**(6): 806-19.
- Wu, G., J. Chai, et al. (2000). "Structural basis of IAP recognition by Smac/DIABLO." *Nature* **408**(6815): 1008-12.
- Wu, G. S., T. F. Burns, et al. (1999). "Induction of the TRAIL receptor KILLER/DR5 in p53-dependent apoptosis but not growth arrest." *Oncogene* **18**(47): 6411-8.

- Xiang, J., D. T. Chao, et al. (1996). "BAX-induced cell death may not require interleukin 1 beta-converting enzyme-like proteases." Proc Natl Acad Sci U S A **93**(25): 14559-63.
- Xu, Q. and J. C. Reed (1998). "Bax inhibitor-1, a mammalian apoptosis suppressor identified by functional screening in yeast." Mol Cell **1**(3): 337-46.
- Yang, L., T. Mashima, et al. (2003). "Predominant Suppression of Apoptosome by Inhibitor of Apoptosis Protein in Non-Small Cell Lung Cancer H460 Cells: Therapeutic Effect of a Novel Polyarginine-conjugated Smac Peptide." Cancer Res **63**(4): 831-837.
- Yeh, W. C., J. L. Pompa, et al. (1998). "FADD: essential for embryo development and signaling from some, but not all, inducers of apoptosis." Science **279**(5358): 1954-8.
- Yin, X. M., K. Wang, et al. (1999). "Bid-deficient mice are resistant to Fas-induced hepatocellular apoptosis." Nature **400**(6747): 886-91.
- Yuan, J., S. Shaham, et al. (1993). "The C. elegans cell death gene ced-3 encodes a protein similar to mammalian interleukin-1 beta-converting enzyme." Cell **75**(4): 641-52.
- Yuan, J. and B. A. Yankner (2000). "Apoptosis in the nervous system." Nature **407**(6805): 802-9.
- Zha, H., C. Aime-Sempe, et al. (1996). "Proapoptotic protein Bax heterodimerizes with Bcl-2 and homodimerizes with Bax via a novel domain (BH3) distinct from BH1 and BH2." J Biol Chem **271**(13): 7440-4.
- Zha, J., S. Weiler, et al. (2000). "Posttranslational N-myristoylation of BID as a molecular switch for targeting mitochondria and apoptosis." Science **290**(5497): 1761-5.
- Zhang, J., D. Cado, et al. (1998). "Fas-mediated apoptosis and activation-induced T-cell proliferation are defective in mice lacking FADD/Mort1." Nature **392**(6673): 296-300.
- Zheng, T. S., S. F. Schlosser, et al. (1998). "Caspase-3 controls both cytoplasmic and nuclear events associated with Fas-mediated apoptosis in vivo." Proc Natl Acad Sci U S A **95**(23): 13618-23.
- Zhu, J., W. Zhou, et al. (1998). "Identification of a novel p53 functional domain that is necessary for mediating apoptosis." J Biol Chem **273**(21): 13030-6.
- Zimmermann, K. C., J. E. Ricci, et al. (2002). "The role of ARK in stress-induced apoptosis in Drosophila cells." J Cell Biol **156**(6): 1077-87.
- Zornig, M., A. O. Hueber, et al. (1998). "p53-dependent impairment of T-cell proliferation in FADD dominant-negative transgenic mice." Curr Biol **8**(8): 467-70.
- Zou, H., W. J. Henzel, et al. (1997). "Apaf-1, a human protein homologous to C. elegans CED-4, participates in cytochrome c-dependent activation of caspase-3." Cell **90**(3): 405-13.
- Zundel, W. and A. Giaccia (1998). "Inhibition of the anti-apoptotic PI(3)K/Akt/Bad pathway by stress." Genes Dev **12**(13): 1941-6.

INDEX

HMGB-1 inhibits cell death in yeast and mammalian cells and is abundantly expressed in human breast carcinoma

Marie-Luise Brezniceanu^{1,5}, Kirsten Völp^{1,5}, Susanne Bösser¹, Christine Solbach², Peter Lichter³, Stefan Joos³, and Martin Zörnig^{1,4}

¹Chemotherapeutisches Forschungsinstitut, Georg-Speyer-Haus
Paul-Ehrlich-Strasse 42-44, 60596 Frankfurt, Germany

²Klinik für Gynäkologie und Geburtshilfe der Johann Wolfgang Goethe-Universität
Theodor-Stern-Kai 7, 60590 Frankfurt, Germany

³Deutsches Krebsforschungszentrum DKFZ
Im Neuenheimer Feld 280, D-69120 Heidelberg, Germany

⁴Correspondence:

Dr. Martin Zörnig
Chemotherapeutisches Forschungsinstitut, Georg-Speyer-Haus
Paul-Ehrlich-Strasse 42-44, 60596 Frankfurt, Germany
Tel.: +49/69-63395115, Fax: +49/69-63395297
e-mail: zoernig@em.uni-frankfurt.de

⁵The first two authors contributed equally to this work

shortened title: The anti-apoptotic HMGB1 is overexpressed in breast carcinoma

Abstract

Apoptosis is a fundamental biological process used to eliminate unwanted cells in a multicellular organism. An increasing number of regulatory proteins have been identified which either promote or inhibit apoptosis. For tumours to arise apoptosis must be blocked in the transformed cells, for example by mutational overexpression of anti-apoptotic proteins which represent attractive target proteins for molecular therapy strategies.

In a functional yeast survival screen designed to select new anti-apoptotic mammalian genes we have identified the chromosomal High-Mobility Group Box-1 protein (HMGB-1) as an inhibitor of yeast cell death induced by the pro-apoptotic Bcl-2 family member Bak. The C-terminal 33 amino acids of HMGB-1 are dispensable for this inhibitory function. HMGB-1 is also able to protect mammalian cells against different death stimuli including UV radiation, CD95-, TRAIL-, Casp-8- and Bax-induced apoptosis. We found high HMGB-1 protein levels in human primary breast carcinoma. *hmgbl* RNA levels are changing during different stages of mouse mammary gland development and are particularly low during lactation and involution. These data suggest that HMGB-1 may participate in the regulation of mammary gland

apoptosis and that its high expression level promotes tumour growth because of its anti-apoptotic properties.

Introduction

Apoptosis is a genetically determined process leading to cell death in mammalian cells [Strasser, 2000 #70; Zornig, 2001 #69]. As the predominant form of physiological cell death it is crucial for the removal of excess, hazardous or damaged somatic cells during development and in the adult organism. The apoptotic process includes mechanisms that organize both packaging and disposal of cell corpses, thereby preventing inflammation of the surrounding tissue [Conradt, 2002 #68]. Apoptosis is characterized by significant morphological features like cell shrinkage, nuclear condensation and fragmentation of the whole cell. Biochemically, activation of apoptosis-specific proteases - the caspases - is observed [Shi, 2002 #67]. Caspases are common effectors of classical metazoan apoptosis. Upon activation they cut a range of substrate proteins whose cleavage either mediates or attends the apoptotic process.

Deregulation of apoptosis is involved in many pathological conditions. While too much apoptosis is implicated for example in neurodegenerative diseases and AIDS, the inhibition of apoptosis is a functional prerequisite for tumourigenesis and certain autoimmune diseases [Thatte, 1997 #65; Thompson, 1995 #66]. Acquired resistance towards apoptosis is a hallmark of most and perhaps all types of cancer and enhanced cell survival is needed for several steps during tumourigenesis [Hanahan, 2000 #64]. This includes suppression of apoptosis in transformed cells harbouring activated oncogenes like *c-myc*, in hypoxic tumour cells and in metastasizing cancer cells which - once deprived of cell-cell contact and of their normal environment - are prone to anoikis (apoptosis upon detachment [Frisch, 2001 #63]). In addition, inhibition of further apoptotic pathways and stimuli is associated with the resistance of tumours against radiation- and chemotherapy [Damiano, 2002 #62].

Decreased apoptotic sensitivity in tumour cells is either due to loss-of-function of pro-apoptotic proteins or to increased activity of anti-apoptotic molecules (gain-of-function; [Hanahan, 2000 #64]). Therefore, anti-apoptotic genes overexpressed in tumours are attractive targets for anti-tumour gene therapy approaches (e.g. *bcl-2* [Gutierrez-Puente, 2002 #60; Nicholson, 2000 #61]) and the identification of additional and novel anti-apoptotic genes activated in tumour cells has become an important issue.

We and others have shown that yeast can undergo cell death accompanied by cellular markers of apoptosis and that both *S. pombe* and *S. cerevisiae* cells are killed upon overexpression of certain mammalian proteins such as the pro-apoptotic Bcl-2 family member Bak [Ink, 1997 #57; Jurgensmeier, 1997 #58; Sato, 1994 #59]. Co-expression of anti-apoptotic Bcl-2 family members like Bcl-x_L inhibits the effective and rapid killing activity of Bak in *S. pombe* [Hanada, 1995 #56; Ink, 1997 #57]. Therefore, screening of mammalian cDNA libraries co-transformed into yeast cells which

express a mammalian killer gene is a powerful system avoiding many of the background problems experienced with similar screens for death-inhibiting genes in mammalian cells. Such a survival screen has already been performed successfully in the yeast *S. cerevisiae* [Greenhalf, 1999 #52; Kampranis, 2000 #51; Matsuyama, 1998 #55; Shaham, 1998 #53; Xu, 1998 #54].

We have established a functional survival assay in the yeast *S. pombe* with the aim to identify anti-apoptotic mammalian genes in tumour-derived cDNA libraries. As a first step we screened an NIH 3T3 mouse fibroblast-derived library and found the mammalian chromosomal High Mobility Group box-1 protein (HMGB-1) as an inhibitor of Bak-induced cell death in *S. pombe* and in mammalian cells. Furthermore, we could show that overexpression of HMGB1 inhibits UV-, CD95-, TRAIL-, Casp-8- and Bax-mediated apoptosis.

HMGB-1 has been implicated in a variety of biologically important processes including transcription, DNA repair, V(D)J recombination [Bianchi, 2000 #7; Kwon, 1998 #8], differentiation, development and extracellular signalling ([Mitsouras, 2002 #49; Muller, 2001 #50] and references herein). As a nuclear protein, HMGB-1 binds to the minor groove of DNA and facilitates the assembly of site-specific DNA binding proteins like P53 at their cognate binding sites within chromatin [Thomas, 2001 #48]. In certain cells, HMGB-1 can be observed at the cell surface where it has been reported to contribute to cellular migration and tumour invasion [Taguchi, 2000 #47]. In addition, the molecule is secreted by activated monocytes and macrophages [Wang, 1999 #46] and released by necrotic, but not apoptotic cells [Scaffidi, 2002 #45]. Under such conditions, HMGB-1 acts as a cytokine and mediates inflammation.

We observed profound HMGB-1 protein expression in primary human breast carcinomas compared to normal breast tissue. *hmgbl* mRNA levels are regulated during mouse mammary gland development and are particularly low during lactation and apoptotic involution. Our results show that a functional yeast survival screen in *S. pombe* is well suited to identify anti-apoptotic mammalian genes and that HMGB-1 might act as an oncoprotein supporting tumourigenesis by inhibiting apoptosis.

Materials and methods

Yeast strains, cell lines and DNA constructs

All *S. pombe* strains used were derived from the wild-type strains 972h- and 975h+. Media and growth conditions were as described previously [Moreno, 1991 #44]. The yeast strain DSI contains stably integrated human *bak* [Ink, 1997 #57] and grows in EMM minimal medium (*Bio 101*) supplemented with leucine (*Bio 101*, 250 mg/l), uracil (*Bio 101*, 250 mg/l) and thiamine (*Sigma*, 5µg/ml, to repress *nmt-1* promoter-driven *bak* expression). To induce Bak expression cells were washed three times before culturing in liquid medium lacking thiamine. For induction of Bak expression in yeast growing on agar plates, colonies were replica-plated at least twice onto thiamine-free agar plates.

The RKO cell line (ATCC number CRL-2577) is a poorly differentiated colon carcinoma cell line containing wildtype *p53*. 293T cells are human embryonic kidney cells immortalized by large T antigen. NRK1 is a normal rat kidney cell line.

The coding sequences of mouse *hmgb-1*, mouse Δ *hmgb-1* and human *bcl-x_L* were cloned into the *S. pombe* constitutive expression vector pArt1 (Dr. Paul Nurse, ICRF, London, UK). For localisation studies, the human *bak* coding sequence was cloned in frame into the yeast vector pREP42/EGFP N (Dr. Paul Nurse) to express an N-terminally GFP-tagged fusion protein with a uracil marker. Mouse *hmgb-1* and Δ *hmgb-1* cDNAs were cloned into pREP41/EGFP N (Dr. Paul Nurse, N-terminal GFP, with leucine marker). For mammalian expression, *bcl-x_L* was cloned into pcDNA3.1+ (*Invitrogen*) and *hmgb-1* and Δ *hmgb-1* into the retroviral vectors pBabe hygro and pBabe puro, respectively (Dr. Hartmut Land, University of Rochester Medical Center, Rochester, USA).

To express a Bak-GFP fusion protein in mammalian cells, the *bak* cDNA was cloned in frame into a modified pEGFP-C1-vector from *Clontech*. This vector contains an *EF* (elongation factor) rather than the usual *CMV* promoter. Casp-8 (aa 1-478) was cloned as a GFP fusion protein into pEGFP-N1 (*Clontech*; kind gift from M. Lenardo, NIH Bethesda, USA). pIC-Bax was a gift from J. Martinou, Departement de Biologie Cellulaire, Sciences III, Geneva, Switzerland.

Yeast transformation

150 ml of yeast culture in EMM medium (*Bio 101*) plus appropriate supplements (leucine, uracil, adenine (all *Bio 101*), thiamine (*Sigma*)) were grown to a density of 1×10^7 cells/ml (O.D.₆₀₀ = 0.5). Yeast cells were washed twice with water (centrifugation at 1,000 g) and resuspended in 1.5 ml fresh 1xTE/1xLiAc (0.1 M) yielding competent cells. 100 ng plasmid DNA (yeast expression construct with appropriate selection marker) were mixed with 0.1 mg denaturated herring sperm DNA (*Bio 101*) and 100 μ l competent yeast cell suspension. 600 μ l 40% PEG 8000 (*Sigma*)/LiAc (0.1 M) were added and the mixture was vortexed for 10 seconds. The cells were incubated at 30°C for 30 minutes with mild shaking, then after adding 70 μ l DMSO the suspension was heat shocked for 15 minutes at 42°C. Afterwards, yeast cells were chilled for 2 minutes on ice, washed, resuspended in 100 μ l TE and plated on EMMA agar plates (*Bio 101*) containing appropriate supplements.

Yeast survival screen and yeast plasmid recovery

S. pombe yeast cells were transformed by electroporation according to standard protocols [Moreno, 1991 #44]. Briefly, a 400 ml yeast culture of DSI cells in rich yeast extract medium (*bak* repressed) was grown to a density of 1×10^7 cells/ml (O.D.₆₀₀ = 0.5). Cells were washed once in ice-cold water (centrifugation 5 minutes at 1,000 g), once in ice-cold 1 M sorbitol (*Sigma*) and resuspended in 2 ml ice-cold 1 M sorbitol. 40 μ l aliquots of the cell suspension were added to chilled Eppendorf tubes each containing 100 ng plasmid library DNA, and incubated on ice for 5 minutes. For the screen, 5 μ g of a REP/cDNA library prepared from exponentially growing mouse NIH 3T3 fibroblasts (provided by Dr. Chris Norbury, ICRF, University of Oxford,

UK) were used. To generate this library, the cDNAs had been cloned into a REP3Xho (pMBS36Leu) *S. pombe* expression vector which contains a thiamine repressible *nmt-1* promoter and a leucine marker. Cells were electroporated with a *BioRad* electroporator (2.25 kV, 200 μ s, 25 μ F), resuspended in 0.9 ml of ice-cold 1 M sorbitol and plated onto EMMA agar plates containing uracil and thiamine to allow growth of the colonies (*bak* off). Replica-plating onto thiamine-free agar plates induced simultaneous *bak* and library *cDNA* expression (*bak* on). In total, 5×10^4 yeast colonies were screened for Bak-resistance. DSI yeasts were re-transformed with library plasmids isolated from surviving colonies to confirm that the protection against Bak-killing was due to the plasmid-encoded library cDNA.

For plasmid recovery from *S. pombe*, yeasts were grown in 50 ml selective EMM medium containing uracil to an O.D.₆₀₀ of 0.5. The cells were resuspended in TE buffer and transferred to a 1.5 ml Eppendorf tube. To 1 volume TE/yeast, 1 volume phenol/chlorophorm and 1 volume glass beads (425-600 micron, *Sigma*) were added. The tube was vortexed for 5 minutes and centrifuged at 13,000 g for 2 min. The upper aqueous phase was transferred to a fresh Eppendorf tube and plasmid DNA was precipitated by adding 2 volumes of 100% ethanol, vortexing and centrifugation for 30 minutes at 13,000 rpm. The DNA pellet was washed with 70% ethanol, resuspended in 100 μ l water plus 5 μ g RNase A (*Roche*), transformed into competent DH5 α bacteria and plated onto ampicillin containing LB agar plates. Plasmid DNA was prepared from growing bacterial colonies by miniprep isolation according to standard procedure.

Yeast growth curves

Yeast strains were grown in liquid EMM medium containing the appropriate supplements (uracil, thiamine (*bak* off)) to an O.D.₆₀₀ of 0.5. The cultures were washed twice in water to remove traces of thiamine and then diluted to O.D.₆₀₀ of 0.03 (lower cell concentrations led to growth arrest) in EMM medium containing uracil and no thiamine (*bak* on). The O.D.₆₀₀ was then measured every 8 hours and the cultures were diluted to keep them in exponential growth (O.D.₆₀₀ max. 0.8). Such dilutions were taken into account when plotting the O.D./cell number kinetic versus time.

Western and Northern blot analysis

Yeast cell lysates were prepared by vortexing yeast cells for 5 min. in lysis buffer (TE buffer/1 mM PMSF, 1 tablet Complete-Mini protease inhibitor cocktail (*Roche*) per 10 ml buffer) and glass beads (1 volume beads per 1 volume yeast suspension). The mixture was centrifuged at 13,000 g and 4°C. The supernatant was used for quantification of protein concentration and Western blot analysis. 5 μ g yeast proteins were loaded on a 12.5% SDS polyacrylamide gel. After transfer by semi-dry blotting onto a PVDF membrane (Immobilon-P, *Millipore*), the membrane was blocked in 5% nonfat milk powder and 0.05% Tween 20 in PBS. The rabbit anti-Bak antibody was purchased from *Calbiochem*, rabbit anti-HMGB-1 from *PharMingen* and goat anti-Hsp27 from *Santa Cruz* (all used at 1:1000).

Yeast RNA was obtained by vortexing yeast cells in Trizol reagent (*Life Technologies*) with glass beads (1 volume beads per 1 volume yeast cell suspension) according to the manufacturer's protocol. 15 µg of total RNA were loaded on a formaldehyde-containing agarose gel. After migration, RNA was transferred onto a Hybond N⁺ membrane (*Amersham*) and hybridized with 100 ng of a ³²[P]-labelled full length human *bak* cDNA probe according to standard protocols. A mouse mammary gland Northern Blot from *RNWAY Laboratories* was hybridized with *Δhmgbl*, *β-actin* and *gapdh* cDNA probes following the manufacturer's instructions. The membrane contains mouse mammary gland mRNA from non-pregnant and pregnant mice as well as from lactating and involuting animals.

Localisation experiments in *S. pombe* using confocal microscopy

For confocal microscopy, a *Leica TCS SL* laser scanning microscope was used. To stain yeast mitochondria, cells were resuspended at 1x10⁶ cells/ml in 10 mM HEPES buffer (pH 7.4) containing 5% glucose. DiOC₆(3) (*Molecular Probes*) was added to a final concentration of 175 nM, before cells were incubated at room temperature for 15 minutes and analyzed by confocal microscopy.

Transfection of mammalian cells

RKO, 293T and NRK1 cells were transfected using the PEI method. Briefly, 13.5µl of a polyethyleneimine solution (10mM in PBS, high molecular weight PEI from *Aldrich*) were diluted with 150µl of PBS. In parallel, 5µl of DNA solution were diluted with 150 µl of PBS and both solutions were mixed and vortexed. After 10 minutes incubation at room temperature, the DNA/PEI mixture was added to the cells (1x10⁶ cell/10cm plate) in serum-free medium. 4 hours later, the medium was replaced with FCS-containing medium.

Quantification of apoptosis

For Death Receptor-induced apoptosis, 10 ng/ml recombinant CD95L (crosslinked with 1 µg/ml anti-Flag antibody M2 from *Sigma*) or 10 ng/ml KILLER TRAIL (both from *Alexis*) were used in combination with 1 µg/ml cycloheximide (*Sigma*). Alternatively, apoptotic cell death was triggered by UV radiation (10 s) or transfection with *bak-gfp*, *bax* or *casp-8-gfp*. Apoptotic cell death was measured using the LIVE/DEAD Viability/Cytotoxicity kit from *Molecular Probes* according to the supplier's protocol. In this assay, living cells are distinguished by the presence of ubiquitous intracellular esterase activity, determined by the enzymatic conversion of the virtually nonfluorescent cell-permeant calcein AM to the intensely green fluorescent calcein (ex/em 495 nm/515 nm). Ethidium homodimer-1 enters cells with damaged membranes and undergoes a 40-fold enhancement of fluorescence upon binding to nucleic acids, thereby producing a bright red fluorescence in dead cells (ex/em 495 nm/635 nm). EthD-1 is excluded by the intact plasma membrane of living

cells. For each experiment, at least 200 green and red cells were counted using a *Nicon* fluorescence microscope (TE300).

Tumour material

All primary human mammary carcinoma samples were collected directly after surgery, frozen in liquid nitrogen and stored at -80° C. They were classified as follows:

Tu.-No.	TNM	Grading	ER/PR	Her2/neu
83	pT3 pN1 M0	3	pos./neg.	neg.
167	pT4 pN0 M0	3	pos./neg.	neg.
249	pT2 pN0 M0	2	pos./neg.	neg.
250	pT2 pN0 M0	3	neg./neg.	neg.
256	pT1 pN0 M0	2	pos./pos.	neg.
611	pT3 pN1	3	neg./neg.	nd
876	pT2 pN0	3	pos./neg.	nd
1096	pT3 pN1	nd	neg./pos.	nd
1132	pT3 pN1	3	nd	nd

Another seven samples were human breast carcinomas passaged in nude mice for several years and tested for human origin. 0.5 cm^3 tumour material was crushed using a homogenizer (Ultra-Turrax T25, *Janke & Kunkel, IKA Labortechnik*) in 1ml lysis buffer (30 mM Tris-HCL (pH7.5), 150 mM NaCl, 1% Triton X-100, 10% Glycerol, 1 mM PMSF, 1 tablet Complete protease inhibitor cocktail (*Roche*) per 10 ml buffer) and centrifuged at 4° C. The supernatant was used for quantification of protein concentration and subsequent Western blot analysis with $40\text{ }\mu\text{g}$ protein per sample and a rabbit anti-HMGB-1 antibody (1:1000, *BD PharMingen Biosciences*).

Breast tissue microarray

Expression of HMGB1 in human breast carcinoma was studied using a tissue microarray (CB2c, *BioCat*) containing 50 breast tumour biopsies and 10 biopsies of normal breast tissue. HMGB1 levels were determined using a rabbit antibody (*BD PharMingen Biosciences*) which was detected using biotinylated anti-rabbit IgG in the first and fluorescein avidin DCS (*Vector laboratories*) in a second step. For quantification purposes, 16-bit grayscale images were acquired from each biopsy of the microarray and intensity values (I_{Biopsie}) were calculated according to:

$$I_{\text{Biopsie}} = \frac{\%Pixel_{\text{Biopsie}} > BG_{\text{local}} + 1SD}{100\%} \times (I_{\text{mean, Biopsie}} - BG_{\text{local}})$$

(BG; background intensity, SD; standard deviation; $I_{\text{mean, Biopsie}}$; mean pixel intensity of a single biopsy on the microarray).

Results

High mobility group-1 protein (HMGB-1) protects against Bak-induced cell death in *S. pombe*

We employed functional yeast survival screens to identify new anti-apoptotic mammalian genes out of tumour-derived libraries. In a first experiment we used an inducible Bak expression system in *S. pombe* to screen a cDNA library prepared from exponentially growing NIH3T3 mouse fibroblasts (see Materials and methods). Altogether 5×10^4 transformed yeast clones were tested for Bak-resistance in a non-saturated library screen. One of the *S. pombe* colonies surviving Bak expression after library transformation contained a truncated deletion mutant of the mouse *hmgbl* gene lacking the C-terminal 33 amino acids. This $\Delta hmgbl$ deletion mutant does not represent a naturally occurring mRNA variant but was rather generated in the cloning process when the oligo-dT primer annealed within the *hmgbl* coding sequence during reverse transcription of the RNA. Δ HMGB-1 still contains the two HMG-boxes identified in the full length HMGB-1 while the highly acidic C-terminal tail is deleted.

We cloned mouse $\Delta hmgbl$ and mouse full length *hmgbl* in a constitutive *S. pombe* expression vector and further analyzed Δ HMGB-1-conferred protection in Bak expressing yeasts. When Bak expression is induced in the *S. pombe* yeast strain DSI growing on agar plates, the yeast cells die within 48 hours (see **Fig. 1A**). Co-expression of either Δ HMGB-1 or full length HMGB-1 protects the yeast colonies from Bak-induced cell death.

We also measured growth curves of the different yeast strains in liquid culture (see **Fig. 1B**). *S. pombe* wildtype cells cease growth and cell division upon Bak expression (DSI, -T). When co-expressing Δ HMGB-1 or full length HMGB-1 the Bak transformed yeasts continue to grow exponentially, as they do when the Bak-antagonist Bcl-x_L is co-expressed.

We then performed Western- and Northern blot analysis to confirm expression of HMGB-1 and Bak in the yeast strains we had used for the experiments (see **Fig. 1C** and **1D**). We could easily detect full length HMGB-1 protein in the transformed yeasts but the anti-HMGB-1 antibody did not recognize Δ HMGB-1 due to the C-terminal deletion. Nevertheless, in similar studies with a $\Delta hmgbl$ -gfp fusion construct Bak killing was inhibited as efficiently as with Δ HMGB-1 and the positive GFP-staining in these cells proved the presence of the Δ HMGB-1 protector (data not shown).

Induction of Bak transcription in the DSI *S. pombe* strain leads to the production of small amounts of Bak mRNA and protein sufficient to kill the DSI strain (see **Fig. 1A** and **1B**). In DSI cells co-transformed with $\Delta hmgbl$ a much higher amount of Bak RNA and protein is detectable and - in the presence of Δ HMGB-1 - tolerated by the yeast cells (**Fig. 1C** and **1D**). Interestingly, we were unable to detect Bak expression in DSI yeast colonies co-transformed with full length *hmgbl*.

These results show that full length HMGB-1 and Δ HMGB-1 protect *S. pombe* cells against Bak-induced yeast killing. While we cannot rule out that the protective effect of full length HMGB-1 involves transcriptional downregulation of the Bak yeast expression construct, the largely increased amount of Bak in $\Delta hmgbl$ co-transformed

yeast cells indicates protection by Δ HMGB-1 against the Bak protein by another mechanism.

HMGB-1 does not interact with Bak in yeast

Having established the protective potential of HMGB-1 against Bak killing in *S. pombe* we set out to analyze the localization of HMGB-1 and Bak in yeast. In mammalian cells, Bak is affiliated with the mitochondrial membrane where it is believed to be involved in the release of Cytochrome c after an apoptotic stimulus [Degenhardt, 2002 #43]. HMGB-1 on the other hand is mostly localized in the nucleus of a mammalian cell [Muller, 2001 #50], although in addition to its intranuclear function as a regulator of transcription, HMGB-1 can also be secreted by certain cells [Wang, 1999 #46].

To facilitate detection of the Bak protein in yeast cells we cloned a *gfp-bak* fusion construct from which expression can be induced in *S. pombe*. The GFP-Bak fusion protein killed the yeast cells as efficiently as the Bak wildtype molecule (data not shown). GFP-Bak accumulated in dotlike structures of varying size within the *S. pombe* cytoplasm (see **Fig. 2A** and **2B**).

The mitochondrial staining of Bak-expressing cells shows the tubular mitochondrial network already reported for exponentially growing *S. pombe* cells [Yaffe, 1996 #42]. With the techniques used for intracellular localisation studies, simultaneous detection of GFP-Bak and DiOC₆(3)-stained yeast mitochondria was not possible. Obviously, the GFP-Bak localization looks different from the typical mitochondrial pattern in the dying yeast cell. However, we cannot exclude that the GFP-Bak accumulations are part of or connect with the *S. pombe* mitochondrial network.

In a similar experiment we transformed the Bak expressing *S. pombe* strain DSI with *Δhmg-1-gfp* and full length *hmg-1-gfp* fusion constructs. The fusion proteins maintained their protective capacity against Bak killing in *S. pombe* (data not shown). **Fig. 2E** represents a typical example of the exclusively nuclear staining of both Δ HMGB-1-GFP and full length HMGB-1-GFP.

The different localization of cytoplasmic Bak and nuclear HMGB-1/ Δ HMGB-1 suggested that HMGB-1 does not inhibit yeast cell death by simply binding and thereby neutralizing Bak. This conclusion was supported by Yeast-Two-Hybrid analysis and co-immunoprecipitation experiments with overexpressed Bak and HMGB-1/ Δ HMGB-1: We could not detect protein interaction between Bak and HMGB-1 or Δ HMGB-1 in such binding assays (data not shown).

HMGB-1 overexpression inhibits apoptosis induced by different stimuli in mammalian cells

Next we wanted to investigate whether HMGB-1 is able to suppress cell death upon Bak overexpression, not only in yeast but also in mammalian cells. For these experiments we used the human embryonic kidney cell line 293T, the human colon carcinoma cell line RKO and the rat kidney cell line NRK1. Transient transfection of all three cell lines with *bak* alone induced apoptosis which was blocked profoundly by co-transfection of either *Δhmg-1* or full length *hmg-1* (see **Fig. 3**). HMGB-1 was as effective in inhibiting Bak killing as was Bcl-x_L in control co-transfections (data not

shown). Transfection of *hmgbl* or Δ *hmgbl* alone did not lead to apoptotic cell death. The observed inhibition of Bak killing was not due to transcriptional downregulation of Bak since cells co-transfected with the protecting Δ *hmgbl* expressed the fluorescent Bak-GFP construct (data not shown).

We also tested whether HMGB1 expression inhibits apoptosis induced by other death stimuli. RKO cells were treated with UV radiation, CD95 Ligand or TRAIL (**Fig.3**). Both HMGB1 and Δ HMGB1 transfection inhibited apoptosis induced by radiation or Death Receptor ligands. In this context, the protection against TRAIL killing was remarkably effective. We also transfected 293T cells with a *casp-8* expression construct and NRK1 cells with the cDNA of another pro-apoptotic member of the Bcl-2 gene family, *bax*. Again, HMGB1 and Δ HMGB1 inhibited both apoptotic insults (**Fig.3**).

Interestingly, endogenous HMGB-1 is expressed at a relatively high level in RKO cells (data not shown), yet further elevation of the HMGB-1 level rescued RKO cells from different apoptotic stimuli.

These data indicate that the protection conferred by HMGB-1 in yeast against Bak-induced cell death is a general phenomenon observable also in mammalian cells. Furthermore, apoptosis mediated by other stimuli as diverse as UV radiation, Death Receptor triggering and Bax and Casp-8 overexpression, is inhibited in different mammalian cell lines by co-expression of HMGB1.

HMGB-1 protein is highly expressed in human breast carcinomas

Mutational activation of anti-apoptotic proteins is one possible mechanism by which transformed cells evade apoptosis and propagate to form tumours. Since HMGB-1 protects against several apoptotic stimuli in mammalian cells we analyzed HMGB-1 protein levels in normal breast and in primary breast carcinoma material by performing Western blot experiments (see **Fig. 4**). We examined six different samples derived from normal breast tissue and they showed hardly any detectable HMGB-1 protein (first six lanes). In comparison, of nine primary breast carcinomas tested, all expressed HMGB-1, six of them in high amounts. We also examined seven human breast carcinomas which were passaged for a long time in nude mice. Such passaging of tumour cells in mice is regarded as an artificial model for tumour metastasis, i.e. genes important for metastasis become upregulated. All seven passaged breast tumours expressed high HMGB-1 protein levels.

These data suggest that the HMGB-1 protein is indeed highly expressed in human breast carcinomas and in a tumour transplantation model.

To screen a larger pannel of breast carcinoma for HMGB1 expression we analyzed a human breast tissue microarray with fixed tissue sections from 10 different normal breast samples and 50 different breast carcinoma. The intensity of the HMGB1 staining was quantified and the results are shown in **Fig. 5**. On average, three times higher HMGB1 protein levels were detected in the tumour samples compared to the normal tissue controls which is consistent with the Western Blot results described above.

hmgb1 mRNA levels are regulated during different stages of mouse mammary gland development

The high expression of HMGB1 protein in human breast carcinoma prompted us to analyze whether HMGB1 levels change during mammary gland development. For this purpose, we used a $\Delta hmgb1$ cDNA probe to hybridize a Northern blot with mouse mammary gland mRNA preparations from different stages before and during pregnancy and from lactating and involuting glands. Quantification of the resulting blot is shown in **Figure 6**. *hmgb1* expression levels were normalized in two different data sets to the mRNA amounts of either of the two housekeeping genes β -actin or *gapdh*. We observed clear differences in *hmgb1* expression during mammary gland development. While significant levels of *hmgb1* RNA are detected in the glands of non-pregnant and pregnant mice, expression of *hmgb1* mRNA is low during lactation and in the involuting glands which undergo apoptosis. This result indicates that HMGB1 may regulate growth and involution of mammary gland tissue, possibly by influencing the apoptotic behaviour of the cells.

Discussion

Programmed cell death (PCD) - in its most prominent form known as apoptosis in metazoa - is also used as an altruistic response for the sake of a colony in unicellular organisms like bacteria or monocellular eukaryotes (e.g. *Trypanosoma cruzi*, *T. brucei rhodesiense*, *Tetrahymena thermophila* and *Dictyostelium discoideum*) [Ameisen, 2002 #39]. Evidence is accumulating that a cell death machinery may also exist in yeast. This includes identification of a metacaspase in *S. cerevisiae* which becomes activated during yeast cell death induced by H₂O₂, acetic acid and ageing [Madeo, 2002 #38].

Yeast has proven itself extremely successful as a model system used to answer many biological questions. In the absence of obvious homologues of major apoptotic regulators like the Bcl-2 family, yeast has also been used to study interactions between heterologously expressed components of apoptotic pathways [Hawkins, 2001 #37]. Interestingly, several pro-apoptotic mammalian proteins kill yeast cells upon overexpression, for example pro-apoptotic members of the Bcl-2 family (Bax and Bak [Ink, 1997 #57; Jurgensmeier, 1997 #58; Sato, 1994 #59]) and caspases (-3 and -8 [Kang, 1999 #36]). We could show some time ago that Bak killing of the fission yeast *S. pombe* is inhibited by co-expression of human Bcl-x_L, and that the same critical BH3 domain of Bak that is required for induction of apoptosis in mammalian cells is also required for inducing death in yeast [Ink, 1997 #57]. These findings, and the fact, that typical phenotypic features of apoptosis are observed during yeast cell death [Ink, 1997 #57; Ligr, 1998 #34; Madeo, 1997 #35], are indicative of an intrinsic cell death program in yeast which can be triggered by pro-apoptotic mammalian proteins.

The molecular mechanisms by which pro-apoptotic Bcl-2 family members induce yeast cell death remain unknown. Bax killing in *S. cerevisiae* requires aspects of mitochondrial biochemistry, including the mitochondrial F₀F₁-ATPase proton pump [Gross, 2000 #32; Matsuyama, 1998 #55; Priault, 1999 #33; Shimizu, 2000 #31]. Reports concerning the release of Cytochrome c (Cyt c) in Bax overexpressing yeast cells appear controversial [Gross, 2000 #32; Manon, 1997 #30; Priault, 1999 #33; Shimizu, 2000 #31] and blocking Cyt c release does not inhibit Bax-induced cell death in *S. cerevisiae* [Roucou, 2000 #29]. Our own overexpression studies with a

functional Bak-GFP-construct in *S. pombe* were not suggestive of an exclusive mitochondrial localization of Bak-GFP in these cells. Remarkably, Bax and Bak have recently been reported to leave the mitochondrial membranes and to coalesce into mitochondria-associated clusters during apoptosis in mammalian cells [Nechushtan, 2001 #71].

Several groups have successfully performed survival screens in *S. cerevisiae* to screen heterologous cDNA libraries for suppressors of Bax killing in yeast [Greenhalf, 1999 #52; Kampranis, 2000 #51; Matsuyama, 1998 #55; Shaham, 1998 #53; Xu, 1998 #54]. We set up an inducible Bak expression system in *S. pombe* with the aim to screen human tumour-derived cDNA libraries to identify potential anti-apoptotic oncogenes. When we transformed Bak expressing *S. pombe* yeast cells in a first experiment with a cDNA library synthesized from mouse NIH 3T3 fibroblasts, we found the chromosomal protein HMGB-1 as a protector against Bak-induced yeast cell death. The deletion mutant Δ HMGB-1, which we isolated in the screen and which lacks the C-terminal 33 amino acids, is even more potent in inhibiting Bak-killing in yeast than the full length protein. Since we only tested 5×10^4 transformed yeast colonies for Bak-resistance, screening of the NIH 3T3 library was by far not complete. This explains why we did not isolate well-known inhibitors of Bak cytotoxicity like Bcl-x_L.

If protected against Bak-killing by overexpression of Δ HMGB-1, *S. pombe* cells grow exponentially while expressing a large amount of Bak (which is much higher than the amount of Bak necessary to kill untransformed yeast cells). These data rule out the possibility that Δ HMGB-1 downregulates Bak-transcription from the *nmt-1* promoter used to express Bak in the yeast. We can also dismiss a scenario where HMGB-1 directly binds to Bak thereby neutralizing Bak's killing activity, similar to the way in which Bcl-x_L prevents Bak-induced cell death. Our localization studies and our negative results in a Yeast-Two-Hybrid-analysis and in co-immunoprecipitation experiments to prove direct Bak-HMGB-1-interactions do not support such a binding model.

We could show that both Δ HMGB-1 and full length HMGB-1 are able to efficiently suppress apoptosis induced by several different stimuli in mammalian cells. The inhibition of apoptosis includes protection against Bak- and Bax-killing as well as prevention of apoptosis induced by overexpression of Casp-8, UV radiation and triggering of the Death Receptors CD95 and the TRAIL receptors. HMGB-1 is an abundant nuclear protein with roughly 1×10^6 molecules per nucleus [Bianchi, 1998 #28]. Yet despite its abundance the protein may be limiting within cells: transient overexpression of HMGB-1 enhances the transcriptional activity of factors such as P53 and steroid hormone receptors. Similarly, an increase of HMGB-1 protein levels in mammalian cells by transfection leads to profound inhibition of apoptosis.

Suppression of apoptosis is a key event at the onset of and during tumorigenesis [Hanahan, 2000 #64]. Increased resistance to the many apoptotic stimuli a tumour cell is exposed to can be achieved by loss-of-function mutations (resulting in inactivation of pro-apoptotic genes) or gain-of-function mutations (resulting in increased activity of anti-apoptotic genes). A prototypic example of the latter is represented by the t(14;18)-translocation involving *bcl-2* which leads to Bcl-2-overexpression in human follicular B-cell lymphoma [Vaux, 1988 #27]. Since we have identified HMGB-1 in a yeast screen for anti-apoptotic genes and because we have shown HMGB-1's anti-apoptotic capacity in mammalian cells, we investigated the expression of the protein in human tumours. Our analysis revealed profound HMGB-1 protein levels in human primary breast carcinomas. We also observed strong HMGB-1 expression in human

breast carcinomas transplanted into nude mice. In contrast, expression of HMGB1 in normal breast tissue was low. This suggests that HMGB1 is involved in the development of mammary carcinomas. Interestingly, *hmgb1* mRNA appears to be regulated during mouse mammary gland development. Its expression is lowest during lactation and involution, when the mammary ducts undergo apoptosis. This finding raises the possibility that HMGB1 participates in the cyclic regulation of mammary gland apoptosis.

Elevated *hmgb-1* mRNA levels have already been reported in human gastrointestinal adenocarcinomas compared to corresponding non-cancerous mucosa [Xiang, 1997 #26]. The authors had suggested a correlation between *hmgb-1* RNA expression and differentiation /staging of the carcinomas. Furthermore, a strong intertumoural variation of *hmgb-1* mRNA expression within 13 breast cancer samples was published by Flohr *et al.* [Flohr, 2001 #25], which corresponds nicely to our tissue microarray results. The authors argue that this variation may contribute to the different response of estrogen receptor-positive breast tumours to endocrine therapy. This argument is based on the observation that HMGB-1 increases binding of the estrogen receptor to its DNA target sequence [Boonyaratanakornkit, 1998 #24]. Comparison of *hmgb-1* mRNA levels in normal breast tissue with expression in breast cancer samples was not included in this study.

Enhanced co-expression of *trx* (thioredoxin) and *hmgb-1* mRNAs has been observed in human hepatocellular carcinomas and higher expression of *trx* correlated with decreasing tumour sensitivity to cisplatin [Kawahara, 1996 #23]. The cytotoxic effect of cisplatin is believed to result from the formation of covalent adducts with DNA (reviewed in [Jamieson, 1999 #22]). HMGB-1 binds with high affinity to DNA damaged by cisplatin, and it is speculated that HMGB-1 contributes to cisplatin cytotoxicity by shielding damaged DNA from repair [Pasheva, 2002 #20; Pil, 1992 #21]. Paradoxically, HMGB-1 overexpression has also been correlated with cisplatin-resistance in cell lines [Imamura, 2001 #19] which could be explained by our data demonstrating anti-apoptotic properties for HMGB-1.

Inhibition of apoptosis by HMGB-1 has to the best of our knowledge not been reported so far. Several other interesting aspects of HMGB-1 biology have however been investigated. The HMGB-1 protein belongs to the high mobility group (HMG) of DNA-binding proteins, which are abundant, heterogeneous, nonhistone components of chromatin [Bianchi, 2000 #7; Grosschedl, 1994 #18]. High mobility group proteins are subdivided into three distinct families: HMGB (with the proteins HMGB-1, -2, -3 (formerly HMG-1, -2, -4)), HMGA (HMGA-1a, b, c, -2 (formerly HMG-I(Y), HMGI-C)) and HMGN (formerly HMG-14/17 [Bustin, 2001 #17]). Members of the structurally distinct HMGA family are highly expressed during embryonic development and in proliferating cells but are rare in adult cells [Chiappetta, 1996 #16]. As critical components of enhanceosomes they participate in gene regulation and their overexpression has been strongly correlated with tumorigenesis ([Fedele, 2002 #15] and references herein).

Both HMGB-1 and HMGB-2 contain two similar, but distinct "HMG boxes" (A and B), and a long acidic C-terminal tail, which is deleted in the Δ HMGB-1 protein identified in our yeast screen (reviewed in [Travers, 2000 #14]). The HMG box consists of approximately 80 amino acids and has a characteristic, twisted, L-shaped fold formed by three α -helical segments [Read, 1993 #12; Weir, 1993 #13]. It binds to DNA through the minor groove and induces site-specific DNA deformations. HMGB proteins recognize and bind to altered DNA conformations, such as stem-loop, four-way-junction, kinked or underwound DNA ([Travers, 2000 #14] and references

herein). Although they possess little or no sequence preference, HMGB-1 interacts with proteins like P53 or steroid hormone receptors and increases the apparent DNA binding affinity of these transcription factors [Jayaraman, 1998 #11; Romine, 1998 #10]. Lack of the protein in *hmgb-1* knockout mice did not disrupt cell growth but rather caused lethal hypoglycaemia in the newborn mice, possibly due to impaired transcriptional glucocorticoid receptor activity [Calogero, 1999 #6]. Such a role for HMGB-1 as a regulator of transcription may influence the apoptotic behaviour of a cell. It has for example been shown that HMGB-1 inhibits both P73 α/β - and P53-dependent transactivation from the *bax* gene promoter in *p53*-deficient SAOS-2 cells [Stros, 2002 #9].

Future studies including transgenic mouse models will investigate whether by suppressing cell death HMGB-1 can act as an oncogene which might be considered for molecular tumour therapy. Our data show that screening of mammalian cDNA libraries in yeast survival assays allows the isolation of new anti-apoptotic tumour-relevant molecules and we are currently using tumour-derived cDNA libraries to identify further cell death-inhibiting oncogenes.

Acknowledgement

The authors would like to thank Dr. Marco Bianchi for providing the full length mouse *hmgb-1* cDNA, Dr. Paul Nurse for providing the yeast vectors pArt1, pREP41/EGFP N and pREP42/EGFP N, Frauke Devens and Daniel Göttel for their help regarding the tissue micorarray experiments and Dr. Winfried Wels and Dr. Catherine Haynes for critically reading the manuscript. This work was supported by the DFG (ZO 110/1-1), the German National Genome Research Network (KR S07T06 and P2T02) and the Heinrich and Erna Schaufler-Stiftung.

Figure and legends

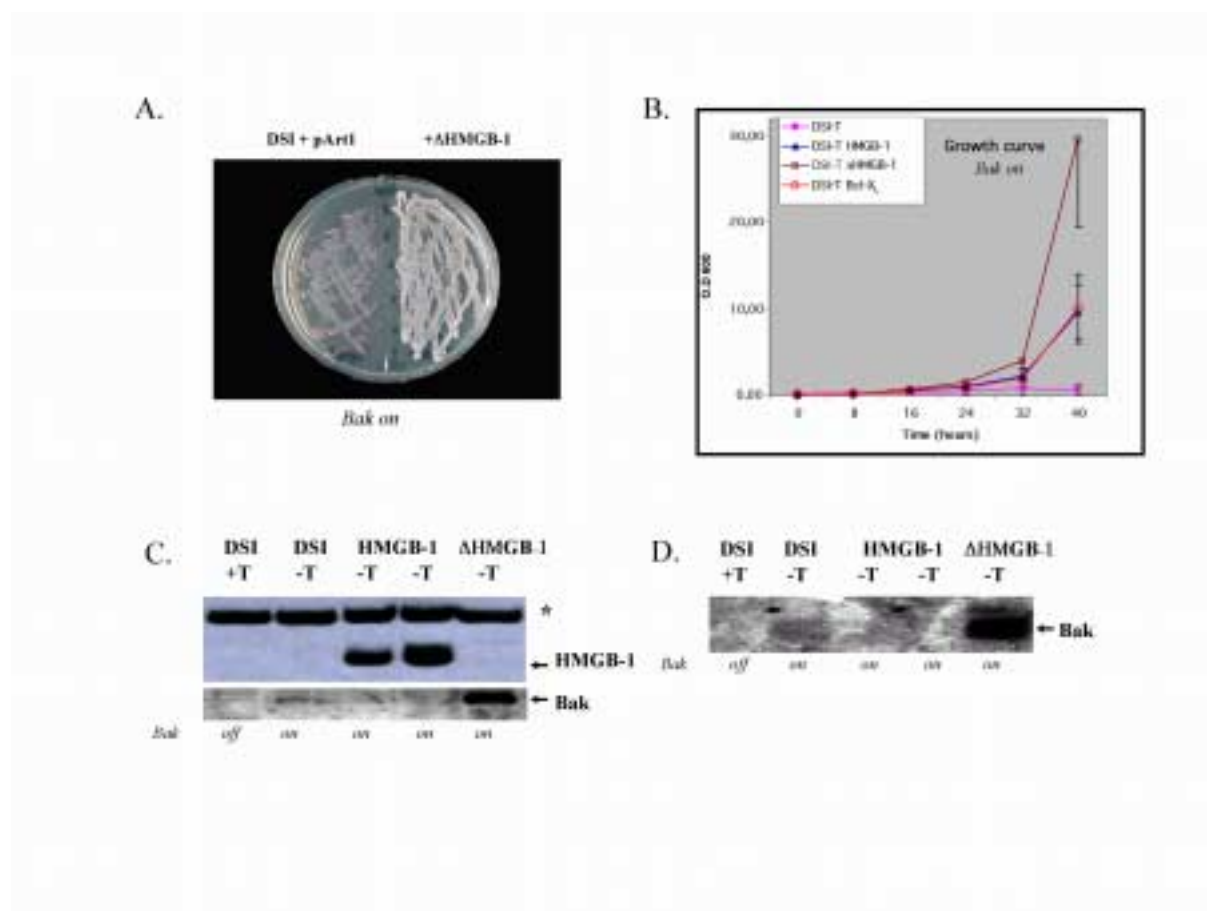


Fig. 1: HMBG-1 inhibits Bak-induced cell death in the yeast *S. pombe*. **A:** DSI cells growing on thiamine-free agar plates with phloxin (5 $\mu\text{g/ml}$, *Sigma*). Dead yeast cells appear dark red, pink colonies are growing. While co-transformation of the empty vector pArt1 cannot rescue colony growth, co-expression of pArt1- Δ hmgb-1 (and full length pArt1-hmgb-1, data not shown) protects against Bak-killing of the yeast. **B:** DSI yeast growth curves in liquid medium lacking thiamine (*bak on*). While pArt1 empty vector-transformed cells cease proliferation and die, Bak-induced cell death is inhibited upon HMGB-1 expression leading to exponential colony growth. Δ hmgb-1-transformed cells grow twice as fast as full length HMGB-1 expressing yeasts, which themselves propagate as quickly as *bcl-x_L*-transformed control cells. The results were obtained by 3 independent experiments. **C:** Western blot analysis showing HMGB-1 expression in two DSI yeast colonies independently co-transformed with pArt1-HMGB-1. The parental DSI strain, either in the presence or absence of thiamine, does not express HMGB-1. Δ HMGB-1 lacking the C-terminus is not recognized by the antibody. An unspecific band marked with an asterisk indicates equal loading of the protein gel. DSI cells in thiamine-free medium express a small amount of Bak protein and *bak* RNA (**D**) sufficient to induce yeast cell death. While we could not detect Bak protein or RNA (**D**) in DSI cells co-transformed with full length HMGB-1, a large amount of Bak protein and RNA (**D**) is present in Δ HMGB-1-expressing DSI cells. **D:** *bak* Northern blot experiment with the same DSI yeast strains as analyzed in C.

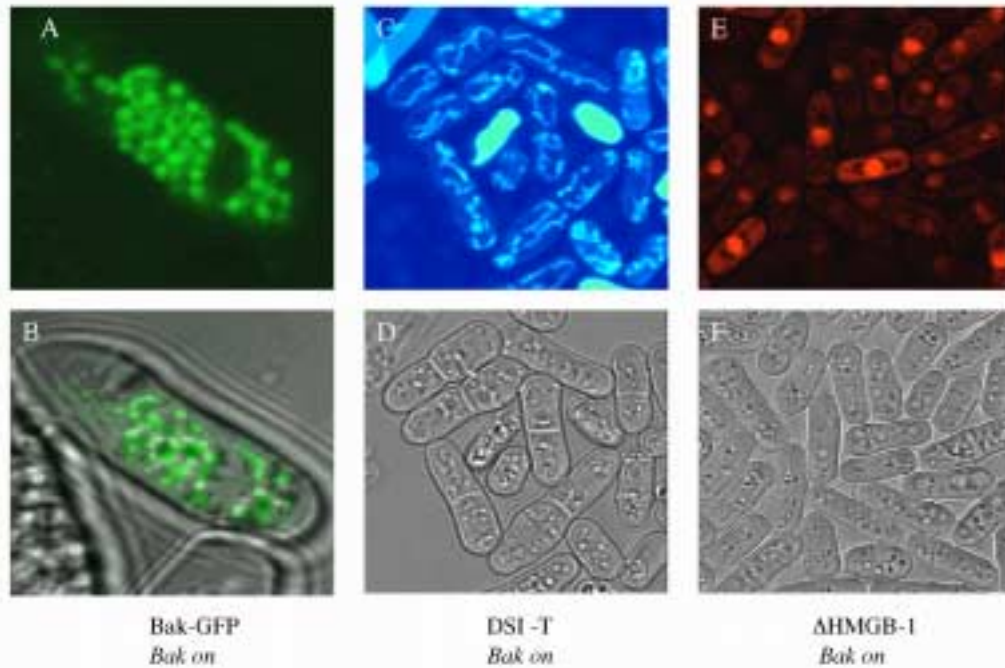


Fig. 2: Localization studies in *S. pombe*. **A:** GFP-Bak accumulates in the cytoplasm. **C:** Yeast cells stained with DiOC₆(3) - the tubular network of mitochondria is clearly visible. **E:** Nuclear localization of the Δ HMGB-1-GFP fusion protein. **B, D, F:** Normal transmission microscopy pictures of the same yeast cells as shown in **A, C** and **E**.

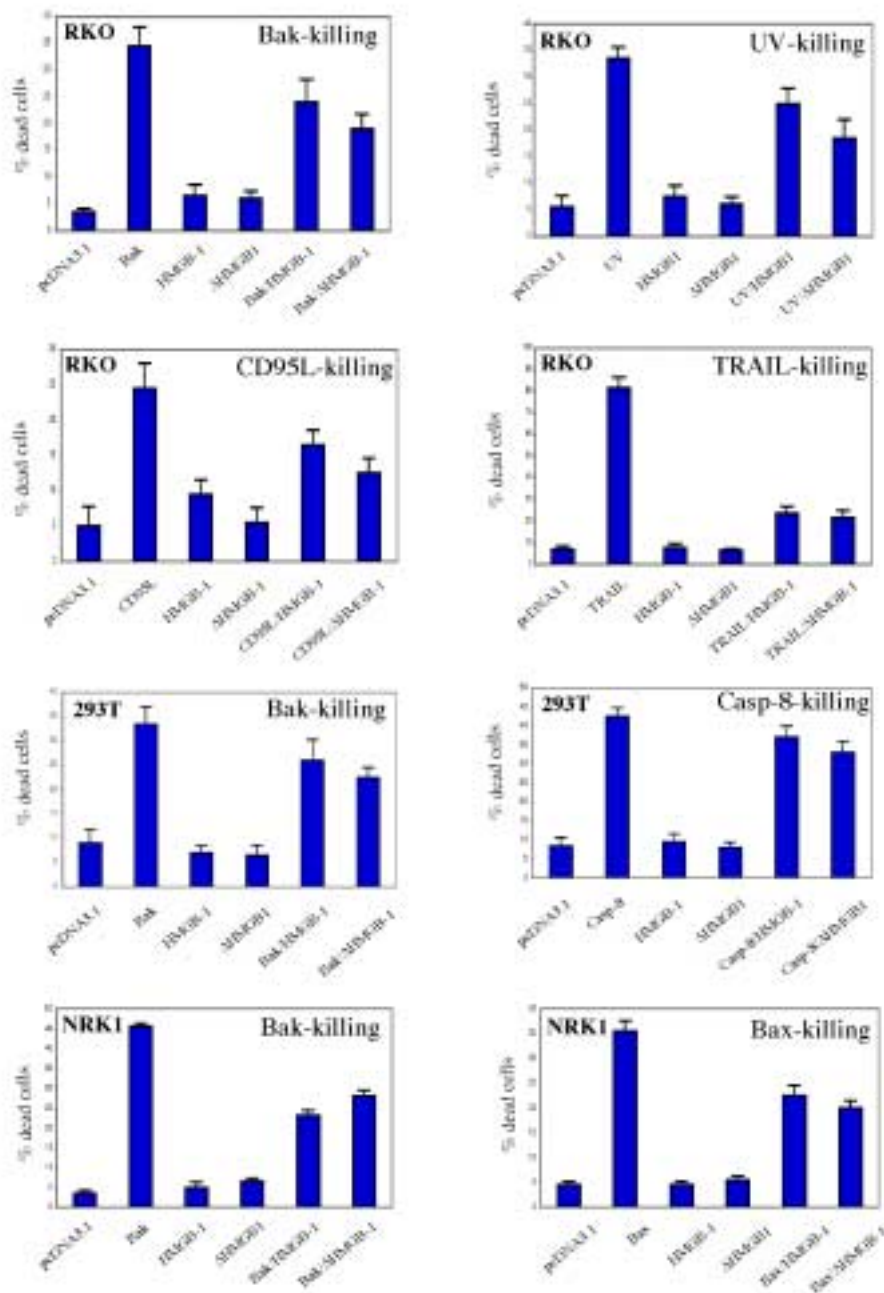


Fig. 3: HMGB-1 and Δ HMGB-1 inhibit apoptosis induced in mammalian cells by different stimuli. RKO, 293T and NRK1 cells were seeded in 10 cm plates at 1×10^6 cells/plate. The next day, $1.3 \mu\text{g}$ *gfp-bak*, *casp-8* or *bax* cDNA together with $4.0 \mu\text{g}$ of either empty vector pcDNA3.1, *hmgbl-1* or Δ *hmgbl-1* cDNA were introduced using the PEI transfection method. 16 hours later, cells were collected (including floating cells) and the percentage of dead cells was determined using the LIVE/DEAD Viability/Cytotoxicity kit from *Molecular Probes*. For UV, CD95L and TRAIL killing, $5 \mu\text{g}$ of either empty vector DNA, *hmgbl-1* or Δ *hmgbl-1* cDNA were transfected. 24 hours after transfection, the cells were treated with either 10 s UV radiation, 10 ng/ml recombinant CD95L plus $1 \mu\text{g}/\text{ml}$ cycloheximide and $1 \mu\text{g}/\text{ml}$ anti-Flag antibody, or with 10 ng/ml TRAIL plus $1 \mu\text{g}/\text{ml}$ cycloheximide. 16 hours

later, apoptosis was quantified using the LIVE/DEAD assay. All apoptotic stimuli were significantly inhibited by overexpression of either *hmgb-1* or Δ *hmgb-1*.

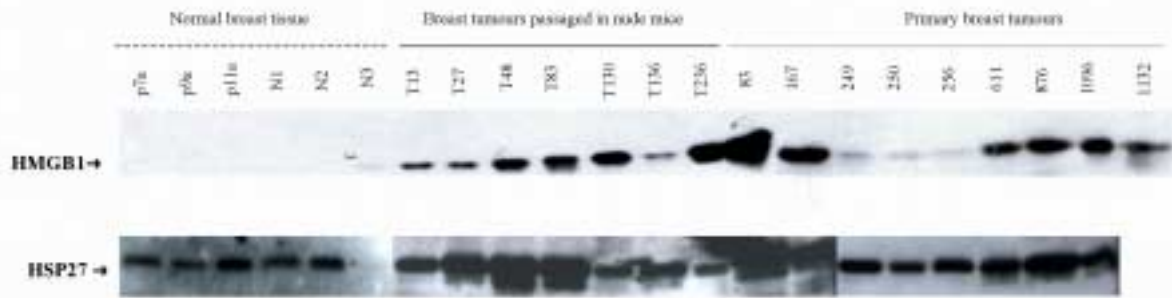


Fig. 4: HMGB-1 protein overexpression in human mammary carcinomas. 40 μ g of protein lysates from normal breast tissue (p7a, p9a, p11a, N1, N2, N3), primary breast tumours (83, 167, 249, 250, 256, 611, 876, 1096, 1132) and breast tumours passaged in nude mice (T13, T27, T48, T83, T130, T136, T236) were analyzed in a Western blot experiment with an anti-HMGB-1 antibody. As a loading control, the membrane was rehybridized with an anti-HSP27 antibody.

Fig.5: Antibody staining of a breast tissue microarray reveals elevated HMGB1 protein expression in breast carcinoma. The array is composed of tissue sections from 10 normal breast samples and 50 different breast carcinoma. **A:** Fluorescent signals

from the sections after incubation with rabbit anti-HMGB1 antibody, followed by treatment with biotinylated anti-rabbit antibody and fluorescein-conjugated avidin. Signal intensities were quantified and averaged for normal and tumour sections and are presented as bars on the right side of the figure. Individual signal strengths are plotted in **B**.

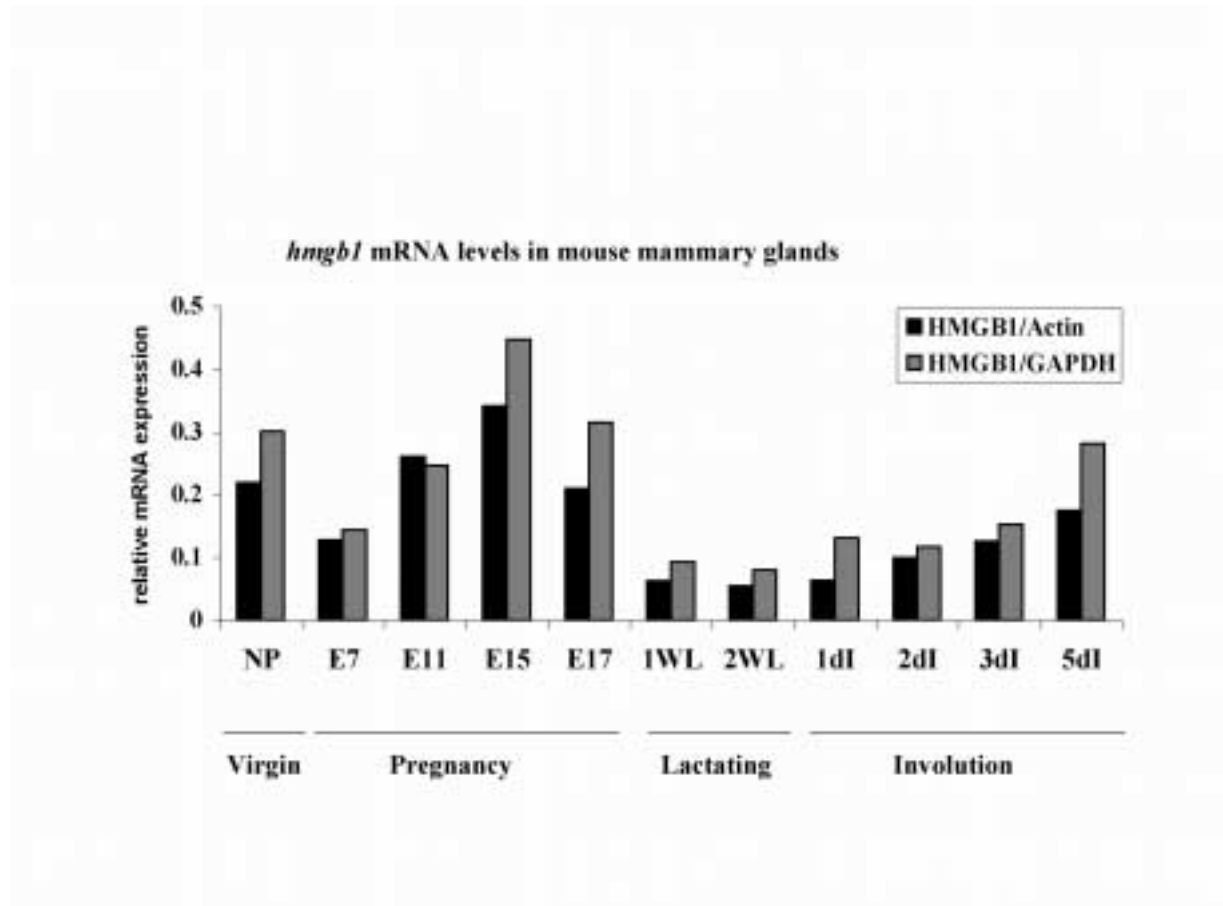


Fig. 6: *hmgb1* mRNA levels are regulated during mouse mammary gland development. Different mRNA preparations of mammary glands from non-pregnant, pregnant (E7-E17), lactating (1WL, 2WL) and involuting (1dI-5dI) mice were used for Northern Blot analysis. The membrane was hybridized sequentially with cDNA probes for mouse $\Delta hmgb1$, β -actin and *gapdh*. *hmgb1* RNA expression was normalized to β -actin (grey bars) or *gapdh* (black bars) RNA levels. *hmgb1* transcription is downregulated during lactation and involution.

BREZNICEANU MARIE-LUISE

28, Beethovenstr., 60325 Frankfurt am Main - Germany

tel: 49 069 74 38 69 98 (home), 49 069 63395121 (lab.)

Brezniceanu@em.uni-frankfurt.de

brezniceanu@gmx.net

EDUCATION

- Sep. 1999 **Currently doing a Ph D in Biology at the Georg-Speyer-Haus Institut in Frankfurt (Germany) under the supervision of Dr. M. Zörnig: Genetic screen for new anti-apoptotic genes downstream of the release of Cytochrome c. Expected end in summer 2003.**
- 1998/99 **National DEA in Toxicology**
Postgraduate Degree at the University of Paris VII.
- 1997/98 Master's degree in Biochemistry; University Reuilly Didrot (Paris VII)
- 1996/98 Bachelor of Science in Biochemistry; University Reuilly Didrot (Paris VII).
- 1994/96 1st year of Medical Studies (P.C.E.M 1), CHU Lariboisiere-St-Louis (Paris VII).
- 1993 French baccalaureate equivalent to high school certificate.
Specialization in maths and physics.

RESEARCH EXPERIENCE

- 1998/99 One year work on a research project: "The metabolism of epothilones by human P450", in the laboratory of Dr. T. Cresteil (CNRS) at the "Gustave Roussy Cancer Research Institut" (IGR).
I obtained the DEA National of Toxicology for this work, together with academic exams.
- 1998 6 month research project: "Intracellular localization of a DNA repair enzyme: the 3-methyladenine DNA glycosylase. Construction of a fusion protein, the human 3-methyladenine DNA glycosylase-EGFP", in the laboratory of Pr. N. Aarsaether at the Preklinisk Institute of Bergen (PKI), Norway. This work was done through participation in the ERASMUS program, and was part of my Master's degree in Biochemistry.

PREVIOUS WORK

1996	One month internship as secretary at SEMA GROUPE firm.
1994/ 95	One month each year, internship at INDOSUEZ bank.
1992	One month work at the pharmaceutical factory ROCHES. One month work at the CNAM (National Center of Arts and Skills).

These were summer jobs which helped finance my studies.

SCIENTIFIC SKILLS

Molecular biology: Bacteria transformations, Cloning techniques, DNA extraction, Southern blotting, Northern blotting, Western blotting, in vitro protein translation and cleavage assays of specific substrates, Micro-array analysis, PCR, RT-PCR, Real-time PCR and protein extraction from cells, organs and tumours.

Metabolism Enzymes kinetic, metabolites extraction.

Technics Cell culture: Mammalian cells, bacteria and Yeast (*S. pombe* and *S. cerevisiae*) transfection and transformation; Electroporation ; Two-Hybrid system ; GST-protein cloning for antibody production and interaction assays ; HPLC and Mass-Spectrometry; FACS analysis (PI and JC-1 staining of fixed or living cells); Confocal Microscopy and Fluorescent Microscopy (for intracellular localizations); Co-immunoprecipitation techniques.

Software HUSAR, Lasergene, Common BLAST, LUCIA (for fluorescent microscopy), LEICA (for the confocal microscopy), QuantityOne (Gel imaging and scintillation analysis of the radioactive arrays). AdobePhotoshop, EXCEL, WORD, Power Point, Cricket Graph.

FOREIGN LANGUAGES

French	Native.
English	Fluent.
Romanian	Fluent.
German	Basic

SCIENTIFIC INTERVENTION

PRESENTATIONS Short talk at the « third international workshop in Apoptosis » Feb 2002.

Short talk at the Foreign Ph. D students, Biocentre Niederursel, 11-12 Oct 2002.

Short talk at the Minisymposia for Doktoranden in Biologie, Frankfurt, 20 Nov 2002.

All the presentations were entitled:

“ Identification of mammalian proteins inhibiting apoptosis downstream of cytochrom c release “

Brezniceanu Marie-Luise and Zörnig Martin

At different stages of this work.

I present my work about twice a year at Research meetings in the GSH, and present interesting published work once per year in our institute's Journal club.

Poster at the NGFN meeting 20-21 Jun 2002:

“Identification of anti-apoptotic genes in a Yeast survival screen.”

Brezniceanu Marie-Luise, Kirsten Völp and Zörnig Martin

I have also trained two high school students for 6 weeks each in laboratory work.

PUBLICATIONS Brezniceanu, M. L., K. Volp, et al. (2003). “HMGB1 inhibits cell death in yeast and mammalian cells and is abundantly expressed in human breast carcinoma.” Faseb J 20: 20.

EXTRACURRICULAR ACTIVITIES

Biochemistry association of Univ.Paris VII : Treasurer (1998).

Trips Several weeks in Germany since 1983 (one or two/year), 6 months in Norway. Visits of Scotland, Thailand, Italy, Austria, Romania, Spain, Belgium, Canada (Ontario and Quebec), Brazil (Rio) and USA (Tennessee).

Hobbies Reading, Kung-Fu and Mountain Hiking.

REFERENCES

Dr. T. CRESTEIL at : cresteil@igr.fr

Dr. M. ZÖRNIG at : Zoernig@em.uni-frankfurt.de

Pr. Dr. B. GRONER at : groner@em.uni-frankfurt.de

Pr. Dr. A. STARTZINSKY-POWITZ at : Starzinski-Powitz@em.uni-frankfurt.de